INVESTIGATION OF THE ROLE OF EXTRA-RENAL 25-HYDROXYVITAMIN D 1-ALPHA HYDROXYLASE (CYP27B1) IN MEDIATING THE BONE PROTECTIVE EFFECTS OF OLEANOLIC ACID

YU WENXUAN

PhD

The Hong Kong Polytechnic University

2021

The Hong Kong Polytechnic University

Department of Applied Biology and Chemical Technology

Investigation of The Role of Extra-Renal 25-Hydroxyvitamin D 1-Alpha Hydroxylase (CYP27B1) in Mediating the Bone Protective Effects of Oleanolic Acid

YU Wenxuan

A thesis submitted in partial fulfilment of the requirements for the degree of Doctor of Philosophy

March 2021

CERTIFICATE OF ORIGINALITY

I hereby declare that this thesis is my own work and that, to the best of my knowledge and belief, it reproduces no material previously published or written, nor material that has been accepted for the award of any other degree or diploma, except where due acknowledgement has been made in the text.

_____ (Signed)

_____YU Wenxuan_____ (Name of student)

Abstract

$1,25(OH)_2D_3$ plays important role in regulating systemic calcium homeostasis and bone mineralization. It is synthesized from its precursor $25OHD_3$ through the hydroxylation by 25-hydroxyvitamin D_3 1-alpha-hydroxylase (CYP27B1). With the discovery of CYP27B1 in other extra-renal sites such as bone, regulation of extra-renal CYP27B1 and the paracrine or autocrine activities of $1,25(OH)_2D_3$ has become the focus of current research. Our previous study showed oleanolic acid (OA), a naturally occurring pentacyclic triterpenoid with bone protective effects, was capable to modulate calcium balance and renal CYP27B1 expression in aged rats. However, the ability of OA to regulate CYP27B1 in extra-renal sites is far from clear. The present study aimed to characterize the effects of OA on modulating extra-renal CYP27B1 expression and activity in extra-renal sites such as osteoblasts and adipocytes, as well as their involvement in the bone protective effects of OA.

In the present study, we first demonstrated that OA effectively elevated circulating $1,25(OH)_2D_3$ levels by upregulating renal CYP27B1 expression, which contributed to the positive calcium balance and the improvement of bone properties in ovariectomized (OVX) mice. Moreover, the expressions of CYP27B1 in iliac crests were significantly increased in response to OA, indicating the potential action of OA to modulate paracrine or autocrine activities of $1,25(OH)_2D_3$ in skeletal microenvironment. The modulatory activities of OA on CYP27B1 expressions and cellular production of $1,25(OH)_2D_3$ in bone cells were confirmed by *in-vitro* experiments using human and rat osteoblast-like cells.

In the following part, OA was shown to significantly induce CYP27B1 expression and cellular synthesis of $1,25(OH)_2D_3$ as well as the expression of bone sialoprotein 2 (BSP2) and osteopontin (OPN), two vitamin D-dependent osteogenic markers in mature osteoblastic lineages. Moreover, the stimulatory effects of OA on OPN expression and ALP activity in human osteoblast-like MG-63 cells were attenuated, at

least in part, in the presence of CYP27B1 siRNA. The results indicated the role of CYP27B1 and local 1,25(OH)$_2$D$_3$ production in mediating the effects of OA on the maturation and mineralization of osteoblasts.

The third part of my study attempted to delineate the underlying mechanisms by which OA regulate CYP27B1 in osteoblasts. Our results showed that the modulatory effects of OA on the expression and activity of CYP27B1 in osteoblasts were mimicked by lithocholic acid (LCA), a bile acid and an agonist of G protein-coupled bile acid receptor 1 (TGR5), indicating the potential role of TGR5 in regulating CYP27B1 in osteoblasts. This speculation was supported by our findings that the effects of OA on CYP27B1 expression were potentiated by overexpression of TGR5 but were attenuated when TGR5 was silenced in MG-63 cells. Further studies demonstrated that OA modulated transcriptional levels of CYP27B1 through activation of TGR5 and subsequent phosphorylation of cAMP-responsive elements-binding protein (CREB).

In the last part, we demonstrated that OA significantly suppressed the accumulation of bone marrow adipose tissues and serum lipids levels, in addition to improvement of bone properties, in OVX mice. Such actions of OA were believed to be associated with its improvement in the balance between adipogenesis and osteogenesis of bone marrow stem cells (BMSCs). *In-vitro* studies showed that OA, act like 1,25(OH)$_2$D$_3$, inhibited adipogenesis and lipid droplets accumulation in adipogenic differentiated hMSCs as well as 3T3-L1 preadipocytes. OA also consistently upregulated CYP27B1 expression and phosphorylated levels of AMP-activated protein kinase alpha (AMPK α) in 3T3-L1 cells, which was mediated by activation of TGR5.

In summary, the present study supported our hypothesis that OA exerts its bone protective effects by modulating extra-renal CYP27B1 expression and activities in osteoblasts and adipocytes. The study extended our understandings of the paracrine or autocrine actions of 1,25(OH)$_2$D$_3$ in bone microenvironment and provides new insights into the approach for modulating CYP27B1 in extra-renal tissues.

List of publication

1. **WX Yu,** Christina CW Poon, Wayne YW Lee, MS Wong. Oleanolic acid modulates 25-Hydroxyvitamin D_3 1-alpha-hydroxylase in osteoblasts and human mesenchymal stem cells. ENDO 2021, Annual Meeting of the Endocrine Society. 2021. Online, USA.

2. Dong, X. L., **Yu, W. X.**, Li, C. M., Zhou, L. P., & Wong, M. S. (2020). Chuanxiong (*Rhizome of Ligusticum chuanxiong*) Protects Ovariectomized Hyperlipidemic Rats from Bone Loss. The American journal of Chinese medicine, 48(02), 463-485.

3. Zhou, L., Wong, K. Y., **Yu, W.**, Poon, C. C. W., Xiao, H., Chan, C. O., ... & Wong, M. S. (2020). Selective Estrogen Receptor Modulator-Like Activities of Herba *epimedii* Extract and its Interactions with Tamoxifen and Raloxifene in Bone Cells and Tissues. Frontiers in Pharmacology, 11.

4. **WX Yu**, XL Dong, SS Cao, MH Li, CO Chan, Daniel KW Mok, MS Wong Osteoprotective effects of oleanolic acid against bone loss are associated with its actions on fatty acid metabolism in aged female rats. Annual Meeting of American Society of Bone and Mineral Research. 2019. Orlando, USA.

5. **W Yu,** S Cao and MS Wong. Investigation of the mechanism of oleanolic acid (OA) in modulating renal vitamin D metabolism *in vitro*. The 15th International Postgraduate symposium on Chinese Medicine. 2019. Hong Kong

6. Zeng, J., **Yu, W.,** Dong, X., Zhao, S., Wang, Z., Liu, Y., ... & Wang, Y. (2019). A nanoencapsulation suspension biomimetic of milk structure for enhanced maternal and fetal absorptions of DHA to improve early brain development. Nanomedicine: Nanotechnology, Biology and Medicine, 15(1), 119-128.

7. Dong, X. L., **Yu, W. X.**, Li, C. M., He, S., Zhou, L. P., Poon, C. W., & Wong, M. S. (2018). Danshen (*Salvia miltiorrhiza*) protects ovariectomized rats fed with high-saturated fat-sucrose diet from bone loss. Osteoporosis International, 29(1), 223-235.

8. Cao, S., Tian, X. L., **Yu, W. X.,** Zhou, L. P., Dong, X. L., Favus, M. J., & Wong, M. S. (2018). Oleanolic acid and ursolic acid improve bone properties and calcium balance and modulate vitamin D metabolism in aged female rats. Frontiers in pharmacology, 9, 1435.

9. Oleanolic acid modulates extra-renal 25-hydroxyvitamin D3 1-alpha-hydroxylase (CYP27B1) in osteoblasts (in preparation)

Acknowledgement

Table of contents

List of figures

List of tables

Abbreviations

1,25(OH)$_2$D	1 alpha,25-Dihydroxyvitamin D
25(OH)D	25-Hydroxyvitamin D
ACATs	Acyl-Coenzyme A: Cholesterol Acyltransferase
ALP	Alkaline Phosphatase
ALT	Alanine Aminotransferase
αMEM	Alpha Modified Eargle Medium
AMPK α	Adenosine Monophosphate -Activated Protein Kinase Alpha
AST	Aspartate Aminotransferase
AV/TV	Adipose Volume/Total Volume
BMC	Bone Mineral Content
BMD	Bone Mineral Density
BMI	Body Mass Index
BMSCs	Bone Marrow Stromal Cells
BSP2	Bone Sialoprotein 2
BV/TV	Bone Volume/Tissue Volume
Ca	Calcium
CA	Cholic Acid
Calbindin D9k	Calcium-Binding Protein Calbindin-D9k
cAMP	Cyclic Adenosine Monophosphate
C/EBP α	CCAAT Enhancer Binding Proteins α
CDCA	Chenodeoxycholic Acid
Col-1	Type 1 Collagen
Conn.D	Connectivity Density
CNS	Central Nervous System
Cr	Creatinine
CRE	Adenosine Monophosphate -Responsive Elements

CREB	Cyclic Adenosine Monophosphate-Responsive Elements-Binding Protein
CT	Computed Tomography
CTX-1	C-Terminal Telopeptide of Type I Collagen
CYP24A1	Vitamin D 24-Hydroxylase
CYP27B1	25-Hydroxyvitamin D 1-Alpha-Hydroxylase
DBP	Vitamin D Binding Protein
DCA	Deoxycholic Acid
DMEM	Dulbecco'S Modified Eargle Medium
DXA	Dual-Energy X-Ray Absorptiometry
E2	Estradiol
ER	Estrogen Receptor
FABPs	Fatty Acid-Binding Proteins
FBS	Fetal Bovine Serum
FDA	Food and Drug Administration
FFAs	Free Fatty Acids
FLL	*Ligustri Lucidi Fructus*
GAPDH	Glyceraldehyde-3-Phosphate Dehydrogenase
GLP-1	Glucagon-Like Peptide-1
GLUT4	Glucose Transporter 4
GPCR	G Protein-Coupled Receptor
GPX	Glutathione Peroxidase
HCD	High Calcium Diet
HDL-C	High-Density Lipoprotein Cholesterol
HFD	High-Fat Diet
LDH	Lactic Dehydrogenase
LDL-C	Low-Density Lipoprotein Cholesterol
LFD	Low-Fat Diet

IBMX	3-Isobuty-1-Methylxanthine
IFNγ	Interferon-γ
IGF-1	Insulin-Like Growth Factor 1
IL-1β	Interleukin 1 Beta
IRS-1	Insulin Receptor Substrate 1
MDA	Malondialdehyde
MAT	Marrow Adipose Tissue
MRI	Magnetic Resonance Imaging
MSCs	Mesenchymal Stromal Cells
NAFLD	Non-Alcoholic Fatty Liver Disease
NEFA	Non-Esterified Fatty Acid
Nrf2	Nuclear Factor Erythroid 2-Related Factor 2
OCN	Osteocalcin
OA	Oleanolic Acid
OPG	Osteoprotogerin
OPN	Osteopontin
OVX	Ovariectomy
P	Phosphorus
PINP	N-Terminal Propeptides of Procollagen Type 1
PKA	Protein Kinase A
PMCA1b	Plasma Membrane Calcium Atpase 1b
PMSF	Phenylmethyl Sulfonyl Fluoride
PPAR γ	Peroxisome Proliferator Activated Receptor Gamma
PTH	Parathyroid Hormone
PVDF	Polyvinylidene Fluoride
RANKL	Receptor Activator of Nuclear Factor Kappa-B Ligand (RANKL)
RT-PCR	Reverse Transcription Polymerase Chain Reaction

Runx2	Runt-Related Transcription Factor 2
RXR	Retinoid-X Receptor
SAT	Subcutaneous Adipose Tissue
siRNAs	Small Interfering RNAs
SMI	Structure Model Index
STAT3	Signal Transducer and Activator of Transcription 3
SOD	Superoxide Dismutase
SREBP-1c	Sterol Regulatory Element-Binding Protein 1c
Tb. N	Trabecular Bone Number
Tb.Sp	Trabecular Bone Separation
Tb.Th	Trabecular Bone Thickness
TC	Total Cholesterol
TG	Triglyceride
TGF-β	Transforming Growth Factor-Beta
TGR5	G Protein-Coupled Bile Acid Receptor 1
TNFα	Tumor Necrosis Factor α
TRPV6	Transient Receptor Potential Vanilloid 6
UVB	Ultraviolet B
VAT	Visceral Adipose Tissue
VDR	Vitamin D Receptor
VDRE	Vitamin D Responsive Element
VDDR	Vitamin D Dependency Rickets

Chapter 1

Introduction

1.1. Osteoporosis and age-related bone loss

Osteoporosis is a systemic skeletal disorder that is characterized by low bone mineral density and deteriorated bone microarchitecture, which further increase bone fragility and induce high risk of fracture. There are two variants of osteoporosis: primary and secondary osteoporosis. Primary osteoporosis is characterized by the increased bone fragility and deterioration with the normal processes of menopause and advancing age. Osteoporosis could also be caused by many endocrinopathies and genetic disorders which may interfere with the achievement of optimal peak bone mass or accelerate the rate of bone loss. Due to its high prevalence worldwide, osteoporosis is considered a serious public health concern. In this Chapter, the prevalence of osteoporosis worldwide and possible influencing factors followed by pathogenic mechanisms involved in the development of osteoporosis will be described. At the end, current interventions or therapies for management of osteoporosis will be reviewed.

1.1.1 Epidemiology of osteoporosis

It is estimated that over 200 million people worldwide suffering from osteoporosis (Reginster et al., 2006). Every year, more than 8.9 million fractures occur as a result of osteoporosis throughout the world (Pisani et al., 2016). In China, 79 million people over 50s are affected and more than 687,000 hip fractures occur as the result of osteoporosis (Lin et al., 2015). Women are at higher risk for osteoporosis, and most of cases occur in postmenopausal women (El Maghraoui et al., 2013). Globally, 1 in 5 men and 1 in 3 women over the age of 50 will experience osteoporotic fractures. In developed countries, 2% - 8% of males but 9% - 38% of females have osteoporosis. About 2 million men and 8 million women in the United States were affected by osteoporosis in 2010 (Wade et al., 2014). In China, the prevalence rate of osteoporosis in the males and females above the age of 50 was 57.6% and 64.6% respectively in 2012 (Chen et al., 2016). Moreover, the incidence of age-related osteoporosis increased more rapidly for females than males.

Besides, the prevalence of osteoporosis becomes more common with age. Globally, approximately 15% of people in their 50s and 70% of them over 80 are affected by osteoporosis. With the increase in ageing population worldwide, it poses significant economic and medical burden to the family and society due to the increased costs of treatment and long-term disability. The United States spend 19 billions USD on healthcare costs associated with osteoporosis in 2005 (Burge et al., 2007). In China, the mean prevalence of osteoporosis in elderly was 34.65 % in 2016, which is projected to increase with the growth of older population in the coming years (Chen et al., 2016). According to the national survey, Chinese people of 60 and above reached 254 million, which account for 18.1% of total population at the end of 2019. By 2050, this proportion is estimated to reach 25 %, thus the corresponding population affected by osteoporosis will increase sharply to 212 million.

1.1.2 Pathogenesis of osteoporosis

There are two key parameters involved in the pathophysiology of osteoporosis: the magnitude of peak bone mass achieved during adolescence and the speed of bone loss during the later adult life. During the process of bone modeling, bone expand and lengthen into its adult form through balanced actions of skeletal deposition and resorption (Parfitt, 1994). Usually this process starts during fetal growth, and stop until the end of second decade of life when epiphyseal fusion happen (Heaney et al., 2000). The bone mass achieved during the bone growth follows sex- and age-specific manners (Fig. 1.1). The peak of bone mineral accretion rate acquired at 14.1 ± 0.95 years in boys and 12.5 ± 0.90 years in girls in Europe (Bailey et al., 1999). By the end of third decade of life, increase in both the cortical and trabecular skeleton provides the accumulation of bone mineral and structural strength of bone (Fig. 1.1). Genome is one the major factors that determines the variability of peak bone mass. Levels of sex hormone, especially estrogen, is another factor that influences bone mass accretion during puberty. In addition, modification of lifestyle in aspects of nutrition, exercise and smoking in

childhood and pubertal years is the effective strategy to optimize the development of peak bone mass.

Bone is a living tissue which could regenerate itself by bone remodeling cycle. This is a tightly coupled process during which bone resorption by osteoclasts at approximate the same rate as bone formation by osteoblasts. Resulting in about 5-10 % of normal bone renewal every year. However, when bone resorption exceeds the speed of bone formation, a rapid decline in bone mass will lead to osteoporosis. Human skeleton is made up of trabecular and cortical bone. Trabecular bone is the porous structural skeleton connected by rods and plates at spines and the ends of long bones like femur and tibia, which contribute to the skeletal strength and bone mass (Weaver et al., 2016). Trabeculae is the active component of bone as the holes in it are filled with bone marrow that provides an environment for keeping skeletal homeostasis. Due to the same reason, trabecular bone is also more sensitive to influences from system or skeletal microenvironment which may result in changes in bone remodeling.

The receptor activator of nuclear factor kappa-B ligand (RANKL) and osteoprotogerin (OPG) are a pair of factors involved in one of the most important pathways in the interaction between osteoblast and osteoclast. RANKL is a surface peptide expressed in osteoblasts and serves as an activator of osteoclastogenesis and subsequent bone resorption once binds to the RANK located on the surface of osteoclasts (J.-Y. Kim et al., 2014). This process could be markedly suppressed by OPG which act as a decoy receptor for RANKL and disturb the interactions of RANKL and RANK, thus inhibiting osteoclastogenesis and bone resorption (Boyle et al., 2003). Expression of OPG in osteoblast lineage cells is significantly regulated by estrogen (Michael et al., 2005; Millán, 2015). Recent studies showed osteocytes inlaying within the bone matrix also could release RANKL which triggers osteolysis when calcium is highly demanded like estrogen deficiency (Xiong et al., 2015). These contribute to the accelerated bone loss in postmenopausal women as rapid decline of ovarian function results in reducing levels of estrogen in these women (Nelson, 2008).
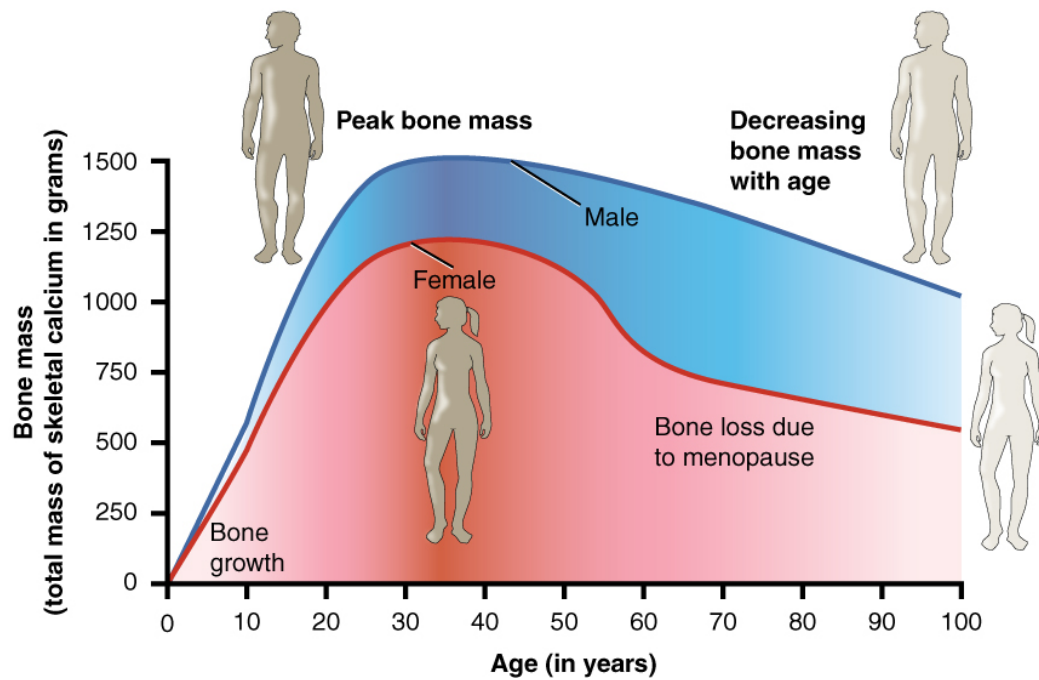
Fig. 1.1 Bone mass across the lifespan of male and female.

Both men and women achieve their peak bone mass at around 30 years old. After that, bone mass decrease gradually with age during the later years of their life. However, women get more rapid bone loss than men after the 50s, the age at which menopause of women approximately started. The deficiency of sexual hormones accelerated age-related bone loss in women.

Adapted from (De Schepper, 2019)

In bone marrow niche, there are two types of stem cells engaged in the formation, maintenance and repairment of skeletal tissue: the hematologic stem cells which could differentiate into osteoclasts, and mesenchymal stromal cells (MSCs) which could give rise to the osteoblasts. In addition to the imbalance between bone resorption in osteoclasts and bone formation in osteoblast, studies suggested that changes in number and function of MSCs are major factors contributing to estrogen deficiency and age-related osteoporosis which affects both men and women (Kiernan et al., 2017). MSCs are the stem cells spindle in shape which could be found in many tissues. Besides the self-renewal ability, MSCs are the multipotential cells which could give rise to various mesodermal lineages including osteoblasts, chondrocytes and adipocytes (da Silva Meirelles et al., 2006). In the ageing process, MSCs shift to differentiation into adipogenesis commitment rather than osteogenesis commitment due to the functional impairment of MSCs with ageing (Coipeau et al., 2009). This leads to the accumulation of adipose tissue but reduction in bone mass in bone tissue, which will ultimately increase the risk of fracture in elderly.

The fate of MSCs commitment towards either the adipocyte or osteoblast lineage is the results of a combination of different regulatory factors in the bone microenvironment (Fig. 1.2). It is well established that activation of CCAAT enhancer binding proteins (C/EBP β, α and γ) and peroxisome proliferator activated receptor gamma (PPAR γ) direct the adipogenesis of MSCs (Lefterova et al., 2008). The upregulated expression of PPAR γ in aged MSCs not only promote adipogenesis but also suppress osteogenesis of MSCs, leading to accelerated age-related bone loss. On the other hand, runt-related transcription factor 2 (Runx2) has been recognized as the initiator of the osteogenic differentiation of MSCs commitment by binding with the cis-element of osteocalcin (OCN) gene (Ducy et al., 1997; Varela et al., 2016). Osterix, also called transcription factor Sp7, is the member of specificity protein 1 family. It is another regulator of osteogenesis and bone formation that functions downstream of Runx2 (Nakashima et al., 2002). The expression of genes for extracellular matrix proteins such as type 1 collagen a1 (Cola1) occurs when the osteogenic commitments differentiate to the pre-

osteoblasts, while maturation of osteoblasts is characterized by the production of osteocalcin and osteopontin. According to Jiang et al. (2008), the expression of Runx2 largely decreased with ageing, resulting in a subsequent lower expression of other osteogenic markers and consequent reduction in number of osteoblasts.
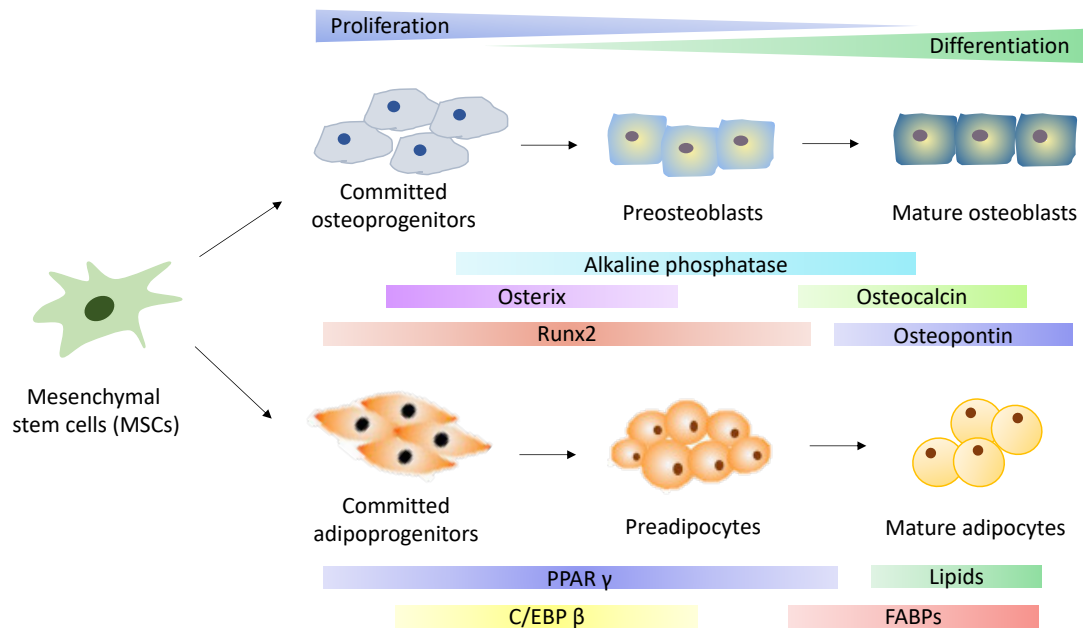
Fig. 1.2 Pathways involved in differentiation of mesenchymal stem cells (MSCs) towards adipocyte and osteoblast commitment.

MSCs are multipotential progenitors that could differentiate into several lineages such as adipocytes and osteoblasts. Differentiation of adipogenic commitment and osteogenic commitment are multiple-stage and well-coordinated process. The adipogenesis of MSCs is regulated by PPAR γ and C/EBP β. Besides, the expression of fatty acid-binding proteins (FABPs) and the production of lipids are important indicators of adipogenesis. On the other hand, osteogenesis of MSCs is directed by Runx2 and Osterix. Alkaline phosphatase, osteocalcin and osteopontin expressed by osteoblast lineage cells at different osteogenic differentiation could serve as indicators of osteogenesis of MSCs.

Adjusted from (Wagner et al., 2010)

1.1.3 Pharmacological therapies of osteoporosis

Osteoporosis is a condition without typical symptoms until a fracture occurs. For such reason, osteoporosis is also called a "silent disease". It is a major chronic disease that may lead to disability and further reduce quality of life of those being affected，bringing significant economic cost to the family and the society. Based on the pathogenesis and risk factors that may cause reduction in bone mass and strength, approaches for prevention or management of osteoporosis in those who are susceptible or being affected are urgent demanded.

Prominent advances in exploring the pathogenesis of osteoporosis in the past two decades made it possible to develop optimal therapies for osteoporosis. A number of pharmacologic agents were approved by the Food and Drug Administration (FDA) to prevent and treat osteoporosis. The mechanisms of actions and adverse events associated with these drugs are listed in Table 1.1. The pharmacological interventions of osteoporosis involve regulating the process of bone remodeling: either by suppressing bone resorption in osteoclast or promoting bone formation in osteoblast, and both of them have been proven to improve bone mass and reduce the occurrence of fracture.

Bisphosphonates are the most used antiresorptive agents for treatment of osteoporosis. Numerous randomized trials have showed both oral and intravenous use of bisphosphonates effectively reduced the hip, vertebral, and non-vertebral fractures (Khosla et al., 2012; McClung et al., 2013). However, adverse effects like upper gastrointestinal symptoms and muscle and joint pain were commonly observed in those taking bisphosphonates. What's more, patients with hypocalcemia or impaired renal function should be more cautious to use bisphosphonates (Khan et al., 2015).

Estrogen not only reduces the bone resorption by osteoclasts, but also has anabolic effects on osteoblasts and osteocytes to enhance bone formation (Chow et al., 1992). According to Women's Health Initiative studies, estrogen therapy significantly reduced

bone loss and prevented the incidence of vertebral, nonvertebral, and hip fractures in postmenopausal women (Cauley et al., 2003). Nevertheless, estrogen therapy is not recommended as a first-line choice due to the risks of breast cancer and cardiovascular disease it may cause (Cosman, 2014). Raloxifene is a selective estrogen receptor modulator which activates estrogen receptors in distinct tissues (Muchmore, 2000). Raloxifene is tempting treatment option as this therapy reduces the risk of breast cancer, although it has weak anti-resorption effects to reduce vertebral but not non-vertebral or hip fracture in postmenopausal women with osteoporosis (Ettinger et al., 1999).

Denosumab is a human monoclonal antibody which binds to RANKL, thereby lead to a pronounced but reversible inhibition of bone resorption (Kostenuik et al., 2009). It is the first biological therapy approved for treatment of osteoporosis. Administration of denosumab by subcutaneous injection at 60 mg twice per year significantly reduced the risk of vertebral, nonvertebral and hip fracture in postmenopausal women with osteoporosis (Cummings et al., 2009). However, high rate of bone resorption and rapid decline in bone mass occurred once the treatment is stopped (Cummings et al., 2018). Treatment with another antiresorptive agent should be kept when denosumab is discontinued.

Teriparatide is an anabolic agent which works by increasing bone formation rather than inhibiting bone resorption. Administration of teriparatide at 20 μg daily by subcutaneous injection for 21 months markedly reduced the risk of vertebral and nonvertebral fractures in postmenopausal women with low BMD (Neer, 2001). Similar to denosumab, benefits of teriparatide will quickly lost once it is stopped, therefore it should be followed by another antiresorptive agent (McClung, 2017).

Table 1.1 Approved pharmacological agents for osteoporosis

	Mechanism of action	**Adverse events**
Bisphosphonates		
Alendronate, risedronate, zoledronic acid	Antiresorptive	Upper gastrointestinal symptoms, flu-like symptoms, muscle and joint pain; atypical femoral fractures, osteonecrosis of the jaw
Estrogens		
Estradiol, estropipate, conjugated estrogen	Antiresorptive and anabolic	Breast cancer, coronary, cerebrovascular, and thrombotic events
Selective estrogen receptor modulators		
Raloxifene, bazedoxifene	Antiresorptive	Vasomotor menopausal symptoms, venous thrombosis, coronary heart disease
RANKL inhibitor		
Denosumab	Antiresorptive	Skin rash and infection, atypical femoral fractures and osteonecrosis
Parathyroid hormone receptor agonist		
Teriparatide	Anabolic	Muscle cramps, hypercalcemia, hypercalciuria, hyperuricemia, osteosarcoma

1.1.4 Nonpharmacological interventions of osteoporosis

Modification of lifestyle that has been linked to the incidence of fracture is highly recommended to slow down the development of osteoporosis as they are easy to implement and few adverse effects that may cause. The amendable lifestyle factors including a balanced diet with adequate calcium and vitamin D, an adequate sunlight exposure and avoidance of the detrimental habit like smoking and excessive intake of alcohol and caffeine, could help to reduce the risk of fracture in men and women (Bliuc et al., 2007). Besides, regular physical activity, especially weight-bearing and muscle-strengthening exercise are encouraged as exercise facilitates the building of peak bone mass and muscle strength thus to improve bone mineral density (BMD) and reduce the risk of fall (Feskanich et al., 2002). Jogging, brisk walking, stair-climbing and dancing are the recommended weight-bearing exercises with proper impact (Ip et al., 2013). Tai Chi, a low-impact traditional Chinese exercise, is proved to retard the trabecular and cortical bone loss in postmenopausal women (Chan et al., 2004), and reduce the risk of fall in elderly (Wolf et al., 1996).

It is well-known that vitamin D is critical for promoting intestinal calcium absorption to guarantee stable serum levels of calcium and phosphate, which further facilitates bone mineralization. However, a local study reported that up to 60% community-dwelling adults over 50 years have vitamin D deficiency (Wat et al., 2007). This phenomenon is more significant in those patients with hip fracture in hospital due to the lack of sunlight exposure (Lau et al., 1989; Pun et al., 1990). Vitamin D deficiency in combination with inadequate consumption of calcium accelerated the bone loss in susceptible elderly population. It has been proved that increasing the daily intake of calcium and vitamin D, either from diet or in the form of supplements, could improve the bone mineral density and reduce the risk of fracture in postmenopausal women and reduce falls in aged people (Shea et al., 2002). As recommended by the UK National Osteoporosis Guideline Group, a daily intake of 1000 mg of calcium and 800 IU of vitamin D_3 is optimal for osteoporosis prevention for those who are aged over 50 and

at high risk of fracture. Moreover, studies showed that supplements of calcium and vitamin D further enhanced the anti-fracture and anti-resorption effects of bisphosphonates (Adami et al., 2006; Bonnick et al., 2007), indicating the importance of maintaining appropriate serum levels of calcium and vitamin D in prevention and treatment of osteoporosis. However, excessive consumption of calcium and vitamin D may give rise to hypercalciuria and hypercalcemia which increased the risk of kidney stones and cardiovascular events (Bolland et al., 2010). Moreover, a meta-analysis by Zhao et al. (2017) showed little association between the use of vitamin D and calcium supplement with the decrease in incidence of fractures in older adults. These contradictory findings to the routine supplements might attribute to the poor intestinal absorption of vitamin D and calcium as well as changes in vitamin D metabolism in older adults.

1.2. Vitamin D and bone health

The predominant activity of vitamin D is to maintain calcium homeostasis by increasing intestinal absorption and renal tubular reabsorption of calcium thus ensure calcium balance and bone mineralization. However, vitamin D deficiency is widely prevalent. Possible reasons for the inadequate levels of vitamin D include insufficient synthesis of vitamin D in the skin due to absence of outdoor activity, sub-optimal intake, or inadequate absorption of vitamin D in the intestine, and impaired synthesis of bioactive form of vitamin D, which might be associated with age-related decline in bone mass and high risk of fall and fracture in elderly. Although the benefit effects of vitamin D in prevention and treatment of osteoporosis and fractures in elderly population are reported in many epidemiological investigations and randomized controlled trials, functions, and role of vitamin D in specific bone cells are still the topic of current research.

1.2.1　Vitamin D metabolism

Vitamin D is a group of fat-soluble secosteroids. There are two major forms of vitamin D which presented in dietary sources with different structures: vitamin D_2 (also called ergocalciferol) and vitamin D_3 (also called cholecalciferol). The former is produced in plants and fungi exposed to ultraviolet B (UVB), while vitamin D_3 can be find in most foods like fish and egg yolk. The structural differences between the two forms are in the side chain where a double bond between C22 and C23 and a methyl group on C24 are absent in vitamin D_3, resulting in closer affinity for vitamin D binding protein (DBP) thus facilitating effective circulation. In addition to natural sources, vitamin D_3 could also be synthesized from 7-dehydrocholesterol under sun exposure (spectrum 280-320 UVB) in the epidermis of skin of most vertebrates, including human (Crissey et al., 2003).

Actually, vitamin D itself is not biologically active, it has to undergo two steps of hydroxylation to produce the bioactive form to exert physiological activities (Kragballe,

1992). The vitamin D obtained from dietary sources or endogenous synthesized in the skin is transported by DBP and stored in the liver and fat. The first step of activation of vitamin D takes place in liver, to 25-hydroxylize vitamin D, under the catalyzation of cytochrome P450 enzymes CYP2R1 and CYP27A1, to form 25-hydroxyvitamin D (25OHD) (Fig. 1.3). As a main circulating form of vitamin D, 25OHD is released into plasma and transported by DBP to the kidney or other tissues for the second step of hydroxylation. In the proximal tubules of the kidney, 25OHD is converted to 1α,25-dihydroxyvitamin D $(1,25(OH)_2D)$ by hydroxylation of 25-hydroxyvitamin D3 1-alpha-hydroxylase (CYP27B1), a mitochondrial CYP450, at the 1α position. After the last step of activation, $1,25(OH)_2D$ is exported into circulation and transported by DBP to the target tissues like intestine and bone (Marriott et al., 2020). It has been generally recognized that renal CYP27B1 is the major source of circulating $1,25(OH)_2D$ which is associated with endocrine activities while other extra-renal CYP27B1 are only responsible for the paracrine or autocrine actions of vitamin D, unless in certain pathological conditions like hematologic malignancies and severe sarcoidosis (Shultz et al., 1983).

Inactivation of 25OHD and $1,25(OH)_2D$ is catalyzed by vitamin D_3 24-hydroxylase (CYP24A1), also a mitochondrial P450 enzyme, via a series of sequential hydroxylation and oxidation. CYP24A1 is expressed in many tissues that are recognized as the targets for vitamin D. $1,25(OH)_2D$ strongly stimulates transcription of CYP24A1 gene via binding to the nuclear vitamin D receptor (VDR) to activate vitamin D response element located in the promoter of CYP24A1, thus preventing excessive amount of $1,25(OH)_2D$ in the circulation. Studies showed that excessive levels of $1,25(OH)_2D$ due to mutation of CYP24A1 may lead to severe disorders such as hypercalciuria, hypercalcaemia, nephrolithiasis and nephrocalcinosis (Dinour et al., 2013).
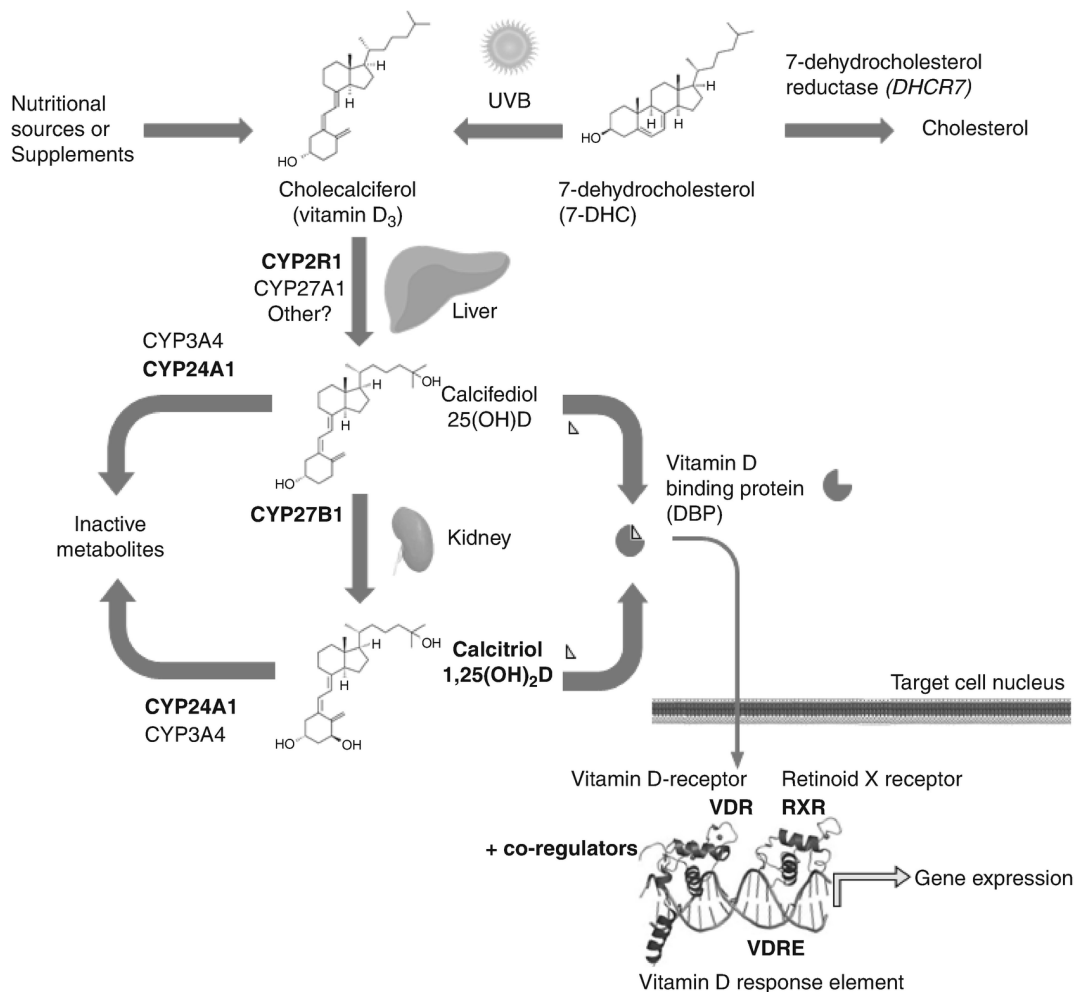
Fig. 1.3 Metabolism and mechanism of actions of vitamin D

Vitamin D obtained from foods and sun exposure is biologically inert, two steps of hydroxylation are needed for activation. In the liver, vitamin D is hydroxylated into the circulating form 25(OH)D, under the actions of CYP2R1 and CYP27A1. 25(OH)D is exported into circulation and is further hydroxylated by CYP27B1 to form the bioactive $1,25(OH)_2D$ in the proximal tubules of the kidney which is the main source of circulating $1,25(OH)_2D$. Both 25(OH)D and $1,25(OH)_2D$ are catabolized by CYP24A1 through a series of sequential hydroxylation and oxidation. To exert the physiological activities, 25(OH)D and $1,25(OH)_2D$ are transported by DBP to target cells and bind to VDR which could form a heterodimer with retinoid-X receptor (RXR). The complex regulates the transcription of target genes by binding the vitamin D responsive element (VDRE) located in those genes.

Adapted from (Bouillon et al., 2020)

1.2.2   25-hydroxyvitamin D 1α-hydroxylase (CYP27B1)

CYP27B1 is considered the sole enzyme that catalyzes the hydroxylation of 25OHD to $1,25(OH)_2D$, the bioactive form of vitamin D, which acts as a central regulator of mineral homeostasis and bone mineralization. It has equal efficiency to hydroxylate $25OHD_2$ and $25OHD_3$ at 1 α position. Coincidentally, CYP27B1 was characterized, sequenced, and cloned from kidney of mouse, rat, and human by different research groups in 1997 (Monkawa et al., 1997; St-Arnaud et al., 1997; Takeyama et al., 1997). Original studies identified that the human *CYP27B1* gene consists of 9 exons and 8 introns spanning 6.5 kb on chromosome 12q13.1-q13.3 (Monkawa et al., 1997). CYP27B1 protein is a mitochondrial cytochrome P450 of 508 amino acids with a molecular weight of 56 kDa.

Human CYP27B1 mutations take place throughout the gene, which results in the defect or misfold of proteins thus abolish activities of the enzyme. Mutations within coding regions leading to inactive or ablated CYP27B1 was recognized in patients with deficiency or absence of serum $1,25(OH)_2D$ despite normal consumption of vitamin D, suggesting the importance of CYP27B1 in synthesis of $1,25(OH)_2D$. This condition, namely vitamin D dependency rickets (VDDR type I), is characterized by resistant-rickets phenotypes such as hypophosphatemia, hypocalcemia, secondary hyperparathyroidism as well as under-mineralized bone (Takeda et al., 1997). The development of CYP27B1-null mice, which showed a short of 1α-hydroxylated vitamin D metabolites in blood and tissues, provided a mouse model of VDDR type I. Administration of a high calcium "rescue diet" (2% calcium, 1.25% phosphorus, 20% lactose) or normal diet supplemented with physiological dosage of $1,25(OH)_2D_3$ (nanogram) largely restored the mineral and skeletal defects in the CYP27B1-null mice (Olivier Dardenne et al., 2003; O Dardenne et al., 2003; HOENDEROP et al., 2002).

The achievement in specific CYP27B1 mRNA and antibodies of CYP27B1 protein made it possible to explore and identify the expression of CYP27B1 in tissues outside

kidney. Using Northern blot analysis, RT-PCT techniques and immunohistochemistry analysis, several research groups demonstrated detectable expression of CYP27B1 in animal and human extra-renal sites such as placenta (Gray et al., 1979), prostate (Whitlatch et al., 2002), colon (Zehnder et al., 2001), muscle (Somjen et al., 2005), and bone (Ichikawa et al., 1995). Accumulated evidence suggested that the presence of CYP27B1 in these tissues may explain the critical role of circulating 25OHD levels which enables cellular production of $1,25(OH)_2D$ and maintaining normal functions of these tissues in a paracrine or autocrine system.

1.2.3   Regulation of 25-hydroxyvitamin D 1α-hydroxylase (CYP27B1)

Numerous studies focused on the regulation of CYP27B1 ever since the enzyme was identified in the proximal tubule of the kidney in the early 1970s. The renal CYP27B1 is tightly controlled by hormonal factors including $1,25(OH)_2D$ itself, and parathyroid hormone (PTH) (Murayama et al., 1999). Other mineral factors like calcium and phosphate, as well as fibroblast growth factor 23 (FGF23) and calcitonin are also essential in regulating the production of $1,25(OH)_2D$ (Chanakul et al., 2013). The vitamin D status is one of the earliest identified regulators that influence the 1α-hydroxylation of 25OHD in kidney cells. The direct negative feedback effect was discovered in the cultured kidney cells or in kidney of animals administrated with $1,25(OH)_2D$. The cloning and identification of CYP27B1 enabled recognition that $1,25(OH)_2D$ regulates the transcription of negative feedback via its nuclear receptor. $1,25(OH)_2D$ binding to VDR generates a liganded VDR/RXR complex which interact with negative VDREs (nVDREs) located in the CYP27B1 promoter to downregulate expression of CYP27B1 (Murayama et al., 1998). Moreover, the elevated CYP27B1 activity and $1,25(OH)_2D$ levels in VDR-null mice expanded our understanding of the role of VDR in this feedback regulation.

In line with the actions of $1,25(OH)_2D$ in regulating CYP27B1, the activity of this enzyme in kidney is also inversely related to the levels of dietary and serum calcium.

PTH was reported to directly mediate this regulation in renal proximal tubule cells in many earlier studies. The decreased levels of serum calcium stimulate parathyroid gland to release PTH and increase renal CYP27B1 activity for calcium absorption and resorption. PTH stimulates CYP27B1 expression at both transcriptional and post-transcriptional levels. The promoter of CYP27B1 gene contains a region that is sensitive to PTH stimulation for its transcription. PTH binding to its membrane receptor (commonly known as PTHR1) results in activation of Gs and production of cAMP, which further initiates protein kinase A (PKA) and the phosphorylation of cAMP-responsive elements (CRE) and its interaction with CRE-binding protein (CREB) site within CYP27B1 promoter (Brenza et al., 1998). Another study by Gao et al. (2002) showed induction of CCAAT box site located in the CYP27B1 promoter also contributes to the stimulation of CYP27B1 by PTH.

FGF23 also acts as an essential regulator of phosphate homeostasis and biosynthesis of $1,25(OH)_2D$. Studies showed that administration of $1,25(OH)_2D_3$ resulted in elevated production of FGF23 in bone followed by the induction in serum phosphate (Inoue et al., 2005). The increased FGF23 in turn suppressed $1,25(OH)_2D_3$ levels by inhibiting CYP27B1 expression and upregulating CYP24A1 expression in kidney, which further suppressed production of FGF23 in bone (Jurutka et al., 2007). To this extent, the negative feedback regulation of $1,25(OH)_2D$ on CYP27B1 is also through the upregulation of FGF23 in bone.
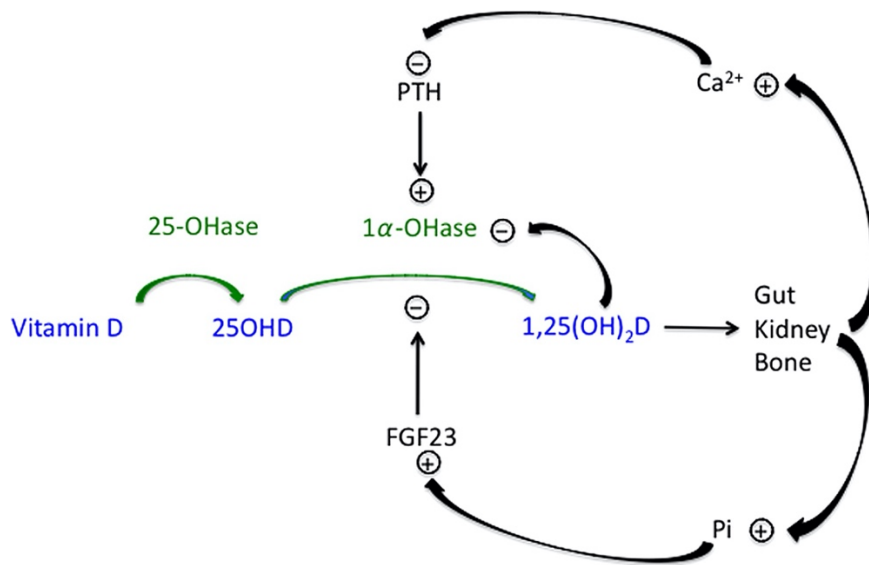
Fig. 1.4 Classic regulation of renal 1α-OHase (CYP27B1)

CYP27B1 is tightly regulated by dietary and hormonal factors. Under low serum calcium levels, renal 1α-hydroxylation of 25OHD to generate bioactive $1,25(OH)_2D$ is upregulated by PTH, resulting in increased absorption of calcium and phosphate in circulation. Elevated calcium and phosphate in turn inhibits PTH secretion and induced FGF23 production in bone. Elevated FGF23 and $1,25(OH)_2D$ suppress renal CYP27B1 and $1,25(OH)_2D$ production in a negative feedback manner.

Adapted from (Füchtbauer et al., 2015)

Regulation of CYP27B1 in extra-renal site has also drawn attention of researchers over the last decade. Accumulating evidence showed that regulation of extra-renal CYP27B1 is different from that in kidney (Bikle et al., 2018). In keratinocytes, expression of CYP27B1 fails to respond to neither $1,25(OH)_2D$ nor PTH. However, an increased production of $1,25(OH)_2D$ in response to PTH was discovered in keratinocytes, indicating that the enzyme might be modulated by PTH in a post-transcriptional manner (Flanagan et al., 2003). $1,25(OH)_2D$ modulates its own levels by stimulating CYP24A1 rather than the feedback regulation of CYP27B1 (St-Arnaud et al., 1997). It seems that cytokines such as interferon-γ (IFNγ) and tumor necrosis factor α (TNFα) act as the major modulators of CYP27B1 in macrophage and keratinocyte (Adams et al., 1985; BIKLE et al., 1991).

The regulation of CYP27B1 in bone remains unclear, although it has been reported that expression of CYP27B1 in osteoblasts did not respond to classic regulators such as PTH and ambient calcium, but was significantly induced by interleukin 1 beta (IL-1β) (van Driel et al., 2006). However, it seems that the regulation of CYP27B1 in MSCs is similar to that in kidney cells. Studies showed that PTH upregulated CYP27B1 expression and $1,25(OH)_2D$ production in MSCs, either via phosphorylation of CREB or the endogenous insulin-like growth factor 1 (IGF-1) signaling (Geng et al., 2011a; S. Zhou et al., 2011). As the expression and activity of CYP27B1 in MSCs decreases with aging, the reduced biosynthesis of $1,25(OH)_2D$ further leads to impaired osteoblastic differentiation.

1.2.4   Mechanisms of action of vitamin D

As the distinct protein that binds $1,25(OH)_2D$ at sub-nanomolar concentrations, VDR mediates most of actions of this hormone, although many rapid and non-genomic signaling of $1,25(OH)_2D$ has been identified (Haussler et al., 1997; Haussler et al., 2011). When transported to target cells, $1,25(OH)_2D$ exerts physiological activities by binding to its nuclear receptor vitamin D receptor (VDR) and initiating transcription of

target genes. To this extent, vitamin D acts more like a hormone. VDR is a member of the nuclear receptor family of steroid hormone and transcription factors. It contains a ligand-binding domain and a DNA-binding domain (Kakuda et al., 2008). In the genomic mode, $1,25(OH)_2D$ binding to VDR causes its conformational alteration that form a heterodimeric complex with the retinoid-X receptor. The complex then enters the nucleus and initiates the transcription of specific genes by binding to the vitamin D responsive element (VDRE) within those genes (Moore et al., 2006). The cell and gene specific complexes contribute to the differential actions of $1,25(OH)_2D$ in different cell types. It has been estimated that over 3% of human genome is directly or indirectly regulated by $1,25(OH)_2D$, which is associated with the genomic actions of $1,25(OH)_2D$ (Bouillon et al., 2008).

The primary action of vitamin D is to maintain mineral homeostasis by increasing intestinal calcium absorption in an endocrine system. $1,25(OH)_2D$/VDR system mediates transcellular and paracellular transport of calcium in intestinal epithelium. When dietary calcium is insufficient, $1,25(OH)_2D$ binds to VDR and induces transcription of apical membrane calcium channel TRPV6 (transient receptor potential vanilloid 6), calcium-binding protein calbindin-D9k (Calbindin D9k), as well as plasma membrane calcium ATPase 1b (PMCA1b) in duodenum, which are responsible for the uptake of calcium from the intestinal lumen into cells, then shuttle of calcium from the apical membrane to the basolateral membrane, and the extrusion of calcium into the blood, respectively. On the other hand, when calcium intake is sufficient, it will be transported through a paracellular flux, which is also mediated by $1,25(OH)_2D$ binding to VDR, thereby increasing transcriptions of tight junction proteins including claudin 2 and 12, cadherin 17 as well as aquaporin 8 in the jejunum and ileum (Goltzman, 2018).

CYP27B1 and VDR are expressed in multiple bone cell types, including osteoblasts, osteoclasts, osteocytes, and chondrocytes, thus enabling $1,25(OH)_2D$ to regulate bone homeostasis via its nuclear receptor. Osteoblasts and osteocytes are considered to be the major mediators of actions of $1,25(OH)_2D$ in bone metabolism as higher expression

levels of VDR were discovered in these cells. A number of genes that encode factors for bone homeostasis and mineralization such as Runx2 (Drissi et al., 2002), osteopontin (OPN) (Noda et al., 1990; Shen et al., 2005), osteocalcin (OCN) (Markose et al., 1990; Ozono et al., 1990), bone sialoprotein (BSP) (Bellows et al., 1999), and RANKL (Kim et al., 2007), are regulated by $1,25(OH)_2D$/VDR system in osteoblasts and osteocytes. However, responses of these factors to $1,25(OH)_2D$ differ at different differentiation stages of osteoblast lineage (Owen et al., 1991). For example, $1,25(OH)_2D$ acts via VDR and initiates production of OPN and OCN in osteoblasts at later stages, but not at early stages, of differentiation (Bikle, 2018). Normal levels of $1,25(OH)_2D$ binding to VDR suppress the ratio of RANKL/OPG in mature osteoblasts, whereas VDR activated by excess levels of $1,25(OH)_2D$ upregulates RANKL/OPG in immature osteoblasts (Goltzman, 2018). Therefore, it seems that $1,25(OH)_2D$/VDR system exerts either anabolic or anticatabolic activities in mature osteoblasts.

1.2.5 Functions of vitamin D in bone

The beneficial effects of vitamin D on bone were first recognized in patients with rickets and osteomalacia. Vitamin D plays a critical role in maintaining mineral homeostasis by promoting intestinal calcium and phosphate absorption and reabsorption in kidney to provide adequate minerals for bone mineralization. Generations of knockout mice with deletion of VDR or CYP27B1 provided an important tool to determine the *in-vivo* functions of $1,25(OH)_2D$. Ablation of these genes seriously impaired development of mice, resulting in growth retardation and the development of severe rickets after weaning (Bouillon et al., 2008). Moreover, mice with CYP27B1 knockout and double knockout of CYP27B1 and VDR have increased bone fragility and reduced osteoblast number or activity, as revealed by decreased rates of mineral apposition in both cortical and trabecular bone as well as reduced expression of ALP (Panda et al., 2004). In line with these observations, the number of mineralized nodules and colony forming units were reduced when bone marrow stromal cells (BMSCs) from the knockout mice were cultured *in vitro*. On the other hand, osteoclast

numbers in trabecular bone were also decreased due to the reduction in expressions of RANKL proteins (Panda et al., 2004). However, overexpression of VDR in mature osteoblastic lineages of mice was found to increase cortical and trabecular bone volume, possibly by increasing cortical bone formation and reducing trabecular bone resorption (Gardiner et al., 2000).

All skeletal cell types, including MSCs, osteoblasts, osteoclasts, osteocytes and chondrocytes, are able to express CYP27B1 and response to 25OHD for endogenous production of $1,25(OH)_2D$, thereby promoting differentiation of these cells. Studies by others showed that silencing of CYP27B1 with siRNA significantly abolished the effects of 25OHD to stimulate differentiation of MSCs and osteoblasts, indicating the paracrine or autocrine activity of $1,25(OH)_2D$ in regulating bone formation (Atkins et al., 2007; Geng et al., 2011b). Other studies demonstrated that overexpression of CYP27B1 in mature osteoblasts resulted in increased bone volume with elevated bone formation but no obvious changes in bone resorption. These anabolic effects have no bearing on circulating $1,25(OH)_2D$ level, emphasizing the critical role of locally produced $1,25(OH)_2D$ in bone (Yang et al., 2012). To this extent, serum levels of 25OHD are supposed to be a predominant positive determinant of bone mineral volume in rodents.

1.3. Fat and bone health

The systemic impact of fat on bone has drawn much attention due to the prevalence of obesity in recent years. Recent studies identified that obesity is one of risk factors on bone that increase risk of osteoporosis and the incident of fractures. Accumulating evidence showed an inverse correlation between bone mineral density (BMD) and body mass index (BMI) (Cohen et al., 2013; Gilsanz et al., 2009). In fact, the systemic effect of fat on bone is complex, with the reported association with factors secreted by peripheral fat such as adipokines. On the other hand, it seems that the local interactions between adiposity and bone in the bone marrow niche also play an important role in the pathogenesis of osteoporosis and age-related bone loss.

1.3.1 Body fat and bone health

Obesity was initially identified to be associated with high BMD and exerting protective effects on bone as the increase in body weight may provide sufficient mechanical loading for promoting bone formation (Albala et al., 1996; Reid et al., 1992). However, these findings were challenged by others in the subsequent years (Janicka et al., 2007; Zhao et al., 2007). In these studies, bone mass and body composition were measured by using dual-energy x-ray absorptiometry (DXA). The results showed a positive association of lean mass and BMD, while an inverse relationship between fat mass (especially trunk fat) and BMD.

Study by Gilsanz et al. (2009) further differentiated visceral adipose tissue (VAT) and subcutaneous adipose tissue (SAT) by using quantitative computed tomography (CT), showed an opposite correlation of VAT and SAT with femoral bone structures and bone strength in young women (15-25 years old). Although SAT is beneficial to acquisition of peak bone mass, VAT acts as a detrimental adipose depot. This observation accounted for the fact that there is a greater accumulation of VAT than SAT, accompanied with a decline in circulating estrogen and decreased bone mass in postmenopausal women (Samaras et al., 2010). Moreover, insulin-like growth factor 1

(IGF-1), which triggers osteoblastic anabolism, was reported to correlate inversely with VAT and bone marrow fat (Bredella et al., 2011). In addition, serum levels of both bone formation markers like N-terminal propeptides of procollagen type 1 (P1NP) and osteocalcin, as well as bone resorption markers including C-telopeptide (CTx) and tartrate-resistant acid phosphatase isoform 5b (TRAP5b), were lower in subjects with higher trunk fat and VAT (Cohen et al., 2013). These findings suggested a universal decrease of bone remodeling rather than an imbalanced bone formation and bone resorption in obesity.

For the perspective of animal studies, the deleterious impact of high-fat diet (HFD) on bone mineral content (BMC) and BMD were widely reported in mice and rats (Beier et al., 2015; Macri et al., 2012; Scheller et al., 2016). Compared with animals fed with low-fat diet (LFD), the HFD groups have higher levels of TRAP5b but lower levels of P1NP, indicating the disrupted fine balance between bone formation and bone resorption in response to HFD. In addition, the negative correlation of VAT and BMD was also underlined in animals fed with HFD (Lac et al., 2008).

1.3.2 Adipose tissue in bone microenvironment

In recent years, a pathophysiological mechanism describing how the increased accumulation of adipose tissue in bone marrow affects bone has drawn much attention from researchers. Similarly, numerous studies showed an increase in vertebral marrow adipose tissue (MAT) in osteoporosis, which is positively correlated with vertebral fractures in men and women (Schwartz et al., 2013; Verma et al., 2002). Given these findings, the enhanced accumulation of MAT was recognized as a critical dominator of age-related bone loss in adults (Duque et al., 2009). These deleterious effects of MAT on bone metabolism may attribute to the interactions of adipocytes with osteoblasts and osteoclasts within the bone marrow niche.

Bone marrow was identified as the only region where fat lies adjacent to bone. It also provides a complex microenvironment where different cell types share growth factors

and cytokines and interact with each other in a common space. As mentioned previously, mesenchymal stem cells (MSCs) in bone marrow serve as the common progenitor of osteoblasts and adipocytes. It is believed that differentiation of MSCs into these two different lineages in a mutually exclusive manner. In other words, accumulation of adipocytes happens at the expense of osteoblasts, which results in gradual decline in bone mass (Muruganandan et al., 2009). These alternative pathways are triggered by the transcription factors runt-related transcription factor 2 (Runx2) for osteogenesis while peroxisome proliferator-activated receptor γ (PPARγ) for adipogenesis, with the cooperation of pro-osteogenic Wnt/β-catenin pathway (Nuttall et al., 2014). Moreover, it has been shown that there is an increase in expression of receptor activator of nuclear factor κ-B ligand (RANKL) in MAT along with aging (Takeshita et al., 2014). Studies reported that bone marrow adipocytes promote osteoclastic bone resorption by expression of RANKL and secretion of inflammatory cytokines (Goto et al., 2011).

In addition, the detrimental effects of adipocytes on osteoblasts were revealed by *in vitro* experiments in which the two cell types were exposed in a co-cultured system. The proliferation and mineralization of osteoblasts were significantly suppressed after exposed to adipocytes. This toxic effect mainly attribute to the fatty acids and cytokines secreted by adipocytes (Maurin et al., 2000). This lipotoxicity could be attenuated by inhibiting fatty acid synthase in adipocytes (Elbaz et al., 2010). On the other hand, bone marrow fat is also essential to supply energy for proper bone functions or to optimize thermogenesis (Lecka-Czernik, 2012).

1.3.3 Hormonal regulation of fat and bone
1.3.3.1 Leptin

In addition to locally derived fatty acids and growth factors, systemic adipokines also play an important role in regulating interactions of bone marrow adipocytes and bone cells. Leptin is a cytokine-like hormone generated by adipose tissues, including those in bone marrow, and is critical in regulating energy metabolism (Chilliard et al., 2005;

Lee et al., 2008). To some extent, increased accumulation of body fat improves leptin levels which directly induce periosteal bone formation via its anabolic effects on osteoblasts (Hamrick et al., 2008). Studies showed peripheral administration of leptin at physiological concentrations reduced bone loss in ovariectomy (OVX) rats and transgenic leptin deficient (*ob/ob*) mice, either by regulating the activities of osteoblasts and osteoclasts or by inducing apoptosis of adipocytes (Burguera et al., 2001; Hamrick et al., 2005). Moreover, leptin managed to indirectly influence the bone metabolism via the central nervous system (CNS), to stimulate the growth hormone/insulin-like growth factor-1 (GH/IGF-1) axis which is critical in promoting growth and mineral acquisition in bone (Hamrick et al., 2008).

1.3.3.2 Estrogen

The significant reduction of circulating estrogen levels is one of the factors accounting for the age-related accumulation of MAT in postmenopausal women. It has been demonstrated that estrogen deficiency in both postmenopausal women and OVX rats was associated with a significant increase in MAT in accompany with a decrease in bone mass, while estradiol (E_2) replacement could reverse these effects by decreasing the number and size of adipocytes (Benayahu et al., 2000; Syed et al., 2008). In line with these findings, Okazaki et al. (2002) reported that estrogen dose-dependently induced osteoblast differentiation and suppressed adipogenesis of mouse bone marrow stromal cell line in a estrogen receptor (ER)-specific manner.

The ability of estrogen to regulate the activities of lipoprotein lipases, lipogenic and lipolytic enzymes in peripheral adipocytes are well established, illustrating the actions of estrogen on adipose tissues through promoting intracellular lipolysis of the lipid droplets and reducing neutral lipid uptake into the adipocyte (Palin et al., 2003). However, there is still a lack of studies demonstrating the mechanisms by which estrogen regulate MAT. It seems that ERα is one of the candidates mediating these

activities as ERα knockout mice demonstrated elevated fat mass accompanied by an increase in production of bone marrow derived adipocytes (Heine et al., 2000).

1.3.3.3 Vitamin D

The association between vitamin D and fat has been widely described in recent years. Studies on vitamin D status have showed that individuals of all ages with higher BMI and fat mass tend to have lower circulating levels of $25OHD_3$, indicating an inverse relationship of vitamin D levels and obesity (Kremer et al., 2009; Parikh et al., 2004). In fact, adipose tissues largely serve as a reservoir for vitamin D. The increased adipose tissues in obesity will require more amount of vitamin D to make the depot saturate, which account for the decreased levels of vitamin D in circulation (Carrelli et al., 2017).

In addition to its role in storage, adipocytes also act as a metabolic organ. The evident expressions of genes encoding CYP27B1 and VDR were identified in adipose tissues of human and rodents, suggesting the adipocytes can generate bioactive $1,25(OH)_2D$ and exerting physiological actions via its receptor in an autocrine or paracrine manner. Experimental studies showed that $1,25(OH)_2D$ plays an important role in regulating adipogenesis and inflammation of adipose tissues. $1,25(OH)_2D_3$ inhibits the adipogenic differentiation of mouse embryonic fibroblast cell line 3T3-L1 in a dose-dependent manner through suppression of adipogenic transcriptional factors such as C/EBP β and PPAR γ (Ji et al., 2015).

The activities of vitamin D on bone marrow adipose tissues were also evaluated in animal studies. Duque et al. (2004) employed senescence-accelerated mice (SAM-P/6), which showed a decreased bone mineral density accompanied with increased accumulation of bone marrow fat, as a senile osteoporosis model. Continuous administration of $1,25(OH)_2D_3$ (18 pmol/day, s.c.) inhibited the adipogenesis in the bone marrow of SAM-P/6 mice. Moreover, mesenchymal stem cells (MSCs) in $1,25(OH)_2D_3$ treated group had decreased expression of PPARγ while accelerated osteoblastogenesis compared to vehicle-treated animals.

1.4. Oleanolic acid (OA)

It has always been of interest to explore bioactive compounds presented in plants as alternative therapeutic strategies for prevention or treatment of chronic diseases such as osteoporosis. Oleanolic acid (OA, 3β-hydroxyolean-12-en-28-oic acid, Fig. 1.5 A) is a natural pentacyclic triterpenoid compound that exists in a lot of plant species involving foods and herbal sources. OA is especially abunda nt in the Oleaceae family plants such as olives, hence the name (Guinda et al., 2004). OA often present with its isomer, ursolic acid (UA, 3β-hydroxyurs-12-en-28-oic acid, Fig. 1.5 B), in various natural plants (Liu, 1995). OA and UA are often employed as criterion in the quality control for many Chinese herbal medicines 3-5. The sole difference in chemical structue between these two compounds is the position of a methyl group. With such similar structures, OA and UA share many common pharmacological properties, including hepatoprotective activities (Liu et al., 1994), antioxidative properties (Alvarado et al., 2018), anti-inflammation activities (Kashyap et al., 2016), anti-diabetic effects (Kalaycıoğlu et al., 2018), anti-tumor activities (Han et al., 2014; Sheng et al., 2019) as well as modulation of calcium balance (Cao et al., 2018). Hence, the potency of combination of OA and UA in are also widely studied (Ali et al., 2006; Cao, Tian, et al., 2018; Ding et al., 2018; Hamza et al., 2016).
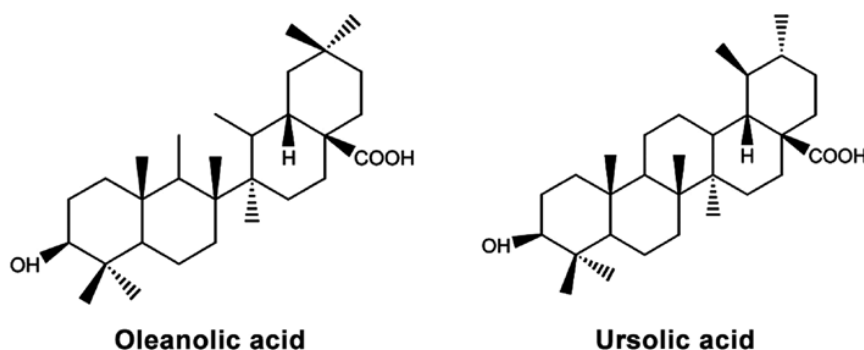
Fig. 1.5 Chemical structures of oleanolic acid (OA) and ursolic acid (UA)

1.4.1 Sources and bioavailability of OA

Pentacyclic triterpenoid compounds like OA are widely spread in the leaves and stem bark of various fruits such as apple, grape, olive, loquat, and elderberry (Jäger et al., 2009). OA is often discovered to be abundant in the plants epicuticular waxes as a free acid, where it acts as a first physical barrier against pathogens and prevents the loss of water (Heinzen et al., 1996). Therefore, the content of OA is much higher in the skin or peel rather than pulp of fruits. Generally, consumptions of fruits including dried fruits with peel and skin can be a good dietary source of OA. Olives and their products like olive oil are also most important sources of OA in human diets. OA also widely presented in a form of aglycone precursor for triterpenoid saponins, by linking to one or more sugar moieties (Szakiel et al., 2003). Roots and fruits of medicinal plants such as ginseng (*Panex sp.*) and wild sage (*Lantana camara L.*), which are commonly used in traditional Chinese medicine (TCM), are also high in OA. OA is also detected with a plentiful quantity in other herbal medicine like *Fructus ligustri lucidi, Chaenomeles sinensis, Vitisvinifera, Mile swertia,* and *Crataegus sp.* (Jiang et al., 2016)*.*

Despite its common presence in human diets, the absorption of OA from the gastrointestinal tract is very low, resulting in poor bioavailability following oral administration (Jeong et al., 2007). It is reported in a human pharmacokinetics study that oral administration of OA (40 mg) resulted in a peak plasma concentration (C_{max}) of 12.1 ng/mL within 5.2 hours, and the half-life ($t_{1/2}$) of 8.7 hours (Song et al., 2006). The intensive metabolism by cytochrome P450 (CYPs) isoenzymes in combination with poor aqueous solubility also contribute to the low bioavailability of OA. Study showed that co-administration of ketoconazole, an uncompetitive CYP3A4 inhibitor, obviously improved the bioavailability of OA in Sprague-Dawley (SD) rats, by suppressing the metabolism of OA (Jiang et al., 2016). To enhance its water solubility and the bioavailability, major advances have been made in design, synthesis and investigate of derivatives and formulations of OA in recent years (Song et al., 2015; Yu et al., 2016; Zhao et al., 2013).

1.4.2 Pharmacological activities of OA

1.4.2.1 Hepatoprotective effects

One of the major pharmacological properties of OA is its hepatoprotective effects, which allows application of OA as an over-the counter medication registered in China for treatment of liver diseases (Liu, 2005). The hepatoprotective effects of OA for prevention and treatment of acute liver injury induced by different hepatotoxic agents, such as alcohol, carbon tetrachloride (CCl_4), metals, and drugs (Liu, 1995). OA was also reported to inhibit bile acid synthesis by CYP7A1, preventing the chronic liver cirrhosis and fibrosis caused by excess accumulation of bile acids in liver (W. Liu et al., 2010).

The effects of OA against CCl_4 induced hepatic injury are indicated by the elevated serum levels of hepatic malondialdehyde (MDA), alanine aminotransferase (ALT), aspartate aminotransferase (AST), and lactic dehydrogenase (LDH), while increasing glutathione peroxidase (GPX) and superoxide dismutase (SOD) (Yu et al., 2016). The underlying mechanisms involve the antioxidative and anti-inflammatory properties. It has been identified by several groups that the nuclear factor erythroid 2-related factor 2 (Nrf2), a major transcriptional regulator for detoxification and the expression of antioxidant enzymes, plays an important role in mediating the hepatoprotective activities of OA (Liu et al., 2008; Reisman et al., 2009; Wang et al., 2010).

Non-alcoholic fatty liver disease (NAFLD) is another prevalent liver disorder associated with disrupted metabolism in patients. It was discovered that oral administration of OA at 25 mg/kg daily for 10 weeks significantly diminished the high fructose-induced fatty liver in rats by suppressing hepatic expressions of sterol regulatory element-binding protein 1c (SREBP-1c), the transcription factor responsible for lipogenesis (Liu et al., 2013). Another study reported that inhibition of liver X receptor alpha (LXR) and pregnane X receptor are (PXR) also involved in inhibitory activities of OA against hepatic lipogenesis (Lin et al., 2018).

1.4.2.2 Anti-diabetic and anti-obesity effects

The beneficial effects of OA on metabolic syndromes mainly involves its anti-diabetic and anti-obesity activities. Studies in rats with diabetes induced by streptozotocin showed that OA markedly suppressed serum glucose levels, improved dysfunctional insulin signaling, and restored glycogen levels and glycogenic enzymes activities in liver and muscle (Musabayane et al., 2010; Ngubane et al., 2011). *In vitro* study showed OA at 25 μmol/L enhanced insulin sensitivity in the insulin resistant HepG2 cells after treatment for 24 hours, by upregulating expressions of glucose transporter 4 (GLUT4) and insulin receptor substrate 1(IRS-1) (M. Li et al., 2015). Other studies showed that treatment of OA (25 mg/kg/day) for 10 weeks also restored the fructose-induced insulin resistance in adipose tissue of rats via IRS-1/PI3K/Akt signaling pathway (Li et al., 2014). Moreover, the combination therapy of metformin and OA exerted a synergetic effect on controlling insulin levels and blood glucose in *db/db* mice (Wang et al., 2015).

OA decreased content of visceral adipose tissue in mice fed with high fat diet (HFD) by modulating fat and carbohydrate metabolism, indicating the anti-obesity activities of OA (de Melo et al., 2010). The actions of OA to regulate lipid metabolism were also revealed by many studies, which showed that OA firmly suppressed serum levels of total cholesterol (TC), triglycerides (TGs), β-lipoprotein, and free fatty acids (FFAs) in hyperlipidemic rabbits and rats fed with HFD (Liu et al., 2007; Yunoki et al., 2008). The underlying mechanisms mediating the effects of OA on lipid metabolism involve suppressing the activity of intestinal acyl-coenzyme A: cholesterol acyltransferase (ACATs) (J. Liu et al., 2010), decreasing the production of visfatin (H.-S. Kim et al., 2014), inhibiting the expression of SREBP-1c and peroxisome proliferator-activated receptor-γ coactivator-1β (PGC-1β) (Li et al., 2014), which play an important role in the lipid homeostasis.

1.4.2.3 Anti-cancer effects

The anti-cancer effects of OA against tumor growth have been reported in a number of *in vitro* and *in vivo* models involving different cancers, including liver cancer (Yan et al., 2010), breast cancer (Chakravarti et al., 2012), lung cancer (Zhao et al., 2015), bladder cancer (Mu et al., 2015), colon cancer (Juan et al., 2008), prostate cancer (Li et al., 2016), gastric cancer (Nie et al., 2016), pancreatic cancer (Wei et al., 2013), as well as the hematological malignancies (Hsu et al., 1997). OA showed its inhibition of carcinogenesis in chemical-induced mouse skin cancer (Tokuda et al., 1986) and in rat colon cancer (Furtado et al., 2008). Numerous studies showed the tumor promotion are also well suppressed by OA via regulating cell cycle arrest at G0/G1 phase (H.-F. Li et al., 2015; R. Zhou et al., 2011). Other studies showed OA suppressed proliferation of tumor cells via antagonizing transforming growth factor-β (TGF-β) as well as nuclear factor-κB (NF-κB), attributing to its anti-inflammation effects (Laszczyk, 2009; Yoshimura et al., 2003).

OA and its derivatives were identified as inhibitors of phosphatidylinositide 3-kinase (PI3K)/ protein kinase B (Akt)/ mammalian target of rapamycin (mTOR)/ ribosomal S6 kinase (S6K) pathway, leading to the activation of downstream signaling and initiation of autophagy (Mu et al., 2015). Induction of apoptosis in cancer cells is a major mechanism involving anti-cancer actions of OA. Studies showed that OA induced mitochondrial apoptosis in pancreas and lung cancer cells through activation of reactive oxygen species (ROS) /apoptosis signal-regulating kinase 1 (ASK1)/p38 mitogen-activated protein kinase (MAPK) signaling (Liu, Wu, et al., 2014). On the other hand, OA induced changes of energy metabolism in cancer cells via activation of adenosine monophosphate-activated protein kinase (AMPK), leading to decreased lipogenesis and protein synthesis (Liu, Zheng, et al., 2014).

1.4.2.4 Anti-osteoporotic effects

Accumulating evidence showed actions of OA to improve bone mineral density (BMD) and bone microarchitecture in osteoporotic animals (Table 1.2). Research by Bian et al. (2012) showed that oral administration of OA (20 mg/kg/day) for 3 months improved bone mass and bone properties in ovariectomized (OVX) mice and the possible mechanism involves the increase in osteoblast numbers and osteogenesis of bone marrow stromal cells (BMSCs). Shu et al. (2017) and colleagues showed OA dose-dependently improved differentiation of hMSCs towards osteoprogenitors, and these actions were mediated by Notch signaling. Nevertheless, Zhao et al. (2018) showed that intraperitoneally injection (i.p.) of OA (10 mg/kg) for 3 months significantly prevented bone loss in OVX mice by inhibiting RANKL-mediated osteoclastic differentiation of bone marrow macrophages (BMMs). Similar actions were reported in osteoprotegerin (OPG) knockout mice which showed OA suppressed the bone loss by attenuating the osteoclast densities (Zhao et al., 2020).

OA (50 mg/kg/day) also significantly restored estrogen deficiency-induced bone loss in OVX mice as revealed by increased BMD and improved bone microarchitecture in proximal tibia, distal femur, as well as lumbar vertebra (L4) after administration for 6 weeks. These properties may associate with the actions of OA to modulate renal CYP27B1 to generate $1,25(OH)_2D_3$ in circulation. As the bioactive form of vitamin D_3, $1,25(OH)_2D_3$ further facilitates duodenal calcium absorption to promote positive calcium balance and bone mineralization (Cao et al., 2018). In the glucocorticoid-induced rat osteoporosis, OA markedly improved BMD and bone minerals in lumbar and femur as well as serum osteocalcin levels (Xu et al., 2018). The potential biomarkers and metabolic pathway involved were identified by metabolomics strategy, which showed the molecular transport, carbohydrate metabolism and lipid metabolism were ameliorated by OA in osteoporotic animals.

Table 1.2 Anti-osteoporotic effects of OA in animal models of osteoporosis

Animal model	Treatment	Mechanism	Reference
OVX mice	OA (20 mg/kg, p.o.) for 3 months	↑ Osteoblast numbers and osteogenesis of bone marrow stromal cells (BMSCs)	(Bian et al., 2012)
OVX mice	OA (10 mg/kg*2 d，i.p.) for 3 months	↓ Osteoclastic differentiation of bone marrow macrophages (BMMs)	(Zhao et al., 2018)
OPG knockout mice	OA (10 mg/kg*2 d，i.p.) for 3 months	↓ The late stage of osteoclastogenesis from RANKL-pretreated BMMs	(Zhao et al., 2020)
Glucocorticoid-treated rats	OA (9 mg/kg, p.o.) for 14 days	Modulating molecular transport, carbohydrate metabolism and lipid metabolism	(Xu et al., 2018)
OVX mice	OA (50 mg/kg, p.o.) for 6 weeks	↑ Renal CYP27B1, serum $1,25(OH)_2D_3$; ↑ Duodenal calcium absorption	(Cao et al., 2018)

1.4.3 Takeda G-protein coupled receptor 5 (TGR5) as a target for OA

The TGR5 (also known as G protein-coupled bile acid receptor 1) is a member of G protein-coupled receptor (GPCR) superfamily and is encoded by the *GPBAR1* gene. It is the first identified cell-surface receptor in humans and animals, to initiate different intracellular signaling upon activated by bile acids (Maruyama et al., 2002). Despite the ubiquitous distribution of TGR5 in various tissues, the regulation of TGR5 in response to certain pathological and physiological conditions remains unclear. It has been identified that TGR5 responded to bile acids by inducing cyclic adenosine monophosphate (cAMP) production (Watanabe et al., 2006). In the Chinese hamster ovary cells (CHO) overexpressed human TGR5 cDNA, bile acids dose-dependently activated TGR5 and induced production of cAMP, in the rank order of potency (EC_{50}) : lithocholic acid (LCA, 0.53 μM) > deoxycholic acid (DCA, 1.01 μM) > chenodeoxycholic acid (CDCA, 4.43 μM) > cholic acid (CA, 7.72 μM) (Kawamata et al., 2003). With the structure resembling that of LCA, OA was also identified as a natural ligand for TGR5 (Sato et al., 2007).

As a pleotropic regulator in bile acids homeostasis, energy metabolism, glucose metabolism, as well as the inflammatory response, TGR5 is recently recognized as a potential target to moderate different human diseases. Activation of TGR5 promoted the secretion of glucagon-like peptide-1 (GLP-1), which plays a critical role in type 2 diabetes (Thomas et al., 2009). OA was also identified to regulate glucose homeostasis in mice fed with high fat diet through activation of TGR5 (Sato et al., 2007). In the brown adipose tissues and muscles, activation of TGR5 promoted energy expenditure by increasing intracellular iodothyronine deiodinase, indicating the role of TGR5 in preventing obesity (Watanabe et al., 2006). Moreover, recent studies also identified TGR5 as a cancer suppressor in colon cancer (Kong et al., 2012), gastric cancer (Guo et al., 2015), as well as liver carcinoma (He et al., 2010), via antagonizing the signal transducer and activator of transcription 3 (STAT3) signaling.

The role of TGR5 in bone metabolism and bone remodeling also draw the attention of researchers. Wang et al. (2018) showed there was an increase in expression of TGR5 with osteogenic differentiation of the pre-osteoblastic MC3T3-E1 cells. Notably, the activation of TGR5 by its specific agonist significantly upregulated expressions of genes encoding osteogenic markers including alkaline phosphatase (ALP), osteocalcin (OCN), and osterix (Osx). They also showed that this process was mediated by AMP-activated protein kinase (AMPK)/ nitric-oxide synthase (eNOS) pathway. Nevertheless, these effects were attenuated by silence of TGR5 using TGR5 siRNA. Subsequently, Li et al. (2019) reported a remarkable bone loss in aged (over 7 months) and ovariectomized (OVX) TGR5 knockout mice, directly proving the role of TGR5 in mediating bone metabolism under pathological conditions. Further studies showed that osteoclastic differentiation of mouse BMMs was suppressed by TGR5 agonists such as LCA, CA, DCA, and OA (Li et al., 2019). Moreover, the activation of cAMP/AMPK signaling was associated with the regulation of osteoclastogenesis by TGR5. However, the detailed actions of TGR5 in bone deserve further investigations, especially those mechanisms involved in pathophysiological processes.

Chapter 2

Hypothesis and objectives

2.1. Hypothesis

With the discovery of 25-hydroxyvitamin D 1-alpha hydroxylase (CYP27B1) in the extrarenal sites, the paracrine or autocrine activities of vitamin D in the local microenvironments become the major focus of research interest. Bone cells, as the major players in the metabolic active bone tissue, are expressing CYP27B1 and vitamin D receptor (VDR). Such expressions indicate the potential role of $1,25(OH)_2D$, the bioactive form of vitamin D, in modulating bone metabolism in a paracrine or autocrine manner in addition to its endocrine activities to calcium homeostasis and bone mineralization. The expression and activity of CYP27B1 is known to be decreased by aging and accompanied with an accumulation of bone marrow adipocytes, leading to the impaired bone properties and increased risk of fractures in elderly, especially postmenopausal women. However, the mechanisms involved in the regulation of CYP27B1 in osteoblasts and adipocytes remains unclear.

Oleanolic acid (OA) is a naturally occurring pentacyclic triterpenoid with pleotropic effects. Its beneficial effects to prevent bone loss induced by estrogen deficiency and glucocorticoid have been reported in a number of studies (Bian et al., 2012; Zhao et al., 2018). Moreover, our previous studies demonstrated the ability of OA to modulate circulating $1,25(OH)_2D_3$ and calcium balance as well as reduce bone loss in aged rats. Most importantly, the beneficial effects of OA on bone and Ca metabolism are shown to be associated with its potential to regulate renal CYP27B1 expression and activity (Cao et al., 2018). However, the ability of OA to regulate CYP27B1 in osteoblasts and bone marrow adipocytes and the role of paracrine or autocrine actions of $1,25(OH)_2D_3$ in skeletal microenvironment in modulating bone health are far from clear.

Thus, the hypothesis of my project is that OA exerts bone protective effects by modulating extra-renal expression and activities of CYP27B1 in osteoblasts and bone marrow adipocytes.

2.2. Objectives

The present study aimed to characterize the actions of OA to modulate extrarenal CYP27B1 in osteoblasts and adipocytes, and the contribution of their interactions in bone microenvironment to the bone protective effects of OA. To validate the hypothesis, the major objectives of the present study are:

1. To determine the effects of OA on renal and extra-renal CYP27B1 in osteoblasts

2. To investigate the involvement of CYP27B1 in mediating the osteogenic effects of OA

3. To study the potential mechanisms involved in mediating regulation of CYP27B1 in osteoblasts

4. To characterize the effects of OA on bone marrow adipose tissues and adipogenesis of bone marrow stromal cells (BMSCs)

Chapter 3

Investigation of the effects of oleanolic acid on expression and activity of renal and skeletal 25-hydroxyvitamin D 1-alpha-hydroxylase (CYP27B1)

3.1 Introduction

It is well recognized that adequate calcium is essential for optimal bone strength and bone mass. Vitamin D plays a critical role in maintaining calcium homeostasis by regulating intestinal and renal calcium absorption, which further facilitates bone mineralization. Unfortunately, studies showed that inadequate serum levels of 25OHD was associated with higher incidence of fracture in elderly (Van Schoor et al., 2008). With the high prevalence of vitamin D deficiency around the world, the risk to develop osteoporosis and fractures in men and women are increased. Calcium and vitamin D supplements appear not to be the optimal choice to prevent bone loss and the development of osteoporosis, as higher risk of cardiovascular disease and kidney stones were observed in postmenopausal women supplemented with calcium and vitamin D (Haghighi et al., 2013). Moreover, a meta-analysis by Zhao et al. (2017) showed little association between use of vitamin D and calcium supplement with decreased incidence of fractures in older adults. These contradictory findings with the routine supplements might attribute to the poor intestinal absorption of vitamin D and calcium in aged people. More importantly, the decreased function of CYP27B1, the hydroxylase catalyzing anabolic metabolism of vitamin D primarily occurring in kidney, is responsible for the inadequate $1,25(OH)_2D$ in circulation and reduced calcium absorption.

Apart from the abundantly expressed CYP27B1 in kidney for generation of circulating $1,25(OH)_2D$ for the endocrine activities, other sites are also identified to express gene encoding CYP27B1 (Adams et al., 2012). The expressions of CYP27B1, CYP24A1 and vitamin D receptor (VDR) in bone cells suggested their ability of $1,25(OH)_2D_3$ anabolism and catabolism and exerting the biological activities via the VDR in themselves and adjacent cells in bone microenvironment. Amongst bone cells, osteoblasts are one of the most active lineages which is responsible for the bone formation. Mechanistic study showed age-related dysfunction of osteoblasts is the main cause of declined bone mass in older populations (Kassem et al., 2011). However, despite activities of CYP27B1 could be an important mediator to improve the functions

and mineralization of osteoblasts, the underlying mechanisms involved in regulating expression and activity of osteoblastic CYP27B1 is far from clear.

The bone-protective effects of oleanolic acid (OA) have been reported by numerous studies showing administration of OA improved bone mass and bone microarchitecture in osteoporotic animals induced by estrogen deficiency and glucocorticoid (Bian et al., 2012; Xu et al., 2018; Zhao et al., 2018) . In addition, previous work by our group demonstrated *Fructus Ligustri Lucidi* (FLL), an OA-rich Chinese herb, enhanced bone mineral density (BMD) and calcium balance in aged female rats (Cao et al., 2018). As a bioactive ingredient of FLL, OA exerted similar effects in aged animals (Cao et al., 2018). More importantly, administration of OA increased circulating $1,25(OH)_2D$ and renal expressions of CYP27B1 accompanied with improved bone properties in ovariectomized (OVX) mice. These studies suggested OA could be a promising molecule for modulating renal CYP27B1 activity and bone metabolism. However, studies to delineate the regulation of CYP27B1 by OA in other extra-renal sites are limiting. It is of interest to explore the effects of OA on osteoblastic CYP27B1 activity and their actions in bone metabolism.

This chapter aimed to evaluate and compare the effects of OA on renal and extrarenal CYP27B1 in bone. First, we employed a stabilized OVX mice model to evaluate the effects of OA on renal and extrarenal CYP27B1 expressions in kidney and iliac crest, under the pathological conditions. This is followed by a series of *in vitro* experiment to determine the effects of OA on expressions and activity of CYP27B1 in human kidney proximal tubular HKC-8 cells, human osteosarcoma MG-63 cells, and rat osteosarcoma UMR-106 cells.

3.2 Methodology

3.2.1 *In vivo* experiment

3.2.1.1 Experimental design

The protocol of the animal study conducted was approved by the Animal Ethics Committee of The Hong Kong Polytechnic University (ASESC No.: 19-20/4-ABCT-R-STUDENT). To systemically investigate the actions of OA on regulating renal and skeletal CYP27B1, thirty-five 4-month-old female C57BL/6J mice weighing 20 ± 1 g were purchased and housed in centralized animal facilities (CAF) of the Hong Kong Polytechnic University in an environment with 12 h light and dark cycle and constancy of temperature (22 ℃). Mice were sham operated or ovariectomized (OVX). After the surgery, mice were maintained with phytoestrogen-free AIN-93M rodent diet (Research diet, USA). After stabilization of the model for 6 weeks, mice were randomly assigned into five groups (n=7/group) and pair fed with 3 g phytoestrogen-free AIN-93M rodent diet (Research diets, USA) (Table 6.1), the estimated daily intake of mice. For each treatment group, the sham-operated and OVX mice were treated with vehicle (Sham and OVX), other OVX mice were orally administrated with 17β-estradiol (E_2, 200 μg/kg/day), high calcium diet (HCD, 1% calcium in AIN-93M based rodent diet), OA (200 ppm in AIN-93M based rodent diet) and OA (400 ppm in AIN-93M based rodent diet) for 8 weeks. OA was administrated by incorporation of OA into AIN-93M based rodent diet. The concentrations of OA in the diet were designed based on the dosage used in our previous study (Cao et al., 2018) and daily dietary intake of mice. E_2 and HCD were employed as positive controls to evaluate the actions of OA on bone metabolism and vitamin D metabolism in OVX mice. Body weight of animals were monitored every week throughout the study. 3 mice in 400 ppm OA group died after administration for 5 weeks. Body weight and dietary intake of the remained mice in this group dropped sharply. Considering accuracy and security of the treatment, the 400 ppm group was excluded in the following studies.

Table 3.1 Composition of modified AIN-93M rodent diet (Research diets, USA)

Diet (Product #)	Phytoestrogen-free AIN-93M rodent diet	High calcium diet (HCD)	OA diet
	D00031602	D19072407	D19072409
Protein (gm%)	14	14	14
Carbohydrate (gm%)	73	72	73
Fat (gm%)	4	4	4
Total (kcal/gm)	3.85	3.80	3.85
Ingredient (gm)			
Casein	140	140	140
L-Cystine	1.8	1.8	1.8
Corn Starch	495.692	495.692	495.692
Maltodextrin 10	125	125	125
Sucrose	100	100	100
Cellulose, BW200	50	50	50
Corn Oil	40	40	40
t-Butylhydroquinone	0.008	0.008	0.008
Mineral Mix S10022M	35	35	35
Calcium Carbonate	0	13	0
Vitamin Mix V10037	10	10	10
Choline Bitartrate	2.5	2.5	2.5
Ca (g)	5.0	10	5.0
Ca (%)	0.5	1	0.5
Oleanolic Acid (mg)	0	0	200
Total (g)	1000	1013	1000.2

3.2.1.2 Sample collection

Before sacrifice, 24-hour urine were collected individually by using metabolic cages. Upon administration of anesthesia, mice were sacrificed by collection of blood via cardiac stick exsanguinations. After clotting at 4 ℃, the blood was centrifuged at 4000 rpm/min for 20 min at 4 ℃. Serum was isolated and stored at - 80 ℃ for further biochemical measurement. Uterus was freshly isolated and wet weight were recorded for assessing the uterine index. Kidney and iliac crest were collected for determination of CYP27B1 expressions. The intact lumbar vertebra and left legs were collected and wrapped with PBS-soaked gauze and stored at - 20 °C for micro-computed tomography (μCT) analysis.

3.2.1.3 Micro-CT analysis

Bone properties of trabecular bone at the fourth lumbar vertebrae (L4) and proximal tibia were determined by μCT system (viva-μCT40; Scanco Medical, Switzerland). The bones were scanned in an axial direction with high resolution (10.5 μm), power of 70 kVp and intensity of 114 μA. A total of 100 continuous slices were scanned in the middle part of the L4 (middle point ± 50 slices), and all of them were used for evaluation. For the proximal tibia, 100 slices were acquired from the growth plate to metaphysis, 50 serials of which were selected for analysis. The volume of interest (VOI) was evaluated using a three-dimensional direct model with a constant threshold of 375. Trabecular bone parameters including bone mineral density (BMD, mg HA/cm^3), bone volume/tissue volume (BV/TV, %), trabecular number (Tb.N, 1/mm), trabecular thickness (Tb.Th, mm), trabecular separation (Tb.Sp, mm), and connectivity density (Conn.D, 1/mm^3) were evaluated.

3.2.1.4 Serum and urine biochemistry

Serum and urinary levels of calcium (Ca) and phosphorus (P) were measured by standard colorimetric methods using commercial kits (Nanjing Jiancheng Bioengineering Institute, China). Urinary Ca and P levels were normalized with urinary creatinine (Cr) levels measured by picric acid methods following the manufacturer's instructions (Nanjing Jiancheng Bioengineering Institute, China). Concentrations of $1,25(OH)_2D_3$ in serum were determined by a mouse 1,25-dihydroxyvitamin D_3 ($1,25(OH)_2D_3$) ELISA kit (BlueGene Biotech, Shanghai, China). Serum levels of procollagen I N-terminal propeptide (PINP) and C-terminal telopeptide of type I collagen (CTX-1) were measured by using mouse PINP ELISA kit and mouse cross linked CTX-I ELISA kit following the manufacturer's instructions, respectively.

3.2.2 *In vitro* experiment

3.2.2.1 Experimental design

Firstly, we determined the effects of OA on vitamin D metabolism in both renal and osteoblast-like cells. Dose responses of CYP27B1 and CYP24A1 mRNA and protein expression to OA were evaluated by RT-PCR and Western blotting analysis in human kidney proximal tubular HKC-8 cells, human osteosarcoma MG-63 cells, and rat osteosarcoma UMR-106 cells, respectively. To further verify the ability of OA to regulate CYP27B1 activity in osteoblasts, both MG-63 and UMR-106 cells were supplied with adequate content of $25OHD_3$ as substrates, concentrations of the hydroxylated product $1,25(OH)_2D_3$ was determined. On the other hand, effects of OA on osteogenesis in osteoblasts were evaluated through measuring mRNA expressions of osteogenic markers by RT-PCR.

3.2.2.2 Cell culture and treatment

HKC-8 cells were cultured in Dulbecco's modified Eagle's medium/Nutrient mixture F-12 (DMEM/F-12, Gibco) containing 5 % heat-inactivated fetal bovine serum (FBS)

and 100 U/ml penicillin-streptomycin (P/S) in a humidified environment with 5 % CO_2 at 37 °C. Cells were routinely subcultured once they reached 80 % confluence. For the experiment, cells were seeded in six-well plates at 3×10^5 cells/well to allow 80 % confluence 24 hours later. FBS in culture medium were then replaced by a supplement containing insulin (5μg/ml), transferrin (5μg/L), triiodothyronine (0.37nmol/L), epidermal growth factor (2.5ng/ml), Na_2SeO_3 (5ng/ml), and hydrocortisone (1nmol/L). 24 hours after changing medium, cells were treated with a series of concentrations of OA (1, 10, 100, 1000, 10000 nM) for determining the responses of CYP27B1 and CYP24A1 expression. Parathyroid hormone (PTH, 100 nM) was used as the positive control for expressions and activity of CYP27B1. $1,25(OH)_2D_3$ (10 nM) was employed as the positive control for study of of CYP24A1 expression.

MG-63 and UMR-106 cells were cultured in DMEM supplemented with 10% heat-inactivated FBS and 100 U/ml P/S in a humidified incubator with 5 % CO_2 at 37 °C. Cells were subcultured twice every week. For the experiment, cells were seeded in six-well plates at a density of 2×10^5 cells/well for MG-63 while 3×10^5 cells/well for UMR-106, to allow 80 % confluence 24 hours later. Culture medium were then replaced by phenol red-free DMEM with 1% charcoal-striped FBS. 24 hours after changing medium, cells were treated with different concentrations of OA (1, 10, 100, 1000, 10000 nM) for relevant experiments. Parathyroid hormone (PTH, 100 nM) was used as a positive control for determination of CYP27B1 expressions and activity. $1,25(OH)_2D_3$ (10 nM) was employed as positive control for expressions of CYP24A1.

3.2.2.3 CYP27B1 activity

Cells were seeded in 12-well plates until 80% confluence. The culture medium was then changed to a phenol red-free and serum-free medium to minimize the interference from sterols for 24 hours before the treatment. Then cells were treated with PTH or OA and supplemented with $25OHD_3$ (1 μM) as a substrate and N, N'-diphenylethylene-diamine (1, 2-dianilinoethane, 10 μM) as an antioxidant (Schwartz et al., 1998). Upon

incubation for 4 hours, the reaction was terminated by placing the plates on ice. The CYP27B1 activity was evaluated by determining the cellular secreted $1,25(OH)_2D_3$ in culture medium (Geng et al., 2011a). Concentrations of $1,25(OH)_2D_3$ in supernatant was qualified with $1,25(OH)_2D_3$ ELISA kit by following manufacturer's instruction (Immundiagnostik AG). To normalize the $1,25(OH)_2D_3$ levels, contents of protein in cells were determined by Bradford assay (Bio-Red, CA, USA).

3.2.2.4 RT-PCR

Around 10 μg of tissues removed from kidneys and iliac crests from *in vivo* study were individually immersed in 500 μl TRIzol reagent (Invitrogen, USA). Upon homogenization with Precellys Evolution tissue homogenizer (Bertin Technologies, France). For *in vitro* experiment, cells were seeded in 6-well plates treated with different concentrations of OA for 24 hours. Total RNA from animal tissues and treated cells was extracted from the respective tissue by following the manufacturer's instructions. 1 μg of RNA was applied for reverse transcription (RT) by using PrimeScript^{TM} RT Master Mix (TaKaRa, Japan) in a 20 μl reaction system for cDNA generation. 500 ng of cDNA products and 0.4 μM primers were added to PCR reaction mixture containing TB Green Premix Ex Taq II (TaKaRa, Japan). Real-time PCR was performed in 7900HT Fast Real-Time PCR System (Applied Biosystems, Carlsbad, CA, USA) under the amplification conditions and procedures: initial denaturation at 95 °C for 30 s, 40 cycles of denaturation at 95 °C for 1 s and 60 °C for 20 s. The sequences of primers for target genes and the housekeeping gene glyceraldehyde-3-phosphate dehydrogenase (GAPDH) are listed in Table 3.2. Relative gene expression was calculated by $2^{-\Delta\Delta CT}$ method.

Table 3.2 Primer sequences for mouse, human and rat genes

Gene		Primer Sequence (5'-3')
Mouse		
CYP27B1	Forward:	GCATCACTTAACCCACTTCC
	Reverse:	CGGGAAAGCTCATAGAGTGT
CYP24A1	Forward:	AAGAGATTCGGGCTCCTTCA
	Reverse:	GCAGGGCTTGACTGATTTGA
GAPDH	Forward:	CAGAACATCATCCCTGCATC
	Reverse:	CTGCTTCACCACCTTCTTGA
Human		
CYP27B1	Forward:	AGAGTTGCTATTGGCGGGAG
	Reverse:	AGAACAGTGGCTGAGGGGTA
CYP24A1	Forward:	ACCCAAAGGAATTGTCCGCA
	Reverse:	ACCACCATCTGAGGCGTATT
ALP	Forward:	TTTATAAGGCGGCGGGGGTG
	Reverse:	AGCCCAGAGATGCAATCGAC
OPN	Forward:	GTACCCTGATGCTACAGACG
	Reverse:	TTCATAACTGTCCTTCCCAC
GAPDH	Forward:	ACCCACTCCTCCACCTTTGAC
	Reverse:	TGTTGCTGTAGCCAAATTCGTT
Rat		
CYP27B1	Forward:	GCATCACTTAACCCACTTCC
	Reverse:	AGGGTCGGCCACATAAACTG
CYP24A1	Forward:	CTCGGACCCTTGACAAACCA
	Reverse:	CGATGCCGAATGGGAGATGA
ALP	Forward:	ACGAGGTCACGTCCATCCT
	Reverse:	CCGAGTGGTGGTCACGAT
OPN	Forward:	CGATGTCCCCAACGGCCGAG
	Reverse:	TGCTCAGAAGCTGGGCAACAGG
GAPDH	Forward:	GTGAGGTGACCGCATCTTCT
	Reverse:	CTTGCCGTGGGTAGAGTCAT

3.2.2.5 Western blotting

Tissues removed from kidneys and iliac crests from *in vivo* study (100 μL/10 mg) as well as treated cells of *in vitro* experiment (10 μL/10^5 cells) were lysed with lysis buffer (Beyotime, Shanghai, China) supplemented with 1mM phenylmethyl sulfonyl fluoride (PMSF) as a protease inhibitor. Following protein extraction, 30 μg proteins of each sample were loaded and separated in a 10% SDS-PAGE, followed by transference onto polyvinylidene fluoride (PVDF) membranes (Millipore, Danvers, USA). The proteins on membranes were blocked with 5 % milk for 1 hour at room temperature and incubated with following primary antibodies overnight at 4°C: rabbit anti-CYP27B1 (1:1000, Invitrogen), rabbit anti-CYP24A1 (1:1000, Invitrogen), or mouse anti-β-Actin (1:5000, Abcam). followed by IgG-HRP-conjugated secondary antibodies anti-rabbit (1:3000, Abcam) or anti-mouse (1:3000, Invitrogen) for 1h at room temperature. Washing with tris-buffered saline with 0.1% Tween 20 detergent (TBST) for 3 times was required between each of incubation. Finally, the blotting was probed and visualized with Clarity^{TM} Western ECL substrate (Bio-Rad, USA) using Azure^{TM} C600 (Azure Biosystems, USA). The relative intensities of the bands were quantified by Image J software (National Institutes of Health, USA) and normalized with β-actin.

3.2.2.6 Statistical analysis

Data from both *in vivo* and *in vitro* experiment were shown as mean ± standard error of mean (SEM) for each treatment group. Inter-group differences were analyzed by one-way analysis of variance (ANOVA) followed by Tukey's Test for multiple comparisons (GraphPad Prism 8.0, USA). A *P* value of less than 0.05 was considered statistically significant.

3.3 Results

3.3.1 Effects of OA on bone properties and bone metabolism in OVX mice

3.3.1.1 Body weight and uterine index

After treatment for 8 weeks, body weight and uterus wet weight of mice were measured and body weight gain and uterus index were calculated, respectively. As shown in Table 3.3, OVX increased body weight gain of mice by more than 3-fold ($P<0.01$) when compared to those with sham operation. This increase in weight gain was markedly suppressed by HCD ($P<0.05$ vs. OVX). Administration of E_2 for 8 weeks strongly accelerated weight loss in OVX mice ($P<0.001$). On the other hand, it seems that mice fed with OA-contained diet acquired lower body weight gain than those of OVX group, although the change did not reach statistical significance. As expected, a remarkable shrinkage of uterus was observed in OVX mice ($P<0.001$ vs. sham) while E_2 increased uterus index in OVX mice by 3.89 folds ($P<0.001$ vs. OVX). Unlike E_2, treatment with HCD and OA did not alter the uterus atrophy in OVX mice.

3.3.1.2 Urine and serum chemistry

Serum and urinary levels of calcium and phosphorus were detected, and the results were listed in Table 3.3. Serum levels of calcium and phosphorus in mice were maintained in a normal range without any differences amongst different treatment groups. OVX significantly increased urinary calcium excretion in mice by one-fold ($P<0.001$ vs. sham). Both E_2 and OA significantly suppressed urinary calcium loss in OVX mice ($P<0.001$). It appeared that HCD did not further increase urinary calcium loss in OVX mice, but it significantly reduced phosphorus excretion in urine ($P<0.01$ vs. OVX).

Table 3.3 Body weight gain, uterine index, serum and urinary biochemistries in ovariectomized (OVX) in response to treatment with 17β-estradiol (E2), high calcium diet (HCD) and oleanolic acid (OA)

	Sham	OVX	E$_2$	HCD	OA
Body weight and uterus index					
Weight gain, %	2.01 ± 1.09**	7.26 ± 0.75	-1.82 ± 0.44 ***	3.20 ± 1.26*	4.23 ± 1.45
Uterus index, mg/g	2.77 ± 0.23***	0.66 ± 0.07	3.23 ± 0.21 ***	0.82 ± 0.08	0.77 ± 0.09
Serum chemistry					
Ca, mg/dL	7.63 ± 0.07	7.75 ± 0.08	7.71 ± 0.08	7.63 ± 0.04	7.91 ± 0.03
P, mg/dL	7.05 ± 0.51	7.66 ± 0.68	8.71 ± 0.39	7.38 ± 0.82	7.12 ± 0.30
Urine chemistry					
Ca/Cr, mg/mg	0.22 ± 0.02***	0.45 ± 0.04	0.21 ± 0.03 ***	0.35 ± 0.03	0.19 ± 0.03 ***
P/Cr, mg/mg	1.97 ± 0.20	1.86 ± 0.14	1.82 ± 0.08	1.20 ± 0.05 **	1.90 ± 0.10

Six-month-old sham operated mice were fed with control diet, the ovariectomized (OVX) mice were orally administrated with vehicle, E$_2$ (200 μg/kg/day), HCD (1% calcium in control diet) and OA (200 ppm in control diet) for 8 weeks. Uterine index was calculated from the wet weight of uterus over the body weight. The urinary calcium (Ca) and phosphorus (P) levels were normalized with concentrations of creatinine (Cr) in urine. Data are shown as mean ± SEM and analyzed by using one-way ANOVA, followed by Tukey's multiple comparison test. * $P < 0.05$, ** $P < 0.01$, *** $P < 0.001$ vs. OVX (n=7/group).

3.3.1.3 Bone mineral density and bone microarchitectural properties at proximal tibia and lumbar vertebra (L4)

The trabecular bone mineral density (BMD) and microarchitectural characteristics of OVX mice were evaluated by micro-CT analysis, and the representative 3D images and related parameters at lumbar vertebra and proximal tibia were shown in Fig. 3.1 and Fig. 3.2, respectively. A marked bone loss and deterioration of bone microarchitecture were observed at both lumbar vertebra (L4) and proximal tibia in OVX mice, as illustrated by the decrease in BMD ($P<0.001$ vs. sham) and the alterations of microarchitectural parameters including the decrease in bone volume/total volume (BV/TV, $P<0.001$ vs. sham), trabecular number (Tb.N, $P<0.01$ vs. sham), connectivity density (Conn.D, $P<0.001$ vs. sham) and trabecular thickness (Tb.Th, $P<0.001$ vs. sham), and the increase in trabecular separation (Tb.Sp, $P<0.01$ vs. sham) and structural model index (SMI, $P<0.001$ vs. sham). Administration of E_2 ($P<0.05$ vs. OVX), HCD ($P<0.05$ vs. OVX) and OA ($P<0.05$ vs. OVX) significantly reversed the changes of trabecular BMD, BV/TV, Tb.N, Conn.D, Tb.Th, Tb.Sp and SMI with different degrees at both sites in OVX mice.

3.3.1.4 Bone turnover biomarkers

Procollagen I N-terminal propeptide (PINP) and C-telopeptide of type I collagen (CTX-1) are a pair of bone turnover biomarkers which are identified for monitoring bone formation and bone resorption, respectively. Compared with mice in sham group, the levels of PINP were 14.93% lower (Fig 3.3 A, $P<0.001$ vs. sham) and the levels of CTX-1 were 42.10% higher (Fig 3.3 B, $P<0.001$ vs. sham) in OVX mice. Treatment with E_2 and OA significantly restored serum levels of PINP in OVX mice (Fig 3.3 A, $P<0.05$ vs. OVX). Besides, E_2 and OA suppressed the increase in serum CTX-1 induced by OVX to the levels similar to that of mice with sham operation (Fig 3.3 B, $P<0.001$ vs. OVX). HCD significantly elevated serum levels of PINP (Fig 3.3 A, $P<0.01$) but not alter CTX-1 levels in OVX mice.
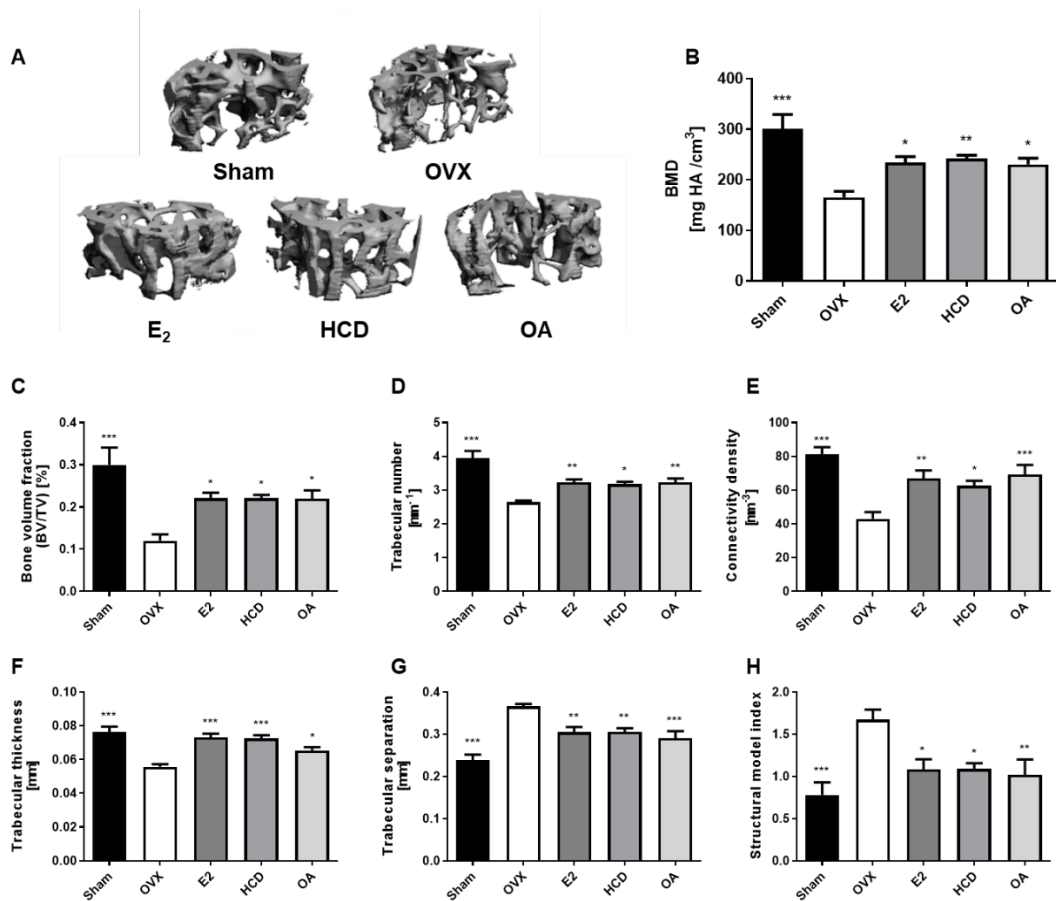
Fig. 3.1 Effects of OA on trabecular bone properties at lumbar vertebra (L4) of OVX mice.

Six-month-old sham operated mice were fed with vehicle diet, the ovariectomized (OVX) mice were orally administrated with vehicle, E_2 (200 μg/kg/day), HCD (1% calcium in control diet) and OA (200 ppm in control diet) for 8 weeks. Trabecular bone properties were evaluated by microcomputed tomography (μCT). (A) representative 3D images of trabecular bone at L4, (B) bone mineral density (BMD), (C) bone volume/total volume (BV/TV), (D) trabecular number (Tb.N), (E) connectivity density (Conn.D), (F) trabecular thickness (Tb.Th), (G) trabecular separation (Tb.Sp), and (H) structural model index (SMI). Data are shown as mean ± SEM and analyzed by using one-way ANOVA, followed by Tukey's multiple comparison test. * $P < 0.05$, ** $P < 0.01$, *** $P < 0.001$ vs. OVX (n=7/group).

Fig. 3.2 Effects of OA on trabecular bone properties at proximal tibia of OVX mice.

Six-month-old sham operated mice were fed with vehicle diet, the ovariectomized (OVX) mice were orally administrated with vehicle, E_2 (200 μg/kg/day), HCD (1% calcium in control diet) and OA (200 ppm in control diet) for 8 weeks. Trabecular bone properties were evaluated by microcomputed tomography (μCT). (A) representative 3D images of trabecular bone at proximal tibia, (B) bone mineral density (BMD), (C) bone volume/total volume (BV/TV), (D) trabecular number (Tb.N), (E) connectivity density (Conn.D), (F) trabecular thickness (Tb.Th), (G) trabecular separation (Tb.Sp), and (H) structural model index (SMI). Data are shown as mean ± SEM and analyzed by using one-way ANOVA, followed by Tukey's multiple comparison test. * $P < 0.05$, ** $P < 0.01$, *** $P < 0.001$ vs. OVX (n=7/group).
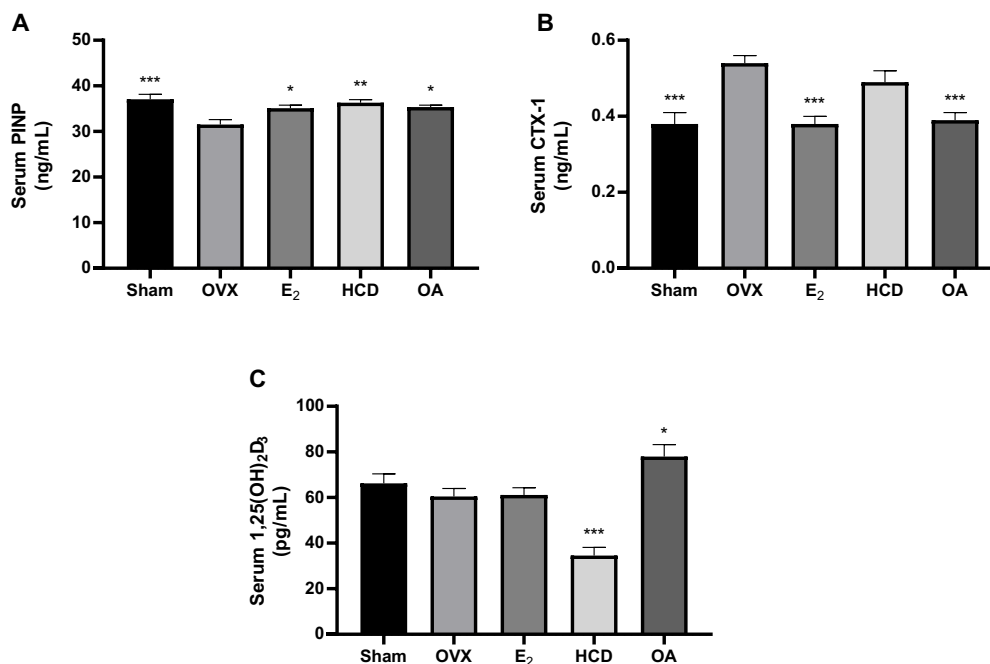
Fig. 3.3 Effects of OA on serum levels on bone turnover makers and 1,25(OH)₂D₃ in OVX mice.

Six-month-old sham operated mice were fed with vehicle diet, the ovariectomized (OVX) mice were orally administrated with vehicle, E_2 (200 µg/kg/day), HCD (1% calcium in control diet) and OA (200 ppm in control diet) for 8 weeks. Serum levels of (A) Procollagen I N-terminal propeptide (PINP), (B) C-telopeptide of type I collagen (CTX-1), and (C) 1,25(OH)₂D₃ were determined by commercial ELISA kits. Data are shown as mean ± SEM and analyzed by using one-way ANOVA, followed by Tukey's multiple comparison test. * $P < 0.05$, ** $P < 0.01$, *** $P < 0.001$ vs. OVX (n=7/group).

3.3.2 Effects of OA on vitamin D metabolism in OVX mice

3.3.1.5 Serum 1,25(OH)$_2$D$_3$ levels

As a biological active hormone mediating systemic calcium homeostasis, circulating levels of 1,25(OH)$_2$D$_3$ remained stable in mice of sham, OVX and E$_2$ groups (Fig 3.3 C). However, there was a significant decrease in circulating 1,25(OH)$_2$D$_3$ in OVX mice in response to HCD (Fig 3.3 C, $P < 0.001$). In contrast, administration of OA in diet significantly increases circulating 1,25(OH)$_2$D$_3$ levels in OVX mice by 28.85% (Fig 3.3 C, $P < 0.05$ vs. OVX).

3.3.1.6 Expressions of vitamin D metabolic enzymes in kidney and iliac crest

To evaluate effects of OA on gene and protein expressions of vitamin D metabolic enzymes in renal and extrarenal tissues, kidney and iliac crests were freshly isolated from treated mice. It appeared that ovariectomy had little impact on mRNA expression of CYP27B1 or CYP24A1 in both kidney and iliac crests (Fig. 3.4), but significantly suppressed protein expression of CYP27B1 (Fig 3.5 A, B, $P < 0.001$ *vs.* sham) and induced that of CYP24A1 (Fig 3.5 A, B, $P < 0.05$ *vs.* sham) in kidney. Similarly, treatment of E$_2$ did not alter gene expressions of CYP27B1 and CYP24A1 at both sites (Fig. 3.4), but markedly increased protein expressions of CYP27B1 in kidney (Fig 3.5 A, B, $P < 0.01$ *vs.* OVX). Mice fed with HCD had significantly higher mRNA levels of CYP24A1 in kidney (Fig 3.4 B, $P < 0.001$ *vs.* OVX) and iliac crest (Fig 3.4 D, $P < 0.05$ *vs.* OVX), but tended to have lower expression of CYP27B1 mRNA at both sites (Fig. 3.4 A, C). Moreover, HCD significantly suppressed protein expressions of CYP27B1 in kidney (Fig 3.5 A, B, $P < 0.01$ *vs.* OVX) but dramatically increased that in iliac crest (Fig 3.5 C, D, $P < 0.05$ *vs.* OVX). On the contrary, OA not only upregulated mRNA and protein expressions of CYP27B1 in kidney for more than 2-fold (Fig 3.4 A, Fig 3.5 B, $P < 0.01$ *vs.* OVX) and iliac crests for more than 3-fold (Fig 3.4 C, Fig 3.5 D, $P < 0.001$ *vs.* OVX), but also significantly induced mRNA expressions of CYP24A1 in iliac crest (Fig 3.4 D, $P < 0.001$ *vs.* OVX) but not in kidney.
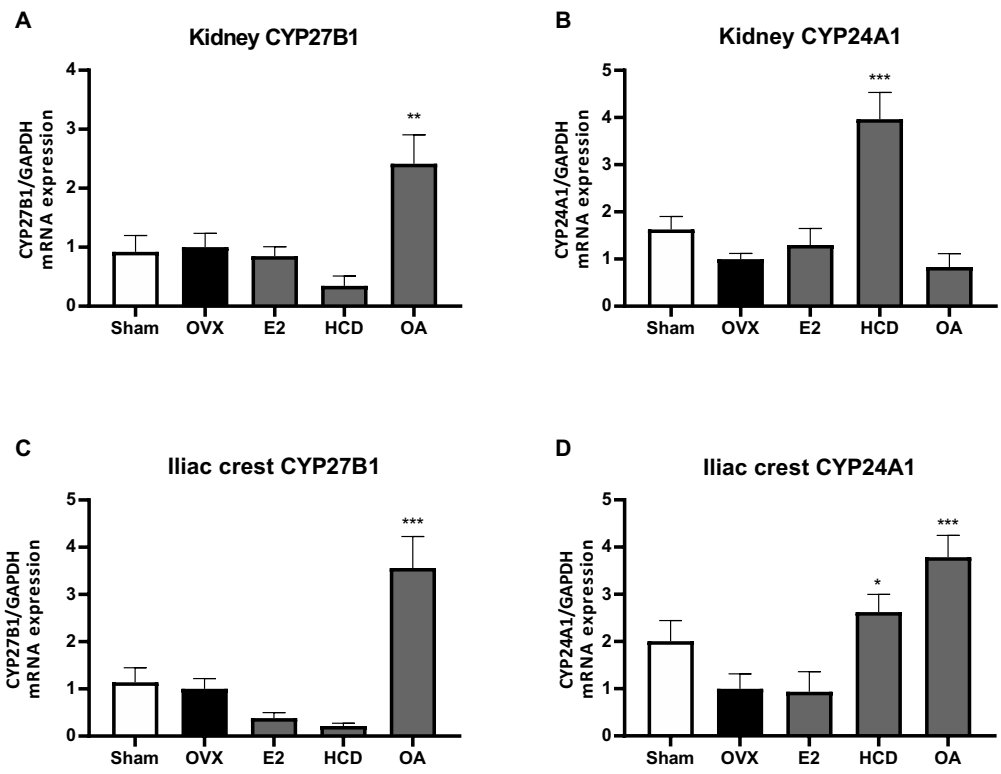
Fig. 3.4 Effects of OA on mRNA expressions of CYP27B1 and CYP24A1 in kidney and iliac crest of OVX mice.

6-month-old sham operated or ovariectomized (OVX) mice were orally administrated with vehicle, E_2 (200 μg/kg/day), HCD (1% calcium in control diet) and OA (200 ppm in control diet) for 8 weeks. mRMA expression levels of (A) CYP27B1 and (B) CYP24A1 in kidney, as well as mRMA expression levels of (C) CYP27B1 and (D) CYP24A1 in iliac crests were determined by RT-PCR. Data are shown as mean ± SEM and analyzed by using one-way ANOVA, followed by Tukey's multiple comparison test. * $P < 0.05$, ** $P < 0.01$, *** $P < 0.001$ vs. OVX (n=7/group).
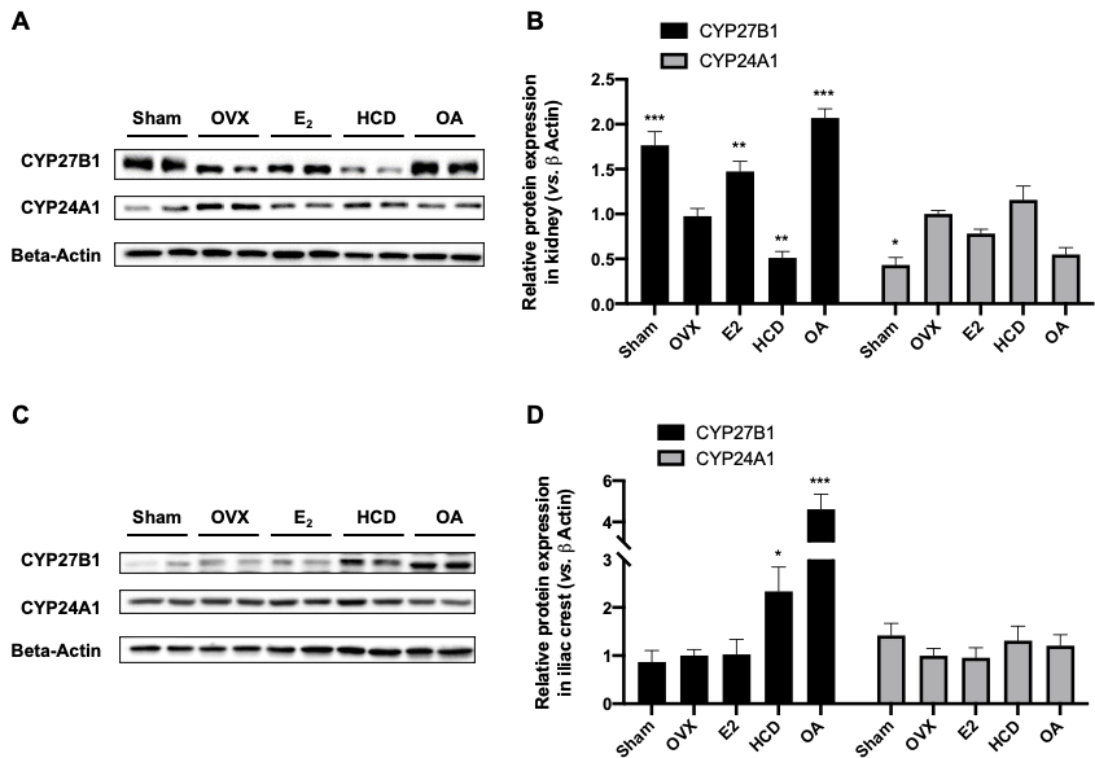
Fig. 3.5 Effects of OA on protein expressions of CYP27B1 and CYP24A1 in kidney and iliac crest of OVX mice.

Six-month-old sham operated mice were fed with vehicle diet, the ovariectomized (OVX) mice were orally administrated with vehicle, E_2 (200 μg/kg/day), HCD (1% calcium in control diet) and OA (200 ppm in control diet) for 8 weeks. Proteins were extracted and expression levels of CYP27B1 and CYP24A1 in kidney and iliac crests were determined by Western blotting. Representative blotting of CYP27B1 and CYP24A1 in kidney (A) and iliac crests (C) of two independent samples from each group were showed. The relative intensities of the bands of CYP27B1 and CYP24A1 in kidney (B) and iliac crests (D) were quantified by Image J with normalizing with β-Actin. Data are shown as mean ± SEM and analyzed by using one-way ANOVA, followed by Tukey's multiple comparison test. * $P < 0.05$, ** $P < 0.01$, *** $P < 0.001$ vs. OVX (n=7/group).
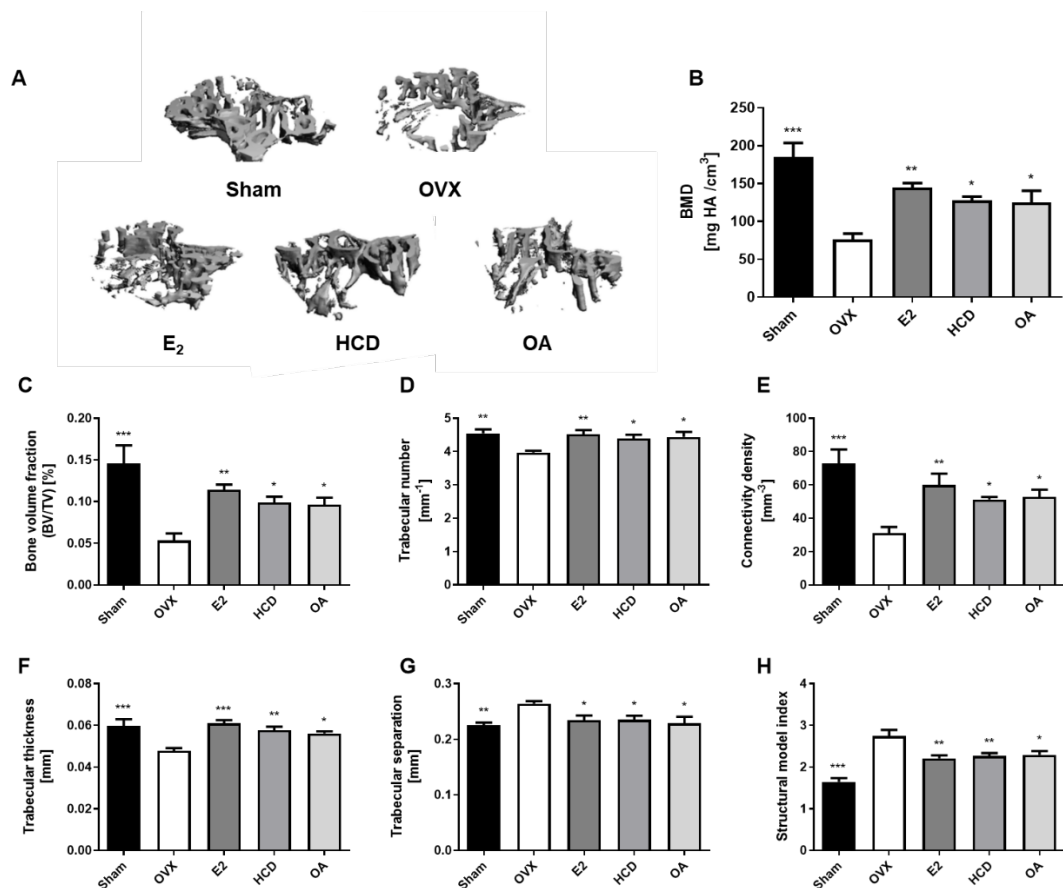
3.3.3 *In-vitro* effects of OA on vitamin D metabolic enzymes in kidney cells and osteoblasts

3.3.3.1 CYP27B1 and CYP24A1 expressions in human kidney cells

Human proximal tubule cells (HKC-8) were employed for evaluating the dose responses of OA on vitamin D metabolic enzymes *in vitro*. Parathyroid hormone (PTH, 100 nM) which was widely reported to induce CYP27B1 expression in kidney, tended to upregulate mRNA and protein expressions of CYP27B1 in HKC-8 cells, although the changes did not reach statistical significance. OA (10 μM) significantly increased mRNA and protein expression levels of CYP27B1 for 1.8-fold (Fig 3.6 A, $P < 0.001$ vs. Control) and 1.3-fold (Fig 3.6 C, $P < 0.01$ vs. Control), respectively, in HKC-8 cells upon incubation for 24 hours. On the other hand, mRNA (Fig 3.6 B, $P < 0.001$ vs. Control) and protein (Fig 3.6 D, $P < 0.01$ vs. Control) levels of CYP24A1 increased dramatically in HKC-8 cells in response to $1,25(OH)_2D_3$ (10 nM). However, no obvious effect of OA on CYP24A1 in HKC-8 cells was observed.

3.3.3.2 CYP27B1 and CYP24A1 expressions in human and rat osteoblasts

Vitamin D metabolic enzymes including CYP27B1 and CYP24A1 are also presented in rat and human osteoblast-like osteosarcoma cells. As shown in Fig 3.7 and Fig 3.8, PTH managed to induce mRNA expression levels of CYP27B1 in UMR-106 cells ($P < 0.05$ vs. Control), as well as mRNA and protein expression levels of CYP27B1 in MG-63 cells ($P < 0.05$ vs. Control). OA not only remarkably increased mRNA ($P < 0.01$ vs. Control) and protein levels ($P < 0.05$ vs. Control) of CYP27B1 at lower concentrations (1-10 nM) in both cells, but also significantly induced CYP27B1 mRNA expressions in UMR-106 ($P < 0.05$ vs. Control) and CYP27B1 protein expressions in MG-63 cells ($P < 0.05$ vs. Control) at higher concentrations (1-10 μM). There was a sharp induction of CYP24A1 expressions in response to $1,25(OH)_2D_3$ ($P < 0.01$ vs. Control), while 24-hour treatment of OA did not significantly affect CYP24A1 expressions in rat and human osteoblast-like cells.
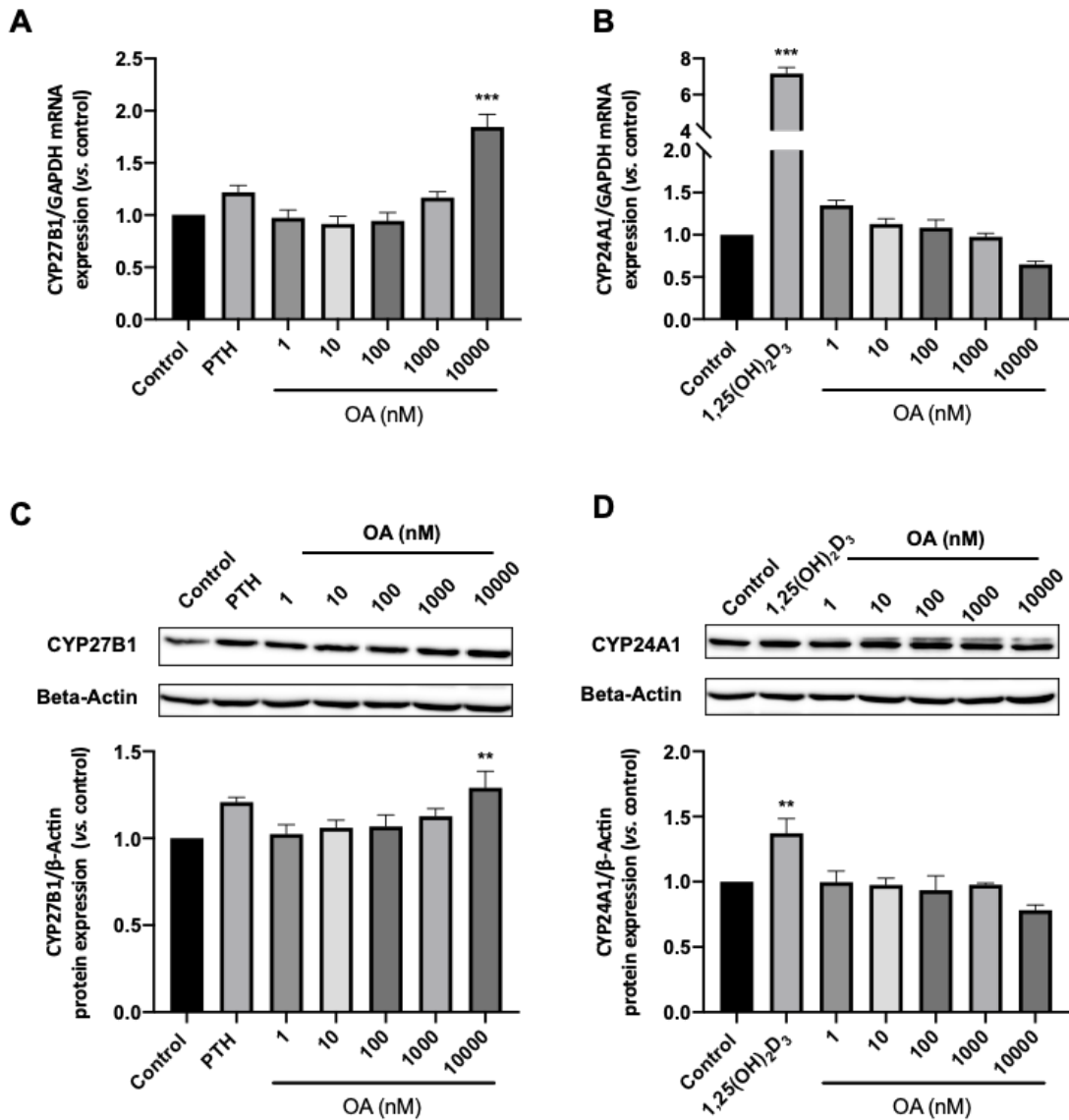
Fig. 3.6 Effects of OA on mRNA and protein expressions of CYP27B1 and CYP24A1 in human kidney proximal tubular HKC-8 cells.

HKC-8 cells were treated with OA (1, 10, 100, 1000, 10000 nM), parathyroid hormone (PTH, 100 nM) or 1,25(OH)$_2$D$_3$ (10 nM) in medium containing a supplement for 24 hours. mRMA expression levels of (A) CYP27B1 and (B) CYP24A1 were determined by RT-PCR. Protein expression levels of (C) CYP27B1 and (D) CYP24A1 were determined by Western blotting. Data are from four independent experiments and are shown as mean ± SEM and analyzed by using one-way ANOVA, followed by Tukey's multiple comparison test. ** $P < 0.01$, *** $P < 0.001$ vs. Control.
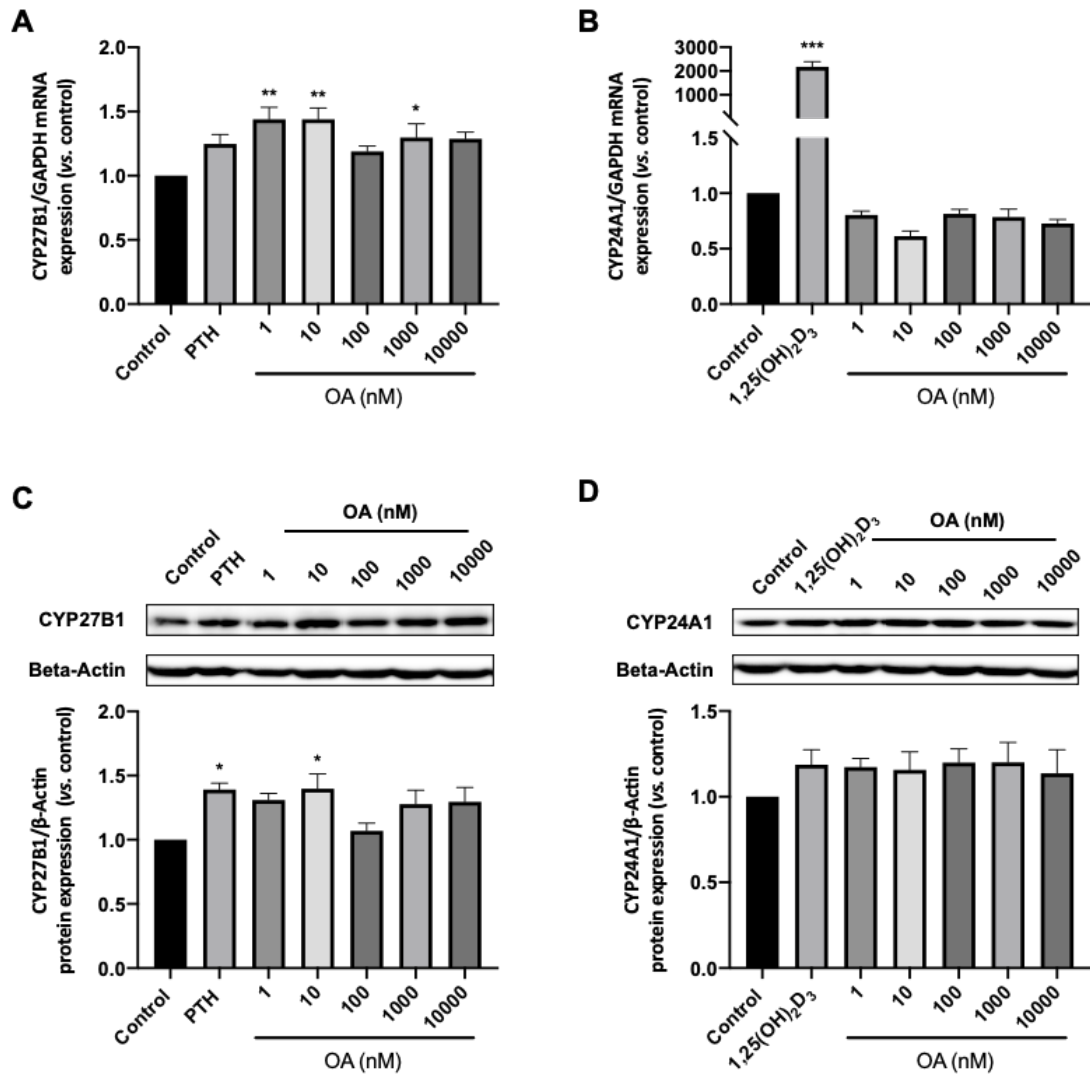
Fig. 3.7 Effects of OA on mRNA and protein expressions of CYP27B1 and CYP24A1 in rat osteosarcoma UMR-106 cells.

UMR-106 cells were treated with OA (1, 10, 100, 1000, 10000 nM), parathyroid hormone (PTH, 100 nM) or 1,25(OH)$_2$D$_3$ (10 nM) in phenol red-free medium for 24 hours. mRMA expression levels of (A) CYP27B1 and (B) CYP24A1 were determined by RT-PCR. Protein expression levels of (C) CYP27B1 and (D) CYP24A1 were determined by Western blotting. Data are from four independent experiments and are shown as mean ± SEM and analyzed by using one-way ANOVA, followed by Tukey's multiple comparison test. * $P < 0.05$, ** $P < 0.01$, *** $P < 0.001$ vs. Control.
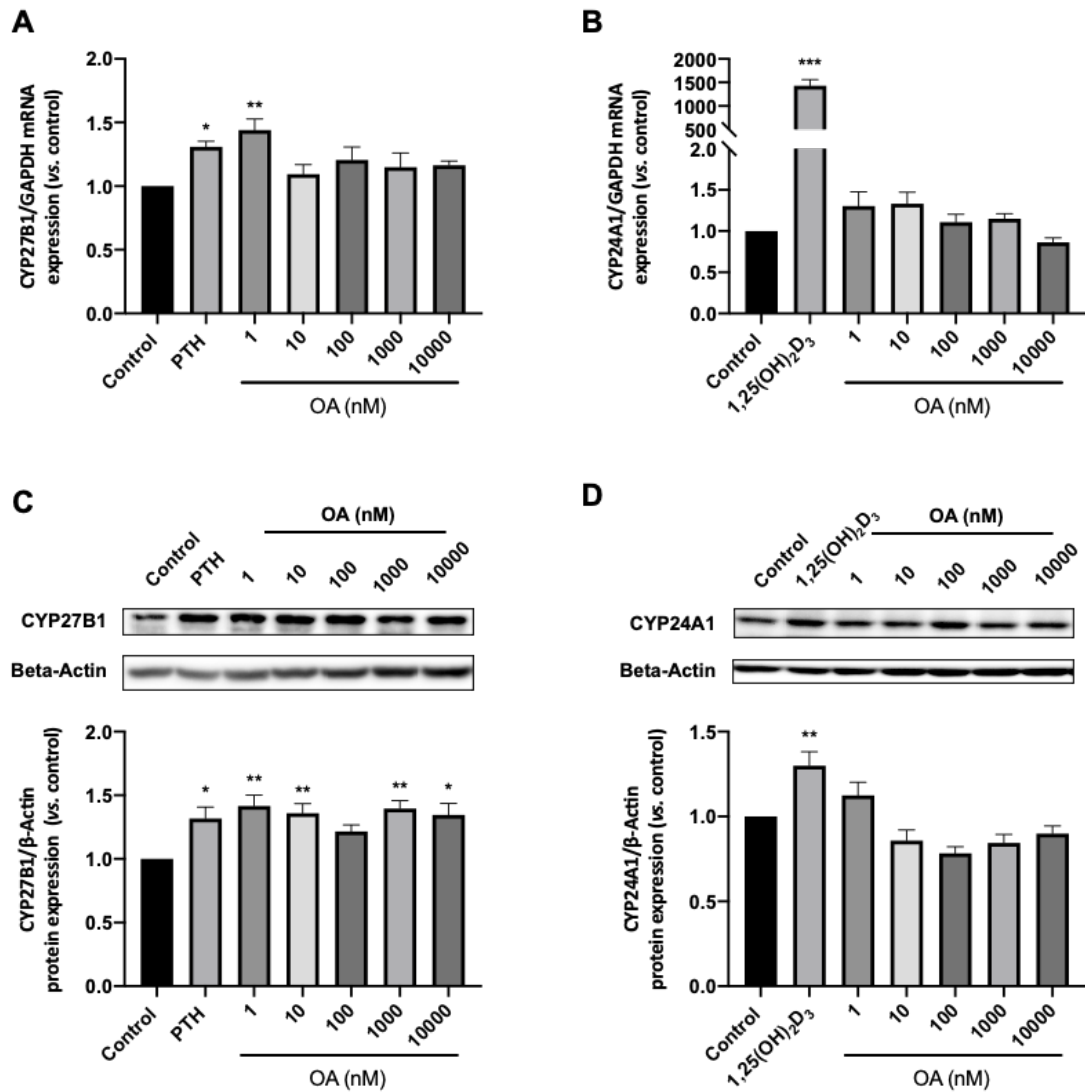
Fig. 3.8 Effects of OA on mRNA and protein expressions of CYP27B1 and CYP24A1 in human osteosarcoma MG-63 cells.

MG-63 cells were treated with OA (1, 10, 100, 1000, 10000 nM), parathyroid hormone (PTH, 100 nM) or $1,25(OH)_2D_3$ (10 nM) in phenol red-free medium for 24 hours. mRMA expression levels of (A) CYP27B1 and (B) CYP24A1 were determined by RT-PCR. Protein expression levels of (C) CYP27B1 and (D) CYP24A1 were determined by Western blotting. Data are from four independent experiments and are shown as mean ± SEM and analyzed by using one-way ANOVA, followed by Tukey's multiple comparison test. * $P < 0.05$, ** $P < 0.01$, *** $P < 0.001$ vs. Control.

3.3.3.3 CYP27B1 activity in human and rat osteoblasts

In addition to mRNA and protein expressions of CYP27B1, the enzymatic activities of CYP27B1 play a critical part in evaluating the effects of OA on vitamin D metabolism in osteoblasts. In this assay, UMR-106 and MG-63 were supplemented with adequate 25OHD$_3$ (1 μM) as substrate for hydroxylation by CYP27B1 in a free radical-scavenged medium. As shown in Fig. 3.9, level of 1,25(OH)$_2$D$_3$ was undetectable in both treated UMR 106 and MG-63 cells in the absence of the substrate 25OHD$_3$. When supplied with same concentrations of substrate, MG-63 tended to have higher efficiency to generate 1,25(OH)$_2$D$_3$ than UMR-106. Treatment with PTH (100 nM) for 4 hours markedly induced CYP27B1 activity, which was indicated by increased cellular secretion of 1,25(OH)$_2$D$_3$, by 49.6% (P <0.05 vs. 25OHD$_3$) in UMR-106 and 33.4% (P <0.05 vs. 25OHD$_3$) in MG-63. OA (1 nM) effectively increased biosynthesis of 1,25(OH)$_2$D$_3$ in MG-63 for 1.4-fold (P <0.05 vs. 25OHD$_3$), but not UMR-106.

3.3.3.4 Bone markers in human and rat osteoblasts

By employing 1,25(OH)$_2$D$_3$ as positive control, effects of OA on mRNA expressions of osteogenic markers in UMR-106 and MG-63 were determined, and the results were showed in Fig. 3.10. Gene expressions of alkaline phosphatase (ALP) and osteopontin (OPN) in both osteoblasts were significantly elevated in response to 24-hour treatment of 1,25(OH)$_2$D$_3$ (P <0.01 vs. Control), although MG-63 seems to be more sensitive to 1,25(OH)$_2$D$_3$. Acting like 1,25(OH)$_2$D$_3$, OA significantly upregulated mRNA levels of ALP for 1.2-fold (P <0.05 vs. Control) at concentration of 1-1000 nM in UMR-106, and 1.4-fold (P <0.05 vs. Control) at 1-10 nM in MG-63. Moreover, gene expressions of OPN in both osteoblasts appeared to be increased by OA (1 nM) for over 1.3-fold, but the changes did not reach statistical significance.
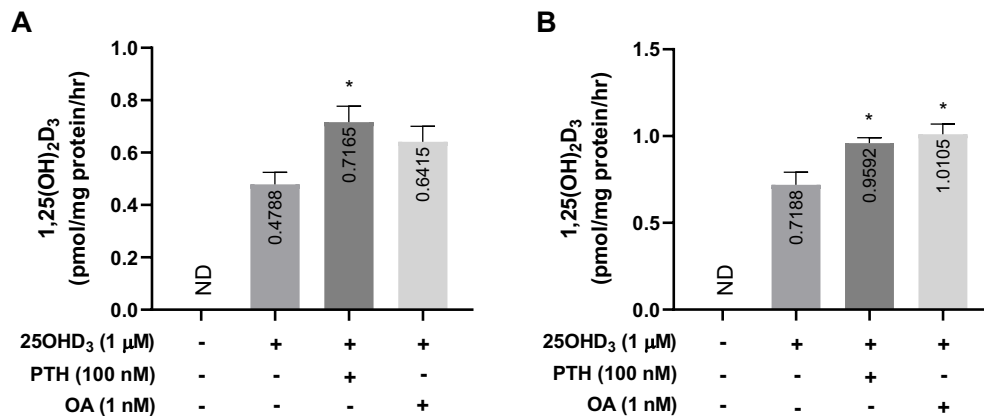
Fig. 3.9 Effects of OA on enzymatic activities of CYP27B1 in rat osteosarcoma UMR-106 cells (A) and human osteosarcoma MG-63 cells (B).

Cells were treated with PTH (100 nM) and OA (1 nM) in phenol red-free and serum-free medium in supplementation of 25(OH)D$_3$ (1 μM) as substrate and N, N'-diphenylethylene-diamine (10 μM) as antioxidant for 4 hours. The CYP27B1 activity was determined by measuring cellular secreted 1,25(OH)$_2$D$_3$ in supernatant per hour. None detected (ND). Data are from three independent experiments and are shown as mean ± SEM and analyzed by using one-way ANOVA, followed by Tukey's multiple comparison test. * $P < 0.05$ vs. Control.
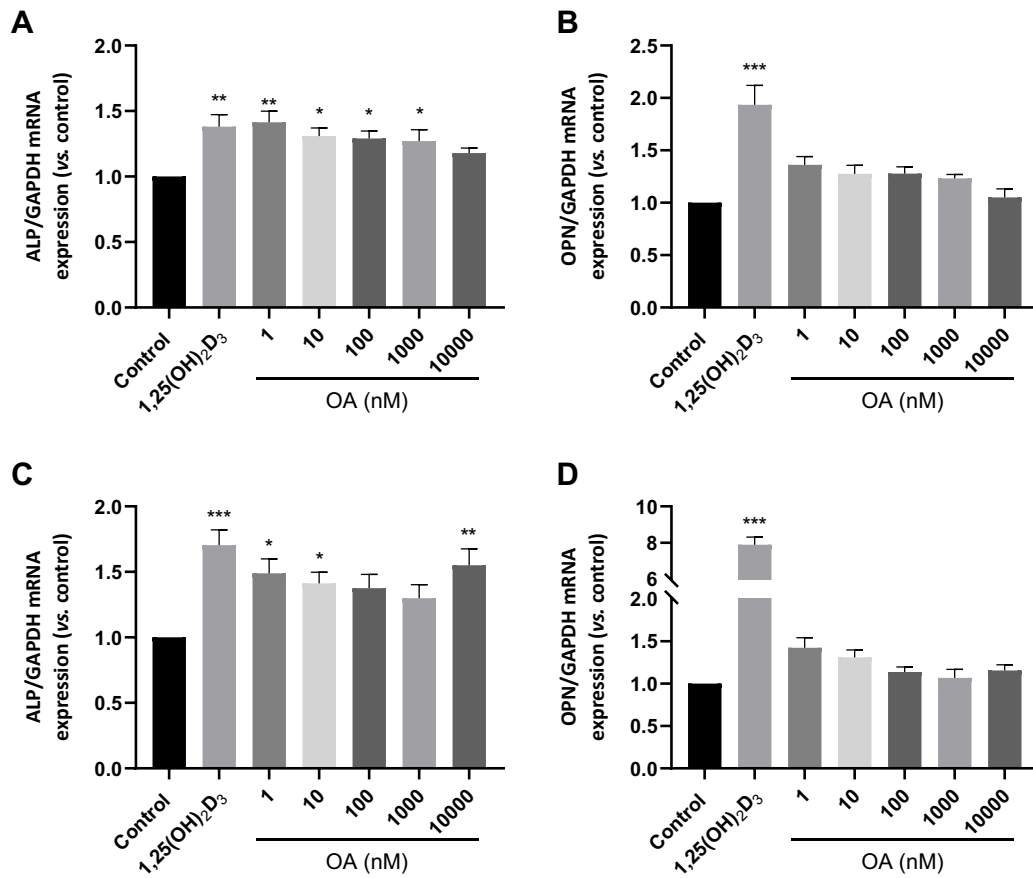
Fig. 3.10 Effects of OA on mRNA expressions of bone markers in rat osteosarcoma UMR-106 cells (A, B) and human osteosarcoma MG-63 cells (C.D).

Cells were treated with $1,25(OH)_2D_3$ (10 nM) and OA (1, 10, 100, 1000, 10000 nM), in phenol red-free medium for 24 hours. mRMA expression levels of alkaline phosphatase (ALP) and osteopontin (OPN) in UMR-106 cells (A, B) and MG-63 cells (C, D) were determined by RT-PCR. Data are from four independent experiments and are shown as mean ± SEM and analyzed by using one-way ANOVA, followed by Tukey's multiple comparison test. * $P < 0.05$, ** $P < 0.01$, *** $P < 0.001$ vs. Control.

3.4 Discussion

Kidney was generally recognized to be the principal site for expressing CYP27B1 and producing $1,25(OH)_2D_3$ for circulation. Since the discovery of CYP27B1 in the extrarenal sites such as bone, intestine, muscle and brain, study of the regulators and functions of CYP27B1 in those tissues has become the main focus. In this chapter, we attempted to characterize the effects of OA on vitamin D metabolism in bone especially in the osteoblasts, and to further compare these actions with that in kidney, by using an *in-vivo* osteoporotic animal model and *in-vitro* cell models.

Given the fact that vitamin D deficiency is prevalent amongst postmenopausal women suffering from osteoporosis and osteoporotic fractures (Glowacki et al., 2003), the present study employed an ovariectomy (OVX)-induced osteoporotic animal model to investigate the effects of OVX on renal and extrarenal vitamin D metabolism. However, we did not find a reduction in circulating levels of $1,25(OH)_2D_3$ in OVX mice, although whose trabecular BMD and bone microarchitecture were significant decreased when compared to that of mice in sham group. In line with our observations, Colin et al. (1999) reported there was no significant changes in serum $1,25(OH)_2D_3$ levels but a marked reduction of intestinal calcium absorption in OVX rats. Our results also showed an accelerated urinary calcium excretion in OVX mice. In accompany with the decreased calcium absorption and increased calcium loss, the calcium released from accelerated bone resorption made it possible for the stable serum levels of calcium in OVX mice.

In addition to the BMD and bone microarchitecture revealed by micro-CT analysis, changes in bone turnover markers also serve to assess the anabolic or catabolic activities of bone in response to different treatment. PINP is a peptide serves as an indicator for bone formation, as it is derived from cleavage of type I procollagen during proliferation of osteoblasts (Han et al., 2007). Moreover, CTX-1 is produced by breakdown of type I collagen during bone resorption and serves as indicator for bone resorption (Tian et al., 2019). In consistent with other studies, our results showed that ovariectomy

significantly accelerated bone turnover rate as reflected by changes in serum levels of PINP and CTX-1 (Cui et al., 2016). E_2 was previously shown to modulate bone formation and bone resorption via the estrogen receptor α and β expressed in osteoblasts and osteoclasts (Nakamura et al., 2007; Zhou et al., 2001). In line with these observations, we also showed the restoration of bone turnover rate in OVX mice after administration with E_2. In the situation of estrogen deficiency, the requirement of calcium from diet is remarkably increased as revealed by worsen bone properties and calcium balance in OVX rats fed with low calcium diet (Morris et al., 2009). Our results shown that these changes could be reversed by feeding OVX mice with high calcium diet (HCD). In addition, the protective actions of HCD on BMD and bone microarchitecture in OVX mice appeared to be contributed by its effect on improving bone formation, as revealed by the increase in serum levels of PINP without changes in levels of CTX-1.

Our results indicated that OA, acting like E_2, significantly improved trabecular bone properties in OVX mice by stimulating bone formation as well as suppressing bone resorption. However, unlike E2, OA did not exert estrogenic effects in the uterus to induce uterine hypertrophy in OVX mice. In fact, the protective actions of OA on bone properties have been demonstrated repeatedly in numerous animal studies, in which suspensions of OA dissolved in physiological saline were orally administrated (Bian et al., 2012; Zhao et al., 2018). However, the strong hydrophobicity of OA contributed to its poor bioavailability as well as difficulties in gavage administration. Therefore, in the present study, OA was administrated by incorporation into control diet and the concentration of OA in the diet were designed based on the daily consumption of diet of mice and the dosage used in our previous study (Cao et al., 2018). However, we discovered that administration of 400 ppm OA diet resulted in a sharp drop in the body weight and food intake of the animals. The urine and skin on feet and lips presented yellow in color, which showed a symptom like cholestasis. In line with our findings, studies reported that long-term or high-dosage administration of OA (>225 mg/kg, p.o. for 10 days) could induce the liver injury and cholestasis in mice (Lu et al., 2013).

It has been well recognized that circulating $1,25(OH)_2D_3$ levels and renal CYP27B1 are tightly controlled by systemic requirement of calcium and phosphate. OVX mice exhibited impaired calcium balance, reduction in renal CYP27B1 expression as well as elevation of renal CYP24A1 expression, although their circulating levels of calcium and $1,25(OH)_2D_3$ were stable compared with sham operated mice. Colin et al. (1999) showed in their study that administration of E_2 restored the impaired intestinal calcium absorption in OVX rats, but this effect was independent of circulating $1,25(OH)_2D_3$ levels. Even so, a significant upregulation of CYP27B1 protein expression in kidney was found in mice in response to E_2, which was also observed in other species (Tanaka et al., 1976; Williams et al., 1988). This increase in renal CYP27B1 expression in response to E_2 facilitated calcium reabsorption in kidney and the decrease in urinary calcium excretion. Moreover, when fed OVX mice with HCD, the system responded to suppress calcium absorption by decreasing renal CYP27B1 expression and circulating $1,25(OH)_2D_3$ levels. In line with our previous study, the present study confirmed that OA significantly elevated circulating levels of $1,25(OH)_2D_3$ in OVX mice by upregulating renal expressions of CYP27B1, contributing to a positive calcium balance and improvement of bone properties (Cao et al., 2018).

The understanding of the regulation of CYP27B1 in bone is limiting, although many studies appeared to show that it was different from that in kidney (Anderson et al., 2010; Anderson et al., 2005; Turner et al., 2007). In supporting of these reported findings, our results showed that ovariectomy did not affect the expressions of CYP27B1 as well as CYP24A1 in iliac crest, at both mRNA and protein expression levels. Similar phenomena were observed in mice administrated with E_2, indicating the status of estrogen has little impact on the vitamin D metabolism in bone. In contrast to the kidney where HCD suppressed renal CYP27B1 expression, the protein expression of CYP27B1 increased in bone of mice in response to feeding with HCD. This phenomenon was also described in studies by Anderson et al. (2010) that high dietary calcium improved mRNA expression of CYP27B1 and mineralization in bone of rats. The upregulation of bone mineralization by HCD appeared to be dependent on the

expression of CYP27B1 in bone. Panda et al. (2004) demonstrated the decreased bone volume and mineral deposition rate in CYP27B1 knockout mice were hardly rescued, although the conditions of hypocalcemia and secondary hyperparathyroidism could be prevented, by feeding high calcium diet in these animals. Most importantly, OA was shown to increase CYP27B1 expression in kidney as well as in iliac crests, suggesting that OA could activate the paracrine or autocrine activity of $1,25(OH)_2D_3$ to modulate cellular proliferation and differentiation in bone.

It appears that regulation of CYP24A1 in extrarenal sites also differs from that in kidney. Generally, renal CYP24A1 was regulated in an opposite manner with CYP27B1. For instance, CYP24A1 was increased in response to elevated circulating levels of $1,25(OH)_2D_3$ and calcium to maintain calcium homeostasis. On contrary to CYP27B1, the activity and expression of CYP24A1 increase with ageing and pathological conditions like chronic renal failure and diabetes (Colussi et al., 2014; Tajiri et al., 2019). In the present study, ovariectomy was found to significantly increase CYP24A1 expressions in kidney, but not in bone. OA significantly increased mRNA expressions of CYP24A1 in iliac crest, although it did not influence renal expressions of CYP24A1. As speculated by Anderson et al. (2005), CYP24A1 expression in bone is more susceptible to levels of locally produced $1,25(OH)_2D_3$. In supporting of this, we discovered the increase of CYP27B1 was followed by an upregulation of CYP24A in bone of mice fed with OA and HCD.

In our *in vitro* experiments, the levels of CYP27B1 expression in both human and rat osteoblast-like cells were comparable to that in proximal tubule cells. In line with other studies, the present study showed that these osteoblasts were capable to generate $1,25(OH)_2D_3$ and modulate osteoblastic activities when supplemented with adequate levels of $25OHD_3$ (Anderson et al., 2007; Atkins et al., 2007; van Driel et al., 2006). PTH is well known to upregulate CYP27B1 activity and expression in kidney cells. Moreover, expressions of CYP27B1 in human mesenchymal stem cells (hMSCs), the progenitors give rise to osteoblasts, were also shown to increase in response to PTH

(Zhou et al., 2011). In the present study, OA at 10 μM was shown to effectively upregulate CYP27B1 in HKC-8 cells, and its effects was even more prominent than that of PTH. Compared with kidney cells, OA at 1-10 nM managed to induce expressions and enzymatic activity of CYP27B1 in UMR-106 and MG-63 cells. These lower effective dosages in osteoblasts seemed more accomplishable in view of the poor gastrointestinal absorption and bioavailability of OA.

Our results showed OA significantly upregulated mRNA levels of ALP in both human and rat osteoblast-like cells. It appears that lower dosages (1-10 nM) of OA exerts a hormone-like effects on the osteogenesis of osteoblasts by increasing cellular production of $1,25(OH)_2D_3$ as indicated in Fig. 3.9. Such actions on $1,25(OH)_2D_3$ are tightly controlled by the catabolic enzyme CYP24A1 and the cellular feedback mechanisms to avoid the possible adverse effects caused by excessive $1,25(OH)_2D_3$. This might be the reason why OA only upregulated the mRNA expression of ALP for 1.2-1.4-fold. A study showed that the mRNA expression of ALP was upregulated for 1.6-fold in response to $1,25(OH)_2D_3$ (10 nM) in primary human osteoblasts (Van Der Meijden et al., 2014). Kyeyune-Nyombi et al. (1991) showed that $1,25(OH)_2D_3$ progressively increased the steady-state level of ALP mRNA from 5 to 24 h of treatment in human bone cells, at which time a plateau was observed. Such observation indicated that the regulation of mRNA expression is time dependent. OA at higher dosage (10000 nM) might improve the osteogenic potential through other mechanisms such as Notch signaling as indicated by other research group (Shu et al., 2017).

Taken together, our results showed OA effectively improved BMD and bone microarchitectures in OVX mice. The bone protective effects of OA partially come from the improved calcium balance by increasing circulating $1,25(OH)_2D_3$ levels via upregulation of renal CYP27B1. On the other hand, OA not only upregulated expressions and enzymatic activity of CYP27B1, but also increased levels of osteogenic markers in osteoblasts. However, it remains a question that the involvement of locally biosynthesized $1,25(OH)_2D_3$ in osteogenic effects of OA in osteoblasts. This will be illustrated in the following chapters.

Chapter 4

The involvement of 25-hydroxyvitamin D 1-alpha-hydroxylase (CYP27B1) in the osteogenic effects of oleanolic acid in osteoblasts

4.1 Introduction

The severe hypocalcemia and osteoporosis as consequences of vitamin D deficiency emphasized the importance of vitamin D in promoting calcium homeostasis and bone mineralization. In the endocrine system, $1,25(OH)_2D$ is produced by CYP27B1 presented in kidney and is released into circulation to exert physiological activities via activating its nuclear receptor presented in the target tissues. For example, $1,25(OH)_2D$ binding to vitamin D binding protein (DBP) in plasma is transported to intestinal epithelium, it binds to vitamin D receptor (VDR) to initiate the transcription of genes encoding calcium transporters. These functions of $1,25(OH)_2D$ were also revealed by the mice with CYP27B1 knockout and double knockout of CYP27B1 and VDR, which exhibit the phenotype of increased bone fragility due to the decreased mineral deposition in both cortical and trabecular bone (Panda et al., 2004).

The presence of CYP27B1 and VDR for biosynthesis and biological activities of $1,25(OH)_2D$ in bone cells suggested the paracrine or autocrine activities of $1,25(OH)_2D$ produced locally in skeletal microenvironment. As the active lineages responsible for the anabolic activities of bone, osteoblasts were implicated to be involved in the local production and activities of $1,25(OH)_2D$. In particular, $1,25(OH)_2D$/VDR system exerts anabolic activities by upregulation of genes that encode factors for bone homeostasis and mineralization such as osteopontin (OPN), osteocalcin (OCN) and bone sialoprotein (BSP) in osteoblasts (Donnelly et al., 2011). Studies observed detectable levels of $1,25(OH)_2D_3$ in cell cultures of human osteosarcoma cells (Anderson et al., 2007), human fetal osteoblasts (van Driel et al., 2006) and human primary osteoblasts (Atkins et al., 2007), when they were supplemented with adequate $25OHD_3$. Moreover, silencing of CYP27B1 with CYP27B1 siRNA abolished alkaline phosphatase (ALP) activity and OCN mRNA expression induced by intracellular produced $1,25(OH)_2D_3$ in osteoblasts. Therefore, modulation of osteoblastic CYP27B1 serves as a promising way for optimizing bone mass and reducing risk of fracture.

Mesenchymal stomal cells (MSCs) in bone marrow, which serve as progenitors of osteoblasts, also express CYP27B1 (Geng et al., 2011a). The locally synthesized $1,25(OH)_2D_3$ enhanced osteoblastic differentiation of MSCs in an autocrine or paracrine manner (Posa et al., 2016). Geng et al. (2011a) showed there is a decline in expression of CYP27B1 with ageing, contributing to the decreased proliferation and osteogenesis of MSCs. Also, knockdown of CYP27B1 with CYP27B1 siRNA resulted in suppression of $1,25(OH)_2D_3$ generation and subsequent osteogenesis of MSCs from younger subjects. However, little is known about the role of CYP27B1 and $1,25(OH)_2D_3$ at different stages of osteogenic differentiation of osteoblasts.

In the previous chapter, we demonstrated that OA, as a naturally occurring small molecule, not only increased circulating $1,25(OH)_2D_3$ and renal expressions of CYP27B1, but also significantly improved local biosynthesis of $1,25(OH)_2D_3$ as well as transcription of ALP and OPN in osteoblasts. All these actions may contribute to the bone protective effects of OA. Recent studies showed that OA increased osteoblast number and osteogenesis of mice bone marrow stromal cells (BMSCs) (Bian et al., 2012). Shu et al. (2017) also demonstrated OA enhanced differentiation of hMSCs towards osteoprogenitor commitment by inhibiting Notch signalling. However, the involvement of intracellular produced $1,25(OH)_2D_3$ by CYP27B1 in the osteogenic effects of OA remains unclear.

This chapter aimed to investigate the involvement of CYP27B1 in the osteogenic effects of OA in osteoblast lineage. We determined expressions and enzymatic activity of CYP27B1 in response to OA at different osteogenic stages of hMSCs. The effects of OA on osteogenesis were also investigated by evaluating expressions of osteogenic markers during the differentiation of hMSCs. To further characterize the involvement of CYP27B1 in the anabolic activities of OA, CYP27B1 was silenced with CYP27B1 siRNA in osteoblast lineage.

4.2 Methodology

4.2.1 Experimental design

Firstly, hMSCs was cultured in osteogenic medium for 7, 14, 21 days to acquire the osteoblast lineages at stages of osteoprogenitors, pre-osteoblasts, and mature osteoblasts, respectively. Cells at different osteogenesis stages were incubated with different concentrations of OA. By using parathyroid hormone (PTH) as positive control, mRNA expressions levels of osteogenic markers and vitamin D metabolism enzymes were determined by RT-PCR. The role of cellular generated $1,25(OH)_2D_3$ by CYP27B1 in osteogenesis of osteoblast lineages were subsequently characterized by silencing of CYP27B1 with CYP27B1 siRNA.

4.2.2 Cell culture and treatment

4.2.2.1 Human mesenchymal stem cells (hMSCs)

hMSCs from a 61-year-old female subject (CREC Ref. No. 2010. 248) were provide by Dr. Lee Yuk wai, Wayne from the Prince of Wales Hospital of the Chinese University of Hong Kong (Lee et al., 2013). Cells were cultured in standard growth medium containing Minimum Essential Medium alpha (α-MEM) with 10% heat-inactivated fetal bovine serum (FBS) and 100 U/mL penicillin-streptomycin in a humidified environment with 5 % CO_2 at 37 ℃. Passage of less than 6 were used, as MSCs display accumulated DNA damage and loss of multipotency with time of culture (Alves et al., 2010). For osteoblastogenic differentiation of hMSCs, 2×10^5 cells/well were seeded in 6-well plates. Upon attaining confluence (day 0), culture medium was replaced with osteogenic induction medium which is composed of standard growth medium supplemented with 10 mM β-glycerophosphate, 1 nM dexamethasone and 50 μg/mL L-ascorbic acid. The medium was changed every 3 days until they were differentiated for 0, 7, 14 and 21 days. After reaching different osteogenic time points, culture medium was then replaced by phenol red-free α-MEM with 1% charcoal-striped FBS. Cells were treated with PTH (100 nM) or OA (1, 10, 100, 1000 nM) for 24 hours and

proceeded for relevant assays. Effects of 10000 nM OA were not studied in hMSCs as OA at such higher concentration was discovered to be toxic to these cells.

4.2.2.2 Human osteosarcoma MG-63

MG-63 cells were cultured in DMEM supplemented with 10% heat-inactivated FBS and 100 U/ml P/S in a humidified incubator with 5 % CO2 at 37 ℃. Cells were subcultured twice every week. For the experiment, cells were seeded in six-well plates at a density of 2×105 cells/well to allow 80 % confluence 24 hours later. Before the treatment, culture medium was replaced by phenol red-free DMEM with 1% charcoal-striped FBS. Osteogenic responses of cells to treatment of OA were evaluated.

4.2.3   RNA interference with CYP27B1 siRNA

To verify if the osteogenesis induced by OA was dependent on intracellular produced $1,25(OH)_2D_3$ by CYP27B1 in osteoblasts, small interfering RNAs (siRNAs) were used to silence CYP27B1. Cells were seeded in 6-well plates until reaching 80% confluence. Transfection was conducted by adding 25 nM SmartPool for human CYP27B1 specific siRNAs or non-silencing control siRNA with 4 uL/well Dharma-Fect-3 reagent (Dharmacon) according to the manufacturer's instructions. 48 hours after transfection, cells were treated with OA for a further 24 hours. Knockdown of CYP27B1 was confirmed by RT-PCR and Western blotting analysis.

4.2.4   Alkaline phosphatase (ALP) activity

Cells were seeded in 24-well plates until reaching 80% confluence. Then they were treated with different concentrations of OA for 7 days in phenol red-free (PRF) medium with 1% charcoal-striped FBS. Medium and treatment were renewed every 3 days. After the treatment, cells were lysed with passive lysis buffer (Promega, USA). ALP activity of the cell lysate was determined with a LabAssay ALP kit (Wako, Japan) by following the manufacturer's instruction. Total protein content was measured by Bradford method to normalize ALP activity.

4.2.5 CYP27B1 activity

Cells were seeded in 12-well plates until reaching 80% confluence. The culture medium was then changed to a phenol red-free and serum-free medium to minimize the interference from sterols for 24 hours before the treatment. Then cells were treated with PTH or OA in supplement with $25OHD_3$ (1 µM) as a substrate and N, N'-diphenylethylene-diamine (1, 2-dianilinoethane, 10 µM) as an antioxidant (Schwartz et al., 1998). Upon incubation for 4 hours, the reaction was terminated by placing the plates on ice. The CYP27B1 activity was evaluated by determining the cellular secreted $1,25(OH)_2D_3$ in culture medium (Geng et al., 2011a). Concentrations of $1,25(OH)_2D_3$ in supernatant was qualified with $1,25(OH)_2D_3$ ELISA kit by following manufacturer's instruction (Immundiagnostik AG). Levels of $1,25(OH)_2D_3$ were normalized to total protein content which were determined by Bradford assay (Bio-Red, CA, USA) to normalize the $1,25(OH)_2D_3$ levels.

4.2.6 RT-PCR

Total RNA from treated cells was extracted using TRIzol reagent (Invitrogen, USA) following the manufacturer's instructions. 1 µg of RNA was applied for reverse transcription (RT) by using PrimeScriptTM RT Master Mix (TaKaRa, Japan) in a 20 µl reaction system for cDNA generation. 500 ng of cDNA products and 0.4 µM primers were added to PCR reaction mixture with TB Green Premix Ex Taq II (TaKaRa, Japan). Real-time PCR was performed in 7900HT Fast Real-Time PCR System (Applied Biosystems, Carlsbad, CA, USA) under the amplification conditions and procedures: initial denaturation at 95 °C for 30 s, 40 cycles of denaturation at 95 °C (1 s) and extension at 60 °C (20 s). The sequences of primers for human and rat genes and the housekeeping gene GAPDH are listed in Table 4.1. Relative gene expression was calculated by $2^{-\Delta\Delta CT}$ method.

Table 4.1 Primer sequences for human genes

Gene	Primer Sequence (5'-3')	
CYP27B1	Forward:	AGAGTTGCTATTGGCGGGAG
	Reverse:	AGAACAGTGGCTGAGGGGTA
CYP24A1	Forward:	ACCCAAAGGAATTGTCCGCA
	Reverse:	ACCACCATCTGAGGCGTATT
VDR	Forward:	CTTCAGGCGAAGGCATGAAGC
	Reverse:	CCTTCATCATGCCGATGTCC
Runx2	Forward:	ACTTCCTGTGCTCGGTGCT
	Reverse:	GACGGTTATGGTCAAGGTGAA
Col-1	Forward:	CACTGGTGATGCTGGTCCTG
	Reverse:	CGAGGTCACGGTCACGAAC
BSP2	Forward:	TTGGGAAAACCACCACCGTT
	Reverse:	CTCGGTAATTGTCCCCACGA
OPN	Forward:	GTACCCTGATGCTACAGACG
	Reverse:	TTCATAACTGTCCTTCCCAC
GAPDH	Forward:	ACCCACTCCTCCACCTTTGAC
	Reverse:	TGTTGCTGTAGCCAAATTCGTT

4.2.7   Western blotting

Treated cells were lysed with lysis buffer (10 μl/10^5 cells) supplemented with 1mM phenylmethyl sulfonyl fluoride (PMSF) as a protease inhibitor. 30 μg proteins of each sample were loaded and separated in a 10% SDS-PAGE, followed by transferring onto polyvinylidene fluoride (PVDF) membranes (Millipore, USA). The proteins on membranes were blocked with 5 % milk for 1 hour at room temperature and incubated with following primary antibodies overnight at 4°C: rabbit anti-CYP27B1 (1:1000, Invitrogen), rabbit anti-osteopontin (1:1000, Invitrogen), or mouse anti-β-Actin (1:5000, Abcam). followed by IgG-HRP-conjugated secondary antibodies anti-rabbit (1:3000, Abcam) or anti-mouse (1:3000, Invitrogen) for 1h at room temperature. Washing with tris-buffered saline with 0.1% Tween 20 detergent (TBST) for 3 times was required between each of incubation. Finally, the blotting was probed and visualized with Clarity^{TM} Western ECL substrate (Bio-Rad, USA) using Azure^{TM} C600 (Azure Biosystems, USA). The relative intensities of the bands were quantified by Image J software (National Institutes of Health, USA) and normalized with β-actin.

4.2.8   Statistical analysis

Data from all experiments were demonstrated as mean ± standard error of mean (SEM) for each treatment group. Inter-group differences were analyzed by one-way analysis of variance (ANOVA) followed by Tukey's Test for multiple comparisons (GraphPad Prism 8.0, USA). A *P* value of less than 0.05 was considered statistically significant.

4.3 Results

4.3.1 Effects of OA on osteogenesis of human mesenchymal stem cells (hMSCs)

4.3.1.1 Osteogenesis of hMSCs

Firstly, osteogenic differentiation of hMSCs were assessed by visualization of the cellular morphology during the process of osteoblastogenesis. As shown in Fig. 4.1 A, under the light microscope with magnification of 200x, hMSCs distributed evenly with an irregular shape at the very beginning of differentiation. In the first week of osteogenic induction, cells with fibroblast-like shape formed gradually. Also, the collagen matrix began to be produced in the second week. Upon induction for 3 weeks, cells aggregated in a spiral shape with extracellular matrix mineralized, indicating the maturation and mineralization of cells.

The patterns of expressions of osteogenic markers confirmed the osteogenic differentiation of hMSCs. A significant increase in the expression of osteoprogenitor marker runt-related transcription factor 2 (Runx2) for 1.9-fold was found in hMSCs upon osteogenic induction for 7 days, suggesting the commitment of hMSCs into osteoprogenitors (Fig. 4.1 B, $P < 0.05$ vs. Day 0). Also, the expression of Runx2 increased continuously in cells throughout the osteogenesis of hMSCs. The expression of collagen type 1 (Col-1) in cells reached highest levels (Fig. 4.1 B, $P < 0.001$ vs. Day 0) after two weeks of osteogenic differentiation, implicating the formation of osteoblasts. Simultaneously, mRNA expression of bone sialoprotein (BSP) and osteopontin (OPN) were also significantly elevated for 3-fold (Fig. 4.1 B, $P < 0.01$ vs. Day 0) and 17-fold (Fig. 4.1 B, $P < 0.001$ vs. Day 0), respectively. The highest expression levels of BSP ($P < 0.001$ vs. Day 0) and OPN ($p < 0.001$ vs. Day 0) in cells were reached after osteogenic differentiation for 3 weeks.

4.3.1.2 Effects of OA on osteogenesis at different osteogenic stages of hMSCs

To characterize the effects of OA on osteogenesis at different osteogenic stages, mRNA expressions of osteoblastic markers in response to OA upon osteogenic differentiation

of hMSCs for 7, 14 and 21 days were evaluated. The results were showed in Fig. 4.2. Neither PTH nor OA posed significant alteration on mRNA levels of Runx2, the osteoprogenitor-related transcription factor, at the early stages of osteogenesis of hMSCs. When the differentiation proceeded to day 21, the mRNA expression level of Runx2 was significantly upregulated in differentiated cells by OA (100 nM) for 1.3-fold (Fig. 4.2 A, $P < 0.01$ vs. Control of Day 21), but not by PTH.

mRNA expressions of the osteoblastic marker Col-1 in hMSCs were not altered by treatment of PTH or OA, at the very beginning or after differentiation for 1 week. Co-I expression level was significantly increased in hMSCs in response to PTH (100 nM) or OA (10 nM) for 1.2-fold upon osteogenic differentiation for 14 days (Fig. 4.2 B, $P < 0.05$ vs. Control of Day 14). Although the basal expression level of Col-1 in the last week decreased slightly compared with the second week, its level was still markedly upregulated by PTH (100 nM) for 1.5-fold ($P < 0.001$ vs. Control of Day 21), or by OA (10-1000 nM) for more than 1.3-fold ($P < 0.05$ vs. Control of Day 21).

BSP2 and OPN are the transcription factors largely expressed in the mature osteoblasts. PTH (100 nM) slightly increased mRNA expression of BSP2 after 7 and 14 days and significantly elevated in hMSCs for 1.8-fold (Fig. 4.2 C, $P < 0.001$ vs. Control of Day 21) by 21 days of osteogenic differentiation. Acting like PTH, OA (10, 100 nM) significantly increased BSP2 expression for 1.7-fold ($P < 0.01$ vs. Control of Day 14) and 1.8-fold ($P < 0.001$ vs. Control of Day 21) in the last two weeks, respectively. With the elevation of OPN in the last phases, not only PTH (100 nM) (Fig. 4.2 D $P < 0.01$) but also OA (1-100 nM) (Fig. 4.2 D $P < 0.05$) significantly improved its mRNA expression compared to the corresponding control groups.
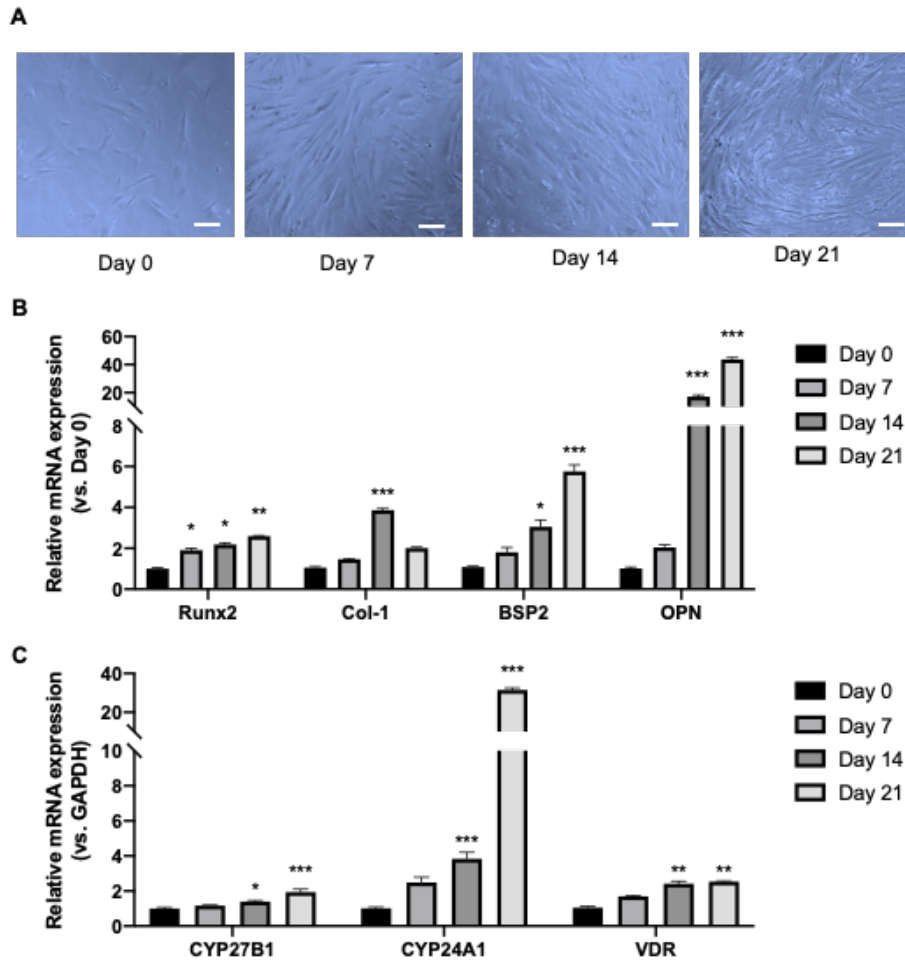
Fig. 4.1 Cellular morphology (A) and mRNA expressions of osteogenic markers (B) and vitamin D metabolism enzymes (C) in human mesenchymal stem cells (hMSCs).

hMSCs from a 61-year-old female subject were incubated in osteogenic induction medium for 7, 14, 21 days to obtain osteoprogenitors, pre-osteoblasts, and mature osteoblasts, respectively. Cellular morphology was visualized by light microscope with magnification of 200x, scale bars: 100 μm. mRNA expressions of runt-related transcription factor 2 (Runx2), collagen type 1 (Col-1), bone sialoprotein 2 (BSP2), osteopontin (OPN), CYP27B1, CYP24A1 and vitamin D receptor (VDR) were determined by RT-PCR. Data are expressed as mean ± SEM, n=3. Differences between treatment group and control were analyzed by one-way ANOVA followed by Tukey's multiple comparison tests. * $P < 0.05$, ** $P < 0.01$, *** $P < 0.001$ vs. Day 0.
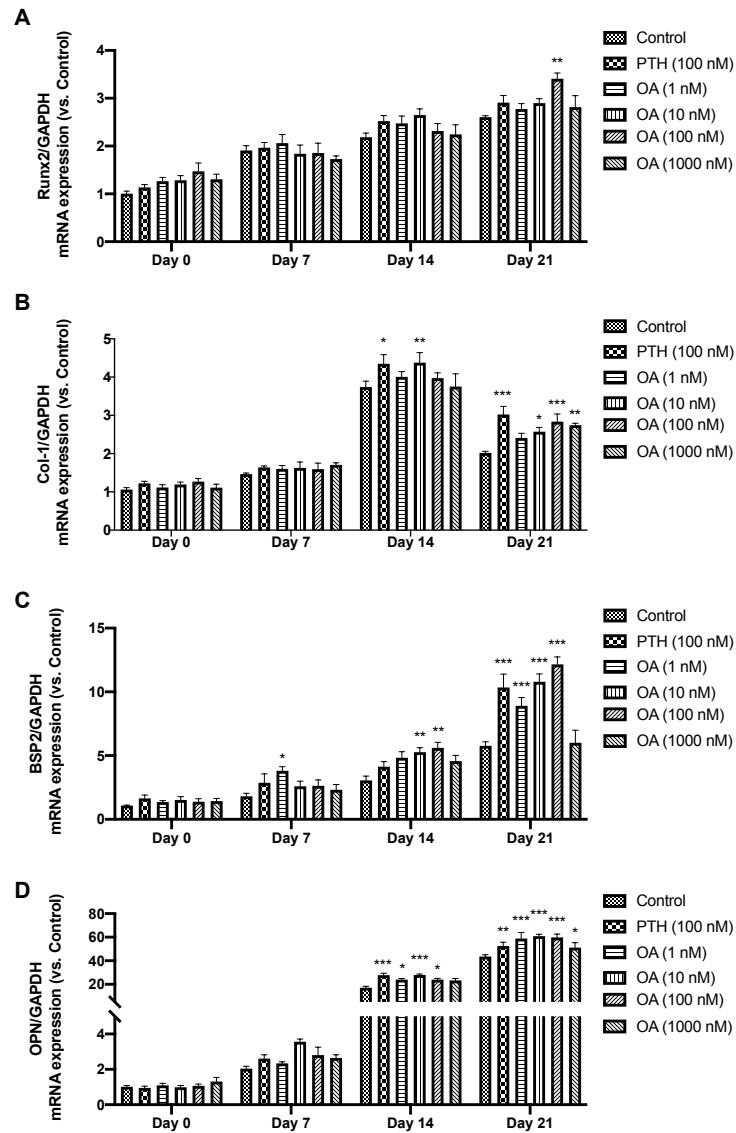
Fig. 4.2 Effects of OA on mRNA expressions of osteogenic markers during osteoblastic differentiation of human mesenchymal stem cells (hMSCs).

hMSCs from a 61-year-old female subject were incubated in osteogenic induction medium for 7, 14, 21 days to obtain osteoprogenitors, pre-osteoblasts, and mature osteoblasts, respectively. At each of osteogenic stages, cells were treated with parathyroid hormone (PTH, 100 nM) or OA (1, 10, 100, 1000 nM) for 24 hours. mRNA expressions of runt-related transcription factor 2 (Runx2, A), collagen type 1 (Col-1, B), bone sialoprotein 2 (BSP2, C) and osteopontin (OPN, D) were determined by RT-PCR. Data are expressed as mean ± SEM, n=3. Differences between treatment group and control were analyzed by one-way ANOVA followed by Tukey's multiple comparison tests. * $P < 0.05$, ** $P < 0.01$, *** $P < 0.001$ vs. control.

4.3.2   Effects of OA on CYP27B1 at different osteogenic stages of hMSCs

4.3.2.1 Basal expressions of vitamin D metabolism markers

Another focus of the present study was the expressions of enzymes involved in vitamin D metabolism as well as vitamin D receptor (VDR) along with the osteogenesis of hMSCs. As shown in Fig. 4.1 C, the expression of CYP27B1 mRNA appeared to increase in hMSCs upon osteogenic differentiation. Compared with the first week of osteogenesis, CYP27B1 expression levels in hMSCs elevated slightly by 40% ($P < 0.05$ vs. Day 0) in the second week and further by 90% ($P < 0.001$ vs. Day 0) in the last week. Also, expressions of CYP24A1 ($P < 0.001$ vs. Day 0) and VDR ($P < 0.001$ vs. Day 0) increased in hMSCs markedly during the last two weeks of osteogenic differentiation, they also reached the highest levels after differentiation for 21 days.

4.3.2.2 Effects of OA on CYP27B1, CYP24A1 and VDR during osteogenesis of hMSCs

By employing PTH (100 nM) as positive control, effects of OA on mRNA expressions of vitamin D metabolism enzymes as well as CYP27B1 activity at different osteogenic stages of hMSCs were evaluated. As shown in Fig. 4.3 A, mRNA levels of CYP27B1 were slightly but not significantly increased by PTH (100 nM) and OA (1, 10 nM) in hMSCs in the first week of osteogenic differentiation. At the second stage of osteogenesis, mRNA expression levels of CYP27B1 in hMSCs were markedly increased for 1.5-fold in response to 24-hour treatment of OA (10, 100 nM) ($P < 0.05$ vs. Control). 21 days after osteogenic induction, PTH significantly improved mRNA expression of CYP27B1 in hMSCs for 1.6-fold ($P < 0.001$ vs. Control). Similarly, OA (1-1000 nM) caused marked increase of CYP27B1 in hMSCs for more than 1.5-fold at days 21 ($P < 0.01$ vs. Control).

Intracellular production of $1,25(OH)_2D_3$ in response to PTH and OA in osteoblast lineages were evaluated by addition of adequate $25(OH)D_3$ (1 μM) to hMSCs at different osteogenic stages. Similar to the effects on CYP27B1 mRNA expression, PTH

and OA did not exert marked regulation of CYP27B1 activity until the later stages of osteogenic differentiation of hMSCs (Fig. 4.4). PTH significantly induced the biosynthesis of 1,25(OH)$_2$D$_3$ in hMSCs by 20% (P <0.01 vs. Control) at day 14 and 16% at day 21 (P <0.05 vs. Control). Similarly, OA (10-1000 nM) markedly improved CYP27B1 activity for more than 1.2-fold at the last two osteogenic stages in hMSCs.

With the differentiation of hMSCs, the expressions of CYP24A1 increased dramatically, and its response to PTH and OA also became obvious accordingly (Fig. 4.3 B). PTH tended to increase expressions of CYP24A1 at day 14, and also significantly elevated its level for 1.5-fold at day 21 (P <0.001 vs. Control). OA (1-1000 nM) also showed significant upregulation of CYP24A1 in the last two weeks (P <0.01 vs. Control). As showed in Fig. 4.3 C, the expressions of VDR also increased with the osteogenesis of hMSCs. OA (10, 100 nM), but not PTH, markedly upregulated expressions of VDR in hMSCs for 1.3-fold (P <0.01 vs. Control). Moreover, mRNA levels of VDR were significantly induced in hMSCs in response to 24-treatment of PTH and OA (1-100 nM) (P <0.05).
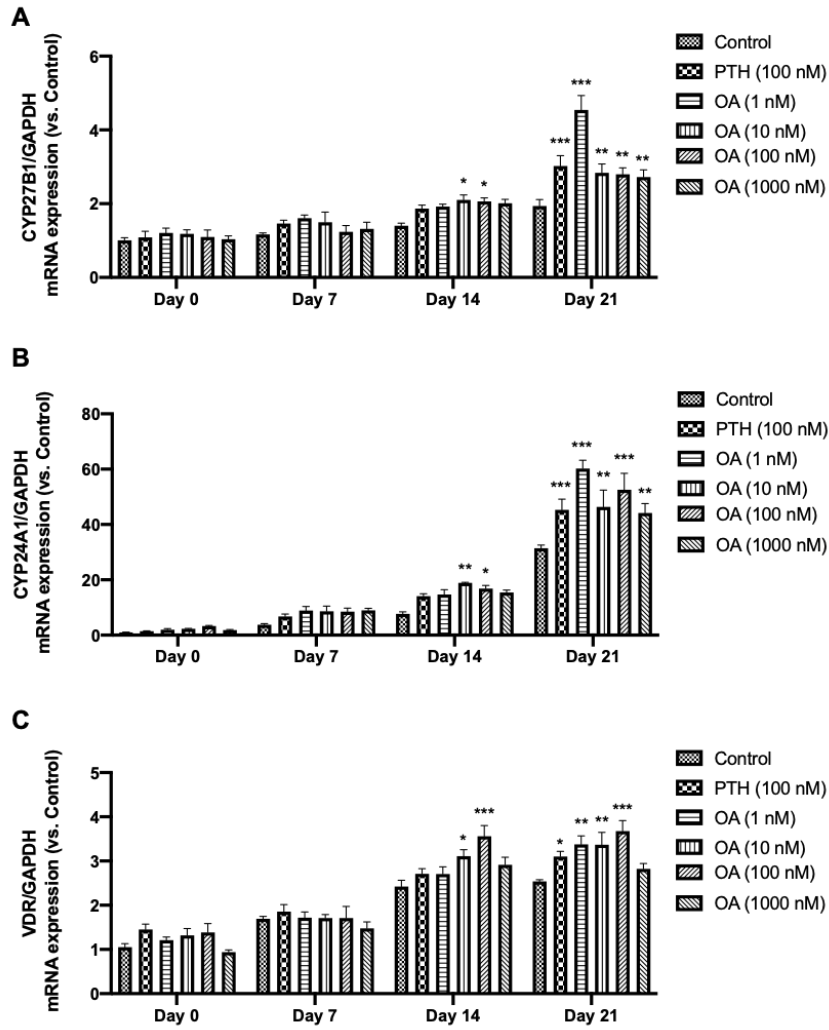
Fig. 4.3 Effects of OA on mRNA expressions of CYP27B1 (A), CYP24A1 (B) and vitamin D receptor (VDR) (C) during osteoblastic differentiation of human mesenchymal stem cells (hMSCs).

hMSCs from a 61-year-old female subject were incubated in osteogenic induction medium for 7, 14, 21 days to obtain osteoprogenitors, pre-osteoblasts, and mature osteoblasts, respectively. At each of osteogenic stages, cells were treated with parathyroid hormone (PTH, 100 nM) or OA (1, 10, 100, 1000 nM) for 24 hours. mRNA expression levels were determined by RT-PCR. Data are expressed as mean ± SEM, n=3. Differences between treatment group and control were analyzed by one-way ANOVA followed by Tukey's multiple comparison tests. * $P < 0.05$, ** $P < 0.01$, *** $P < 0.001$ vs. control.
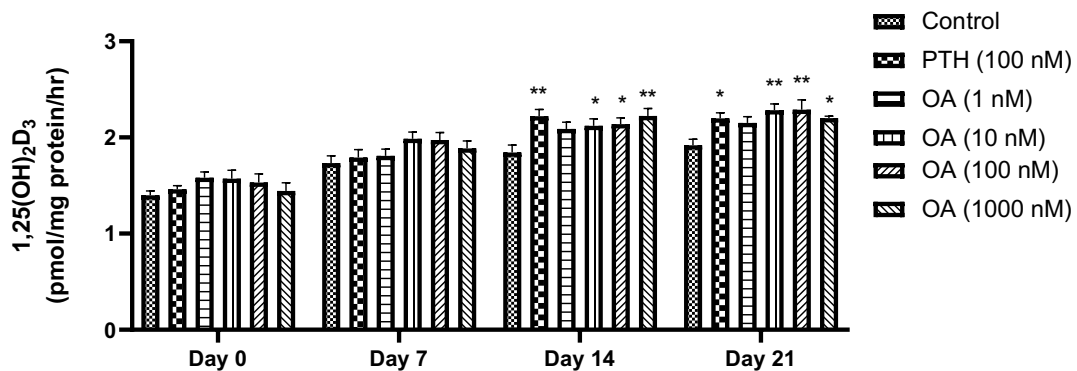
Fig. 4.4 Effects of OA on CYP27B1 activity during osteoblastic differentiation of human mesenchymal stem cells (hMSCs).

hMSCs from a 61-year-old female subject were incubated in osteogenic induction medium for 7, 14, 21 days to obtain osteoprogenitors, pre-osteoblasts, and mature osteoblasts, respectively. At each of osteogenic stages, cells were treated with PTH (100 nM) or OA (1, 10, 100, 1000 nM) in phenol red-free and serum-free medium in supplementation of $25(OH)D_3$ (1 μM) as substrate and N, N'-diphenylethylene-diamine (10 μM) as antioxidant for 4 hours. The CYP27B1 activity was determined by measuring cellular secreted $1,25(OH)_2D_3$ in supernatant per hour. Data are expressed as mean ± SEM, n=3. Differences between treatment group and control were analyzed by one-way ANOVA followed by Tukey's multiple comparison tests. * $P < 0.05$, ** $P < 0.01$, *** $P < 0.001$ vs. control.

4.3.3 Role of CYP27B1 in osteogenic effects of OA in mature osteoblasts

4.3.3.1 Effects of OA on CYP27B1 and osteogenesis in MG-63 cells

To further confirm the osteogenic effects and regulation of CYP27B1 by OA in mature osteoblast lineages, the osteoblast-like MG-63 cells were employed. As shown in Fig. 4.5, OA (1-1000 nM) effectively upregulated protein expression of CYP27B1 by 20% after 24-hour treatment (P <0.05 vs. Control). On the other hand, $1,25(OH)_2D_3$ (10 nM) dramatically induced protein expression of OPN for 1.2-fold (Fig. 4.5 C, P <0.001 vs. Control) and improved ALP activity for 4-fold (Fig. 4.5 D, P <0.01 vs. Control), suggesting the stimulatory effects of $1,25(OH)_2D_3$ on osteogenesis of MG-63 cells. Similarly, OA (1-100 nM) showed significant osteogenic effects through increasing OPN expression for 1.2-fold (P <0.01 vs. Control) and inducing ALP activity for 1.3-fold (P <0.05 vs. Control).

4.3.3.2 Effects of OA on osteogenesis in MG-63 cells in supplementation of 25(OH)D$_3$

Serving as the substrate for enzymatic activity of CYP27B1, $25(OH)D_3$ increases intracellular production of $1,25(OH)_2D_3$ and exerts subsequent osteogenic activities in osteoblasts. To further evaluate the regulation of CYP27B1 by OA and its involvement in osteogenesis of osteoblasts, MG-63 cells were pre-treated with $25(OH)D_3$ before exposing to OA. As shown in Fig. 4.6, expression of CYP27B1 were significantly increased for 1.3-fold in response to $25(OH)D_3$ treatment (P <0.05 vs. Control). More importantly, OA (10-1000 nM) further enhanced this effect of $25(OH)D_3$ (P <0.01 vs. $25(OH)D_3$). In addition, treatment of $25(OH)D_3$ promoted osteogenesis of MG-63 cells by effectively upregulation of expression of OPN and ALP activity (P <0.01 vs. Control). Compared with $25(OH)D_3$ alone, addition of OA (10, 100 nM) markedly increased OPN expression by 25% (P <0.05), and also significantly increased ALP activity by 25% (P <0.05) in MG-63 cells.
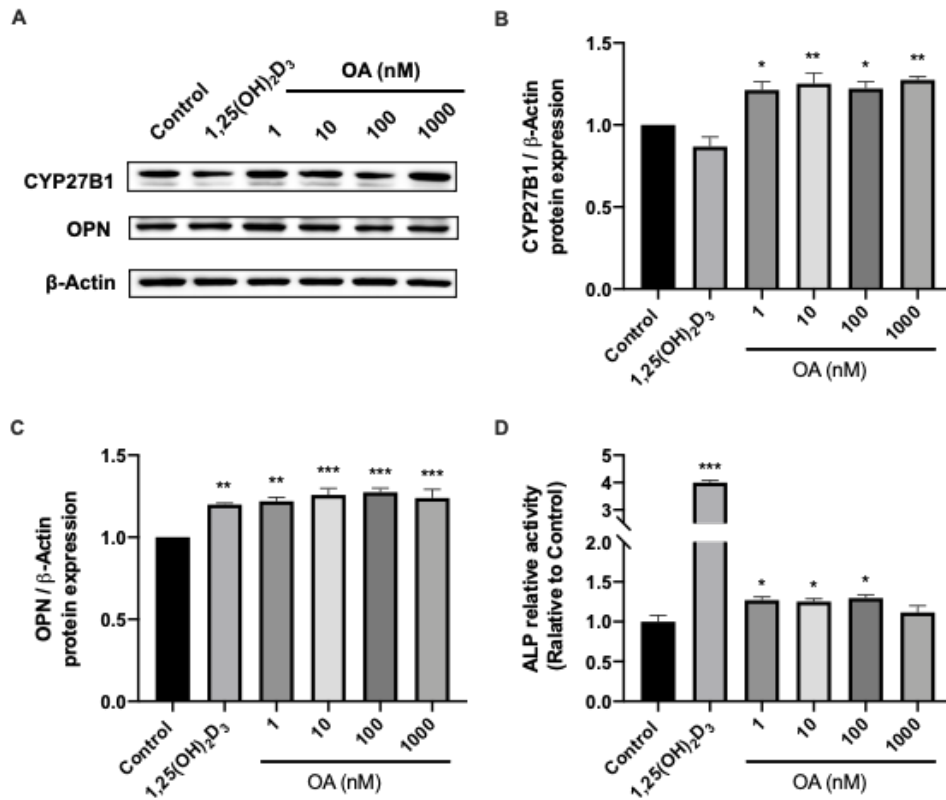
Fig. 4.5 Effects of OA on protein expressions of CYP27B1 (A, B) and osteopontin (OPN) (A, C), as well as alkaline phosphatase (ALP) activity (D) in MG-63 cells. Cells were exposed to 1,25(OH)₂D₃ (10 nM) or OA (1, 10, 100, 1000 nM) in phenol red-free medium for 24 hours, protein expressions of CYP27B1 and OPN were determined by Western blotting. ALP activity was determined after treatment of 1,25(OH)₂D₃ or OA for 7 days. Data are expressed as mean ± SEM, n=3. Differences between treatment group and control were analyzed by one-way ANOVA followed by Tukey's multiple comparison tests. $*$ $P < 0.05$, $**$ $P < 0.01$, $***$ $P < 0.001$ vs. control.
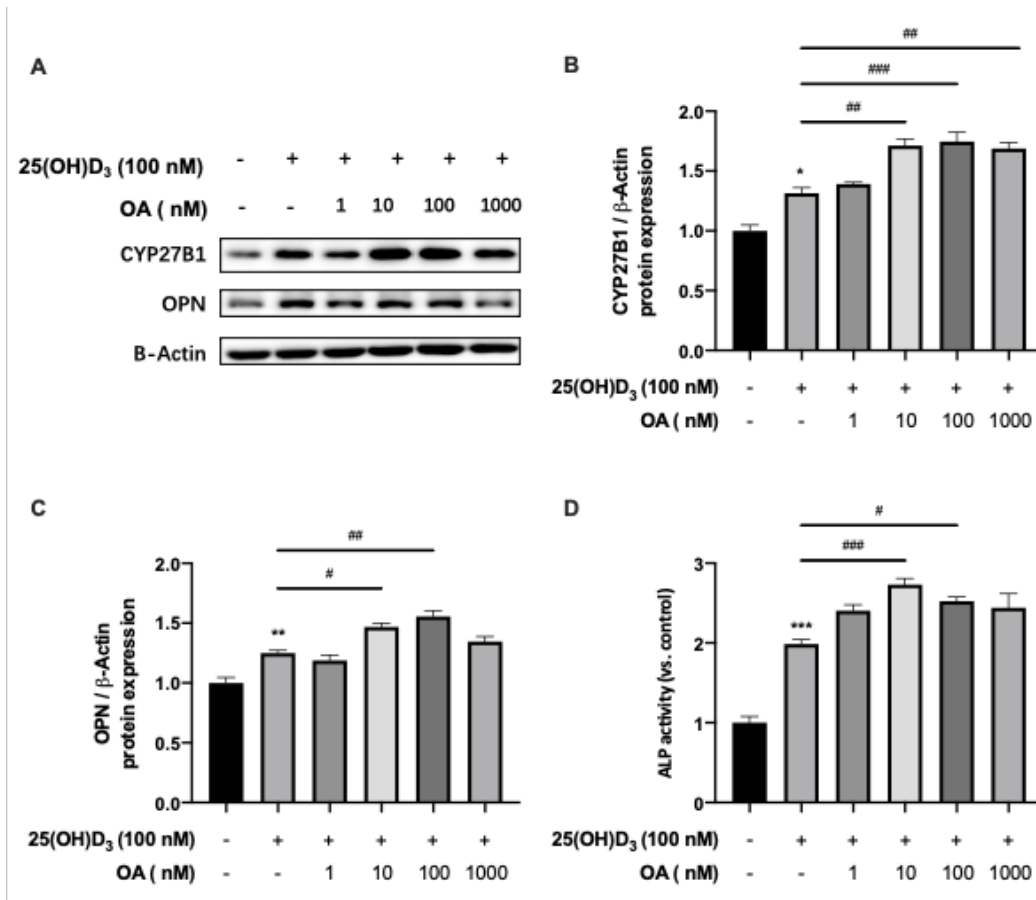
Fig. 4.6 Effects of OA on ALP activity (A) and protein expressions of CYP27B1 (B, C) and osteopontin (OPN) (B, D) in MG-63 cells in supplement with 25(OH)D₃. Cells were pre-treated with 25(OH)D₃ (100 nM) for 12 hours, followed by treatment of OA (1-1000 nM) for 7 days to determine responses of ALP activity. Protein expressions of CYP27B1 and OPN were determined in cells pre-treated with 25(OH)D₃ (100 nM) for 12 hours before further treatment with OA for another 24 hours. Data are expressed as mean ± SEM, n=3. Differences between treatment group and control were analyzed by one-way ANOVA followed by Tukey's multiple comparison tests. * $P < 0.05$, ** $P < 0.01$, *** $P < 0.001$ vs. control; # $P < 0.05$, ## $P < 0.01$, ### $P < 0.001$ vs. 25(OH)D₃.

4.3.3.3 Effects of OA on osteogenesis in MG-63 cells transfected with CYP27B1 siRNA

In the last part, the role of CYP27B1 in osteogenic effects of OA was determined in MG-63 cells with the knockdown of CYP27B1. Here 1 nM and 10 nM were selected as the optimal concentrations of OA, because these concentrations are within the range of serum levels of OA (10 ng/ml) after administration by healthy adults (Song et al., 2006). As shown in Fig. 4.7, transfection of CYP27B1 siRNA significantly silenced protein expression of CYP27B1 by 55% (P <0.01 vs. Non-silencing control siRNA), which showed the effective knockdown of CYP27B1. OA at 1 nM and 10 nM showed significant induction of CYP27B1 expression in cells transfected with non-silencing siRNA (P <0.01), while did not alter the CYP27B1 expression in cells in the presence of CYP27B1 siRNA. Also, the increased expression of CYP27B1 were markedly attenuated with the knockdown of CYP27B1 (P <0.001 vs. Non-silencing control siRNA). Similarly, transfection of CYP27B1 siRNA abolished the osteogenesis in MG-63 cells as revealed by decreased expression of OPN and ALP activity compared to the non-silencing control group (P <0.01). Moreover, the upregulated OPN expression and ALP activity in response to OA were significantly suppressed by knockdown of CYP27B1 in the cells (P <0.001). It seemed that when cells were transfected with CYP27B1 siRNA, OA failed to modulate expression of OPN or ALP activity, indicating the importance of CYP27B1 in the osteogenic effects of OA in MG-63 cells.
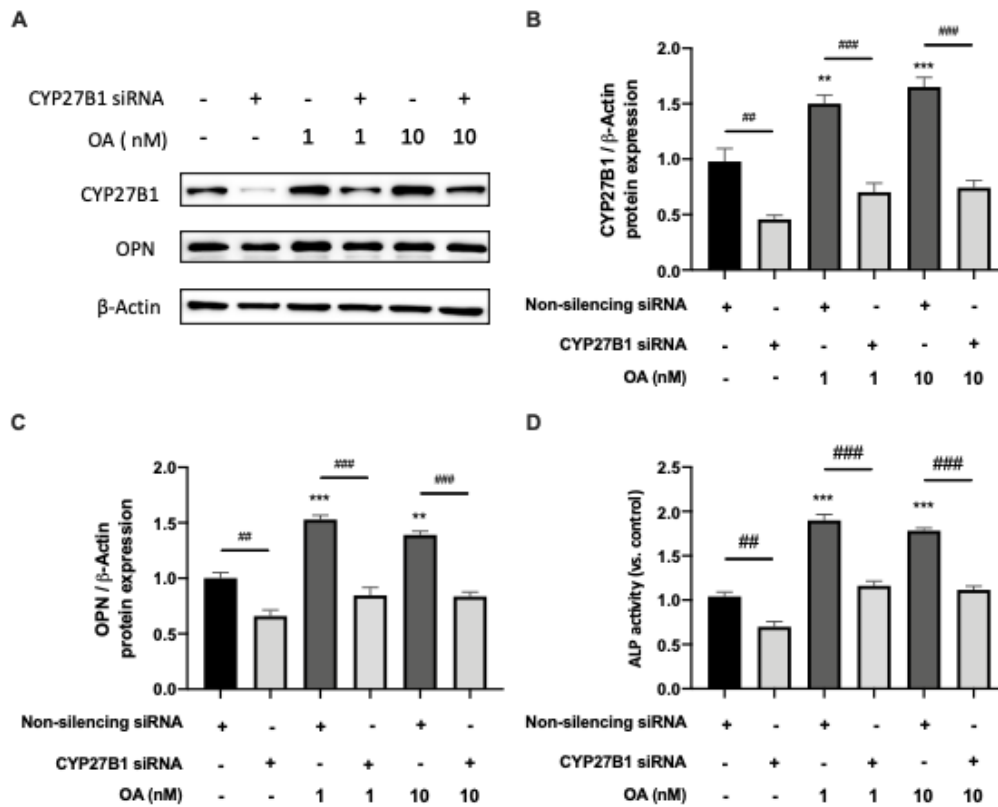
Fig. 4.7 Effects of CYP27B1 knockdown on protein expressions of CYP27B1 (A, B) and osteopontin (OPN) (A, C) and ALP activity (D) induced by OA in MG-63 cells.

Cells were transfected with non-silencing control siRNA or CYP27B1 siRNA for 48 hours. Protein expressions of CYP27B1 and OPN in response to OA in the presence or absence of CYP27B1 siRNA were determined in cells after treatment for 24 hours. ALP activity was determined in cells treated with OA (1, 10 nM) for 7 days. Data are expressed as mean ± SEM, n=3. Differences between treatment group and control were analyzed by one-way ANOVA followed by Tukey's multiple comparison tests. * $P <$ 0.05, ** $P < 0.01$, *** $P < 0.001$ vs. control; # $P <0.05$, ## $P < 0.01$, ### $P < 0.001$ vs. treatment group transfected with Non-silencing control siRNA.

4.4 Discussion

The discovery of CYP27B1 in bone cells improved our understanding of the paracrine or autocrine activities of locally produced $1,25(OH)_2D_3$ in bone microenvironment. Among the bone cells, osteoblasts express CYP27B1 and also respond to $1,25(OH)_2D_3$ to mediate osteogenesis and bone mineralization. In this chapter, we attempted to characterize the expressions and enzymatic activity of CYP27B1 at different stages during the process of osteogenesis, and to further evaluate the involvement of endogenously produced $1,25(OH)_2D_3$ on osteogenic effects of OA by supplying cells with $25(OH)D_3$ or knockdown of CYP27B1 by utilizing siRNA.

Human and rodent mesenchymal stem cells (MSCs) derived from bone marrow are the multipotential cells which could give rise to osteoblasts, adipocytes, and chondrocytes (da Silva Meirelles et al., 2006). *In vitro*, with the induction of dexamethasone, β-glycerophosphate and ascorbic acid, MSCs could differentiate into osteoblastic lineage (Heng et al., 2004) The different stages of osteoblastogenesis are characterized by sequentially expressed osteogenic markers. During the first phase of osteogenesis induction, lineage expand by intensive proliferation thus give rise to a committed osteoprogenitor (Nakashima et al., 2002). Our results showed runt-related transcription factor 2 (Runx2), a master regulator that is required at both early and late stages of osteogenesis, is highly expressed in this process, and its expression increase continuously until the end of differentiation (Fig. 4.1). Following the lineage commitment, MSCs amplify the expressions of transcription factors engaged in osteogenesis, indicating their differentiation towards pre-osteoblasts. At this intermediate stage, cells take to secrete an extracellular matrix containing type 1 collagen (Col-1), osteocalcin, bone sialoprotein (BSP) as well as osteopontin (OPN), which were expressed under the control of Runx2 (Marie et al., 2015). BSP is a heavily glycosylated protein which serves as the nucleator for mineralization of the matrix (Bianco et al., 1991). OPN is a phosphorylated glycoprotein which has the affinity for calcium ions and hydroxyapatite (Somerman et al., 1987). Our results showed that

BSP2 and OPN increased their expressions at later stages of differentiation, which is consistent with their functions in osteoblast maturation and mineralization. Thereby, both the cellular morphology and the kinetics of osteogenic gene expressions confirmed the differentiation of hMSCs towards osteoblasts.

Our results showed a time-dependent increase of CYP27B1 expression as well as cellular production of $1,25(OH)_2D_3$ along with the process of osteogenesis of hMSCs, implicating the requirement of $1,25(OH)_2D_3$ for osteogenesis and functions of osteoblasts. Also, we and others (Olivares-Navarrete et al., 2012) showed the hMSCs improved their expressions of VDR following the osteogenic induction. Acting through binding to VDR, $1,25(OH)_2D_3$ modulate transcription of osteogenic factors including osteocalcin, collagen type 1, bone sialoprotein and osteopontin. However, responses of these factors to $1,25(OH)_2D_3$ differ at different differentiation stages of osteoblast lineage (Owen et al., 1991). For example, $1,25(OH)_2D_3$ acts via VDR and initiates production of OPN and OCN in osteoblasts at later stages, but not at early stages, of differentiation (Bikle, 2018). It is worth noting that most of these factors are matrix protein that engaged in the extracellular matrix mineralization and maturation of the osteoblasts (Donnelly et al., 2011). This is positively correlated with our results showing that there is a robust in expressions of BSP2 and OPN with increased expression of VDR at later stages of osteogenesis of hMSCs. Actions of $1,25(OH)_2D_3$ on osteogenic differentiation of hMSCs were also demonstrated by Lou et al. (2017), they showed supplementation of 10 nM $1,25(OH)_2D_3$ in osteogenic medium resulted in significant improvement of gene expressions of OPN and osteocalcin, but not Runx2, after 21 days of osteogenic differentiation of hMSCs.

Apart from $1,25(OH)_2D_3$, many hormonal factors are also reported to play a positive impact on functions of osteoblasts as well as osteogenesis of MSCs including IGF-1, PTH and PTHrP (Hock et al., 1990; Huang et al., 2010; White et al., 2005). Geng et al. (2011a) showed PTH at 100 nM improved CYP27B1 and the osteogenic responsiveness to $25(OH)D_3$ in hMSCs. Our results showed the effects of PTH on

CYP27B1 and osteogenesis were more marked at later stages, rather than the onset of osteogenic induction, although it seems that expressions of BSP2 and OPN were also upregulated by PTH in the first week of differentiation. Acting like PTH, OA significantly increased CYP27B1 expressions and cellular production of $1,25(OH)_2D_3$ with the formation of extracellular matrix. Given the physiological functions of $1,25(OH)_2D_3$ on systemic calcium and phosphate homeostasis, the paracrine or autocrine activity of $1,25(OH)_2D_3$ in osteoblasts seems regulate matrix deposition and mineral homeostasis by modulating matrix proteins such as BSP2, OPN and Col-1. This is supported by our results which showed elevated CYP27B1 expression as well as BSP2, OPN and Col-1 by PTH and OA at later osteogenic stages where higher levels of calcium and phosphate is required for bone formation.

We and others (Lou et al., 2017) noticed that the effective concentration of $1,25(OH)_2D_3$ *in vitro* (10 nM) is much higher than its physiological level as well as the intracellular synthesized level (0.03-0.14 nM) (Vieth et al., 2002). This variation between the exogenous and endogenous levels means that it is hard for osteoblasts to respond to the circulating $1,25(OH)_2D_3$ generated from renal proximal tubule cells, owing to the short half-life of $1,25(OH)_2D_3$ which is less than 4 hours (Boullata, 2010) as well as its inferior level than that required for osteogenesis. Moreover, the increased expression of CYP24A1 which is sensitive to the induction of $1,25(OH)_2D_3$ indicated that the intracellular synthesized $1,25(OH)_2D_3$ was enough to exert the biological effects in osteoblast lineages. In addition, regulation of systemic calcium homeostasis by $1,25(OH)_2D_3$ is prior of that in bone (Carmeliet et al., 2015). The excessive levels of $1,25(OH)_2D_3$ in circulation trigger the bone resorption in osteoclasts to maintain mineral homeostasis, in the condition of negative calcium balance (Maierhofer et al., 1983). In addition, the presence of CYP24A1 in osteoblasts prevent the toxicity induced by excessive intracellular $1,25(OH)_2D_3$ and maintain the optimal level of $1,25(OH)_2D_3$ to regulate anabolic activities of osteoblasts. These observations underlined that with optimal levels, locally produced $1,25(OH)_2D_3$ plays significant role in the osteogenesis and mineralization of osteoblasts. Lending support to this concept, our results showed

97

OA improved locally produced $1,25(OH)_2D_3$ at later osteogenic stages and thus modulated the expressions of vitamin D-regulated osteogenic genes in osteoblast lineages, emphasizing the importance of osteoblastic CYP27B1 in mediating the regulatory effects of OA.

To further confirm the involvement of CYP27B1 in osteogenic effects of OA in mature osteoblasts, we determined protein expression of OPN as well as ALP activity which is a generally used marker for osteogenesis, in human osteosarcoma MG-63 as these cells consistently express CYP27B1 as well as osteogenic markers for mature osteoblasts (Atkins et al., 2007; Pautke et al., 2004). Our results showed OA not only markedly upregulated CYP27B1 expression, but also act like $1,25(OH)_2D_3$ to improve the expression of OPN and ALP activity in mature osteoblasts. By using of CYP27B1 siRNA which silenced expression of CYP27B1 at a post-translational level, our results showed OA failed to induce OPN expression as well as ALP activity in the absence, or at least in part, of CYP27B1 in MG-63 cells. Again, these results emphasized the importance of cellular production of $1,25(OH)_2D_3$ induced by OA in the osteogenesis of mature osteoblast.

Lou et al. (2017) in their study showed that the presence of $25(OH)D_3$ in osteogenic medium improved osteogenesis and mineralization of MSCs by improving ALP, OPN and osteocalcin. By supplement of $25(OH)D_3$ in culture medium, we attempted to mimic the physiological condition and determine the effects of OA on vitamin D metabolism as well as osteogenesis of osteoblasts. In line with previous study (Atkins et al., 2007), our results showed exposure of mature osteoblastic cells to the physiological levels of $25(OH)D_3$ resulted in not only the upregulation of CYP27B1 but also the induction of $1,25(OH)_2D_3$ responsive markers in these cells. More importantly, these induction by $25(OH)D_3$ were further enhanced by adding of OA as revealed by elevated OPN expression as well as ALP activity. Considering the reduced bone mass and osteogenesis of osteoblasts with ageing, which has been associated with reduced expression of CYP27B1 in osteoblast lineages, treatment of OA could, at least

in part, increase the activity of CYP27B1 thus to improve osteogenesis of osteoblasts in ageing adults.

Taken together, our results showed an increased expression of CYP27B1 along with the process of osteogenic differentiation of hMSCs. Treatment of OA further enhanced the expression of CYP27B1 as well as cellular production of $1,25(OH)_2D_3$ at later stages rather than the early stages of osteogenic differentiation, which in turn improved the expressions of $1,25(OH)_2D_3$ responsive genes including Col-1, BSP2 and OPN in mature osteoblast lineage. These findings provided evidence for the differential regulation of paracrine or autocrine activity of $1,25(OH)_2D_3$ at different osteogenic stages of osteoblasts. Moreover, the locally produced $1,25(OH)_2D_3$ by CYP27B1 is essential in mediating the osteogenic effects of OA by facilitating the maturation and mineral homeostasis in osteoblasts.

Chapter 5

Investigation of the potential mechanism mediating the effects of oleanolic acid on osteoblastic 25-hydroxyvitamin D 1-alpha-hydroxylase (CYP27B1)

5.1 Introduction

Since the critical role of this enzyme in biosynthesis of $1,25(OH)_2D_3$ was identified by Fraser et al. (1970), numerous studies focused on the regulation of its expression and activity in kidney. Parathyroid hormone (PTH) was reported to directly regulate transcription of CYP27B1 through a cyclic adenosine monophosphate (cAMP) transduction mechanism (HENRY et al., 1989). PTH binds to its membrane receptor (commonly known as PTHR1), a G protein-coupled receptor (GPCR), and results in the activation of Gs and production of cAMP and subsequent initiation of protein kinase A (PKA) and the phosphorylation of cAMP-responsive elements-binding protein (CREB) (Brenza et al., 1998). In mesenchymal stem cells (MSCs), the regulation of CYP27B1 seems to be similar to that in kidney cells. Geng et al. (2011a) has reported that CYP27B1 acutely responded to the stimulation of PTH via phosphorylation of CREB in human MSCs.

Van der Meijden et al. (2016) showed that CYP27B1 in primary human osteoblasts responded differently to classic regulators of renal CYP27B1 such as PTH, calcitonin and calcium, suggesting that the regulation of CYP27B1 in osteoblasts is different from that in kidney. Our previous study demonstrated that oleanolic acid (OA), a naturally occurring pentacyclic triterpenoid compound, managed to improve circulating $1,25(OH)_2D_3$ and calcium balance by regulating renal CYP27B1 expression and activities (Cao et al., 2018). More importantly, we also found OA markedly increased maturation and mineralization of osteoblast lineages. These actions were associated with its upregulation of CYP27B1 expression and locally synthesis of $1,25(OH)_2D_3$ in mature osteoblasts. However, the mechanism by which OA regulates osteoblastic CYP27B1 remains unclear.

Three potential cAMP-responsive elements (CRE) sites were identified in the promoter of CYP27B1, which were found to mediate the direct regulation of CYP27B1 transcriptional activity by cAMP. Based on these findings, forskolin, a specific inducer

for cAMP, was shown to stimulate CYP27B1 promoter activity and mRNA expressions in kidney cells (Armbrecht et al., 2003; Brenza et al., 2000). Similarly, the promoter activity and mRNA level of CYP27B1 was significantly increased when the kidney cells were incubated with a cAMP analog 8-Bromo-cAMP (Armbrecht et al., 2003). However, the involvement of cAMP-activated pathway in regulating CYP27B1 in osteoblasts remains unclear.

Takeda G-protein coupled receptor 5 (TGR5), encoded by GPBAR1 gene, is a member of GPCR superfamily. It was reported to initiate intracellular signaling by inducing the production of cAMP upon activated by bile acids such as lithocholic acid (LCA) (Fiorucci et al., 2009). Since it was discovered in 2002, TGR5 has been identified to be ubiquitously expressed in various tissues such as kidney, intestine, gall bladder and bone (Duboc et al., 2014). TGR5 is recently recognized as a potential target to moderate different human diseases due to its role as a pleotropic regulator in bile acids homeostasis, energy metabolism, glucose metabolism, as well as the inflammatory response (Jin et al., 2021). With a structure resembling that of LCA, OA has been identified as an agonist of TGR5 in a CRE-driven luciferase reporter assay based on studies using Chinese Hamster Ovary (CHO) cell line transfected with TGR5 expression plasmid (Sato et al., 2007). Thus, it is of interest to determine whether TGR5 is involved in mediating the effects of OA on CYP27B1 expression.

In the present chapter, we attempted to delineate role of TGR5 in mediating the regulatory effects of OA on CYP27B1 in osteoblasts. We first determined the time-dependent response of CYP27B1 expression to the treatment of OA. Based on the findings, we speculated that OA might regulate CYP27B1 expression via activation of acute signaling. To test the hypothesis, we determined the impact of TGR5 on CYP27B1 expressions by transfection of TGR5 overexpression plasmid or TGR5 siRNA. Finally, the involvement of CREB signaling in the regulation of CYP27B1 in osteoblasts were determined.

5.2 Methodology

5.2.1 Experimental design

The time course of the response of CYP27B1 expression to the treatment of OA was determined by RT-PCR and Western blotting analysis in human osteosarcoma MG-63 cells. To characterize the impact of activation of TGR5 on the expression and activity of CYP27B1, cells were treated with lithocholic acid (LCA) which has been identified as a specific TGR5 agonist. We also overexpressed or silenced TGR5 by transfection of a TGR5 cDNA vector or TGR5 siRNA in cells, respectively, to evaluate the dependence of CYP27B1 induced by OA on TGR5. To further determine the underlining mechanisms, the regulatory effects of phosphorylation of CREB on the promoter activity and protein expression of CYP27B1 were determined by using a chemical blocker for TGR5.

5.2.2 Cell culture and treatment

MG-63 cells were cultured in DMEM supplemented with 10% heat-inactivated FBS and 100 U/ml P/S in a humidified incubator with 5 % CO_2 at 37 °C. Cells were sub-cultured twice every week. For the experiment, cells were seeded in six-well plates at a density of 2×10^5 cells/well, to allow reaching 80 % confluence 24 hours later. Culture medium were then replaced by phenol red-free DMEM with 1% charcoal-striped FBS. 24 hours after changing medium, cells were treated with OA or LCA for relevant experiments.

5.2.3 CYP27B1 activity

Cells were seeded in 12-well plates until 80% confluence. The culture medium was then changed to a phenol red-free and serum-free medium to minimize the interference from sterols for 24 hours before the treatment. Then cells were treated with LCA in the presence of $25OHD_3$ (1 μM) as a substrate and N, N'-diphenylethylene-diamine (1, 2-dianilinoethane, 10 μM) as an antioxidant (Schwartz et al., 1998). Upon incubation for

4 hours, the reaction was terminated by placing the plates on ice. The CYP27B1 activity was evaluated by determining the cellular secreted $1,25(OH)_2D_3$ in culture medium (Geng et al., 2011a). Concentrations of $1,25(OH)_2D_3$ in supernatant was qualified with $1,25(OH)_2D_3$ ELISA kit by following manufacturer's instruction (Immundiagnostik AG). To normalize the $1,25(OH)_2D_3$ levels, contents of protein in cells were determined by Bradford assay (Bio-Red, CA, USA).

5.2.4 Overexpression of human GPBAR1 (TGR5) gene

To study the relationship between TGR5 and CYP27B1 expressions in osteoblasts, cells were transfected with a human GPBAR1 gene open reading frame (ORF) cDNA clone expression plasmid (Sino Biological, China). For transfection, cells were seeded in 6-well plates to reach 80% confluence. TGR5 expression plasmid (4 μg/well) and a negative control plasmid (pCMV3) (4 μg/well) were transfected by combining with Lipofectamine^{TM} 2000 reagent (Invitrogen, USA) (4 μL/well) in antibiotics-free medium for 48 hours. The medium was then replaced with phenol red-free DMEM and cells were treated with OA (1-10 nM) for 2 hours. The transfection efficiency and response of OA were determined by studying the protein expression of TGR5 analyzed by Western blotting.

5.2.5 RNA interference with TGR5 siRNA

To verify if TGR5 could mediate the effects of OA on CYP27B1 expression in osteoblasts, MG-63 cells were transfected with a pool of 4 independent small interfering RNAs (siRNAs) to silence the expression of TGR5. Cells were seeded in 6-well plates until reaching 80% confluence. Transfection was conducted by adding 25 nM SmartPool for human GPBAR1 (TGR5) specific siRNAs (Dharmacon, USA) or non-silencing control siRNA (Dharmacon, USA) with 4 uL/well Dharma-Fect-3 reagent (Dharmacon, USA) according to the manufacturer's instructions. 48 hours after transfection, cells were treated with OA for a further 2 hours. Knockdown of TGR5

was confirmed by studying their mRNA and protein expression using RT-PCR and Western blotting.

5.2.6 Dual luciferase reporter assay

To determine the effects of OA on transcriptional activity of CYP27B1 promoter, MG-63 cells were seeded in 24-well plates until reaching 80%. Cells were transiently transfected with CYP27B1-promoter construct which contains a full-length insert of 1567bp CYP27B1 promoter region in pGL-3 vector. Transfection was conducted by combining the CYP27B1 promoter plasmid (0.4 μg/well) and constitutive thymidine kinase plasmid (Promega, USA) (0.1 μg/well), an internal control for normalization of efficiency of transfection, with Lipofectamine™ 2000 reagent (Invitrogen, USA) (1 μL/well) in antibiotics-free medium for 6 hours. The medium was then replaced with phenol red-free DMEM and cells were pretreated with triamterene (100 nM) for 30 min followed by treatment with OA (1-10 nM) for 2 hours. Treated cells were lysed with Passive Lysis Bufer (Promega, USA) and subject to dual-luciferase reporter assay according to the protocol (Promega, USA).

5.2.7 RT-PCR

Cells were seeded in 6-well plates and treated with different concentrations of OA for 24 hours. Total RNA from treated cells was extracted in TRIzol reagent by following the manufacturer's instructions. 1 μg of RNA was applied for reverse transcription (RT) by using PrimeScript™ RT Master Mix (TaKaRa, Japan) in a 20 μl reaction system for cDNA generation. 500 ng of cDNA products and 0.4 μM primers were added to PCR reaction mixture containing TB Green Premix Ex Taq II (TaKaRa, Japan). Real-time PCR was performed in 7900HT Fast Real-Time PCR System (Applied Biosystems, Carlsbad, CA, USA) under the amplification conditions and procedures: initial denaturation at 95 °C for 30 s, 40 cycles of denaturation at 95 °C for 1 s and 60 °C for 20 s. The sequences of primers for target genes and the housekeeping gene

glyceraldehyde-3-phosphate dehydrogenase (GAPDH) are listed in Table 5.1. Relative gene expression was calculated by $2^{-\Delta\Delta CT}$ method.

5.2.8 Western blotting

Treated cells were lysed with lysis buffer (Beyotime, Shanghai, China) (10 μL/10^5 cells) supplemented with 1mM phenylmethyl sulfonyl fluoride (PMSF) as a protease inhibitor. 30 μg extracted proteins of each sample were loaded and separated in a 10% SDS-PAGE, followed by transblotting onto polyvinylidene fluoride (PVDF) membranes (Millipore, Danvers, USA). The proteins on membranes were blocked with 5 % milk for 1 hour at room temperature and incubated with following primary antibodies overnight at 4°C: rabbit anti-CYP27B1 (1:1000, Invitrogen, USA), rabbit anti-TGR5 (1:1000, Invitrogen, USA), mouse anti-p-CREB1 (1:500, Santa Cruz, USA), mouse anti-CREB1 (1:500, Santa Cruz, USA), or mouse anti-β-Actin (1:5000, Abcam, UK), followed by IgG-HRP-conjugated secondary antibodies anti-rabbit (1:3000, Abcam, UK) or anti-mouse (1:3000, Invitrogen, USA) for 1h at room temperature. Washing with tris-buffered saline with 0.1% Tween 20 detergent (TBST) for 3 times was required between each of incubation. Finally, the blotting was probed and visualized with Clarity™ Western ECL substrate (Bio-Rad, USA) using Azure™ C600 (Azure Biosystems, USA). The relative intensities of the bands were quantified by ImageJ software (National Institutes of Health, USA) and normalized with β-actin.

5.2.9 Statistical analysis

Data from both *in vivo* and *in vitro* experiment were shown as mean ± standard error of mean (SEM) for each treatment group. Inter-group differences were analyzed by one-way analysis of variance (ANOVA) followed by Tukey's Test for multiple comparisons (GraphPad Prism 8.0, USA). A *P* value of less than 0.05 was considered statistically significant.

Table 5.1 Primer sequences for human genes

Gene		Primer Sequence (5'-3')
CYP27B1	Forward:	AGAGTTGCTATTGGCGGGAG
	Reverse:	AGAACAGTGGCTGAGGGGTA
TGR5	Forward:	CAGTGTCGACCTGGACTTGA
	Reverse:	TAACGGCCAGAGGAGCTTTA
GAPDH	Forward:	ACCCACTCCTCCACCTTTGAC
	Reverse:	TGTTGCTGTAGCCAAATTCGTT

5.3 Results

5.3.1 Time course of CYP27B1 expression in response to OA

In the previous chapters, we demonstrated that OA at 1 nM upregulated expression and activity of CYP27B1 in MG-63 cells in 24 hours. The time-dependent effects of OA (1 nM) on CYP27B1 expression at transcriptional and translational levels were further determined in this chapter. As shown in Fig 5.1 A, the induction of CYP27B1 by OA was rapid and transient. OA significantly increased mRNA expression of CYP27B1 for 2.2-fold (P <0.001 vs. 0 h) within 1 hour of incubation, and this induction was maintained until 6 hours of incubation (P <0.05 vs. 0 h). For protein expression, there were two peaks of increase in CYP27B1 upon treatment with OA for 2 hours and 6 hours, with the fold changes of 1.6-fold (Fig. 5.1 B, P <0.001 vs. 0 h) and 1.4-fold (P <0.01 vs. 0 h), respectively. The result suggests that OA regulates CYP27B1 through rapid signaling cascade.
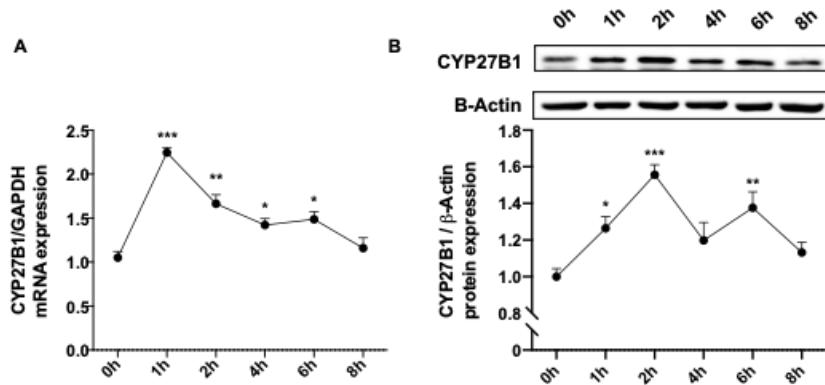
Fig. 5.1 Time course of effects of OA on mRNA (A) and protein (B) expressions of CYP27B1 in human osteosarcoma MG-63 cells.

MG-63 cells were treated with OA (1 nM) in phenol red-free medium for 1, 2, 4, 6, 8 hours. mRNA and protein expression levels of CYP27B1 were determined by RT-PCR and Western blotting, respectively. Data are expressed as mean $\pm$ SEM, n=3. Differences between time points were analyzed by one-way ANOVA followed by Tukey's multiple comparison tests. $*$ $P < 0.05$, $**$ $P < 0.01$, $***$ $P < 0.001$ vs. control.

5.3.2 Effects of TGR5 agonist on CYP27B1 expression

To evaluate if TGR5 activation could mediate the induction of CYP27B1 expression in osteoblasts, lithocholic acid (LCA), a well identified TGR5 agonist, was used as an induction agent. As shown in Fig 5.2, LCA appears to induce the expressions of TGR5 in MG-63 cell dose-dependently. LCA at 10 μM significantly improved mRNA levels of TGR5 for 7.2-fold (Fig. 5.2 A, P <0.001 vs. control) and its protein levels for 1.3-fold (Fig. 5.2 C, P <0.01 vs. control) in MG-63 cells upon treatment for 24 hours. In addition, the mRNA levels of CYP27B1 were significantly upregulated in response to LCA at 1μM for 1.9-fold (Fig. 5.2 B, P <0.001 vs. control) and at 10 μM for 3.2-fold (P <0.001 vs. control) in MG-63 cells. Similarly, the protein expression of CYP27B1 in MG-63 cells were markedly elevated by LCA (Fig. 5.2 D, P <0.01 vs. control). The cellular production of $1,25(OH)_2D_3$ in response to LCA were also evaluated in MG-63 cells in the presence of adequate levels (1 μM) of $25(OH)D_3$ (Fig. 5.3). Compared with cells treated with $25(OH)D_3$ alone, LCA at 1 μM and 10 μM significantly induced CYP27B1 activity to produce $1,25(OH)_2D_3$ by 29 % (P <0.01) in MG-63 cells. Thus, activation of TGR5 by LCA was positively associated with its induction of CYP27B1expression and activity in MG-63 cells.
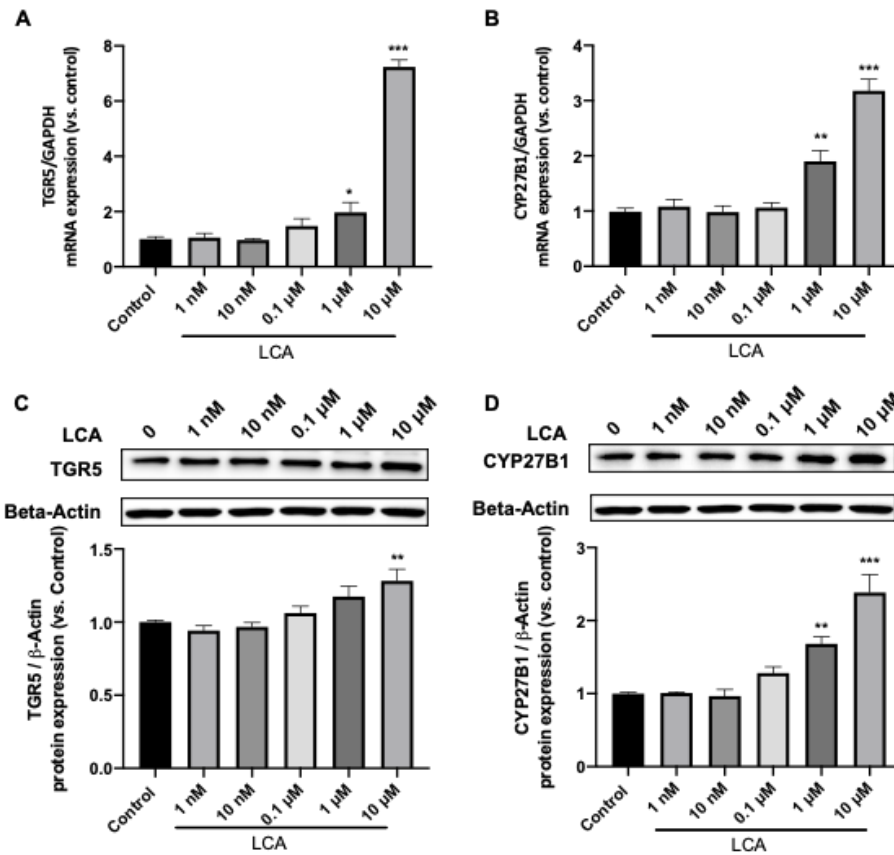
Fig. 5.2 Effects of lithocholic acid (LCA) on mRNA and protein expressions of TGR5 and CYP27B1 in human osteosarcoma MG-63 cells.

MG-63 cells were treated with lithocholic acid (LCA) (1, 10, 100, 1000, 10000 nM), in phenol red-free medium for 24 hours. mRMA expression levels of (A) TGR5 and (B) CYP27B1 were determined by RT-PCR. Protein expression levels of (C) TGR5 and (D) CYP27B1 were determined by Western blotting. Data are expressed as mean ± SEM, n=3. Differences between time points were analyzed by one-way ANOVA followed by Tukey's multiple comparison tests. * $P < 0.05$, ** $P < 0.01$, *** $P < 0.001$ vs. control.
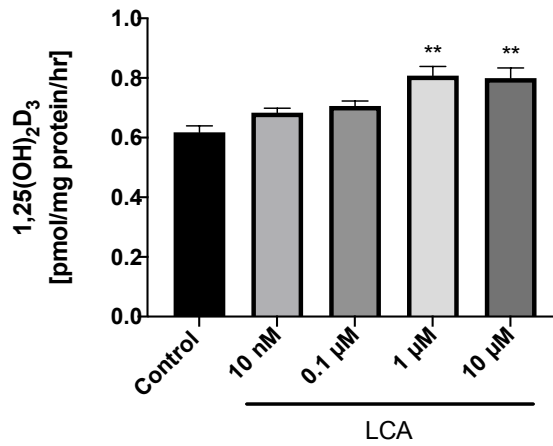
Fig. 5.3 Effects of lithocholic acid (LCA) on enzymatic activities of CYP27B1 in human osteosarcoma MG-63 cells.

Cells were treated with lithocholic acid (LCA) (10, 100, 1000, 10000 nM) in phenol red-free and serum-free medium in supplementation of $25(OH)D_3$ (1 μM) as substrate and N, N'-diphenylethylene-diamine (10 μM) as antioxidant for 4 hours. The CYP27B1 activity was determined by measuring cellular secreted $1,25(OH)_2D_3$ in supernatant per hour. Data are expressed as mean ± SEM, n=3. Differences between time points were analyzed by one-way ANOVA followed by Tukey's multiple comparison tests. ** $P <$ 0.01 vs. control.

5.3.3 Involvement of TGR5 in mediating effects of OA on CYP27B1 expression

5.3.3.1 Effects of OA on CYP27B1 expression in MG-63 cells transfected with TGR5 expression plasmid

To evaluate the role of TGR5 in mediating the effects of OA on CYP27B1 expressions in osteoblasts, MG-63 cells were transfected with a human TGR5 cDNA expression plasmid. As shown in Fig. 5.4, protein expression of TGR5 was successfully increased by 1.6-fold (P <0.01 vs. control plasmid) in MG-63 cells upon transfection with 4 μg TGR5 expression plasmid for 48 hours. More importantly, overexpression of TGR5 not only resulted in a marked induction of CYP27B1 in osteoblasts (P <0.05 vs. control plasmid), but also potentiated the effects of OA to induce CYP27B1 expression by 35% at 1 nM (P <0.05) and 43% at 10 nM (P <0.01) in MG-63 cells upon treatment for two hours, when compared to the corresponding treatment group transfected with pCMV-control plasmid. These results suggested the rapid effects of OA on CYP27B1 in MG-63 cells might be dependent on the level of membrane receptor TGR5 expression.

5.3.3.2 Effects of OA on CYP27B1 expression in MG-63 cells transfected with TGR5 siRNA

To further verify the role of TGR5 in mediating the effects of OA, MG-63 cells were transfected with TGR5 siRNA to interfere with the expression of TGR5, followed by studying the effects of OA on CYP27B1 expression (Fig. 5.5). Transient transfection of TGR5 siRNA significantly reduced mRNA and protein expressions of TGR5 in MG-63 cells by 38% (P <0.05 vs. Non-silencing control siRNA) and 46% (P <0.001 vs. Non-silencing control siRNA), respectively, indicating the effective knockdown of TGR5 in these cells. Treatment of OA at 1 nM and 10 nM for two hours significantly induced TGR5 mRNA expression for 1.35-fold (P <0.05) in MG-63 cells transfected with non-silencing siRNA but did not alter the TGR5 expression in cells in the presence of TGR5 siRNA. It is notable that transfection of TGR5 siRNA markedly attenuated the expression of CYP27B1 in MG-63 cells for more than 52% (P <0.001 vs. Non-

silencing control siRNA) at both transcriptional and translational levels. Moreover, the upregulated mRNA and protein expressions of CYP27B1 in response to OA were significantly suppressed by knockdown of TGR5 in MG-63 cells (P <0.001 vs. Non-silencing control siRNA).
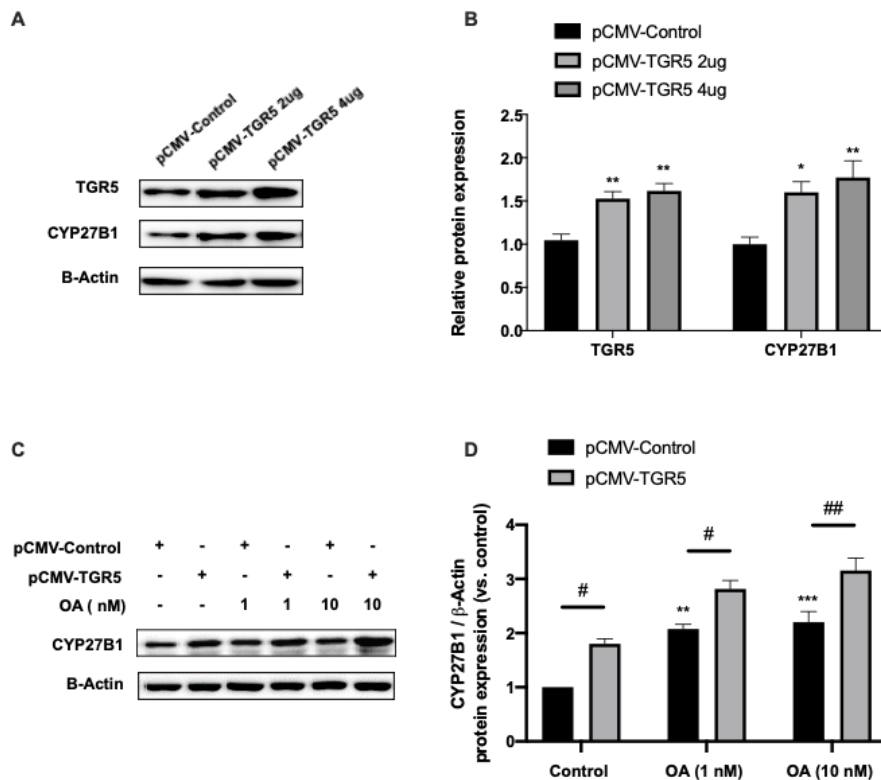
Fig. 5.4 Effects of OA on protein expression of CYP27B1 in human osteosarcoma MG-63 cells with TGR5 overexpression.

MG-63 cells were transfected with pCMV-Control plasmid or pCMV-TGR5 plasmid for 48 hours, followed by treatment of OA (1, 10 nM) for 2 hours. The transfection efficiency (A) and effects of OA (B) were determined by Western blotting. Data are expressed as mean ± SEM, n=3. Differences between time points were analyzed by one-way ANOVA followed by Tukey's multiple comparison tests. $*$ $P < 0.05$, $**$ $P < 0.01$, $***$ $P < 0.001$ vs. control; $\#$ $P < 0.05$, $\#\#$ $P < 0.01$ vs. treatment group transfected with pCMV-Control.
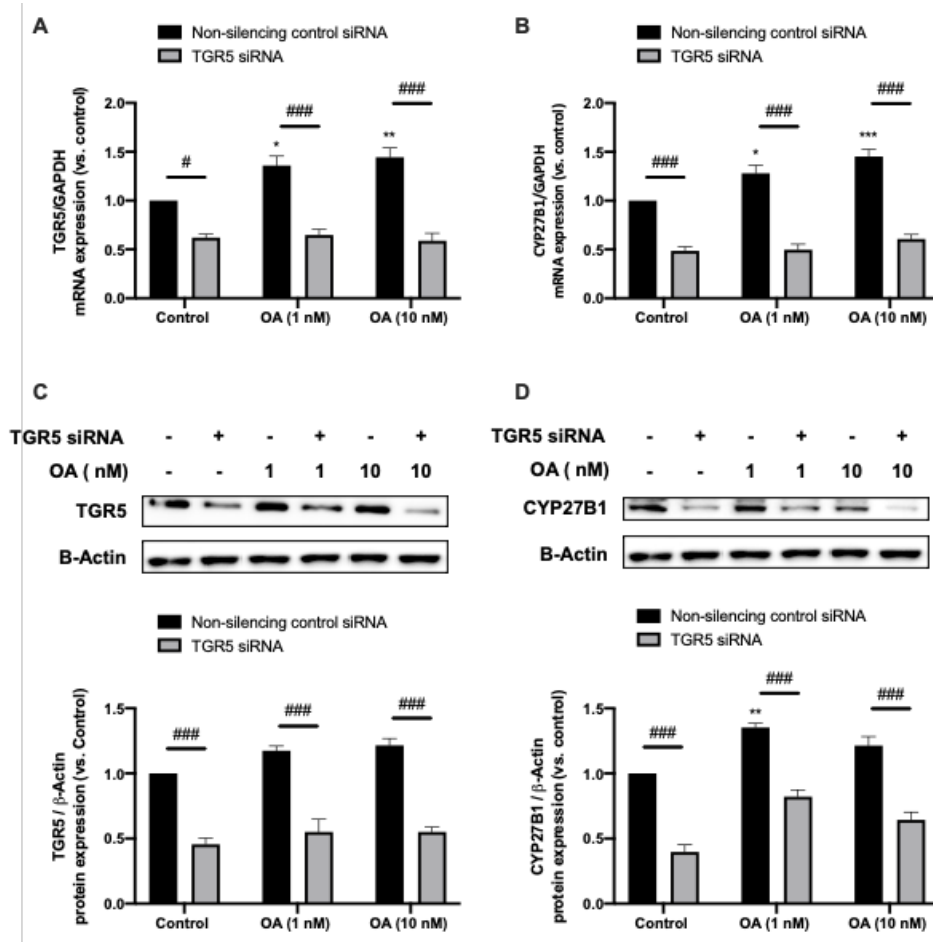
Fig. 5.5 Effects of OA on mRNA and protein expressions of TGR5 and CYP27B1 in human osteosarcoma MG-63 cells with TGR5 knockdown.

Cells were transfected with non-silencing control siRNA or TGR5 siRNA for 48 hours, followed by treatment of OA (1, 10 nM) for 2 hours. mRNA expressions of TGR5 (A) and CYP27B1 (B) in the presence or absence of CYP27B1 siRNA were determined by RT-PCR. Protein expressions of TGR5 (C) and CYP27B1 (D) in the presence or absence of CYP27B1 siRNA were determined by Western blotting. Data are expressed as mean ± SEM, n=3. Differences between treatment group and control were analyzed by one-way ANOVA followed by Tukey's multiple comparison tests. * $P < 0.05$, ** $P < 0.01$, *** $P < 0.001$ vs. control; # $P < 0.05$, ## $P < 0.01$, ### $P < 0.001$ vs. treatment group transfected with Non-silencing control siRNA.

5.3.4 Involvement of CREB signaling in mediating effects of OA on CYP27B1 expression

5.3.4.1 Time course of CREB phosphorylation and CYP27B1 expression

It has been reported that phosphorylation of CREB, a nuclear transcription factor, is one of the signaling pathway by which activated TGR5 modulates the expression of genes (Pearman et al., 1996). Hence, we assessed the time-dependent changes in phosphorylation of CREB and expression of CYP27B1 in MG-63 cells in response to OA treatment. As shown in Fig. 5.6, protein expression of TGR5 and total CREB were not significantly affected in MG-63 cells by treatment with OA. CREB phosphorylation was induced in MG-63 cells in response to treatment with OA (1 nM) at two time points. OA rapidly induced phosphorylation of CREB at 10 minutes of treatment for 1.2-fold (P <0.001 vs. 0 minute) and the induction continued to 30 minutes followed by a slow decline thereafter in MG-63 cells. A second induction of CREB phosphorylation by OA was observed at 120 minutes of treatment in MG-63 cells for 1.2-fold (P <0.001 vs. 0 minute). For CYP27B1, OA did not alter its expression in MG-63 cells until 90 minutes of incubation. OA (1 nM) markedly upregulated protein expressions of CYP27B1 in MG-63 cells for 1.3-fold (P <0.001) and 1.2- fold (P <0.01) at 90 minutes and 120 minutes, respectively. The results showed that the stimulation of CREB phosphorylation by OA preceded its induction of CYP27B1 protein expression in MG-63 cells, indicating the potential of OA to alter CYP27B1 transcription through induction of CREB phosphorylation.
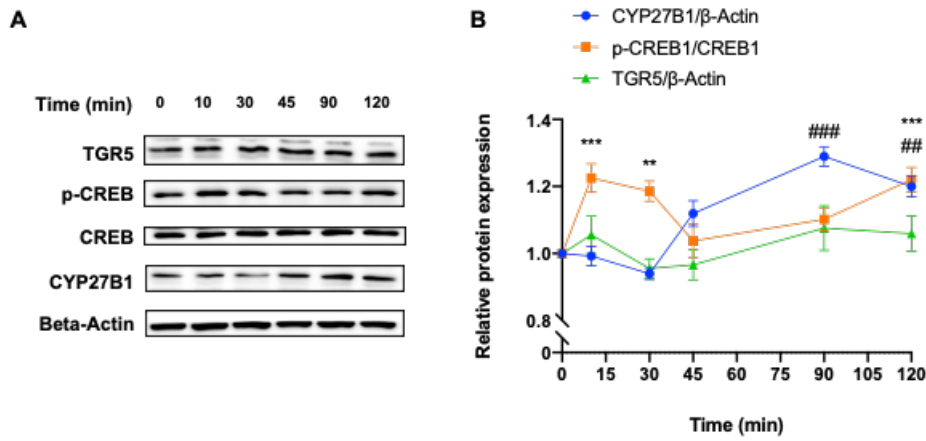
**Fig. 5.6 Time course of effects of OA on CREB phosphorylation and CYP27B1 in human osteosarcoma MG-63 cells.**

MG-63 cells were treated with OA (1 nM) in phenol red-free medium for 10, 30, 45, 90, 120 minutes. Protein expression levels of TGR5, phosphorylation of CREB and CYP27B1 were determined by Western blotting, respectively. Data are expressed as mean ± SEM, n=3. Differences between time points were analyzed by one-way ANOVA followed by Tukey's multiple comparison tests. ** $P < 0.01$, *** $P < 0.001$ vs. p-CREB at 0 minute; ## $P < 0.01$, ### $P < 0.001$ vs. CYP27B1 at 0 minute.

5.3.4.2 Effects of OA on CREB phosphorylation and CYP27B1 expression in the presence of TGR5 inhibitor

In the last part, we evaluated the role of TGR5 in inducing CREB phosphorylation and CYP27B1 expression by using a chemical inhibitor of TGR5. Triamterene has been identified as a chemical inhibitor of TGR5 *in vivo* and *in vitro* (Li et al., 2017). Our results showed that treatment of MG-63 cells with triamterene markedly decreased the promoter activity of CYP27B1 (Fig. 5.7, P <0.05 vs. control without inhibitor). Similarly, pre-treatment of triamterene significantly reduced basal expression of phosphorylated CREB and CYP27B1 (Fig. 5.8, P <0.05 vs. control without inhibitor) in MG-63 cells without altering the expression of TGR5. In the absence of triamterene pre-treatment, OA at 1 nM and 10 nM markedly increased phosphorylation of CREB in MG-63 cells for 1.4-fold (Fig. 5.8, P <0.01 vs. control without inhibitor). In addition, the promoter activity (Fig. 5.7) and protein expression (Fig. 5.8) of CYP27B1 were significantly elevated MG-63 cells upon treatment with OA for 2 hours (P <0.05 vs. control without inhibitor). However, when MG-63 cells were pretreated with triamterene, OA failed to induce phosphorylation of CREB and expression of CYP27B1. Inhibiting of TGR5 activation by triamterene significantly abolished the stimulatory effects of OA on CYP27B1, as revealed by the decreased expression of phosphorylated CREB (P <0.001) and CYP27B1 (P <0.001) when compared to each treatment group without inhibitor. Thus, our results suggested that OA might stimulate CYP27B1 transcription through the activation of TGR5 and subsequent CREB phosphorylation.
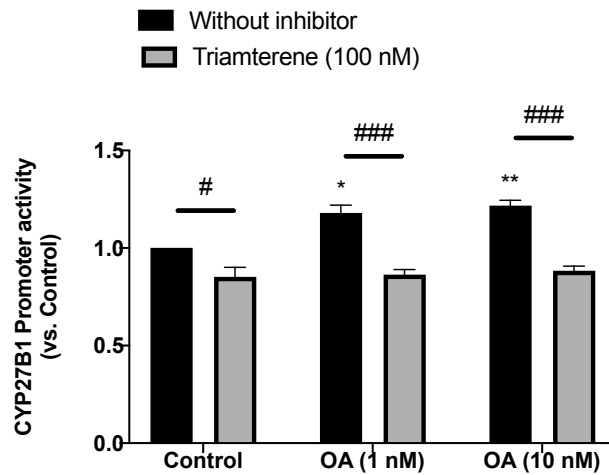
Fig. 5.7 Involvement of TGR5 in OA-induced CYP27B1 promoter activity in human osteosarcoma MG-63 cells.

Cells were transfected with CYP27B1-promoter plasmid for 6 hours. Then cells were pre-treated with triamterene (100 nM) for 30 minutes, followed by treatment of OA (1, 10 nM) for 2 hours. CYP27B1 promoter activity in the presence or absence of triamterene, the inhibitor for TGR5, was determined by dual luciferase reporter assay. Data are expressed as mean ± SEM, n=3. Differences between treatment group and control were analyzed by one-way ANOVA followed by Tukey's multiple comparison tests. * $P < 0.05$, ** $P < 0.01$ vs. control; # $P < 0.05$, ### $P < 0.001$ vs. treatment group without inhibitor.
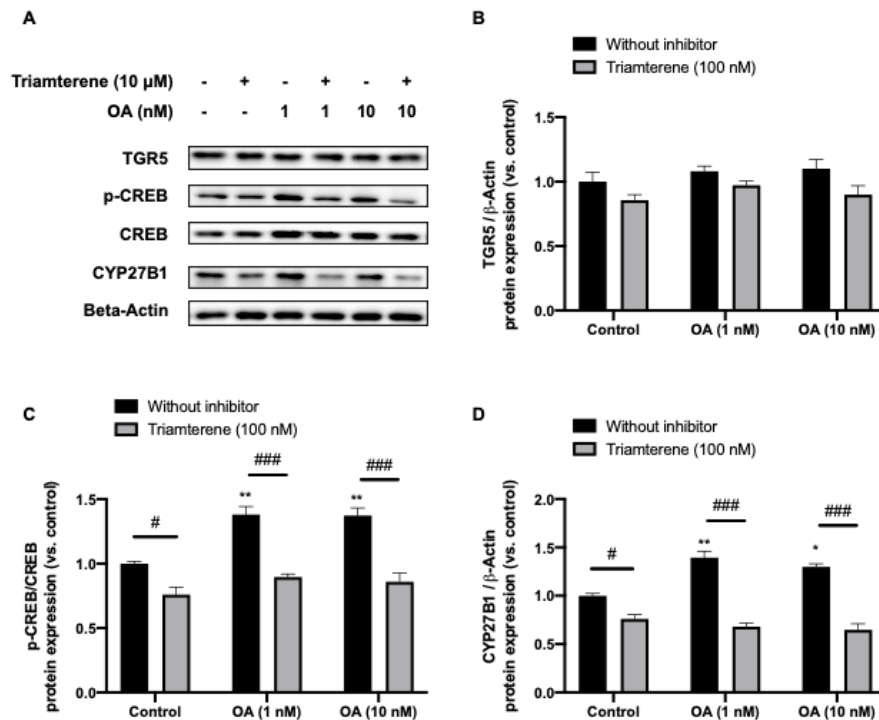
Fig. 5.8 Involvement of TGR5 in OA-induced CREB phosphorylation and CYP27B1 in human osteosarcoma MG-63 cells.

Cells were pre-treated with triamterene (100 nM) for 30 minutes, followed by treatment of OA (1, 10 nM) for 2 hours. Protein expressions of TGR5 (A, B), phosphorylation of CREB (A, C) and CYP27B1 (A, D) in the presence or absence of triamterene, the inhibitor for TGR5, were determined by Western blotting. Data are expressed as mean $\pm$ SEM, n=3. Differences between treatment group and control were analyzed by one-way ANOVA followed by Tukey's multiple comparison tests. * $P < 0.05$, ** $P < 0.01$ vs. control; ### $P < 0.001$ vs. treatment group without inhibitor.

5.4 Discussion

Regulating CYP27B1 in osteoblasts has been the major focus since the discovery of CYP27B1 in extra-renal sites. As a naturally occurring compound, OA was identified to upregulate CYP27B1 expression and cellular biosynthesis of $1,25(OH)_2D_3$ in human osteoblastic cells in our previous study. Given the fact that OA is a natural agonist of the G protein-coupled bile acid receptor 1 (TGR5), we attempted to characterize the involvement of TGR5 and its downstream signaling in mediating the actions of OA to regulate CYP27B1 in osteoblasts.

Emerging as a transmembrane receptor for bile acids, TGR5 was identified to respond to lithocholic acid (LCA) in a dose-dependent manner by increasing the production of cAMP in the Chinese hamster ovary cells (CHO) overexpressed human TGR5 cDNA (Kawamata et al., 2003). Our preliminary results showed TGR5 was consistently expressed in the human osteoblast-like MG-63 cells. By using MG-63 as osteoblastic cells model, our results showed the regulatory effects of OA on CYP27B1 was mimicked by LCA. Treatment of LCA for 24 hours dose-dependently upregulated expressions of CYP27B1 and cellular production of $1,25(OH)_2D_3$ in MG-63 cells, indicating the potential of regulating CYP27B1 by activation of TGR5 in osteoblasts. This was supported by our findings that the expression of CYP27B1 decreased slightly when the activation of TGR5 was blocked by using the small molecule inhibitor. Two experimental approaches were used to determine the role of TGR5 in OA upregulation of CYP27B1: specific overexpression of TGR5 and targeted silencing of TGR5 in MG-63 cells. It seems that expression of CYP27B1 was associated with the expression of TGR5. Overexpression or silencing of TGR5 not only significantly changed TGR5 expression but also result in the corresponding alteration of CYP27B1 expressions. Moreover, overexpression of TGR5 potentiated the effects of OA on CYP27B1, while OA failed to alter CYP27B1 expression when the expression of TGR5 was decreased by transfection of TGR5 siRNA. These results illustrated TGR5 is critical for the

expressions of CYP27B1 as well as stimulatory effects of OA on CYP27B1 in osteoblasts.

The classical pathway involving activation of TGR5 is similar to those of other G protein-coupled receptors, which is usually accompanied by the alteration of intracellular second messengers (such as cAMP), subsequent alteration of the activities of protein kinases (such as protein kinase A), resulting in the change in activities of the transcription factor (such as CREB) via phosphorylation (Kim et al., 2013). CREB binding to the cAMP response element (CRE) initiates the transcription of target genes upon the phosphorylation of CREB by activated protein kinases at Ser 133 (Altarejos et al., 2011). Indeed, CREs were being identified within the promoter region of CYP27B1 gene and the phosphorylation of CREB is a critical modulator for transcription of CYP27B1 (Kong et al., 1999). In line with this, the stimulation of CYP27B1 by PTH in human mesenchymal stem cells (hMSCs) was reported to be attenuated by the presence of KG501, an inhibitor that blocks the interaction between p-CREB and CREB-binding protein, or the CREB siRNA (Geng et al., 2011a). Our results showed that the increase in phosphorylated levels of CREB in response to OA was completely obliterated by pre-treatment with TGR5 inhibitor, indicating that the phosphorylation of CREB induced by OA attribute to its activation of TGR5. In addition, the induction of promoter activity and mRNA expression of CYP27B1 in MG-63 cells by OA was completely obliterated in the presence of TGR5 inhibitor. These results suggested that the activation of TGR5 by OA resulted in the phosphorylation of CREB that subsequently lead to the induction of CYP27B1 transcription in osteoblasts.

Forskolin, a TGR5-independent cAMP activator, was reported to upregulate CREB phosphorylation to a maximal level in kidney cells upon treatment for 15 minutes (Armbrecht et al., 2003). It is worth noting that our results showed OA rapidly increased CREB phosphorylation in 10 minutes in osteoblastic cells. In line with our findings, OA was reported to stimulate CREB phosphorylation in human vascular smooth muscle cells in 5 minutes and to the highest level at 15 minutes (Martinez-Gonzalez et al.

(2008). This rapid induction implicated the potential of OA to induce cAMP-activated rapid signaling through activation of the transmembrane receptor TGR5. Following the first episode of the increase in CREB phosphorylation, mRNA and protein expressions of CYP27B1 were stimulated to the maximal levels in MG-63 cells upon treatment with OA for 1 hour and 2 hours, respectively. These results provided evidence for the modulation of CYP27B1 in osteoblastic cells by OA at the transcriptional level. We also found a second stimulation of CREB phosphorylation and an induction of CYP27B1 promoter activity by treatment with OA for 2 hours, indicating that OA activated TGR5 in an intermittent manner. Moreover, OA significantly increased TGR5 mRNA expression in MG-63 cells upon treatment for two hours. The modest induction of TGR5 signaling and CYP27B1 ensured the cells with adequate levels of intracellular $1,25(OH)_2D_3$ for biological activities and also prevented the cells from the toxic effects induced by excessive intracellular $1,25(OH)_2D_3$. As indicated by Goltzman (2018), high levels of $1,25(OH)_2D_3$ increased expression of RANKL/OPG by binding the VDR in osteoblasts, which further promoted the osteoclastic bone resorption.

CYP27B1 is known to express in numerous renal and extra-renal sites, which is responsible for the circulating and intracellular $1,25(OH)_2D_3$ to exert endocrine and autocrine activities (Bikle et al., 2018). Mapping studies has described a wide distribution of TGR5 gene expression in various human and rodents tissues such as liver, kidney, brain, adipose tissue and muscles, although the level of TGR5 expression varied in these sites (Duboc et al., 2014; Kawamata et al., 2003). These ubiquitous distribution of TGR5 made it possible for OA to regulate the expression of CYP27B1 and cellular production of $1,25(OH)_2D_3$ in other tissues. Emerging evidence showed that apart from OA and LCA, plenty of natural bile acids and synthesized compounds could activate TGR5 and induce the production of cAMP (Budzik et al., 2010; Pellicciari et al., 2009). Thus, it is of interest to know if other selective TGR5 agonists could also modulate CYP27B1 expression and the biosynthesis of $1,25(OH)_2D_3$ in different tissues to exert cell-specific activities.

Our previous studies showed that OA improved osteogenesis and mineralization of osteoblastic lineages at the mature stages by increasing locally produced $1,25(OH)_2D_3$ by CYP27B1. Our findings are supported by a recent report by Wang et al. (2018) that TGR5 expression increased with the osteogenic differentiation of pre-osteoblast MC3T3-E1 cells. Such an increase in TGR5 expressions further facilitate the effects of OA to induce CYP27B1 expression and activities in mature osteoblasts, which has been demonstrated by our study with TGR5 overexpression in MG-63 cells. Moreover, treatment of a specific TGR5 agonist was reported to improve osteogenesis of MC3T3-E1 cells by upregulation of alkaline phosphatase (ALP) activity and gene expressions of osteocalcin and type I collagen (Wang et al., 2018). These findings were also consistent with the results of our study reported in Chapter 4 that OA treatment could improve the expressions of $1,25(OH)_2D_3$ responsive genes in hMSCs. Taken together, these studies suggest that the osteogenic differentiation induced by activation of TGR5 might be mediated by the increase in cellular produced $1,25(OH)_2D_3$ by CYP27B1 in the osteoblasts.

Renal CYP27B1 expression are known to be regulated by calciotropic hormones such as parathyroid hormone (PTH) and calcitonin through the activation of the corresponding functional GPCRs (Armbrecht et al., 2003; Yoshida et al., 1999). However, the regulation of CYP27B1 in extrarenal sites, especially in osteoblasts, was controversial (Van der Meijden et al., 2016). The present study was the first to investigate the possible involvement of TGR5 signaling in the regulation of CYP27B1 in human osteoblastic cells. Further studies are required to determine the role of TGR5 in regulation of CYP27B1 in other tissues. Moreover, the involvement of TGR5 in mediating the regulation of CYP27B1 and $1,25(OH)_2D_3$ levels should further be confirmed in animals with targeted ablation of TGR5.

Taken together, our results showed that the expression of CYP27B1 in MG-63 cell was partially dependent on the presence of TGR5. Also, TGR5 was required for mediating the effects of OA on the expression of CYP27B1 in osteoblasts. Moreover, the

activation of TGR5 by OA resulted in rapid induction of CREB phosphorylation and subsequent activation of CYP27B1 transcription. Our results are the first to demonstrate that CYP27B1 expression and cellular production of $1,25(OH)_2D_3$ in extra-renal site can be modulated by small molecules via the GPCR-activated rapid signaling.

Chapter 6

Characterization of the effects of oleanolic acid on adipogenesis and 25-hydroxyvitamin D 1-alpha-hydroxylase (CYP27B1) in bone marrow stem cells (BMSCs)

6.1 Introduction

Obesity and osteoporosis are considered the major threat to public health due to their increasing prevalence worldwide (Melton III, 1995). The systemic impact of fat on bone health has drawn much attention in the last decade. Accumulating evidence showed that the body mass index (BMI) was inversely correlated with bone mineral density (BMD) in healthy adults, indicating the detrimental effects of obesity on bone metabolism (Bredella et al., 2013; Cohen et al., 2013). The development of imaging techniques enabled researchers to accurately differentiate and quantify the adipose tissues in bone marrow cavities. By using magnetic resonance imaging (MRI), researchers discovered that the content of vertebral marrow fat is much higher in postmenopausal women with osteoporosis, which account for bone fragility and increased risk of fracture in elder women (Yong et al., 2009). Moreover, marrow adipose tissues (MAT) has been recognized as a critical dominator of age-related bone loss as the content of MAT was discovered to be positively associated with fractures in elderly (Schwartz et al., 2013).

Bone marrow has been identified as the only region where fat tissues lie adjacently to bone. Moreover, it also provides a complex microenvironment where different cell types interact with each other by sharing growth factors and cytokines in a common space. In the bone marrow, mesenchymal stem cells (MSCs) serve as the progenitors that give rise to both osteoblasts and adipocytes. MSCs are believed to differentiate to these two different lineages in a mutually exclusive manner (Muruganandan et al., 2009). Accumulation of adipose tissue will occur in the expense of osteoblasts, leading to a gradual decrease of bone mass (Muruganandan et al., 2009). The alternative commitment of MSCs toward either the adipocyte or osteoblast lineages is the results of different transcription factors. Adipogenesis of MSCs is directed by the activation of peroxisome proliferator activated receptor gamma (PPAR γ) and CCAAT enhancer binding proteins (C/EBP α), while runt-related transcription factor 2 (Runx2) and Osterix trigger the osteogenesis of MSCs (Lefterova et al., 2008; Nakashima et al., 2002).

128

Increasing number of studies reported vitamin D and its bioactive metabolites play important roles in adipose tissues, including effects on adipogenesis and inflammation. In murine pre-adipocytes 3T3-L1, treatment of $1,25(OH)_2D_3$ suppressed adipogenesis in a dose-dependent manner (Chang et al., 2016). Also, the inhibitory effects of $1,25(OH)_2D_3$ on MAT has been reported in senescence-accelerated mice (SAM-P/6) (Duque et al., 2004). In fact, the expressions of CYP27B1 and vitamin D receptor (VDR) were well described in human and rodents adipose tissues (Li et al., 2008; Wamberg et al., 2013), indicating the potential of $1,25(OH)_2D_3$ locally synthesized by adipocytes to exert autocrine or paracrine activities via its nuclear receptor. However, the regulation of CYP27B1 in adipocytes and role of locally produced $1,25(OH)_2D_3$ in adipogenesis have not been reported.

The anti-obesity activities of oleanolic acid (OA) were reported in mice fed with high fat diet (HFD) (Liu et al., 2007; Yunoki et al., 2008). Studies showed that OA suppressed the increase in visceral adipose tissue in HFD fed animals by improving carbohydrate and lipid metabolism (Liu et al., 2007; Yunoki et al., 2008). Sung et al. (2010) showed OA dose-dependently suppressed adipogenesis and cellular lipid accumulation of 3T3-L1 cells at the dose of 1-25 μM. However, the effects of lower concentrations of OA have not been reported. In Chapter 3 and 4, we reported that OA upregulated the production of $1,25(OH)_2D_3$ by CYP27B1 in kidney and osteoblasts, which were believed to exert endocrine and autocrine activity to regulate systemic mineral homeostasis and osteoblasts mineralization. However, it is unclear if OA modulates the expression and activity of CYP27B1 in another extra-renal site, adipocytes, to exert their beneficial effects on bone.

This chapter aimed to evaluate the effects of OA on adipogenesis of and CYP27B1 in BMSCs. First, we employed a stabilized ovariectomized (OVX) mice model to evaluate the effects of OA on bone marrow adipose tissues and adipogenesis of BMSCs in these animals. This is followed by a series of *in vitro* experiment to determine the effects of OA on CYP27B1 expressions in the process of adipogenesis of human mesenchymal stem cells (hMSCs) and murine 3T3-L1 preadipocytes. Also, the role of TGR5 in

mediating regulatory effects of OA on CYP27B1 and adipogenesis were evaluated in adipogenic differentiated 3T3-L1 cells.

6.2 Methodology

6.2.1 *In vivo* experiment

6.2.1.1 Experimental design

The protocol of the animal study conducted was approved by the Animal Ethics Committee of The Hong Kong Polytechnic University (ASESC No.: 19-20/4-ABCT-R-STUDENT). To investigate the actions of OA on bone marrow adipose tissues, forty 4-month-old female C57BL/6J mice weighing 20 ± 1 g were purchased and housed in centralized animal facilities (CAF) of the Hong Kong Polytechnic University in an environment with 12 h light and dark cycle and constancy of temperature (22 °C). Mice were sham operated or ovariectomized (OVX) after acclimation for one week. Following the surgery, mice were maintained with phytoestrogen-free AIN-93M rodent diet (Research diet, USA). After stabilization of the model for 6 weeks, mice were randomly assigned into five groups (n=8/group) and pair fed with 3 g phytoestrogen-free AIN-93M rodent diet (Research diets, USA) (Table 6.1), the estimated daily intake of mice. For each treatment group, the sham-operated (Sham) and OVX mice (OVX) were treated with vehicle, other OVX mice were orally administrated with 17β-estradiol (E_2, 200 μg/kg/day), high calcium diet (HCD, 1% calcium in AIN-93M based rodent diet) and OA (200 ppm in AIN-93M based rodent diet) for 8 weeks. Mice in Sham, OVX and E_2 treatment groups were fed with AIN-93M rodent diet. OA was administrated by incorporation of OA into AIN-93M based rodent diet at the concentration of 200 mg OA/kg diet. The concentration of OA in the diet was designed based on the dosage used in our previous study (Cao et al., 2018) and daily dietary intake of mice. E_2 and HCD were employed as positive controls to evaluate the actions of OA on bone metabolism and adipogenesis in OVX mice. Body weight of animals were monitored every week throughout the study.

Table 6.1 Composition of modified AIN-93M rodent diet (Research diets, USA)

Diet (Product #)	Phytoestrogen-free AIN-93M rodent diet	High calcium diet (HCD)	OA diet
	D00031602	D19072407	D19072409
Protein (gm%)	14	14	14
Carbohydrate (gm%)	73	72	73
Fat (gm%)	4	4	4
Total (kcal/gm)	3.85	3.80	3.85
Ingredient (gm)			
Casein	140	140	140
L-Cystine	1.8	1.8	1.8
Corn Starch	495.692	495.692	495.692
Maltodextrin 10	125	125	125
Sucrose	100	100	100
Cellulose, BW200	50	50	50
Corn Oil	40	40	40
t-Butylhydroquinone	0.008	0.008	0.008
Mineral Mix S10022M	35	35	35
Calcium Carbonate	0	13	0
Vitamin Mix V10037	10	10	10
Choline Bitartrate	2.5	2.5	2.5
Ca (g)	5.0	10	5.0
Ca (%)	0.5	1	0.5
Oleanolic Acid (mg)	0	0	200
Total (g)	1000	1013	1000.2

6.2.1.2 Sample collection

Upon anesthesia, mice were sacrificed by collection of blood via cardiac stick exsanguinations. After clotting, the blood was centrifuged at 4000 rpm/min for 20 min at 4 ℃. Serum was isolated and stored at - 80 ℃ for further biochemical measurement. Uterus were freshly isolated and wet weight were recorded for assessing the uterine index. The left legs were collected and wrapped with PBS-soaked gauze and stored at - 20 °C for micro-computed tomography (μCT) analysis. Bone marrow stromal cells (BMSCs) were freshly isolated from right legs for the measurement of the expression of osteogenic markers and adipogenic markers.

6.2.1.3 Micro-CT analysis for bone marrow adipose tissues

Bone marrow adipose tissues in tibia were stained with osmium tetroxide followed by visualization and quantification by micro-CT following the protocol by Scheller et al. (2014). Briefly, the tibias were immediately immersed in 10% neutral buffered formalin (Thermo Fisher, USA) after removing the soft tissues from legs. After fixation at 4 ℃ for 3 days, the bones were decalcified in 4.14 % EDTA solution (pH 7.0-7.4) at 4 ℃ for two weeks during which the decalcification solution were changed every 3-4 days. The decalcified bones were then stained with 1% osmium tetroxide at room temperature for 48 hours. Adipose tissues in the entire bone marrow cavity were scanned by micro-CT system (viva-μCT40; Scanco Medical, Switzerland) in an axial direction with power of 55 kVp and high resolution (10.5 μm). The fractional volume of adipose tissue stained by osmium tetroxide was evaluated by a three-dimensional direct model with a constant threshold of 420 and Gaussian filtering (support=1, σ=0.8). The data was expressed as adipose volume/total volume (AV/TV) which was similar with the bone volume fraction (BV/TV).

6.2.1.4 Micro-CT analysis for bone properties

Bone properties of trabecular bone at the proximal tibia were determined by μCT system (viva-μCT40; Scanco Medical, Switzerland). The bones were scanned in an axial direction with high resolution (10.5 μm), power of 70 kVp and intensity of 114 μA. A total of 100 continuous slices were scanned from the growth plate to metaphysis, 50 serials of which were selected for analysis. The volume of interest (VOI) was evaluated by using a three-dimensional direct model with a constant threshold of 375. Trabecular bone parameters including bone mineral density (BMD, mg HA/cm^3), bone volume/tissue volume (BV/TV, %), trabecular number (Tb.N, 1/mm), trabecular thickness (Tb.Th, mm), trabecular separation (Tb.Sp, mm), and connectivity density (Conn.D, 1/mm^3) were evaluated.

6.2.1.5 Serum analysis

Serum levels of total cholesterol (TC), triglyceride (TG), low-density lipoprotein cholesterol (LDL-C), high-density lipoprotein cholesterol (HDL-C) and non-esterified fatty acids (NEFA) were measured by standard colorimetric methods using commercial kits (Nanjing Jiancheng Bioengineering Institute, China). Concentrations of $1,25(OH)_2D_3$ in serum were determined by a mouse 1,25-dihydroxyvitamin D_3 ($1,25(OH)_2D_3$) ELISA kit (BlueGene Biotech, Shanghai, China). Serum levels of procollagen I N-terminal propeptide (PINP) and C-terminal telopeptide of type I collagen (CTX-1) were tested by using mouse PINP ELISA kit (ABclonal, USA) and mouse cross linked CTX-I ELISA kit (CUSABIO technology, USA) following the manufacturer's instructions, respectively.

6.2.1.6 Isolation of BMSCs

BMSCs were freshly isolated from right legs of treated animals upon sacrifice following protocol by Huang et al. (2015). Briefly, the soft tissues were thoroughly removed from the bones followed by washing the bones with Hanks' Balanced Salt

Solution (HBSS, Gibco) containing 1% penicillin-streptomycin (P/S, Gibco). Then the proximal and distal ends of long bones were cut off, the bone marrow were slowly flushed out with low glucose DMEM (L-DMEM, Gibco) containing 10% heat-inactivated fetal bovine serum (FBS) by using syringe equipped with a 23-gauge needle, until the diaphysis become pale. The cell clumps were dissociated by slowly pull the cell suspension up and down using a 25-gauge. Then the cells were centrifuged at 800 rpm for 5 minutes, followed by resuspension with L-DMEM containing 1% and 10% FBS. After incubation at 37 °C in a humidity environment with 5 % CO_2 for 7 days, the suspension blood cells were discarded. The adherent BMSCs were collected in 500 μl TRIzol reagent (Invitrogen, USA) for further analysis.

6.2.1.7 RT-PCR

Total RNA from BMSCs isolated from legs of treated animals was extracted by using 500 μl TRIzol reagent (Invitrogen, USA) following the manufacturer's instructions. 1 μg of RNA was applied for reverse transcription (RT) by using PrimeScript^{TM} RT Master Mix (TaKaRa, Japan) in a 20 μl reaction system for cDNA generation. 500 ng of cDNA products and 0.4 μM primers were added to PCR reaction mixture containing TB Green Premix Ex Taq II (TaKaRa, Japan). Real-time PCR was performed in 7900HT Fast Real-Time PCR System (Applied Biosystems, Carlsbad, CA, USA) under the amplification conditions and procedures: initial denaturation at 95 °C for 30 s, 40 cycles of denaturation at 95 °C for 1 s and 60 °C for 20 s. The sequences of primers for target genes and the housekeeping gene glyceraldehyde-3-phosphate dehydrogenase (GAPDH) are listed in Table 6.1. Relative gene expression was calculated by $2^{-\Delta\Delta CT}$ method.

Table 6.2 Primer sequences for mouse genes

Gene		Primer Sequence (5'-3')
Mouse		
CYP27B1	Forward:	GCATCACTTAACCCACTTCC
	Reverse:	CGGGAAAGCTCATAGAGTGT
CYP24A1	Forward:	AAGAGATTCGGGCTCCTTCA
	Reverse:	GCAGGGCTTGACTGATTTGA
Runx2	Forward:	CGCACGACAACCGCACCAT
	Reverse:	CAGCACGGAGCACAGGAAGTT
Osterix	Forward:	CTCGTCTGACTGCCTGCCTAG
	Reverse:	GCGTGGATGCCTGCCTTGTA
PPAR γ	Forward:	GGTTGACACAGAGATGCCATTC
	Reverse:	ATCACGGAGAGGTCCACAGAG
C/EBP α	Forward:	ACTAGGAGATTCCGGTGCCT
	Reverse:	GAATTCTCCCCTCCTCGCAG
GAPDH	Forward:	CAGAACATCATCCCTGCATC
	Reverse:	CTGCTTCACCACCTTCTTGA

6.2.2 *In vitro* experiment

6.2.2.1 Experimental design

To verify the effects of OA on adipogenesis and CYP27B1 expression in adipogenic MSCs, hMSCs were maintained in adipogenic medium to induce their commitment to adipogenic lineages. The effects of OA on CYP27B1 and PPAR γ expressions at different adipogenic time points were determined by Western blotting. Subsequently, the role of TGR5 in mediating the modulating effects of OA on CYP27B1 expression and adipogenesis were evaluated in murine pre-adipocyte 3T3-L1. Cells were treated with different concentrations of OA in adipogenic medium in the presence or absence of triamterene, a chemical inhibitor for TGR5, for 7 days. The protein expression of CYP27B1 was evaluated by Western blotting. The effects of different treatment on adipogenesis were determined by studying the protein expressions of PPAR γ by Western blotting. Moreover, the lipid accumulation in 3T3-L1 in response to treatment with OA were evaluated by Oil Red O staining.

6.2.2.2 Cell culture and adipogenesis

hMSCs from a 61-year-old female subject (CREC Ref. No. 2010. 248) were provide by Dr. Lee Yuk wai, Wayne from the Prince of Wales Hospital of the Chinese University of Hong Kong (Lee et al., 2013). The cells were cultured in standard growth medium containing Minimum Essential Medium alpha (α-MEM) with 10% heat-inactivated fetal bovine serum (FBS) and 100 U/mL penicillin-streptomycin in a humidified environment with 5 % CO_2 at 37 °C. For adipogenic differentiation, hMSCs at passage 4-7 were seeded in 6-well plates at the density of 2×10^5 cells/well. Upon attaining confluence (day 0), culture medium was replaced with adipogenic induction medium which consist of high glucose DMEM supplemented with 500 μM 3-isobuty-1-methylxanthine (IBMX), 1 μM dexamethasone, 100 μM indomethacin, and 10 μg/mL insulin (all from Sigma-Aldrich, UK). The medium was changed every 2 days until they were differentiated for 7 and 14 days. At each osteogenic time point, culture medium

was then replaced by phenol red-free α-MEM with 1% charcoal-striped FBS. Cells were treated with $1,25(OH)_2D_3$ (10 nM) or OA (1 nM, 10 nM, 100 nM) for 24 hours and proceeded for relevant assays.

Mouse fibroblast preadipocytes 3T3-L1 were maintained in DMEM supplemented with 10% heat-inactivated FBS and 100 U/ml P/S in a humidified incubator with 5 % CO_2 at 37 °C. Cells were sub-cultured twice every week. For adipogenic differentiation, cells were seeded in 12-well plates or 6-well plates to allow 100% confluence (day 0). Then cells were treated with $1,25(OH)_2D_3$ (10 nM) or OA (1 nM, 10 nM, 100 nM) in adipogenic induction medium which consist of standard growth medium supplemented with 500 μM 3-isobuty-1-methylxanthine (IBMX), 500 nM dexamethasone, and 10 μg/mL insulin (all from Sigma-Aldrich, UK) for two days. Treatment was continued for additional 5 days in normal culture medium supplemented with 10 μg/mL insulin, during which the medium was changed every 2 days.

6.2.2.3 Oil red O staining

Adipogenesis of 3T3-L1 were determined by measuring lipid accumulation in cells using Oil Red O (Sigma-Aldrich, UK) staining method. A working solution of Oil Red O was prepared by mixing stock solution (60 mg Oil Red O in 20 mL isopropanol) with distilled water at a ratio of 3:2. The working solution was filtered through a 0.45 μm filter before use. 3T3-L1 cells treated and differentiated in 12-well plates were fixed with 10% neutral buffered formalin (Thermo Fisher, USA) at room temperature for 1 hour before incubation with Oil Red O working solution for 20 minutes. Upon rinsing for 5 times, lipid droplets were visualized under light microscope. After that, the Oil Red O stain in cells was eluted in isopropanol and measured at 492 nm.

6.2.2.4 Western blotting

Cells (10 μL/10^5 cells) were lysed with lysis buffer (Beyotime, Shanghai, China) supplemented with 1mM phenylmethyl sulfonyl fluoride (PMSF) as a protease inhibitor.

Following protein extraction, 30 μg proteins of each sample were loaded and separated in a 10% SDS-PAGE, followed by transblotting onto polyvinylidene fluoride (PVDF) membranes (Millipore, Danvers, USA). The membrane blots were blocked with 5 % milk for 1 hour at room temperature and incubated with following primary antibodies overnight at 4°C: rabbit anti-CYP27B1 (1:1000, Invitrogen, USA), rabbit anti-TGR5 (1:1000, Invitrogen, USA), rabbit anti-phospho-AMPKα (Thr^{172}) (1:1000, Cell Signaling, USA), rabbit anti-AMPKα (1:1000, Cell Signaling, USA), mouse anti-PPAR γ (1:1000, Abcam, UK), or mouse anti-β-Actin (1:5000, Abcam, UK). followed by IgG-HRP-conjugated secondary antibodies anti-rabbit (1:3000, Abcam, UK) or anti-mouse (1:3000, Invitrogen, USA) for 1h at room temperature. Washing with tris-buffered saline with 0.1% Tween 20 detergent (TBST) for 3 times was required between each of incubation. Finally, the blotting was probed and visualized with Clarity^{TM} Western ECL substrate (Bio-Rad, USA) using Azure^{TM} C600 (Azure Biosystems, USA). The relative intensities of the bands were quantified by Image J software (National Institutes of Health, USA) and normalized with β-actin.

6.2.3 Statistical analysis

Data from both *in vivo* and *in vitro* experiment were shown as mean ± standard error of mean (SEM) for each treatment group. Inter-group differences were analyzed by one-way analysis of variance (ANOVA) followed by Tukey's Test for multiple comparisons (GraphPad Prism 8.0, USA). A *P* value of less than 0.05 was considered statistically significant.

6.3 Results

6.3.1　Effects of OA on bone properties and bone metabolism in OVX mice

6.3.1.1 Body weight and uterine index

Upon treatment for 8 weeks, body weight and uterus wet weight were recorded, body weight gain and uterus index were calculated accordingly (Table 6.3). Body weight gain of mice in sham group was 2.27% upon treatment with vehicle for 8 weeks. Body weight gain of OVX mice was 7.99% and was more than 3-fold of that of the sham-operated mice (P <0.001). This accelerated weight gain was markedly suppressed in E_2 treated mice by more than 10-fold (P <0.001 vs. OVX). HCD and OA also decreased body weight gain in OVX mice by 1.85-fold (P <0.05) and 1.76-fold (P <0.05), respectively. As expected, estrogen deficiency in OVX mice resulted a marked shrinkage of uterus (P <0.001 vs. sham). E_2 significantly increased uterus index in OVX mice by 2.82-flod (P <0.05). Unlike E_2, administration with HCD and OA-contained diet did not alter the atrophy of uterus in OVX mice.

6.3.1.2 Bone properties at proximal tibia

The trabecular bone mineral density (BMD) and bone microarchitectural properties at proximal tibia of mice in different treatment group were characterized by micro-CT analysis (Table 6.4). As compared to sham-operated mice, OVX markedly reduced BMD for 2.5-fold (P <0.001) and also significantly deteriorated bone microarchitectures as revealed by the decrease in bone volume fraction (BV/TV, P <0.001), trabecular number (Tb. N, P <0.05), trabecular thickness (Tb. Th, P <0.001) and connectivity density (Conn. D, P <0.001), as well as the increase in trabecular separation (Tb. Sp, P <0.01) and structural model index (SMI, P <0.001). Serving as positive control for monitoring bone protective effects, E_2 and HCD not only markedly improved BMD (P <0.001, vs OVX mice), but also improved bone microarchitectural parameters in OVX mice. Like E_2 and HCD, OA prevented OVX-induced bone loss in mice as revealed by the increase in BMD for 1.5-fold (P <0.05), as well as the changes

in trabecular BV/TV (P <0.05), Tb.N (P <0.05), Conn.D (P <0.05), Tb.Th (P <0.05), Tb.Sp (P <0.01) and SMI (P <0.05).

6.3.1.3 Bone turnover markers and serum 1,25(OH)$_2$D$_3$

Serum levels of bone turnover markers can be used for monitoring the effects of oleanolic acids on bone metabolism. Procollagen I N-terminal propeptide (PINP) and C-telopeptide of type I collagen (CTX-1) are a pair of bone turnover biomarkers for monitoring the effects on bone formation and bone resorption, respectively. As shown in Table 6.3, OVX significantly increased bone resorption but decreased bone formation of mice. Serum CTX-1 levels were 45 % higher (P <0.001) while PINP levels were 17 % lower (P <0.001) in OVX mice when compared to sham operated mice. Treatment with E$_2$, HCD and OA significantly restored bone formation in OVX mice as they significantly increased serum PINP levels for more than 10% (P <0.05 vs. OVX). On the other hand, the increase in serum CTX-1 levels induced by OVX were markedly suppressed by E$_2$ and OA, but not HCD, for more than 50% (P <0.001 vs. OVX).

1,25(OH)$_2$D$_3$ is a calciotropic hormone which remains stable in circulation in normal physiological conditions. OVX appeared to slightly decrease the circulating level of 1,25(OH)$_2$D$_3$ in mice, but the change did not reach statistical significance. Levels of 1,25(OH)$_2$D$_3$ was suppressed by 46% in OVX mice (P <0.01 vs. OVX) in response to fed with HCD. In contrast, circulating levels of 1,25(OH)$_2$D$_3$ increased by 56% in OVX mice fed with OA-contained diet (P <0.01 vs. OVX).

Table 6.3 Body weight gain, uterine index, serum markers in ovariectomized (OVX) in response to treatment with 17β-estradiol (E$_2$), high calcium diet (HCD) and oleanolic acid (OA)

	Sham	OVX	E$_2$	HCD	OA
Body weight and uterus index					
Weight gain, %	2.27 ± 1.17***	7.99 ± 0.93	0.75 ± 1.10 ***	4.30 ± 0.91*	4.55 ± 0.48*
Uterus index, mg/g	3.81 ± 0.35***	0.67 ± 0.09	1.89 ± 0.14 ***	0.69 ± 0.04	0.65 ± 0.05
Serum markers					
PINP, ng/mL	36.92 ± 0.96 ***	31.45 ± 1.00	35.34 ± 0.99 **	36.00 ± 0.67 **	35.01 ± 0.53 *
CTX-I, ng/mL	0.40 ± 0.04 ***	0.58 ± 0.02	0.35 ± 0.03 ***	0.52 ± 0.04	0.38 ± 0.02 ***
1,25(OH)$_2$D$_3$, pg/mL	55.58 ± 4.73	48.22 ± 6.10	48.28 ± 4.68	26.18 ± 3.45 **	75.28 ± 6.61 **

Six-month-old sham operated mice were fed with phytoestrogen-free AIN-93M diet, the ovariectomized (OVX) mice were orally administrated with vehicle, E$_2$ (200 µg/kg/day), HCD (1% calcium in AIN-93M based rodent diet) and OA (200 ppm in AIN-93M based rodent diet) for 8 weeks. Uterine index was calculated from the wet weight of uterus over the body weight, respectively. Procollagen I N-terminal propeptide (PINP), C-telopeptide of type I collagen (CTX-1). Data are shown as mean ± SEM and analyzed by using one-way ANOVA, followed by Tukey's multiple comparison test. * $P < 0.05$, ** $P < 0.01$, *** $P < 0.001$ vs. OVX (n=8/group).

Table 6.4 Bone microarchitectural parameters at proximal tibia in ovariectomized (OVX) mice in response to treatment with 17β-estradiol (E$_2$), high calcium diet (HCD) and oleanolic acid (OA)

	Sham	OVX	E$_2$	HCD	OA
BMD (mg HA/cm^3)	185.33 ± 15.95 ***	73.64 ± 7.00	144.49 ± 5.15 ***	128.00 ± 4.22 ***	116.39 ± 6.99 *
BV/TV (%)	14.60 ± 1.86 ***	5.34 ± 0.74	11.44 ± 0.52 ***	9.91 ± 0.60 *	9.69 ± 0.72 *
Tb.N (1/mm)	4.51 ± 0.10 *	3.99 ± 0.05	4.49 ± 0.11 *	4.46 ± 0.12 *	4.51 ± 0.20 *
Tb.Th (mm)	59.64 ± 2.81 ***	49.30 ± 1.49	61.06 ± 1.25 ***	57.80 ± 1.33 **	56.51 ± 1.46 *
Tb.Sp (mm)	228.34 ± 4.33 **	255.52 ± 2.27	226.14 ± 6.32 ***	233.57 ± 4.99 *	231.80 ± 5.64 **
Conn.D (1/mm^3)	75.34 ± 6.43 ***	34.47 ± 2.96	65.53 ± 7.23 ***	52.57 ± 1.66 *	53.36 ± 3.68 *
SMI	1.61 ± 0.06 ***	2.70 ± 0.14	2.14 ± 0.07 **	2.34 ± 0.12 *	2.32 ± 0.09 *

Six-month-old sham operated mice were fed with phytoestrogen-free AIN-93M diet, the ovariectomized (OVX) mice were orally administrated with vehicle, E$_2$ (200 μg/kg/day), HCD (1% calcium in AIN-93M based rodent diet) and OA (200 ppm in AIN-93M based rodent diet) for 8 weeks. Trabecular bone properties were evaluated by microcomputed tomography (μCT). (A) representative 3D images of trabecular bone at L4, (B) bone mineral density (BMD), (C) bone volume/total volume (BV/TV), (D) trabecular number (Tb.N), (E) connectivity density (Conn.D), (F) trabecular thickness (Tb.Th), (G) trabecular separation (Tb.Sp), and (H) structural model index (SMI). Data are shown as mean ± SEM and analyzed by using one-way ANOVA, followed by Tukey's multiple comparison test. * $P < 0.05$, ** $P < 0.01$, *** $P < 0.001$ vs. OVX (n=8/group).

6.3.2 Effects of OA on bone marrow adipose tissues and adipogenesis of BMSCs in OVX mice

6.3.2.1 Serum lipid profile

Considering the fact that osteoporosis in postmenopausal women is usually accompanied with dyslipidemia which may contribute to the development of bone marrow adipose tissues (Bone et al., 2007), we evaluated effects of OA on circulating lipid profile in OVX mice. As shown in Fig. 6.1, OVX significantly increased serum levels of TG and LDL-C (P <0.05 vs. sham), but did not alter the levels of TC, HDL-C and NEFA. E_2 treatment markedly improved lipid metabolism in OVX mice, as revealed by the reduction of serum levels of TC, TG, LDL-C and NEFA and the induction of HDL-C level (P <0.05 vs. OVX). Serum TG and NEFA in OVX mice were also significantly suppressed by HCD and OA for more than 30% (P <0.01 vs. OVX). In addition, HCD and OA improved serum HDL-C for 1.4-fold and 1.3-fold, respectively. OA also significantly suppressed elevated serum LDL-C in OVX mice by 32% (P <0.01 vs. OVX).
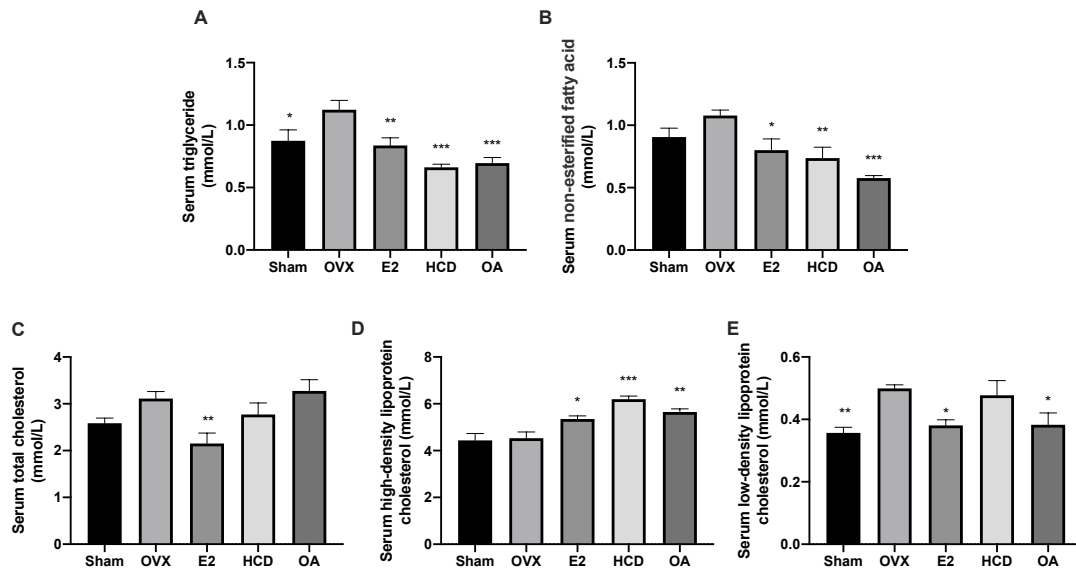
Fig. 6.1 Effects of OA on serum lipid profile in OVX mice.

Six-month-old sham operated mice were fed with phytoestrogen-free AIN-93M diet, the ovariectomized (OVX) mice were orally administrated with vehicle, E_2 (200 μg/kg/day), HCD (1% calcium in AIN-93M based rodent diet) and OA (200 ppm in AIN-93M based rodent diet) for 8 weeks. Serum levels of (A) triglyceride (TG), (B) non-esterified fatty acid (NEFA), (C) total cholesterol (TC), (D) high-density lipoprotein cholesterol (HDL-C), and (E) low-density lipoprotein cholesterol (LDL-C) was determined by commercial kits. Data are shown as mean ± SEM and analyzed by using one-way ANOVA, followed by Tukey's multiple comparison test. * $P < 0.05$, ** $P < 0.01$, *** $P < 0.001$ vs. OVX (n=8/group).

6.3.2.2 Bone marrow adipose tissues in tibia

By using osmium tetroxide staining with micro-CT, we were able to visualize the amount of marrow adipose tissues (MAT) accumulated in bone marrow cavity. Distribution of bone marrow adipose tissues in mice tibia in response to different treatment were shown in Fig. 6.2. In sham-operated mice, bone marrow adipose tissues (MAT) were mostly distributed at the growth plate and distal tibia near the ankle, which account for around 10% of total volume of tibia. OVX significantly increased the accumulation of MAT at proximal to middle tibia by 3.5-fold in mice when compared to those with sham operation (P <0.001 vs Sham). E_2 treatment significantly suppressed MAT accumulation in OVX mice by 37% (P <0.001 vs OVX). Similarly, marked reduction in MAT accumulation were also observed in OVX mice fed with HCD and OA-contained diet, in which MAT fraction was decreased in OVX mice by 24% (P <0.01 vs. OVX) and 40% (P <0.001 vs OVX), respectively.
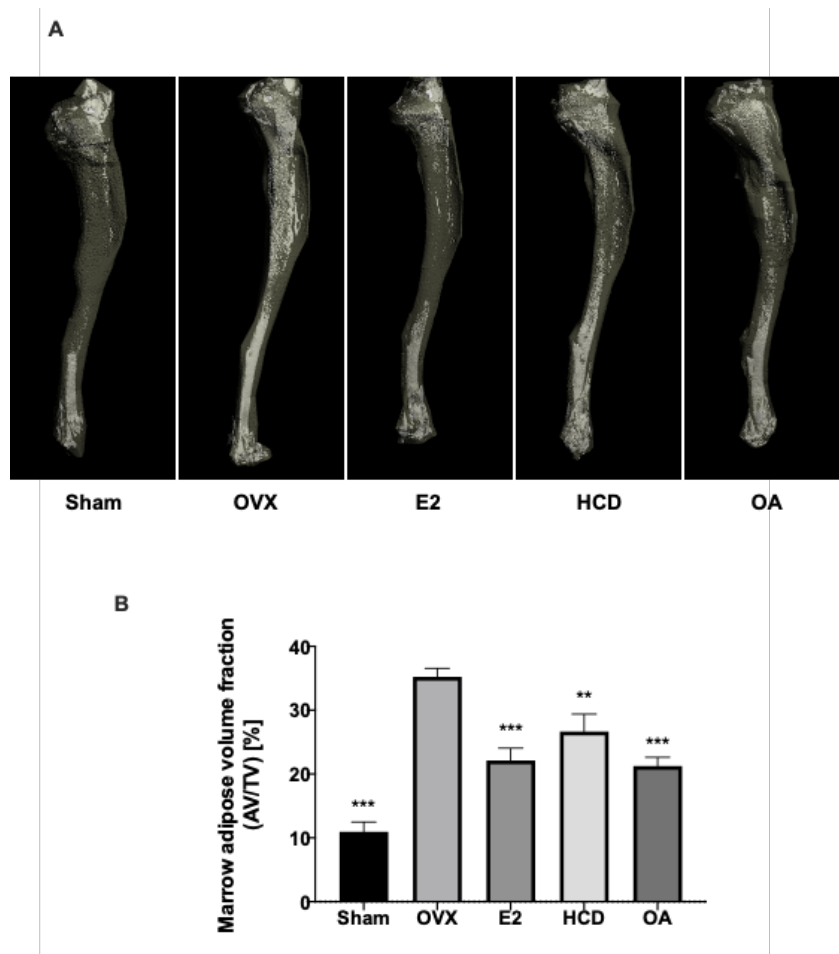
Fig. 6.2 Effects of OA on bone marrow adipose tissues in tibias of OVX mice.

Six-month-old sham operated mice were fed with phytoestrogen-free AIN-93M diet, the ovariectomized (OVX) mice were orally administrated with vehicle, E_2 (200 µg/kg/day), HCD (1% calcium in AIN-93M based rodent diet) and OA (200 ppm in AIN-93M based rodent diet) for 8 weeks. Accumulation of bone marrow adipose tissue in tibias were evaluated by Osmium tetroxide staining with microcomputed tomography (µCT). (A) representative 3D images of adipose tissue in in the entire bone marrow cavity of tibias, (B) bone adipose volume fraction (adipose volume/total volume, AV/TV). Gray, bone; white, marrow adipose tissue. Data are shown as mean ± SEM and analyzed by using one-way ANOVA, followed by Tukey's multiple comparison test. * $P < 0.05$, ** $P < 0.01$, *** $P < 0.001$ vs. OVX (n=8/group).

6.3.2.3 Osteogenic markers and adipogenic markers in BMSCs

To investigate the *in-vivo* effects of OA on osteogenesis and adipogenesis of BMSCs, mRNA expressions of osteogenic markers (Runx2 and Osterix) and adipogenic markers (PPAR γ and C/EBP α) in BMSCs of treated mice were determined. As shown in Fig. 6.3, OVX significantly suppressed osteogenesis of BMSCs, as revealed by 44% and 54% reduction in mRNA expressions of Runx2 ($P < 0.01$ vs sham) and Osterix ($P < 0.01$, vs Sham), respectively. E_2 and HCD significantly restored osteogenesis of BMSCs in OVX mice by upregulating mRNA expressions of Runx2 and Osterix for more than 1.6-fold ($P < 0.05$ vs. OVX). In contrast, OVX resulted in a marked elevation of mRNA expression of adipogenic markers in BMSCs of mice. Levels of PPAR γ and C/EBP α mRNA expression in BMSCs were increased by 2.8-fold ($P < 0.001$ vs. sham) and 4.3-fold ($P < 0.001$ vs. sham) in OVX mice. Such increases in OVX mice could be significantly suppressed in mice in response to treatment with E_2 and HCD ($P < 0.05$ vs. OVX). Similarly, OA not only significantly improved osteogenesis of BMSCs by increasing mRNA expressions of Runx2 by 1.4-fold ($P < 0.001$ vs. OVX) and Osterix by 1.5-fold ($P < 0.001$ vs. OVX), but also suppressed adipogenesis of BMSCs by decreasing mRNA expressions of PPAR γ and C/EBP α by 34% ($P < 0.01$ vs. OVX) and 72% ($P < 0.001$ vs. OVX), respectively.

6.3.3   Effects of OA on CYP27B1 and CYP24A1 of BMSCs in OVX mice

To investigate if CYP27B1 play a role in mediating the modulating effects of OA on adipogenesis or osteogenesis of BMSCs, we determined mRNA expressions of CYP27B1 and CYP24A1 in BMSCs in treated mice. As shown in Fig. 6.4, it appeared that the mRNA expressions of CYP27B1 and CYP24A1 were not altered in mice BMSCs in response to OVX as well as E_2 treatment. However, the mRNA expression levels of CYP27B1 and CYP24A1 were significantly upregulated in BMSCs from mice fed with OA by 2.3-fold (P <0.01 vs. OVX) and 1.6-fold (P <0.05 vs. OVX), respectively. Moreover, mice fed with HCD appeared to have higher expression of CYP24A1 in BMSCs, but its level did not reach statistical significance.
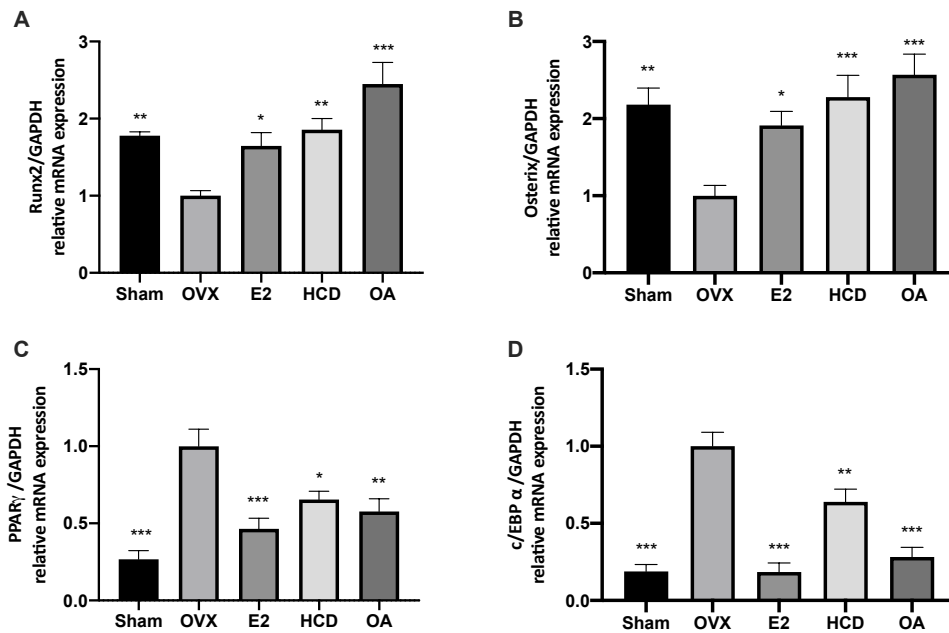
Fig. 6.3 Effects of OA on mRNA expressions of osteogenic markers and adipogenic markers in BMSCs of OVX mice.

Six-month-old sham operated mice were fed with phytoestrogen-free AIN-93M diet, the ovariectomized (OVX) mice were orally administrated with vehicle, E_2 (200 μg/kg/day), HCD (1% calcium in AIN-93M based rodent diet) and OA (200 ppm in AIN-93M based rodent diet) for 8 weeks. mRMA expression levels of (A) runt-related transcription factor 2 (Runx2), (B) osterix (Osx) (C) peroxisome proliferator-activated receptor gamma (PPAR γ) and (D) CCAAT/enhancer binding protein-alpha (C/EBP α) in BMSCs were determined by RT-PCR. Data are shown as mean ± SEM and analyzed by using one-way ANOVA, followed by Tukey's multiple comparison test. * $P < 0.05$, ** $P < 0.01$, *** $P < 0.001$ vs. OVX (n=8/group).
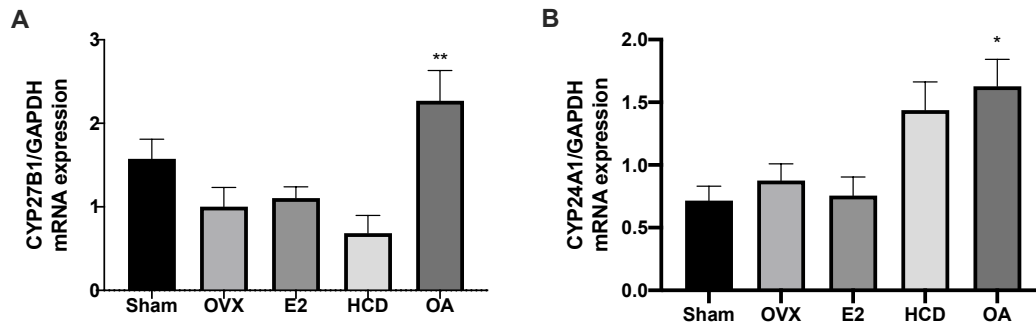
Fig. 6.4 Effects of OA on mRNA expressions of CYP27B1 and CYP24A1 in BMSCs of OVX mice.

Six-month-old sham operated mice were fed with phytoestrogen-free AIN-93M diet, the ovariectomized (OVX) mice were orally administrated with vehicle, E_2 (200 µg/kg/day), HCD (1% calcium in AIN-93M based rodent diet) and OA (200 ppm in AIN-93M based rodent diet) for 8 weeks. mRNA expression levels of (A) CYP27B1 and (B) CYP24A1 in BMSCs were determined by RT-PCR. Data are shown as mean ± SEM and analyzed by using one-way ANOVA, followed by Tukey's multiple comparison test. * $P < 0.05$, ** $P < 0.01$, *** $P < 0.001$ vs. OVX (n=8/group).

6.3.4 Effects of OA on adipogenesis and CYP27B1 expression in hMSCs

We first determined the protein expressions of CYP27B1 and PPAR γ during the adipogenic differentiation of hMSCs. As shown in Fig. 6.5A & B, the protein expression of PPAR γ increased continuously along with the process of adipogenesis in hMSCs, indicating the commitment of hMSCs to become adipoprogenitors. In contrast, the protein expression of CYP27B1 decreased significantly in hMSCs with the development of adipocytes. Upon differentiation for 14 days, the protein expression of PPAR γ in hMSCs reached maximal levels (1.6-fold of day 0, $P < 0.001$) while the protein expression level of CYP27B1 in hMSCs was approximately 40 % of that at day 0.

We also determined the effects of OA on protein expressions of CYP27B1 and PPAR γ at different adipogenic stages using $1,25(OH)_2D_3$ (1 nM) as positive control. $1,25(OH)_2D_3$ slightly suppressed CYP27B1 protein expression in hMSCs at day 0, but this suppression became more significant in the immature ($P < 0.001$ vs. Control of Day 7) and mature ($P < 0.01$ vs. Control of Day 14) adipocytes which were differentiated for 7 days and 14 days, respectively. On the contrary, protein expressions of CYP27B1 were significantly upregulated in hMSCs in response to treatment with OA (1 nM and 10 nM) for more than 10% ($P < 0.05$ vs. Control of Day 0) at day 0 and 21% ($P < 0.05$ vs. Control of Day 7) at day 7. Moreover, OA at 10 nM and 100 nM markedly improved the protein expression of CYP27B1 in hMSCs which are adipogenic differentiated for 2 weeks ($P < 0.001$ vs. Control of Day 14). On the other hand, $1,25(OH)_2D_3$ significantly suppressed adipogenesis of hMSCs by decreasing the protein expressions of PPAR γ by 65 % ($P < 0.001$ vs. Control of Day 0), 60% ($P < 0.001$ vs. Control of Day 7) and 64% ($P < 0.001$ vs. Control of Day 14) at day 0, day 7 and day 14, respectively. Similarly, OA (1 nM and 10 nM) markedly downregulated the expressions of PPAR γ by 15% at day 0 ($P < 0.05$ vs. Control of Day 0), 42% at day 7 ($P < 0.05$ vs. Control of Day 7) and 33% at day 14 ($P < 0.05$ vs. Control of Day 14).
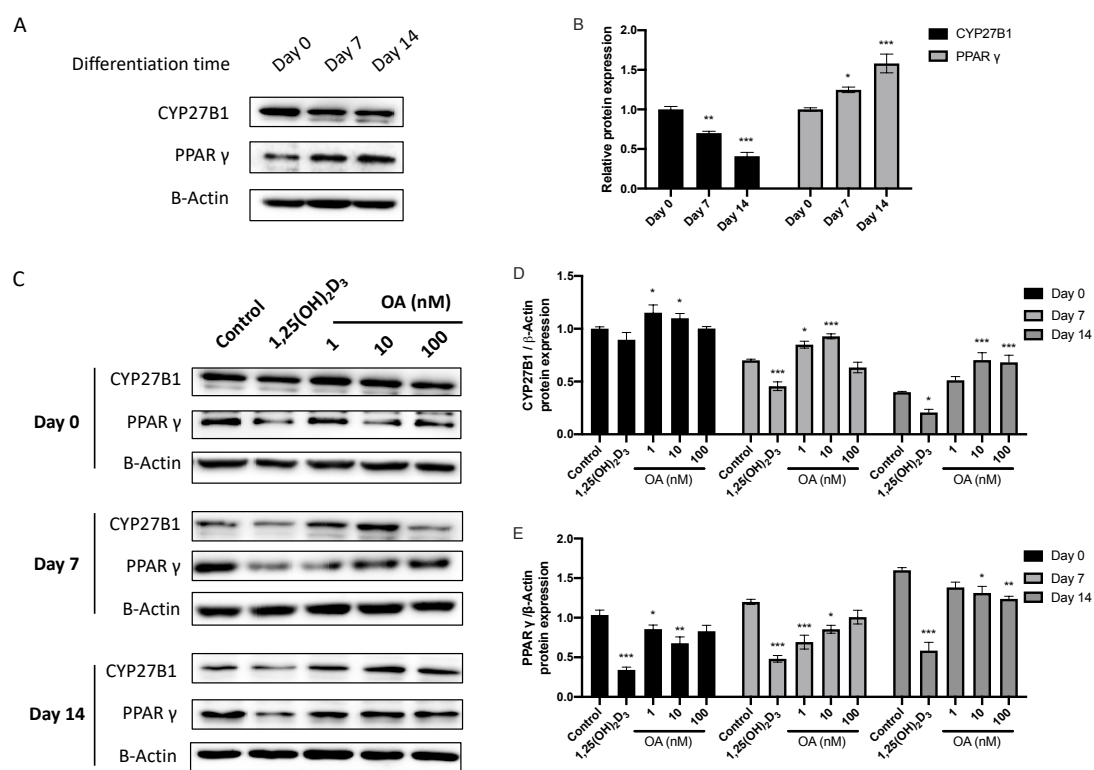
Fig. 6.5 Effects of OA on adipogenesis and CYP27B1 protein expression in hMSCs.
hMSCs from a 61-year-old female subject were differentiated in adipogenic medium
for 0, 7 and 14 days. (A, B) Protein expressions of peroxisome proliferator-activated
receptor gamma (PPAR γ) and CYP27B1 were determined by Western blotting. At
each of adipogenic time point, cells were treated with $1,25(OH)_2D_3$ (1 nM) or OA (1,
10, 100 nM) for 24 hours. Protein expressions of PPAR γ (C, D) and CYP27B1 (C, E)
were determined by Western blotting. Data are expressed as mean ± SEM, n=3.
Differences between treatment group and control were analyzed by one-way ANOVA
followed by Tukey's multiple comparison tests. * $P < 0.05$, ** $P < 0.01$, *** $P < 0.001$
vs. control

## 6.3.5 Effects of OA on adipogenesis and lipid accumulation in 3T3-L1 preadipocytes

Apart from the expressions of adipogenic marker PPARγ, the accumulation of lipid droplets in adipocytes could also serve as an indicator for adipogenesis. The effects of OA on lipid accumulation in 3T3-L1 preadipocytes were showed in Fig. 6.6. Adipogenic differentiation resulted in a dramatic increase in intracellular lipid accumulation in 3T3-L1 cells by 5-fold (P <0.001 vs. non differentiated cells). These induction of lipid droplets were significantly decreased by 56% (P <0.001 vs. differentiated control) when cells were differentiated in the presence of $1,25(OH)_2D_3$. OA also markedly prevented lipid accumulation in 3T3-L1 cells in a dose-dependent manner. OA at 10 nM and 100 nM significantly suppressed the accumulation of lipid droplets in differentiated cells by 30 % (P <0.01) and 45% (P <0.001), respectively.

6.3.6 Involvement of TGR5 in effects of OA on adipogenesis in 3T3-L1 preadipocytes

We evaluated the role of TGR5 in mediating the modulatory actions on adipogenesis and CYP27B1 expression in adipogenic differentiated 3T3-L1 preadipocytes using triamterene, which has been identified as a chemical inhibitor of TGR5 *in vivo* and *in vitro* (Li et al., 2017),. As shown in Fig. 6.7, a significant drop in protein expressions of TGR5 (P <0.05 vs. undifferentiated control) and CYP27B1 (P <0.05 vs. undifferentiated control) was accompanied by an elevation of PPAR γ expression (P <0.001 vs. undifferentiated control) upon adipogenic differentiation of 3T3-L1 cells.

The induction of PPARγ expressions could be significantly suppressed in 3T3-L1 cells treated with $1,25(OH)_2D_3$ (1 nM) and OA (10 nM and 100 nM) by more than 52% (P <0.01 vs. differentiated control) and 41% (P <0.05 vs. differentiated control), respectively. Moreover, the presence of triamterene not only increased protein expression of PPARγ in 3T3-L1 cells by 1.6-fold (P <0.01 vs. differentiated control), but also significantly (P <0.001) abolished the suppressive effects of OA on PPAR γ

expression, indicating the important role of TGR5 in regulating the process of adipogenesis in 3T3-L1 cells. Incubation of 3T3-L1 cells with 10 nM and 100 nM OA significantly restored the expressions of TGR5 by more than 1.4-fold (P <0.05 vs. differentiated control), and the expressions of CYP27B1 by more than 1.7-fold (P <0.001 vs. differentiated control), to the levels that were comparable with that in undifferentiated cells. However, the effects of OA on protein expressions of TGR5 and CYP27B1 were also markedly (P <0.05) attenuated in 3T3-L1 cells in the presence of triamterene.

Activation of AMP-activated protein kinase α (AMPK α) via phosphorylation at Thr 172 plays a central role in regulating cellular energy homeostasis involving glucose and lipid metabolism (Kim et al., 2016). Our results showed that the phosphorylated levels of AMPKα in adipogenic differentiated cells was significantly increased in 3T3-L1 cells treated with $1,25(OH)_2D_3$ (1 nM) and OA (10 nM and 100 nM) by more than 2-fold (P <0.001 vs. differentiated control). Similarly, the effects of OA on phosphorylation of AMPK α were also markedly (P <0.001) abolished in 3T3-L1 cells in the presence of triamterene.
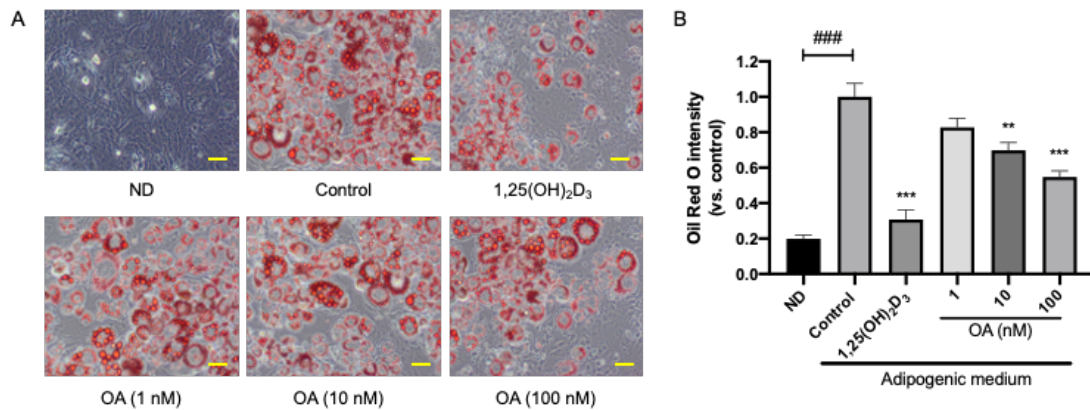
Fig. 6.6 Effects of OA on lipid accumulation of 3T3-L1 preadipocytes.

3T3-L1 preadipocytes were differentiated in adipogenic medium in the presence of 1,25(OH)$_2$D$_3$ (1 nM) or OA (1, 10, 100 nM) for 2 days, followed by treatment in adipocyte maintenance medium for another 5 days. (A) Intracellular lipid droplets were stained with Oil Red O and visualized by light microscope with magnification of 200x, scale bars: 100 μm. (B) The absorbance of Oil Red O staining intensity was measured at 492 nm. Non differentiated (ND). Data are from three independent experiments and are shown as mean ± SEM and analyzed by using one-way ANOVA, followed by Tukey's multiple comparison test. ### $P < 0.001$ vs. ND; * $P < 0.05$, ** $P < 0.01$, *** $P < 0.001$ vs. Control.
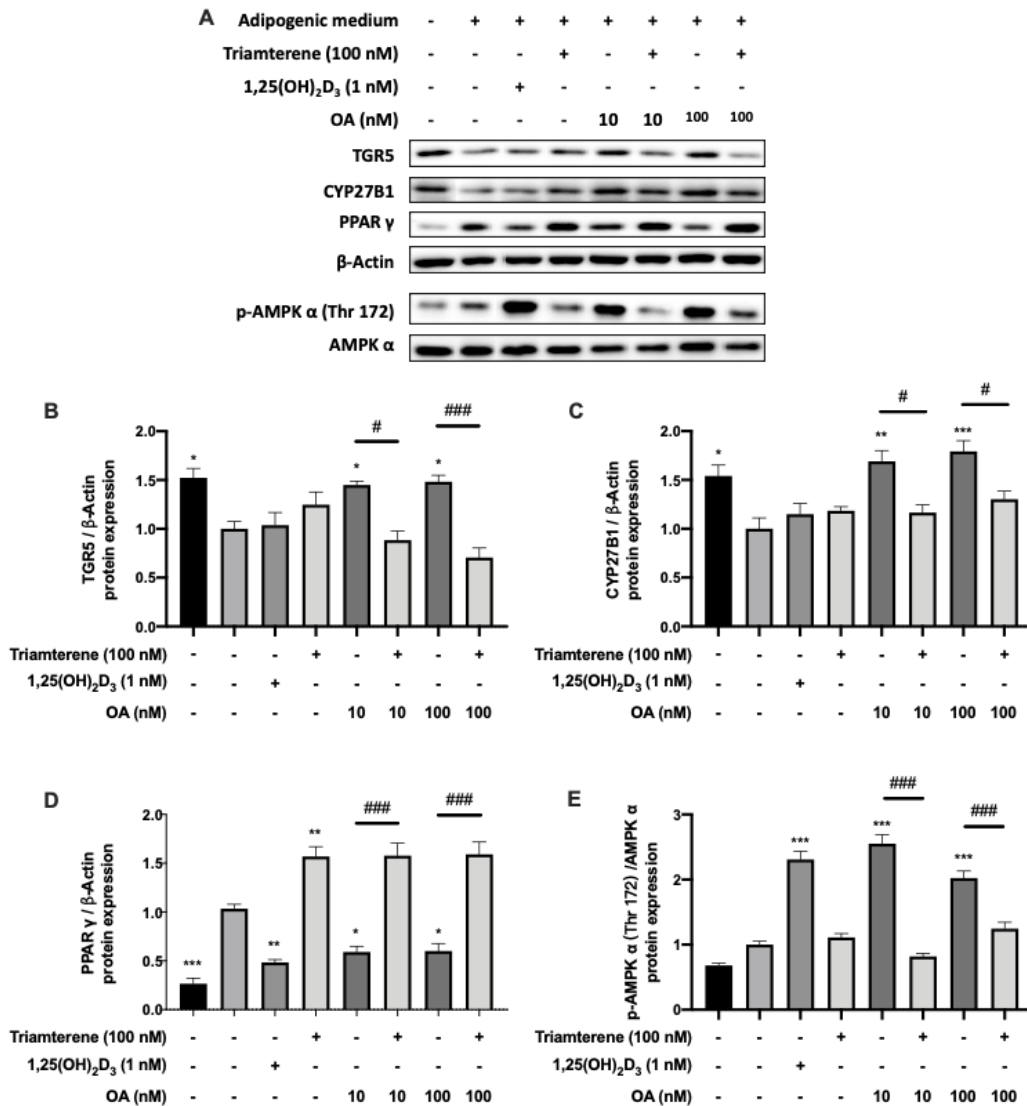
Fig. 6.7 Involvement of TGR5 in mediating effects of OA in 3T3-L1 preadipocytes.
3T3-L1 preadipocytes were differentiated in adipogenic medium in the presence of
1,25(OH)$_2$D$_3$ (1 nM) or OA (1, 10, 100 nM) for 2 days, followed by treatment in
adipocyte maintenance medium in the presence or absence of triamterene (100 nM) for
another 5 days. Protein expressions of TGR5 (A, B), CYP27B1 (A, C), PPAR γ (A, D)
and p-AMPK α (A, E) were determined by Western blotting. Data are from three
independent experiments and are shown as mean ± SEM and analyzed by using one-
way ANOVA, followed by Tukey's multiple comparison test. * $P < 0.05$, ** $P < 0.01$,
*** $P < 0.001$ vs. differentiated Control; # $P < 0.05$, ### $P < 0.001$ vs. treatment group
without inhibitor.

6.4 Discussion

The role of bone marrow adipose tissue (MAT) has drawn much attention as its amount increase with age, obesity and other metabolic disorders (Paccou et al., 2015). As the major components within the bone marrow cavity, MAT plays an important role in regulating bone homeostasis (Li et al., 2018). In this chapter, we attempted to characterize the potential effect of OA in modulating MAT accumulation and adipogenesis of BMSCs in ovariectomized (OVX) mice, and to further evaluate its actions on CYP27B1 expression and involvement in the process of adipogenesis and commitment to the adipogenic lineages *in vitro*.

In the present study, we found an intense accumulation of MAT accompanied with an accelerated bone loss in estrogen-deficient mice. In line with our findings, clinical studies reported an inverse association between BMD and the number and size of bone marrow adipocytes in osteoporotic postmenopausal women (Syed et al., 2008). It has been recognized that MAT located at distal skeleton, also known as constitutive MAT (cMAT), are formed in early life. MAT located within proximal and middle regions of tibia, femur and lumbar vertebra, also known as regulated MAT (rMAT), tends to develop in later life and is sensitive to the environmental stimuli such as estrogen deficiency and dyslipidemia (Scheller et al., 2015). Lending support to this concept, our results showed that OVX significantly elevated MAT accumulation at the proximal to middle tibia, while treatment of E_2 not only suppressed the increase in rMAT but also significantly prevented estrogen deficiency-induced bone loss. These E_2 actions might be associated with its regulatory effects on osteogenesis of BMSCs by promoting the expressions of Runx2 and Osterix, and on adipogenesis by suppressing expressions of PPARγ and C/EBP α in BMSCs induced by OVX. Our results also agreed with those of Okazaki et al. (2002) which reported that estrogen dose-dependently induced osteoblastic differentiation and suppressed adipogenesis of mouse bone marrow stromal cell line in a estrogen receptor (ER)-specific manner.

Besides the increase in MAT content, body weight gain was significantly increased in OVX mice in the present study, even though their level of food intake was controlled to be similar to that of the sham-operated mice. Such estrogen-deficiency induced weight gain is often accompanied with the condition of hyperlipidemia in postmenopausal women, and was reported to be associated with the incidence of osteoporotic fractures in these women (Bredella et al., 2013; Papakitsou et al., 2004). Our results showed an elevated levels of serum triglyceride (TG) and low-density lipoprotein cholesterol (LDL-C) with decreased BMD in OVX mice, confirming the detrimental effects of serum lipids on bone metabolism. Accumulating evidence has suggested that increased levels of lipid and lipoproteins in serum posed an inhibitory effects on osteoblastic differentiation while promoted differentiation and survival of osteoclast lineages (Parhami et al., 2001; Tintut et al., 2004). Our results showed that treatment of E_2 attenuated these damages as indicated by the restoration of serum levels of PINP and reduction in serum CTX-1. These effects of E_2 appeared to be associated with its actions to suppress serum levels of non-esterified fatty acids (NEFA, also known as free fatty acids), TG and LDL-C (Fig. 6.1). Besides, MAT accumulation in tibia of OVX mice was significantly suppressed upon treatment with E_2 for 8 weeks. Our findings are in line with the clinical observations reported by Bredella et al. (2013) in which a positive relationship between serum TG levels and the content of MAT was found in obese men and women, indicating that TG could serve as an important predictor of bone marrow fat. Moreover, high-density lipoprotein cholesterol (HDL-C), which has been reported to be positively correlated with BMD Bredella et al. (2013), was significantly elevated by E_2.

An inadequate calcium intake in individuals of all ages were reported to be associated with higher BMI and fat mass (Kremer et al., 2009; Parikh et al., 2004). Moreover, the beneficial effects of calcium on regulating body weight and lipid metabolism were reported in elderly women (Caron-Jobin et al., 2011). Our results were in agreement with these observations by showing that intake of high calcium diet (HCD) significantly suppressed body weight gain as well as serum levels of TG and NEFA in OVX mice.

Numerous studies have reported that supplementation of calcium and/or vitamin D favored the reduction in visceral adipose tissue (VAT) in obese adults (Caron-Jobin et al., 2011; Rosenblum et al., 2012). Our present study was the first to report the inhibitory effects of HCD on MAT accumulation in OVX mice, although some studies reported MAT was positively correlated with VAT in overweight women (Bredella et al., 2011). Moreover, our results showed that as a result of restoration of imbalanced osteogenesis and adipogenesis of BMSCs, HCD improved bone properties and decreased accumulation of MAT in OVX mice.

The results of the present study confirmed our previous observations that OA induced a marked elevation of circulating levels of $1,25(OH)_2D_3$ in OVX mice (Cao et al., 2018). Such an increase will favor intestinal calcium absorption and renal reabsorption of calcium to improve Ca balance in OVX mice. Our results indicated that OA, acting like HCD, significantly suppressed body weight gain and hyperlipidemia in OVX mice induced by estrogen deficiency. Similar actions of OA on periphery adipose tissues and lipid metabolism were also found in animals fed with high fat diet (Liu et al., 2007; Yunoki et al., 2008). Moreover, our study showed that the decrease in BMD and the deterioration of bone microarchitecture were markedly improved in OVX mice upon treatment with OA. It is possible that OA, through its modulatory effects on lipid metabolism, attenuated the detrimental effects of elevated serum lipids on the balance between bone formation and bone resorption in OVX mice. This concept was supported by our findings that OA significantly restored the changes in serum levels of PINP and CTX-1 in mice induced by OVX. More importantly, OA effectively decreased the accumulation of MAT in OVX mice, indicating the balance between osteoblasts and adipocytes in bone marrow niche was improved.

Accumulating evidence demonstrate that the physiological effects of $1,25(OH)_2D_3$ are not limited to the regulation of calcium homeostasis. The presence of CYP27B1 and vitamin D receptor (VDR) in adipose tissues indicated the presence of paracrine or autocrine activities of $1,25(OH)_2D_3$ in such extra-renal site. It has been reported that

the adipogenic potential of MSCs increases with aging, and contributes to the increase in MAT accumulation and age-related bone loss in elderly (Bateman et al., 2017). Based on these findings, we evaluated the effects of OA on adipogenesis of MSCs in the present study by employing hMSCs from a 61-year-old female subject. Our results showed a significant reduction in CYP27B1 expression along with the adipogenic differentiation of hMSCs, indicating a reduced bioactivation of vitamin D at later phase of adipogenesis. Treatment of OA significantly increased CYP27B1 expression at different adipogenic stages of hMSCs. Moreover, our results showed that $1,25(OH)_2D_3$ and OA exerted inhibitory effects on adipogenesis of hMSCs and 3T3-L1 preadipocytes, as revealed by the reduction in the protein expressions of PPARγ as well as the decrease in accumulation of lipid droplets in adipogenic differentiated 3T3-L1 cells. Our findings are in agreement with those reported previously in which $1,25(OH)_2D_3$ was shown to modulate adipogenic differentiation and energy metabolism in 3T3-L1 preadipocytes through binding VDR (Kong et al., 2006).

It is worth noting that TGR5, a potential target of OA, also plays a part in mediating the modulatory effects of OA on CYP27B1 expression in differentiated preadipocytes. Moreover, inhibition of TGR5 abolished the inhibitory effects of OA on adipogenesis of 3T3-L1 cells, indicating the important role of TGR5 in regulating adipogenesis. Our results are in agreement with the findings of previous studies in which diet-induced body weight gain in mice was prevented by dietary supplementation of bile acids and specific agonists for TGR5 (Velazquez-Villegas et al., 2018; Watanabe et al., 2006). In addition, our results showed that the phosphorylated levels of AMPK, a signaling protein that involved in regulation of lipolysis and fatty acid oxidation, were significantly increased in 3T3-L1 cells in response to treatment of $1,25(OH)_2D_3$ and OA. Such an increase in phosphorylation of AMPK might account for the decrease in lipid droplets in adipogenic differentiated 3T3-L1 cells in response to these treatments. Our study indicated that the increase in AMPK phosphorylation might be associated with the activation of TGR5 by OA in 3T3-L1 cells, as our results showed that inhibition of TGR5 by triamterene suppressed the AMPK phosphorylation in these cells.

Such observation was also supported by others (Velazquez-Villegas et al., 2018) in which specific knockout of TGR5 in adipose tissues was found to impair AMPK-regulated mitochondrial function and lipolysis. Future study will be needed to determine if causal relationship exists between TGR5 and AMPK phosphorylation in adipose tissue.

Taken together, our results demonstrated the inverse relationship between BMD and the content of MAT in mice. The modulating effects of OA on bone properties and bone marrow fat accumulation appear to be associated with its actions on improving the balance between osteogenesis and adipogenesis of BMSCs. OA consistently upregulated CYP27B1 expression in adipocytes, which might be involved in its inhibitory effects on adipogenesis. In addition, TGR5 plays an important role in mediating the bone protective effects of OA by serving as a membrane target for the actions of OA to regulate vitamin D and lipid metabolism.

Chapter 7

Summary and conclusion

7.1 Summary

Osteoporosis has been considered a serious public health concern due to its increasing prevalence among men and women, especially the elderly. It has been recognized that the increase in bone fragility and risk of fractures are closely related to the vitamin D deficiency and inadequate calcium intake. However, emerging studies reported that the use of vitamin D and calcium supplement could not reduce the incidence of fractures in older adults (Zhao et al., 2017). Possible reasons for this contradiction are the poor absorption of vitamin D and calcium in intestine and the deterioration in the vitamin D bioactivation in older people. Thus, improvement of vitamin D activation and calcium absorption become the major focus of the present study.

Oleanolic acid is a natural pentacyclic triterpenoid compound with pleiotropic effects. The activities of OA in bone protection are also documented. Moreover, our previous study demonstrated the ability of OA to modulate circulating $1,25(OH)_2D_3$ and calcium absorption in ovariectomized (OVX) mice. These beneficial effects of OA on Ca balance and bone properties might be associated with its modulatory effects on renal CYP27B1 (Cao et al., 2018). Paracrine or autocrine activities of $1,25(OH)_2D_3$ in skeletal microenvironment has also drawn much attention due to the ubiquity of CYP27B1 and vitamin D receptor (VDR) in extrarenal sites including bone. Moreover, a reduced CYP27B1 activity was reported to be accompanied with an increase in bone marrow adipose tissue accumulation with aging, which in turn contribute to the impaired bone properties and increased risk of fractures in elderly.

Based on these findings, the hypothesis of the present study is that OA exerts bone protective effects by modulating extra-renal expression and activities of CYP27B1 in osteoblasts and bone marrow adipocytes. To validate the hypothesis, we characterized the effectiveness and the underlying mechanisms of OA to modulate extrarenal CYP27B1 in osteoblasts. In addition, the actions of intracellular produced $1,25(OH)_2D_3$ induced by OA in mediating osteogenesis were evaluated. Considering the important

role of bone marrow adipose tissues (MAT) in bone homeostasis, the effects of OA on MAT and its interaction with osteoblastic lineages in bone marrow niche were investigated. The details were illustrated in four parts.

7.1.1 OA upregulated CYP27B1 expression and activity in kidney and osteoblasts

In Chapter 3, we employed OVX mice as osteoporotic animal model to investigate the effects of OA to regulate vitamin D metabolism and bone metabolism, given the fact that vitamin D deficiency is prevalent in postmenopausal women suffering from osteoporotic fractures. We confirmed the bone protective effects of OA, as revealed by the increase in bone mineral density (BMD) and the improvement of bone microarchitectural parameters in OVX mice administrated with OA (200 ppm in diet) for 8 weeks. Such actions of OA were partially attributed to the restoration of bone turnover rate in the midst of negative calcium balance due to estrogen deficiency, as supported by the significant reduction in urinary calcium excretion of mice fed with OA-contained diet.

It has been well recognized that circulating $1,25(OH)_2D_3$ levels and renal CYP27B1 activity are tightly controlled by systemic requirement of calcium and phosphate. Our results showed that calcium balance and vitamin D metabolism were impaired in OVX mice. OA effectively elevated circulating $1,25(OH)_2D_3$ levels by upregulating renal CYP27B1 expression, which contribute to a positive calcium balance and the improvement of bone properties in mice. More importantly, the expressions of CYP27B1 in iliac crests were significantly increased in response to OA, indicating the potential action of OA to modulate paracrine or autocrine activities of $1,25(OH)_2D_3$ in skeletal microenvironment.

The modulatory activities of OA on CYP27B1 expressions in kidney and bone cells were confirmed by *in-vitro* experiments using human proximal tubule cells as well as human and rat osteoblast-like cells. Our results indicated that the effective dosages of

OA in osteoblasts (1-10 nM) appeared more accomplishable than that in kidney cells (10 μM) in view of the poor gastrointestinal absorption and bioavailability of OA. Most importantly, our results indicated the abilities of the osteoblasts to generate $1,25(OH)_2D_3$ for cellular activities when the cells were incubated with $25(OH)D_3$ (1 μM) as substrate. Moreover, the production of $1,25(OH)_2D_3$ was effectively enhanced in osteoblasts in response to treatment with OA (1 nM). Our results also demonstrated that the actions of OA on cellular production of $1,25(OH)_2D_3$ was associated with its induction of the expressions of alkaline phosphatase (ALP) and osteopontin (OPN) in osteoblasts.

7.1.2 CYP27B1 is critical in mediating osteogenic effects of OA in mature osteoblasts

In the second part, we determined the expressions and enzymatic activity of CYP27B1 at different osteogenic stages of human mesenchymal stem cells (hMSCs), which were characterized by sequentially expressed osteogenic markers including runt-related transcription factor 2 (Runx2), containing type 1 collagen (Col-1), bone sialoprotein (BSP) and OPN. Our results showed a time-dependent increase in CYP27B1 expression as well as cellular production of $1,25(OH)_2D_3$ along with the process of osteogenesis of hMSCs, implicating the requirement of $1,25(OH)_2D_3$ for osteogenesis and functions of mature osteoblasts. This concept was supported by our results which demonstrated a robust increase in expressions of BSP2 and OPN, the matrix proteins engaged in the extracellular matrix mineralization and maturation, with the increase in expression of VDR at mature stages of osteogenesis in hMSCs. In addition, OA further enhanced CYP27B1 expression and cellular production of $1,25(OH)_2D_3$ in mature osteoblastic lineages, where higher levels of calcium and phosphate is required for bone formation. The expressions of Col-1, BSP2 and OPN were also upregulated by OA, indicating the involvement of intracellular synthesized $1,25(OH)_2D_3$ in mediating the effects of OA on maturation of osteoblastic lineages.

We further determined the involvement of CYP27B1 in the osteogenic effects of OA in the mature osteoblastic MG-63 cells. In line with our findings in Chapter 3, OA markedly upregulated expression of CYP27B1 in MG-63 cells. OA also markedly improved OPN expression and ALP activity in these cells, which resemble the actions of $1,25(OH)_2D_3$. However, such actions were attenuated, at least in part, in osteoblasts in the presence of CYP27B1 siRNA. Again, these results emphasized the important role of cellular production of $1,25(OH)_2D_3$ induced by OA in the osteogenesis of mature osteoblast. Moreover, OA potentiated the actions of $25(OH)D_3$ to regulate CYP27B1 and osteogenesis when the cells were incubated with physiological levels of $25(OH)D_3$ (100 nM). The results indicated that OA could modulate vitamin D metabolism and osteogenesis of mature osteoblasts independent of the vitamin D status.

These findings provided evidence for the differential regulation of paracrine or autocrine activity of $1,25(OH)_2D_3$ at different osteogenic stages of osteoblasts. Moreover, the locally produced $1,25(OH)_2D_3$ by CYP27B1 is essential in mediating the osteogenic effects of OA by facilitating the maturation and mineral homeostasis in osteoblasts.

7.1.3 TGR5 was required for mediating the actions of OA on modulating CYP27B1 transcription in osteoblasts

Regulating CYP27B1 in osteoblasts has been the major focus since the discovery of CYP27B1 in extra-renal sites (Bikle et al., 2018). In Chapter 4, we characterized the involvement of G protein-coupled bile acid receptor 1 (TGR5) in mediating the regulatory effects of OA on CYP27B1 expression in MG-63 cells. With a structure resembling bile acids, OA has been identified as a natural ligand for the activation of TGR5 (Sato et al., 2007). Our results showed that the modulatory effects of OA on the expression and activity of CYP27B1 in osteoblasts were mimicked by lithocholic acid (LCA), a bile acid and an agonist of TGR5, indicating the potential role of TGR5 in

regulating CYP27B1 in osteoblasts. This was supported by the decreased expression of CYP27B1 in osteoblasts in the presence of TGR5 inhibitor.

Moreover, specific overexpression of TGR5 not only improved CYP27B1 expression in MG-63 cells, but also potentiated the effects of OA on CYP27B1 expression. However, these changes were attenuated in MG-63 cells when TGR5 was silenced with TGR5 siRNA. Wang et al. (2018) showed an increase in TGR5 expression with the osteogenic differentiation of pre-osteoblast MC3T3-E1 cells. Such elevated TGR5 expressions could further facilitate the effects of OA to induce CYP27B1 expression and activities in mature osteoblasts.

Subsequently, we determined the actions of OA on the phosphorylation of cAMP-responsive elements-binding protein (CREB) in osteoblasts, a transcription factor that was involved in the classical pathway for activation of TGR5 as well as activation of CYP27B1 transcription. The results showed that OA (1 nM) rapidly induced CREB phosphorylation in MG-63 cells, which was followed by the stimulation of mRNA and protein expressions of CYP27B1 to the maximal levels by 1 hour and 2 hours, respectively. However, the increase in CREB phosphorylation and CYP27B1 promoter activity in response to OA was completely obliterated by pre-treatment with TGR5 inhibitor. These results provided evidence for the modulation of CYP27B1 transcription in osteoblastic cells through the activation of TGR5 and CREB phosphorylation by OA.

7.1.4 OA suppressed the accumulation of MAT and adipogenesis of BMSCs

In Chapter 6, we characterized the potential effect of OA in modulating MAT accumulation and adipogenesis of BMSCs in OVX mice. In line with those findings in the clinical studies, our results showed an intense accumulation of MAT accompanied with the condition of hyperlipidemia in estrogen-deficient mice. In addition to the improvement in BMD and bone microarchitectures, OA significantly suppressed the accumulation of MAT and levels of serum lipids in OVX mice. It has been reported

that increased levels of lipid and lipoproteins in serum posed detrimental effects on bone metabolism by suppressing osteoblastic differentiation and improving the differentiation and survival of osteoclasts (Parhami et al., 2001; Tintut et al., 2004). It is possible that the modulation of lipid metabolism contributes to the restoration of bone turnover rate, as supported by our findings that OA significantly restored the changes in serum levels of PINP and CTX-1 in OVX mice.

The balance between adipocytes and osteoblasts also drawn our attention due to the fact that they shared common progenitors in bone marrow niche. It is believed that the differentiation of MSCs towards these two different lineages is in a mutually exclusive manner in which the accumulation of adipose tissue will occur in the expense of osteoblasts (Muruganandan et al., 2009). Our results showed that OA significantly improved the balance between adipogenesis and osteogenesis of BMSCs, as indicated by the decrease in expressions of peroxisome proliferator activated receptor gamma (PPAR γ) and CCAAT enhancer binding proteins (C/EBP α) while the increase in expressions of runt-related transcription factor 2 (Runx2) and Osterix in BMSCs of OA-fed mice.

Our results showed a significant reduction in CYP27B1 expression along with the adipogenic differentiation of hMSCs and murine 3T3-L1 preadipocytes, indicating a reduced bioactivation of vitamin D in mature adipocytes. Treatment of OA significantly inhibited adipogenesis of hMSCs and 3T3-L1 preadipocytes. Meanwhile, OA improved the expression of CYP27B1 in adipogenic differentiated cells, which was believed to partially contribute to the inhibitory effects of OA on adipogenesis and lipid droplets accumulation. Moreover, the phosphorylated levels of AMP-activated protein kinase alpha (AMPK α), the master regulator of lipid metabolism, in differentiated 3T3-L1 cells were increased in response to $1,25(OH)_2D_3$ and OA. It is worth noting that these actions of OA could be abolished when the cells were co-treated with TGR5 inhibitor, indicating that TGR5 plays an important role in mediating the bone protective effects

of OA by serving as a membrane target for the actions of OA to regulate vitamin D and lipid metabolism.

7.2 Conclusion

In conclusion, the results of the present study support our hypothesis that OA effectively upregulated the expression and activity of CYP27B1 in renal and extra-renal sites such as osteoblasts and bone marrow adipocytes, which in turn contribute to its bone protective effects (Fig. 7.1). On the one hand, OA improved calcium balance by its actions on increasing circulating $1,25(OH)_2D_3$ levels via the upregulation of renal CYP27B1. On the other hand, OA increased locally production of $1,25(OH)_2D_3$ by CYP27B1 in mature osteoblasts, which further facilitated the maturation and mineral homeostasis in osteoblasts. Moreover, OA consistently upregulated CYP27B1 expression in adipocytes that were associated with its effects on adipogenesis and lipid metabolism in BMSCs. More importantly, our results demonstrated that the actions of OA on regulating CYP27B1 expressions in osteoblasts and adipocytes were mediated by a membrane receptor TGR5 via a rapid induction of CREB phosphorylation and subsequent activation of CYP27B1 transcription.

This study provides evidence for the use of small molecule to modulate CYP27B1 expression and cellular production of $1,25(OH)_2D_3$ in extra-renal sites via the activation of TGR5 and improves our understanding of the paracrine or autocrine activities of $1,25(OH)_2D_3$ in the skeletal microenvironment.
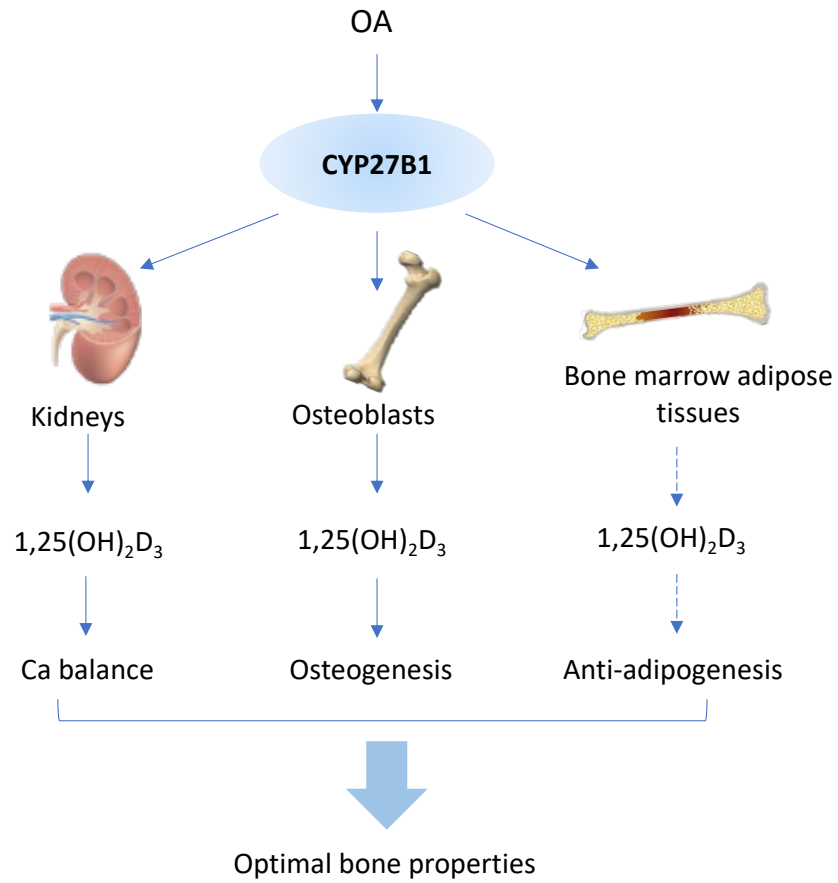
Fig. 7.1 Diagram illustrating the proposed effects of OA on the expression and activity of CYP27B1 in renal and extra-renal sites and their contribution to the optimal bone properties.

7.3 Limitation and future studies

To investigate the effects of OA on the age-related changes in CYP27B1 expression as well as osteogenesis or adipogenesis of MSCs, the present study employed hMSCs from a 61-year-old female donor. However, the results might be not be representative due to the limitation in sample size. With such consideration, hMSCs from different subjects should be included in the future study.

In the present study, the dependence of OA-regulated CYP27B1 expression on TGR5 was determined in *in-vitro* experiments using transient transfection of TGR5 siRNA. However, the efficiency of knockdown varied in each transfection. The involvement of TGR5 in mediating the regulation of CYP27B1 and $1,25(OH)_2D_3$ levels should further be confirmed in animals with targeted ablation of TGR5.

We employed 3T3-L1, preadipocytes from murine peripheral adipose tissues, for the characterization of the effects of OA on MAT formation and lipid metabolism. However, although the peripheral adipocytes used in present study resemble those bone marrow adipocytes in many ways, evident differences between them exist due to their unique localization and functions. Therefore, advances in techniques for isolating bone marrow adipose tissues are urgently needed to fully understand the actions of OA on vitamin D metabolism and energy metabolism in them.

References

Adami, S., Isaia, G., Luisetto, G., Minisola, S., Sinigaglia, L., Gentilella, R., . . . Nuti, R. (2006). Fracture incidence and characterization in patients on osteoporosis treatment: the ICARO study. *Journal of bone and mineral research, 21*(10), 1565-1570.

Adams, J., & Hewison, M. (2012). Extrarenal expression of the 25-hydroxyvitamin D-1-hydroxylase. *Archives of biochemistry and biophysics, 523*(1), 95-102.

Adams, J. S., & Gacad, M. (1985). Characterization of 1 alpha-hydroxylation of vitamin D3 sterols by cultured alveolar macrophages from patients with sarcoidosis. *The Journal of experimental medicine, 161*(4), 755-765.

Albala, C., Yanez, M., Devoto, E., Sostin, C., Zeballos, L., & Santos, J. (1996). Obesity as a protective factor for postmenopausal osteoporosis. *International journal of obesity and related metabolic disorders: journal of the International Association for the Study of Obesity, 20*(11), 1027-1032.

Ali, H., Houghton, P., & Soumyanath, A. (2006). α-Amylase inhibitory activity of some Malaysian plants used to treat diabetes; with particular reference to Phyllanthus amarus. *Journal of ethnopharmacology, 107*(3), 449-455.

Altarejos, J. Y., & Montminy, M. (2011). CREB and the CRTC co-activators: sensors for hormonal and metabolic signals. *Nature reviews Molecular cell biology, 12*(3), 141-151.

Alvarado, H. L., Calpena, A. C., Garduno-Ramirez, M. L., Ortiz, R., Melguizo, C., Prados, J. C., & Clares, B. (2018). Nanoemulsion strategy for ursolic and oleanic acids isolates from Plumeria obtusa improves antioxidant and cytotoxic activity in melanoma cells. *Anti-Cancer Agents in Medicinal Chemistry (Formerly Current Medicinal Chemistry-Anti-Cancer Agents), 18*(6), 847-853.

Alves, H., Munoz-Najar, U., De Wit, J., Renard, A. J., Hoeijmakers, J. H., Sedivy, J. M., . . . De Boer, J. (2010). A link between the accumulation of DNA damage and loss of multi-potency of human mesenchymal stromal cells. *Journal of cellular and molecular medicine, 14*(12), 2729-2738.

Anderson, P., Atkins, G., Findlay, D., Oloughlin, P., Welldon, K., Vincent, C., & Morris, H. (2007). RNAi-mediated silencing of CYP27B1 abolishes 1, 25 (OH) 2D3 synthesis and reduces osteocalcin and CYP24 mRNA expression in human osteosarcoma (HOS) cells. *The Journal of steroid biochemistry and molecular biology, 103*(3-5), 601-605.

Anderson, P. H., Iida, S., Tyson, J. H., Turner, A. G., & Morris, H. A. (2010). Bone CYP27B1 gene expression is increased with high dietary calcium and in mineralising osteoblasts. *The Journal of Steroid Biochemistry and Molecular Biology, 121*(1-2), 71-75.

Anderson, P. H., O'Loughlin, P. D., May, B. K., & Morris, H. A. (2005). Modulation of CYP27B1 and CYP24 mRNA expression in bone is independent of circulating 1, 25 (OH) 2D3 levels. *Bone, 36*(4), 654-662.

Armbrecht, H., Hodam, T., & Boltz, M. (2003). Hormonal regulation of 25-hydroxyvitamin D3-1α-hydroxylase and 24-hydroxylase gene transcription in opossum kidney cells. *Archives of biochemistry and biophysics, 409*(2), 298-304.

Atkins, G. J., Anderson, P. H., Findlay, D. M., Welldon, K. J., Vincent, C., Zannettino, A. C., . . . Morris, H. A. (2007). Metabolism of vitamin D3 in human osteoblasts: evidence for autocrine and paracrine activities of 1α, 25-dihydroxyvitamin D3. *Bone, 40*(6), 1517-1528.

Bailey, D., McKay, H., Mirwald, R., Crocker, P., & Faulkner, R. (1999). A six-year longitudinal study of the relationship of physical activity to bone mineral accrual in growing children: the university of Saskatchewan bone mineral accrual study. *Journal of bone and mineral research, 14*(10), 1672-1679.

Bateman, M. E., Strong, A. L., McLachlan, J. A., Burow, M. E., & Bunnell, B. A. (2017). The effects of endocrine disruptors on adipogenesis and osteogenesis in mesenchymal stem cells: a review. *Frontiers in endocrinology, 7*, 171.

Beier, E. E., Inzana, J. A., Sheu, T.-J., Shu, L., Puzas, J. E., & Mooney, R. A. (2015). Effects of combined exposure to lead and high-fat diet on bone quality in juvenile male mice. *Environmental health perspectives, 123*(10), 935-943.

Bellows, C. G., Reimers, S., & Heersche, J. N. (1999). Expression of mRNAs for type-I collagen, bone sialoprotein, osteocalcin, and osteopontin at different stages of osteoblastic differentiation and their regulation by 1, 25 dihydroxyvitamin D 3. *Cell and tissue research, 297*(2), 249-259.

Benayahu, D., Shur, I., & Ben-Eliyahu, S. (2000). Hormonal changes affect the bone and bone marrow cells in a rat model. *Journal of Cellular Biochemistry, 79*(3), 407-415.

Bian, Q., Liu, S.-f., Huang, J.-h., Yang, Z., Tang, D.-z., Zhou, Q., . . . Shen, Z.-y. (2012). Oleanolic acid exerts an osteoprotective effect in ovariectomy-induced osteoporotic rats and stimulates the osteoblastic differentiation of bone mesenchymal stem cells in vitro. *Menopause, 19*(2), 225-233.

Bianco, P., Fisher, L. W., Young, M. F., Termine, J. D., & Robey, P. G. (1991). Expression of bone sialoprotein (BSP) in developing human tissues. *Calcified tissue international, 49*(6), 421-426.

Bikle, D. D. (2018). Vitamin D Biochemistry and Physiology. In *Extraskeletal Effects of Vitamin D* (pp. 1-40): Springer.

Bikle, D. D., Patzek, S., & Wang, Y. (2018). Physiologic and pathophysiologic roles of extra renal CYP27b1: Case report and review. *Bone reports, 8*, 255-267.

BIKLE, D. D., PILLAI, S., GEE, E., & HINCENBERGS, M. (1991). Tumor necrosis factor-α regulation of 1, 25-dihydroxy vitamin D production by human keratinocytes. *Endocrinology, 129*(1), 33-38.

Bliuc, D., Nguyen, T. V., & Eisman, J. A. (2007). Risk of subsequent fracture after low-trauma fracture in men and women. *Jama, 297*(4), 387-394.

Bolland, M. J., Avenell, A., Baron, J. A., Grey, A., MacLennan, G. S., Gamble, G. D., & Reid, I. R. (2010). Effect of calcium supplements on risk of myocardial infarction and cardiovascular events: meta-analysis. *Bmj, 341*, c3691.

Bone, H. G., Kiel, D. P., Lindsay, R. S., Lewiecki, E. M., Bolognese, M. A., Leary, E. T., . . . McClung, M. R. (2007). Effects of atorvastatin on bone in postmenopausal women with dyslipidemia: a double-blind, placebo-controlled, dose-ranging trial. *The Journal of Clinical Endocrinology & Metabolism, 92*(12), 4671-4677.

Bonnick, S., Broy, S., Kaiser, F., Teutsch, C., Rosenberg, E., DeLucca, P., & Melton, M. (2007). Treatment with alendronate plus calcium, alendronate alone, or calcium alone for postmenopausal low bone mineral density. *Current medical research and opinion, 23*(6), 1341-1349.

Bouillon, R., Carmeliet, G., Verlinden, L., van Etten, E., Verstuyf, A., Luderer, H. F., . . . Demay, M. (2008). Vitamin D and human health: lessons from vitamin D receptor null mice. *Endocrine reviews, 29*(6), 726-776.

Bouillon, R., & Laurent, M. R. (2020). Vitamin D and Bone Health: Basic and Clinical Aspects. In *Osteoporosis* (pp. 71-87): Springer.

Boullata, J. I. (2010). Vitamin D supplementation: a pharmacologic perspective. *Current Opinion in Clinical Nutrition & Metabolic Care, 13*(6), 677-684.

Boyle, W. J., Simonet, W. S., & Lacey, D. L. (2003). Osteoclast differentiation and activation. *Nature, 423*(6937), 337-342.

Bredella, M. A., Gill, C. M., Gerweck, A. V., Landa, M. G., Kumar, V., Daley, S. M., . . . Miller, K. K. (2013). Ectopic and serum lipid levels are positively associated with bone marrow fat in obesity. *Radiology, 269*(2), 534-541.

Bredella, M. A., Torriani, M., Ghomi, R. H., Thomas, B. J., Brick, D. J., Gerweck, A. V., . . . Miller, K. K. (2011). Vertebral bone marrow fat is positively associated with visceral fat and inversely associated with IGF-1 in obese women. *Obesity, 19*(1), 49-53.

Brenza, H. L., & DeLuca, H. F. (2000). Regulation of 25-hydroxyvitamin D3 1α-hydroxylase gene expression by parathyroid hormone and 1, 25-dihydroxyvitamin D3. *Archives of biochemistry and biophysics, 381*(1), 143-152.

Brenza, H. L., Kimmel-Jehan, C., Jehan, F., Shinki, T., Wakino, S., Anazawa, H., . . . DeLuca, H. F. (1998). Parathyroid hormone activation of the 25-hydroxyvitamin D3-1α-hydroxylase gene promoter. *Proceedings of the National Academy of Sciences, 95*(4), 1387-1391.

174

Budzik, B. W., Evans, K. A., Wisnoski, D. D., Jin, J., Rivero, R. A., Szewczyk, G. R., . . . Yu, H. (2010). Synthesis and structure–activity relationships of a series of 3-aryl-4-isoxazolecarboxamides as a new class of TGR5 agonists. *Bioorganic & medicinal chemistry letters, 20*(4), 1363-1367.

Burge, R., Dawson-Hughes, B., Solomon, D. H., Wong, J. B., King, A., & Tosteson, A. (2007). Incidence and economic burden of osteoporosis-related fractures in the United States, 2005–2025. *Journal of bone and mineral research, 22*(3), 465-475.

Burguera, B., Hofbauer, L. C., Thomas, T., Gori, F., Evans, G. L., Khosla, S., . . . Turner, R. T. (2001). Leptin reduces ovariectomy-induced bone loss in rats. *Endocrinology, 142*(8), 3546-3553.

Cao, S., Dong, X.-L., Ho, M.-X., Yu, W.-X., Wong, K.-C., Yao, X.-S., & Wong, M.-S. (2018). Oleanolic acid exerts osteoprotective effects and modulates vitamin D metabolism. *Nutrients, 10*(2), 247.

Cao, S., Tian, X.-L., Yu, W.-X., Zhou, L.-P., Dong, X.-L., Favus, M. J., & Wong, M.-S. (2018). Oleanolic acid and ursolic acid improve bone properties and calcium balance and modulate vitamin D metabolism in aged female rats. *Frontiers in pharmacology, 9*, 1435.

Carmeliet, G., Dermauw, V., & Bouillon, R. (2015). Vitamin D signaling in calcium and bone homeostasis: a delicate balance. *Best Practice & Research Clinical Endocrinology & Metabolism, 29*(4), 621-631.

Caron-Jobin, M., Morisset, A. S., Tremblay, A., Huot, C., Légaré, D., & Tchernof, A. (2011). Elevated serum 25 (OH) D concentrations, vitamin D, and calcium intakes are associated with reduced adipocyte size in women. *Obesity, 19*(7), 1335-1341.

Carrelli, A., Bucovsky, M., Horst, R., Cremers, S., Zhang, C., Bessler, M., . . . Silverberg, S. J. (2017). Vitamin D storage in adipose tissue of obese and normal weight women. *Journal of bone and mineral research, 32*(2), 237-242.

Cauley, J. A., Robbins, J., Chen, Z., Cummings, S. R., Jackson, R. D., LaCroix, A. Z., . . . Neuner, J. (2003). Effects of estrogen plus progestin on risk of fracture and bone mineral density: the Women's Health Initiative randomized trial. *Jama, 290*(13), 1729-1738.

Chakravarti, B., Maurya, R., Siddiqui, J. A., Bid, H. K., Rajendran, S., Yadav, P. P., & Konwar, R. (2012). In vitro anti-breast cancer activity of ethanolic extract of Wrightia tomentosa: role of pro-apoptotic effects of oleanolic acid and urosolic acid. *Journal of ethnopharmacology, 142*(1), 72-79.

Chan, K., Qin, L., Lau, M., Woo, J., Au, S., Choy, W., . . . Lee, S. (2004). A randomized, prospective study of the effects of Tai Chi Chun exercise on bone mineral density in postmenopausal women. *Archives of physical medicine and rehabilitation, 85*(5), 717-722.

Chanakul, A., Zhang, M. Y., Louw, A., Armbrecht, H. J., Miller, W. L., Portale, A. A., & Perwad, F. (2013). FGF-23 regulates CYP27B1 transcription in the kidney and in extra-renal tissues. *PloS*

one, 8(9), e72816.

Chang, E., & Kim, Y. (2016). Vitamin D decreases adipocyte lipid storage and increases NAD-SIRT1 pathway in 3T3-L1 adipocytes. *Nutrition, 32*(6), 702-708.

Chen, P., Li, Z., & Hu, Y. (2016). Prevalence of osteoporosis in China: a meta-analysis and systematic review. *BMC public health, 16*(1), 1039.

Chilliard, Y., Delavaud, C., & Bonnet, M. (2005). Leptin expression in ruminants: nutritional and physiological regulations in relation with energy metabolism. *Domestic animal endocrinology, 29*(1), 3-22.

Chow, J., Tobias, J., Colston, K., & Chambers, T. (1992). Estrogen maintains trabecular bone volume in rats not only by suppression of bone resorption but also by stimulation of bone formation. *The Journal of clinical investigation, 89*(1), 74-78.

Cohen, A., Dempster, D. W., Recker, R. R., Lappe, J. M., Zhou, H., Zwahlen, A., . . . Lang, T. (2013). Abdominal fat is associated with lower bone formation and inferior bone quality in healthy premenopausal women: a transiliac bone biopsy study. *The Journal of Clinical Endocrinology & Metabolism, 98*(6), 2562-2572.

Coipeau, P., Rosset, P., Langonné, A., Gaillard, J., Delorme, B., Rico, A., . . . Sensebé, L. (2009). Impaired differentiation potential of human trabecular bone mesenchymal stromal cells from elderly patients. *Cytotherapy, 11*(5), 584-594.

Colin, E., Van Den Bemd, G., Van Aken, M., Christakos, S., De Jonge, H., Deluca, H., . . . Pols, H. (1999). Evidence for involvement of 17β-estradiol in intestinal calcium absorption independent of 1, 25-dihydroxyvitamin D3 level in the rat. *Journal of Bone and Mineral Research, 14*(1), 57-64.

Colussi, G., Ganon, L., Penco, S., De Ferrari, M. E., Ravera, F., Querques, M., . . . Dinour, D. (2014). Chronic hypercalcaemia from inactivating mutations of vitamin D 24-hydroxylase (CYP24A1): implications for mineral metabolism changes in chronic renal failure. *Nephrology Dialysis Transplantation, 29*(3), 636-643.

Cosman, F. (2014). Anabolic and antiresorptive therapy for osteoporosis: combination and sequential approaches. *Current osteoporosis reports, 12*(4), 385-395.

Crissey, S. D., Ange, K. D., Jacobsen, K. L., Slifka, K. A., Bowen, P. E., Stacewicz-Sapuntzakis, M., . . . Ward, A. (2003). Serum concentrations of lipids, vitamin D metabolites, retinol, retinyl esters, tocopherols and selected carotenoids in twelve captive wild felid species at four zoos. *The Journal of nutrition, 133*(1), 160-166.

Cui, H., Zhu, Y., Yang, Q., Zhao, W., Zhang, S., Zhou, A., & Jiang, D. (2016). Necrostatin-1 treatment inhibits osteocyte necroptosis and trabecular deterioration in ovariectomized rats. *Scientific reports, 6*(1), 1-13.

Cummings, S. R., Ferrari, S., Eastell, R., Gilchrist, N., Jensen, J. E. B., McClung, M., . . . Wang, A. T. (2018). Vertebral fractures after discontinuation of denosumab: a post hoc analysis of the randomized placebo‑controlled FREEDOM trial and its extension. *Journal of bone and mineral research, 33*(2), 190-198.

Cummings, S. R., Martin, J. S., McClung, M. R., Siris, E. S., Eastell, R., Reid, I. R., . . . Wang, A. (2009). Denosumab for prevention of fractures in postmenopausal women with osteoporosis. *New England Journal of Medicine, 361*(8), 756-765.

da Silva Meirelles, L., Chagastelles, P. C., & Nardi, N. B. (2006). Mesenchymal stem cells reside in virtually all post-natal organs and tissues. *Journal of cell science, 119*(11), 2204-2213.

Dardenne, O., Prud'Homme, J., Hacking, S. A., Glorieux, F. H., & St‑Arnaud, R. (2003). Rescue of the pseudo‑vitamin D deficiency rickets phenotype of CYP27B1‑deficient mice by treatment with 1, 25‑dihydroxyvitamin D3: biochemical, histomorphometric, and biomechanical analyses. *Journal of bone and mineral research, 18*(4), 637-643.

Dardenne, O., Prud'Homme, J., Hacking, S., Glorieux, F., & St-Arnaud, R. (2003). Correction of the abnormal mineral ion homeostasis with a high-calcium, high-phosphorus, high-lactose diet rescues the PDDR phenotype of mice deficient for the 25-hydroxyvitamin D-1α-hydroxylase (CYP27B1). *Bone, 32*(4), 332-340.

de Melo, C. L., Queiroz, M. G. R., Fonseca, S. G., Bizerra, A. M., Lemos, T. L., Melo, T. S., . . . Rao, V. S. (2010). Oleanolic acid, a natural triterpenoid improves blood glucose tolerance in normal mice and ameliorates visceral obesity in mice fed a high-fat diet. *Chemico-biological interactions, 185*(1), 59-65.

De Schepper, J. (2019). Bone Development During Childhood and Adolescence: Peak Bone Mass.

Ding, H., Hu, X., Xu, X., Zhang, G., & Gong, D. (2018). Inhibitory mechanism of two allosteric inhibitors, oleanolic acid and ursolic acid on α-glucosidase. *International journal of biological macromolecules, 107*, 1844-1855.

Dinour, D., Beckerman, P., Ganon, L., Tordjman, K., Eisenstein, Z., & Holtzman, E. J. (2013). Loss-of-function mutations of CYP24A1, the vitamin D 24-hydroxylase gene, cause long-standing hypercalciuric nephrolithiasis and nephrocalcinosis. *The Journal of urology, 190*(2), 552-557.

Donnelly, E., & Boskey, A. L. (2011). Mineralization. In *Vitamin D* (pp. 381-401): Elsevier.

Drissi, H., Pouliot, A., Koolloos, C., Stein, J. L., Lian, J. B., Stein, G. S., & Van Wijnen, A. J. (2002). 1, 25-(OH) 2-vitamin D3 suppresses the bone-related Runx2/Cbfa1 gene promoter. *Experimental cell research, 274*(2), 323-333.

Duboc, H., Taché, Y., & Hofmann, A. F. (2014). The bile acid TGR5 membrane receptor: from basic research to clinical application. *Digestive and Liver Disease, 46*(4), 302-312.

Ducy, P., Zhang, R., Geoffroy, V., Ridall, A. L., & Karsenty, G. (1997). Osf2/Cbfa1: a transcriptional activator of osteoblast differentiation. *cell, 89*(5), 747-754.

Duque, G., Macoritto, M., & Kremer, R. (2004). 1, 25 (OH) 2D3 inhibits bone marrow adipogenesis in senescence accelerated mice (SAM-P/6) by decreasing the expression of peroxisome proliferator-activated receptor gamma 2 (PPARγ2). *Experimental gerontology, 39*(3), 333-338.

Duque, G., Rivas, D., Li, W., Li, A., Henderson, J. E., Ferland, G., & Gaudreau, P. (2009). Age-related bone loss in the LOU/c rat model of healthy ageing. *Experimental gerontology, 44*(3), 183-189.

El Maghraoui, A., Ngbanda, A., Bensaoud, N., Bensaoud, M., Rezqi, A., & Tazi, M. (2013). Age-adjusted incidence rates of hip fractures between 2006 and 2009 in Rabat, Morocco. *Osteoporosis international, 24*(4), 1267-1273.

Elbaz, A., Wu, X., Rivas, D., Gimble, J. M., & Duque, G. (2010). Inhibition of fatty acid biosynthesis prevents adipocyte lipotoxicity on human osteoblasts in vitro. *Journal of cellular and molecular medicine, 14*(4), 982-991.

Ettinger, B., Black, D. M., Mitlak, B. H., Knickerbocker, R. K., Nickelsen, T., Genant, H. K., . . . Stakkestad, J. (1999). Reduction of vertebral fracture risk in postmenopausal women with osteoporosis treated with raloxifene: results from a 3-year randomized clinical trial. *Jama, 282*(7), 637-645.

Feskanich, D., Willett, W., & Colditz, G. (2002). Walking and leisure-time activity and risk of hip fracture in postmenopausal women. *Jama, 288*(18), 2300-2306.

Fiorucci, S., Mencarelli, A., Palladino, G., & Cipriani, S. (2009). Bile-acid-activated receptors: targeting TGR5 and farnesoid-X-receptor in lipid and glucose disorders. *Trends in pharmacological sciences, 30*(11), 570-580.

Flanagan, J. N., Wang, L., Tangpricha, V., Reichrath, J., Chen, T. C., & Holick, M. F. (2003). Regulation of the 25-hydroxyvitamin D-1α-hydroxylase gene and its splice variant. In *Vitamin D Analogs in Cancer Prevention and Therapy* (pp. 157-167): Springer.

Fraser, D., & Kodicek, E. (1970). Unique biosynthesis by kidney of a biologically active vitamin D metabolite. *Nature, 228*(5273), 764-766.

Füchtbauer, L., Brusgaard, K., Ledaal, P., Frost, M., & Frederiksen, A. L. (2015). Case report: vitamin D‐dependent rickets type 1 caused by a novel CYP27B1 mutation. *Clinical case reports, 3*(12), 1012.

Furtado, R. A., Rodrigues, E. P., Araujo, F. R., Oliveira, W. L., Furtado, M. A., Castro, M. B., . . . Tavares, D. C. (2008). Ursolic acid and oleanolic acid suppress preneoplastic lesions induced by 1, 2-dimethylhydrazine in rat colon. *Toxicologic pathology, 36*(4), 576-580.

Gao, X.-H., Dwivedi, P. P., Choe, S., Alba, F., Morris, H. A., Omdahl, J. L., & May, B. K. (2002). Basal and parathyroid hormone induced expression of the human 25-hydroxyvitamin D 1α-hydroxylase gene promoter in kidney AOK-B50 cells: role of Sp1, Ets and CCAAT box protein binding sites. *The international journal of biochemistry & cell biology, 34*(8), 921-930.

Gardiner, E. M., Baldock, P. A., Thomas, G. P., Sims, N. A., Henderson, N. K., Hollis, B., . . . Walsh, W. R. (2000). Increased formation and decreased resorption of bone in mice with elevated vitamin D receptor in mature cells of the osteoblastic lineage. *The FASEB Journal, 14*(13), 1908-1916.

Geng, S., Zhou, S., & Glowacki, J. (2011a). Age‐related decline in osteoblastogenesis and 1α-hydroxylase/CYP27B1 in human mesenchymal stem cells: stimulation by parathyroid hormone. *Aging Cell, 10*(6), 962-971.

Geng, S., Zhou, S., & Glowacki, J. (2011b). Effects of 25‐hydroxyvitamin D3 on proliferation and osteoblast differentiation of human marrow stromal cells require CYP27B1/1α-hydroxylase. *Journal of bone and mineral research, 26*(5), 1145-1153.

Gilsanz, V., Chalfant, J., Mo, A. O., Lee, D. C., Dorey, F. J., & Mittelman, S. D. (2009). Reciprocal relations of subcutaneous and visceral fat to bone structure and strength. *The Journal of Clinical Endocrinology & Metabolism, 94*(9), 3387-3393.

Glowacki, J., Hurwitz, S., Thornhill, T. S., Kelly, M., & LeBoff, M. S. (2003). Osteoporosis and vitamin-D deficiency among postmenopausal women with osteoarthritis undergoing total hip arthroplasty. *JBJS, 85*(12), 2371-2377.

Goltzman, D. (2018). Functions of vitamin D in bone. *Histochemistry and cell biology, 149*(4), 305-312.

Goto, H., Hozumi, A., Osaki, M., Fukushima, T., Sakamoto, K., Yonekura, A., . . . Baba, H. (2011). Primary human bone marrow adipocytes support TNF-α-induced osteoclast differentiation and function through RANKL expression. *Cytokine, 56*(3), 662-668.

Gray, T. K., Lester, G. E., & Lorenc, R. S. (1979). Evidence for extra-renal 1 alpha-hydroxylation of 25-hydroxyvitamin D3 in pregnancy. *Science, 204*(4399), 1311-1313.

Guinda, Á., Pérez-Camino, M. C., & Lanzón, A. (2004). Supplementation of oils with oleanolic acid from the olive leaf (Olea europaea). *European journal of lipid science and technology, 106*(1), 22-26.

Guo, C., Su, J., Li, Z., Xiao, R., Wen, J., Li, Y., . . . Huang, W. (2015). The G-protein-coupled bile acid receptor Gpbar1 (TGR5) suppresses gastric cancer cell proliferation and migration through antagonizing STAT3 signaling pathway. *Oncotarget, 6*(33), 34402.

Haghighi, A., Samimagham, H., & Gahardehi, G. (2013). Calcium and vitamin D supplementation and risk of kidney stone formation in postmenopausal women. *Iranian journal of kidney diseases, 7*(3), 210-213.

Hamrick, M. W., Della-Fera, M. A., Choi, Y. H., Pennington, C., Hartzell, D., & Baile, C. A. (2005). Leptin treatment induces loss of bone marrow adipocytes and increases bone formation in leptin-deficient ob/ob mice. *Journal of bone and mineral research, 20*(6), 994-1001.

Hamrick, M. W., & Ferrari, S. L. (2008). Leptin and the sympathetic connection of fat to bone. *Osteoporosis International, 19*(7), 905-912.

Hamza, M., Nadir, M., Mehmood, N., & Farooq, A. (2016). In vitro effectiveness of triterpenoids and their synergistic effect with antibiotics against Staphylococcus aureus strains. *Indian journal of pharmacology, 48*(6), 710.

Han, B., Copeland, M., Geiser, A. G., Hale, L. V., Harvey, A., Ma, Y. L., . . . Hale, J. E. (2007). Development of a highly sensitive, high-throughput, mass spectrometry-based assay for rat procollagen type-I N-terminal propeptide (PINP) to measure bone formation activity. *Journal of proteome research, 6*(11), 4218-4229.

Han, Y.-Y., Xue, X.-W., Shi, Z.-M., Wang, P.-Y., Wu, X.-R., & Wang, X.-J. (2014). Oleanolic acid and ursolic acid inhibit proliferation in transformed rat hepatic oval cells. *World Journal of Gastroenterology: WJG, 20*(5), 1348.

Haussler, M. R., Haussler, C., Jurutka, P., Thompson, P., Hsieh, J.-C., Remus, L., . . . Whitfield, G. K. (1997). The vitamin D hormone and its nuclear receptor: molecular actions and disease states. *Journal of Endocrinology, 154*(3_Suppl), S57-S73.

Haussler, M. R., Jurutka, P. W., Mizwicki, M., & Norman, A. W. (2011). Vitamin D receptor (VDR)-mediated actions of 1α, 25 (OH) 2vitamin D3: genomic and non-genomic mechanisms. *Best practice & research Clinical endocrinology & metabolism, 25*(4), 543-559.

He, G., Yu, G.-Y., Temkin, V., Ogata, H., Kuntzen, C., Sakurai, T., . . . Karin, M. (2010). Hepatocyte IKKβ/NF-κB inhibits tumor promotion and progression by preventing oxidative stress-driven STAT3 activation. *Cancer cell, 17*(3), 286-297.

Heaney, R., Abrams, S., Dawson-Hughes, B., Looker, A., Marcus, R., Matkovic, V., & Weaver, C. (2000). Peak bone mass. *Osteoporosis international, 11*(12), 985.

Heine, P., Taylor, J., Iwamoto, G., Lubahn, D., & Cooke, P. (2000). Increased adipose tissue in male and female estrogen receptor-α knockout mice. *Proceedings of the National Academy of Sciences, 97*(23), 12729-12734.

Heinzen, H., de Vries, J. X., Moyna, P., Remberg, G., Martinez, R., & Tietze, L. F. (1996). Mass spectrometry of labelled triterpenoids: thermospray and electron impact ionization analysis. *Phytochemical Analysis, 7*(5), 237-244.

Heng, B. C., Cao, T., Stanton, L. W., Robson, P., & Olsen, B. (2004). Strategies for directing the differentiation of stem cells into the osteogenic lineage in vitro. *Journal of Bone and Mineral*

Research, 19(9), 1379-1394.

HENRY, H. L., & LUNTAO, E. M. (1989). Interactions between intracellular signals involved in the regulation of 25-hydroxyvitamin D3 metabolism. *Endocrinology, 124*(5), 2228-2234.

Hock, J., & Fonseca, J. (1990). Anabolic effect of human synthetic parathyroid hormone-(1-34) depends on growth hormone. *Endocrinology, 127*(4), 1804-1810.

HOENDEROP, J. G., DARDENNE, O., VAN ABEL, M., VAN DER KEMP, A. W., VAN OS, C. H., ST.-ARNAUD, R., & BINDELS, R. M. (2002). Modulation of renal Ca2+ transport protein genes by dietary Ca2+ and 1, 25‑dihydroxyvitamin D3 in 25hydroxyvitamin D3‑1α‑hydroxylase knockout mice. *The FASEB Journal, 16*(11), 1398-1406.

Hsu, H.-Y., Yang, J.-J., & Lin, C.-C. (1997). Effects of oleanolic acid and ursolic acid on inhibiting tumor growth and enhancing the recovery of hematopoietic system postirradiation in mice. *Cancer letters, 111*(1-2), 7-13.

Huang, S., Xu, L., Sun, Y., Wu, T., Wang, K., & Li, G. (2015). An improved protocol for isolation and culture of mesenchymal stem cells from mouse bone marrow. *Journal of orthopaedic translation, 3*(1), 26-33.

Huang, Z., Ren, P.-G., Ma, T., Smith, R. L., & Goodman, S. B. (2010). Modulating osteogenesis of mesenchymal stem cells by modifying growth factor availability. *Cytokine, 51*(3), 305-310.

Ichikawa, F., Sato, K., Nanjo, M., Nishii, Y., Shinki, T., Takahashi, N., & Suda, T. (1995). Mouse primary osteoblasts express vitamin D3 25-hydroxylase mRNA and convert 1α-hydroxyvitamin D3 into 1α, 25-dihydroxyvitamin D3. *Bone, 16*(1), 129-135.

Inoue, Y., Segawa, H., Kaneko, I., Yamanaka, S., Kusano, K., Kawakami, E., . . . Saito, H. (2005). Role of the vitamin D receptor in FGF23 action on phosphate metabolism. *Biochemical Journal, 390*(1), 325-331.

Ip, T.-P., Cheung, S., Cheung, T.-C., Choi, T.-C., Chow, S., Ho, Y., . . . Leung, K. (2013). The Osteoporosis Society of Hong Kong (OSHK): 2013 OSHK guideline for clinical management of postmenopausal osteoporosis in Hong Kong. *Hong Kong Med J, 19*(Suppl 2), 1-40.

Jäger, S., Trojan, H., Kopp, T., Laszczyk, M. N., & Scheffler, A. (2009). Pentacyclic triterpene distribution in various plants–rich sources for a new group of multi-potent plant extracts. *Molecules, 14*(6), 2016-2031.

Janicka, A., Wren, T. A., Sanchez, M. M., Dorey, F., Kim, P. S., Mittelman, S. D., & Gilsanz, V. (2007). Fat mass is not beneficial to bone in adolescents and young adults. *The Journal of Clinical Endocrinology & Metabolism, 92*(1), 143-147.

Jeong, D. W., Kim, Y. H., Kim, H. H., Ji, H. Y., Yoo, S. D., Choi, W. R., . . . Lee, H. S. (2007). Dose-

linear pharmacokinetics of oleanolic acid after intravenous and oral administration in rats. *Biopharmaceutics & drug disposition, 28*(2), 51-57.

Ji, S., Doumit, M. E., & Hill, R. A. (2015). Regulation of adipogenesis and key adipogenic gene expression by 1, 25-dihydroxyvitamin D in 3T3-L1 cells. *PloS one, 10*(6), e0126142.

Jiang, Q., Yang, X., Du, P., Zhang, H., & Zhang, T. (2016). Dual strategies to improve oral bioavailability of oleanolic acid: Enhancing water-solubility, permeability and inhibiting cytochrome P450 isozymes. *European Journal of Pharmaceutics and Biopharmaceutics, 99*, 65-72.

Jiang, Y., Mishima, H., Sakai, S., Liu, Y. k., Ohyabu, Y., & Uemura, T. (2008). Gene expression analysis of major lineage-defining factors in human bone marrow cells: effect of aging, gender, and age-related disorders. *Journal of Orthopaedic Research, 26*(7), 910-917.

Jin, P., Deng, S., Tian, M., Lenahan, C., Wei, P., Wang, Y., . . . Gao, Y. (2021). INT-777 prevents cognitive impairment by activating Takeda G protein-coupled receptor 5 (TGR5) and attenuating neuroinflammation via cAMP/PKA/CREB signaling axis in a rat model of sepsis. *Experimental Neurology, 335*, 113504.

Juan, M. E., Planas, J. M., Ruiz-Gutierrez, V., Daniel, H., & Wenzel, U. (2008). Antiproliferative and apoptosis-inducing effects of maslinic and oleanolic acids, two pentacyclic triterpenes from olives, on HT-29 colon cancer cells. *British Journal of Nutrition, 100*(1), 36-43.

Jurutka, P. W., Bartik, L., Whitfield, G. K., Mathern, D. R., Barthel, T. K., Gurevich, M., . . . Haussler, M. R. (2007). Vitamin D receptor: key roles in bone mineral pathophysiology, molecular mechanism of action, and novel nutritional ligands. *Journal of bone and mineral research, 22*(S2), V2-V10.

Kakuda, S., Okada, K., Eguchi, H., Takenouchi, K., Hakamata, W., Kurihara, M., & Takimoto-Kamimura, M. (2008). Structure of the ligand-binding domain of rat VDR in complex with the nonsecosteroidal vitamin D3 analogue YR301. *Acta Crystallographica Section F: Structural Biology and Crystallization Communications, 64*(11), 970-973.

Kalaycıoğlu, Z., Uzaşçı, S., Dirmenci, T., & Erim, F. B. (2018). α-Glucosidase enzyme inhibitory effects and ursolic and oleanolic acid contents of fourteen Anatolian Salvia species. *Journal of pharmaceutical and biomedical analysis, 155*, 284-287.

Kashyap, D., Sharma, A., S Tuli, H., Punia, S., & K Sharma, A. (2016). Ursolic acid and oleanolic acid: pentacyclic terpenoids with promising anti-inflammatory activities. *Recent patents on inflammation & allergy drug discovery, 10*(1), 21-33.

Kassem, M., & Marie, P. J. (2011). Senescence-associated intrinsic mechanisms of osteoblast dysfunctions. *Aging cell, 10*(2), 191-197.

Kawamata, Y., Fujii, R., Hosoya, M., Harada, M., Yoshida, H., Miwa, M., . . . Shintani, Y. (2003). AG

protein-coupled receptor responsive to bile acids. *Journal of Biological Chemistry, 278*(11), 9435-9440.

Khan, A. A., Morrison, A., Hanley, D. A., Felsenberg, D., McCauley, L. K., O'Ryan, F., . . . Tetradis, S. (2015). Diagnosis and management of osteonecrosis of the jaw: a systematic review and international consensus. *Journal of bone and mineral research, 30*(1), 3-23.

Khosla, S., Bilezikian, J. P., Dempster, D. W., Lewiecki, E. M., Miller, P. D., Neer, R. M., . . . Potts, J. T. (2012). Benefits and risks of bisphosphonate therapy for osteoporosis. *The Journal of Clinical Endocrinology & Metabolism, 97*(7), 2272-2282.

Kiernan, J., Davies, J. E., & Stanford, W. L. (2017). Concise review: musculoskeletal stem cells to treat age‐related osteoporosis. *Stem Cells Translational Medicine, 6*(10), 1930-1939.

Kim, H.-S., Han, S.-Y., Sung, H.-Y., Park, S.-H., Kang, M.-K., Han, S.-J., & Kang, Y.-H. (2014). Blockade of visfatin induction by oleanolic acid via disturbing IL-6-TRAF6-NF-κB signaling of adipocytes. *Experimental biology and medicine, 239*(3), 284-292.

Kim, J., Yang, G., Kim, Y., Kim, J., & Ha, J. (2016). AMPK activators: mechanisms of action and physiological activities. *Experimental & molecular medicine, 48*(4), e224-e224.

Kim, J.-Y., Cheon, Y.-H., Yoon, K.-H., Lee, M. S., & Oh, J. (2014). Parthenolide inhibits osteoclast differentiation and bone resorbing activity by down-regulation of NFATc1 induction and c-Fos stability, during RANKL-mediated osteoclastogenesis. *BMB reports, 47*(8), 451.

Kim, J. M., Choi, J. S., Kim, Y. H., Jin, S. H., Lim, S., Jang, H. J., . . . Suh, P. G. (2013). An activator of the cAMP/PKA/CREB pathway promotes osteogenesis from human mesenchymal stem cells. *Journal of cellular physiology, 228*(3), 617-626.

Kim, S., Yamazaki, M., Shevde, N. K., & Pike, J. W. (2007). Transcriptional control of receptor activator of nuclear factor-κB ligand by the protein kinase A activator forskolin and the transmembrane glycoprotein 130-activating cytokine, oncostatin M, is exerted through multiple distal enhancers. *Molecular endocrinology, 21*(1), 197-214.

Kong, J., & Li, Y. C. (2006). Molecular mechanism of 1, 25-dihydroxyvitamin D3 inhibition of adipogenesis in 3T3-L1 cells. *American Journal of Physiology-Endocrinology and Metabolism, 290*(5), E916-E924.

Kong, X. F., Zhu, X. H., Pei, Y. L., Jackson, D. M., & Holick, M. F. (1999). Molecular cloning, characterization, and promoter analysis of the human 25-hydroxyvitamin D3-1α-hydroxylase gene. *Proceedings of the National Academy of Sciences, 96*(12), 6988-6993.

Kong, Y., Bai, P.-s., Sun, H., Nan, K.-j., Chen, N.-z., & Qi, X.-g. (2012). The deoxycholic acid targets miRNA-dependent CAC1 gene expression in multidrug resistance of human colorectal cancer. *The international journal of biochemistry & cell biology, 44*(12), 2321-2332.

Kostenuik, P. J., Nguyen, H. Q., McCabe, J., Warmington, K. S., Kurahara, C., Sun, N., . . . Van, G. (2009). Denosumab, a fully human monoclonal antibody to RANKL, inhibits bone resorption and increases BMD in knock‑in mice that express chimeric (murine/human) RANKL. *Journal of bone and mineral research, 24*(2), 182-195.

Kragballe, K. (1992). Treatment of psoriasis with calcipotriol and other vitamin D analogues. *Journal of the American Academy of Dermatology, 27*(6), 1001-1008.

Kremer, R., Campbell, P. P., Reinhardt, T., & Gilsanz, V. (2009). Vitamin D status and its relationship to body fat, final height, and peak bone mass in young women. *The Journal of Clinical Endocrinology & Metabolism, 94*(1), 67-73.

Kyeyune-Nyombi, E., Lau, K.-H. W., Baylink, D. J., & Strong, D. D. (1991). 1, 25-Dihydroxyvitamin D3 stimulates both alkaline phosphatase gene transcription and mRNA stability in human bone cells. *Archives of biochemistry and biophysics, 291*(2), 316-325.

Lac, G., Cavalie, H., Ebal, E., & Michaux, O. (2008). Effects of a high fat diet on bone of growing rats. Correlations between visceral fat, adiponectin and bone mass density. *Lipids in health and disease, 7*(1), 16.

Laszczyk, M. N. (2009). Pentacyclic triterpenes of the lupane, oleanane and ursane group as tools in cancer therapy. *Planta medica, 75*(15), 1549-1560.

Lau, E., Woo, J., Swaminathan, R., MacDonald, D., & Donnan, S. (1989). Plasma 25-hydroxyvitamin D concentration in patients with hip fracture in Hong Kong. *Gerontology, 35*(4), 198-204.

Lecka-Czernik, B. (2012). Marrow fat metabolism is linked to the systemic energy metabolism. *Bone, 50*(2), 534-539.

Lee, N. K., & Karsenty, G. (2008). Reciprocal regulation of bone and energy metabolism. *Trends in Endocrinology & Metabolism, 19*(5), 161-166.

Lee, W. Y., Zhang, T., Lau, C. P., Wang, C., Chan, K.-M., & Li, G. (2013). Immortalized human fetal bone marrow-derived mesenchymal stromal cell expressing suicide gene for anti-tumor therapy in vitro and in vivo. *Cytotherapy, 15*(12), 1484-1497.

Lefterova, M. I., Zhang, Y., Steger, D. J., Schupp, M., Schug, J., Cristancho, A., . . . Liu, X. S. (2008). PPARγ and C/EBP factors orchestrate adipocyte biology via adjacent binding on a genome-wide scale. *Genes & development, 22*(21), 2941-2952.

Li, H.-F., Wang, X.-A., Xiang, S.-S., Hu, Y.-P., Jiang, L., Shu, Y.-J., . . . Ye, Y.-Y. (2015). Oleanolic acid induces mitochondrial-dependent apoptosis and G0/G1 phase arrest in gallbladder cancer cells. *Drug Design, Development and Therapy, 9*, 3017.

Li, J., Byrne, M. E., Chang, E., Jiang, Y., Donkin, S. S., Buhman, K. K., . . . Teegarden, D. (2008). 1α,

25-Dihydroxyvitamin D hydroxylase in adipocytes. *The Journal of steroid biochemistry and molecular biology, 112*(1-3), 122-126.

Li, M., Han, Z., Bei, W., Rong, X., Guo, J., & Hu, X. (2015). Oleanolic acid attenuates insulin resistance via NF-κB to regulate the IRS1-GLUT4 pathway in HepG2 cells. *Evidence-Based Complementary and Alternative Medicine, 2015*.

Li, Q., Wu, Y., & Kang, N. (2018). Marrow adipose tissue: its origin, function, and regulation in bone remodeling and regeneration. *Stem cells international, 2018*.

Li, X., Song, Y., Zhang, P., Zhu, H., Chen, L., Xiao, Y., & Xing, Y. (2016). Oleanolic acid inhibits cell survival and proliferation of prostate cancer cells in vitro and in vivo through the PI3K/Akt pathway. *Tumor Biology, 37*(6), 7599-7613.

Li, Y., Cheng, K. C., Niu, C.-S., Lo, S.-H., Cheng, J.-T., & Niu, H.-S. (2017). Investigation of triamterene as an inhibitor of the TGR5 receptor: Identification in cells and animals. *Drug design, development and therapy, 11*, 1127.

Li, Y., Wang, J., Gu, T., Yamahara, J., & Li, Y. (2014). Oleanolic acid supplement attenuates liquid fructose-induced adipose tissue insulin resistance through the insulin receptor substrate-1/phosphatidylinositol 3-kinase/Akt signaling pathway in rats. *Toxicology and applied pharmacology, 277*(2), 155-163.

Li, Z., Huang, J., Wang, F., Li, W., Wu, X., Zhao, C., . . . Qian, M. (2019). Dual Targeting of Bile Acid Receptor-1 (TGR5) and Farnesoid X Receptor (FXR) Prevents Estrogen-Dependent Bone Loss in Mice. *Journal of bone and mineral research, 34*(4), 765-776.

Lin, X., Xiong, D., Peng, Y.-Q., Sheng, Z.-F., Wu, X.-Y., Wu, X.-P., . . . Liao, E.-Y. (2015). Epidemiology and management of osteoporosis in the People's Republic of China: current perspectives. *Clinical interventions in aging, 10*, 1017.

Lin, Y.-N., Chang, H.-Y., Wang, C. C., Chu, F.-Y., Shen, H.-Y., Chen, C.-J., & Lim, Y.-P. (2018). Oleanolic acid inhibits liver X receptor alpha and pregnane X receptor to attenuate ligand-induced lipogenesis. *Journal of agricultural and food chemistry, 66*(42), 10964-10976.

Liu, C., Li, Y., Zuo, G., Xu, W., Gao, H., Yang, Y., . . . Li, Y. (2013). Oleanolic Acid diminishes liquid fructose-induced Fatty liver in rats: role of modulation of hepatic sterol regulatory element-binding protein-1c-mediated expression of genes responsible for de novo Fatty Acid synthesis. *Evidence-Based Complementary and Alternative Medicine, 2013*.

Liu, J. (1995). Pharmacology of oleanolic acid and ursolic acid. *Journal of ethnopharmacology, 49*(2), 57-68.

Liu, J. (2005). Oleanolic acid and ursolic acid: research perspectives. *Journal of ethnopharmacology, 100*(1-2), 92-94.

Liu, J., Liu, Y., Mao, Q., & Klaassen, C. D. (1994). The effects of 10 triterpenoid compounds on experimental liver injury in mice. *Fundamental and Applied Toxicology, 22*(1), 34-40.

Liu, J., Rajendram, R., & Zhang, L. (2010). Effects of oleanolic acid and maslinic acid on glucose and lipid metabolism: implications for the beneficial effects of olive oil on health. *Olives and olive oil in health and disease prevention*, 1423-1429.

Liu, J., Sun, H., Wang, X., Mu, D., Liao, H., & Zhang, L. (2007). Effects of oleanolic acid and maslinic acid on hyperlipidemia. *Drug Development Research, 68*(5), 261-266.

Liu, J., Wu, N., Ma, L.-N., Zhong, J.-T., Liu, G., Zheng, L.-H., & Lin, X.-K. (2014). p38 MAPK signaling mediates mitochondrial apoptosis in cancer cells induced by oleanolic acid. *Asian Pacific Journal of Cancer Prevention, 15*(11), 4519-4525.

Liu, J., Wu, Q., Lu, Y.-F., & Pi, J. (2008). New insights into generalized hepatoprotective effects of oleanolic acid: key roles of metallothionein and Nrf2 induction. *Biochemical pharmacology, 76*(7), 922-928.

Liu, J., Zheng, L., Wu, N., Ma, L., Zhong, J., Liu, G., & Lin, X. (2014). Oleanolic acid induces metabolic adaptation in cancer cells by activating the AMP-activated protein kinase pathway. *Journal of agricultural and food chemistry, 62*(24), 5528-5537.

Liu, W., & Wong, C. (2010). Oleanolic acid is a selective farnesoid X receptor modulator. *Phytotherapy Research: An International Journal Devoted to Pharmacological and Toxicological Evaluation of Natural Product Derivatives, 24*(3), 369-373.

Lou, Y.-R., Toh, T. C., Tee, Y. H., & Yu, H. (2017). 25-Hydroxyvitamin D 3 induces osteogenic differentiation of human mesenchymal stem cells. *Scientific reports, 7*(1), 1-12.

Lu, Y.-F., Wan, X.-L., Xu, Y., & Liu, J. (2013). Repeated oral administration of oleanolic acid produces cholestatic liver injury in mice. *Molecules, 18*(3), 3060-3071.

Macri, E. V., Chaves, M. M. G., Rodriguez, P. N., Mandalunis, P., Zeni, S., Lifshitz, F., & Friedman, S. M. (2012). High-fat diets affect energy and bone metabolism in growing rats. *European journal of nutrition, 51*(4), 399-406.

Maierhofer, W. J., Gray, R. W., Cheung, H. S., Lemann Jr, J., & Maierhofer, W. (1983). Bone resorption stimulated by elevated serum 1, 25-(OH) 2-vitamin D concentrations in healthy men. *Kidney international, 24*(4), 555-560.

Marie, P. J., Fromigué, O., & Modrowski, D. (2015). Deregulation of osteoblast differentiation in primary bone cancers. In *Bone Cancer* (pp. 39-54): Elsevier.

Markose, E. R., Stein, J. L., Stein, G. S., & Lian, J. B. (1990). Vitamin D-mediated modifications in protein-DNA interactions at two promoter elements of the osteocalcin gene. *Proceedings of the*

National Academy of Sciences, 87(5), 1701-1705.

Marriott, B. P., Birt, D. F., Stalling, V. A., & Yates, A. A. (2020). *Present Knowledge in Nutrition: Basic Nutrition and Metabolism*: Academic Press.

Martinez-Gonzalez, J., Rodriguez-Rodriguez, R., Gonzalez-Diez, M., Rodriguez, C., Herrera, M. D., Ruiz-Gutierrez, V., & Badimon, L. (2008). Oleanolic acid induces prostacyclin release in human vascular smooth muscle cells through a cyclooxygenase-2-dependent mechanism. *The Journal of nutrition, 138*(3), 443-448.

Maruyama, T., Miyamoto, Y., Nakamura, T., Tamai, Y., Okada, H., Sugiyama, E., . . . Tanaka, K. (2002). Identification of membrane-type receptor for bile acids (M-BAR). *Biochemical and biophysical research communications, 298*(5), 714-719.

Maurin, A., Chavassieux, P., Frappart, L., Delmas, P., Serre, C., & Meunier, P. (2000). Influence of mature adipocytes on osteoblast proliferation in human primary cocultures. *Bone, 26*(5), 485-489.

McClung, M., Harris, S. T., Miller, P. D., Bauer, D. C., Davison, K. S., Dian, L., . . . Lewiecki, E. M. (2013). Bisphosphonate therapy for osteoporosis: benefits, risks, and drug holiday. *The American journal of medicine, 126*(1), 13-20.

McClung, M. R. (2017). Using osteoporosis therapies in combination. *Current osteoporosis reports, 15*(4), 343-352.

Melton III, J. L. (1995). Perspectives: how many women have osteoporosis now? *Journal of Bone and Mineral Research, 10*(2), 175-177.

Michael, H., Härkönen, P. L., Väänänen, H. K., & Hentunen, T. A. (2005). Estrogen and testosterone use different cellular pathways to inhibit osteoclastogenesis and bone resorption. *Journal of bone and mineral research, 20*(12), 2224-2232.

Millán, M. M. (2015). The role of estrogen receptor in bone cells. *Clinical Reviews in Bone and Mineral Metabolism, 13*(2), 105-112.

Monkawa, T., Yoshida, T., Wakino, S., Shinki, T., Anazawa, H., Deluca, H. F., . . . Saruta, T. (1997). Molecular cloning of cDNA and genomic DNA for human 25-hydroxyvitamin D31α-hydroxylase. *Biochemical and biophysical research communications, 239*(2), 527-533.

Moore, D. D., Kato, S., Xie, W., Mangelsdorf, D. J., Schmidt, D. R., Xiao, R., & Kliewer, S. A. (2006). International Union of Pharmacology. LXII. The NR1H and NR1I receptors: constitutive androstane receptor, pregnene X receptor, farnesoid X receptor α, farnesoid X receptor β, liver X receptor α, liver X receptor β, and vitamin D receptor. *Pharmacological reviews, 58*(4), 742-759.

Morris, H. A., Moore, A., Moore, R., Need, A., O'Loughlin, P., Nordin, C., & Anderson, P. (2009).

Dietary calcium and oestradiol protect osteocyte density and bone structure against the effects of ovariectomy. *Bone*(44), S61.

Mu, D.-W., Guo, H.-Q., Zhou, G.-B., Li, J.-Y., & Su, B. (2015). Oleanolic acid suppresses the proliferation of human bladder cancer by Akt/mTOR/S6K and ERK1/2 signaling. *International journal of clinical and experimental pathology, 8*(11), 13864.

Muchmore, D. B. (2000). Raloxifene: a selective estrogen receptor modulator (SERM) with multiple target system effects. *The Oncologist, 5*(5), 388-392.

Murayama, A., Takeyama, K.-i., Kitanaka, S., Kodera, Y., Hosoya, T., & Kato, S. (1998). The promoter of the human 25-hydroxyvitamin D31α-hydroxylase gene confers positive and negative responsiveness to PTH, calcitonin, and 1α, 25 (OH) 2D3. *Biochemical and biophysical research communications, 249*(1), 11-16.

Murayama, A., Takeyama, K.-i., Kitanaka, S., Kodera, Y., Kawaguchi, Y., Hosoya, T., & Kato, S. (1999). Positive and negative regulations of the renal 25-hydroxyvitamin D3 1α-hydroxylase gene by parathyroid hormone, calcitonin, and 1α, 25 (OH) 2D3 in intact animals. *Endocrinology, 140*(5), 2224-2231.

Muruganandan, S., Roman, A., & Sinal, C. (2009). Adipocyte differentiation of bone marrow-derived mesenchymal stem cells: cross talk with the osteoblastogenic program. *Cellular and molecular life sciences, 66*(2), 236-253.

Musabayane, C., Tufts, M., & Mapanga, R. (2010). Synergistic antihyperglycemic effects between plant-derived oleanolic acid and insulin in streptozotocin-induced diabetic rats. *Renal failure, 32*(7), 832-839.

Nakamura, T., Imai, Y., Matsumoto, T., Sato, S., Takeuchi, K., Igarashi, K., . . . Yamamoto, Y. (2007). Estrogen prevents bone loss via estrogen receptor α and induction of Fas ligand in osteoclasts. *Cell, 130*(5), 811-823.

Nakashima, K., Zhou, X., Kunkel, G., Zhang, Z., Deng, J. M., Behringer, R. R., & De Crombrugghe, B. (2002). The novel zinc finger-containing transcription factor osterix is required for osteoblast differentiation and bone formation. *cell, 108*(1), 17-29.

Neer, R. (2001). Teriparatide reduces fracture risk in postmenopausal osteoporosis. *Inpharma, 1288*, 19.

Nelson, H. D. (2008). Menopause. *Lancet, 371*(9614), 760-770. doi:10.1016/S0140-6736(08)60346-3

Ngubane, P. S., Masola, B., & Musabayane, C. T. (2011). The effects of Syzygium aromaticum-derived oleanolic acid on glycogenic enzymes in streptozotocin-induced diabetic rats. *Renal failure, 33*(4), 434-439.

Nie, H., Wang, Y., Qin, Y., & Gong, X. G. (2016). Oleanolic acid induces autophagic death in human

gastric cancer cells in vitro and in vivo. *Cell biology international, 40*(7), 770-778.

Noda, M., Vogel, R. L., Craig, A. M., Prahl, J., DeLuca, H. F., & Denhardt, D. T. (1990). Identification of a DNA sequence responsible for binding of the 1, 25-dihydroxyvitamin D3 receptor and 1, 25-dihydroxyvitamin D3 enhancement of mouse secreted phosphoprotein 1 (SPP-1 or osteopontin) gene expression. *Proceedings of the National Academy of Sciences, 87*(24), 9995-9999.

Nuttall, M. E., Singh, V., Thomas-Porch, C., Frazier, T., & Gimble, J. M. (2014). Adipocytes and the regulation of bone remodeling: a balancing act. *Calcified tissue international, 94*(1), 78-87.

Okazaki, R., Inoue, D., Shibata, M., Saika, M., Kido, S., Ooka, H., . . . Matsumoto, T. (2002). Estrogen promotes early osteoblast differentiation and inhibits adipocyte differentiation in mouse bone marrow stromal cell lines that express estrogen receptor (ER) α or β. *Endocrinology, 143*(6), 2349-2356.

Olivares-Navarrete, R., Sutha, K., Hyzy, S. L., Hutton, D. L., Schwartz, Z., McDevitt, T., & Boyan, B. D. (2012). Osteogenic differentiation of stem cells alters vitamin D receptor expression. *Stem cells and development, 21*(10), 1726-1735.

Owen, T. A., ARONOW, M. S., Barone, L. M., BETTENCOURT, B., Stein, G. S., & Lian, J. B. (1991). Pleiotropic effects of vitamin D on osteoblast gene expression are related to the proliferative and differentiated state of the bone cell phenotype: dependency upon basal levels of gene expression, duration of exposure, and bone matrix competency in normal rat osteoblast cultures. *Endocrinology, 128*(3), 1496-1504.

Ozono, K., Liao, J., Kerner, S., Scott, R., & Pike, J. W. (1990). The vitamin D-responsive element in the human osteocalcin gene. Association with a nuclear proto-oncogene enhancer. *Journal of Biological Chemistry, 265*(35), 21881-21888.

Paccou, J., Hardouin, P., Cotten, A., Penel, G., & Cortet, B. (2015). The role of bone marrow fat in skeletal health: usefulness and perspectives for clinicians. *The Journal of Clinical Endocrinology & Metabolism, 100*(10), 3613-3621.

Palin, S., McTernan, P., Anderson, L., Sturdee, D., Barnett, A., & Kumar, S. (2003). 17β-Estradiol and anti-estrogen ICI: compound 182,780 regulate expression of lipoprotein lipase and hormone-sensitive lipase in isolated subcutaneous abdominal adipocytes. *Metabolism, 52*(4), 383-388.

Panda, D. K., Miao, D., Bolivar, I., Li, J., Huo, R., Hendy, G. N., & Goltzman, D. (2004). Inactivation of the 25-hydroxyvitamin D 1α-hydroxylase and vitamin D receptor demonstrates independent and interdependent effects of calcium and vitamin D on skeletal and mineral homeostasis. *Journal of Biological Chemistry, 279*(16), 16754-16766.

Papakitsou, E., Margioris, A., Dretakis, K., Trovas, G., Zoras, U., Lyritis, G., . . . Stergiopoulos, K. (2004). Body mass index (BMI) and parameters of bone formation and resorption in postmenopausal

women. *Maturitas, 47*(3), 185-193.

Parfitt, A. (1994). The two faces of growth: benefits and risks to bone integrity. *Osteoporosis international, 4*(6), 382-398.

Parhami, F., Tintut, Y., Beamer, W. G., Gharavi, N., Goodman, W., & Demer, L. L. (2001). Atherogenic high‑fat diet reduces bone mineralization in mice. *Journal of Bone and Mineral Research, 16*(1), 182-188.

Parikh, S. J., Edelman, M., Uwaifo, G. I., Freedman, R. J., Semega-Janneh, M., Reynolds, J., & Yanovski, J. A. (2004). The relationship between obesity and serum 1, 25-dihydroxy vitamin D concentrations in healthy adults. *The Journal of Clinical Endocrinology & Metabolism, 89*(3), 1196-1199.

Pautke, C., Schieker, M., Tischer, T., Kolk, A., Neth, P., Mutschler, W., & Milz, S. (2004). Characterization of osteosarcoma cell lines MG-63, Saos-2 and U-2 OS in comparison to human osteoblasts. *Anticancer research, 24*(6), 3743-3748.

Pearman, A. T., Chou, W.-Y., Bergman, K. D., Pulumati, M. R., & Partridge, N. C. (1996). Parathyroid hormone induces c-fos promoter activity in osteoblastic cells through phosphorylated cAMP response element (CRE)-binding protein binding to the major CRE. *Journal of Biological Chemistry, 271*(41), 25715-25721.

Pellicciari, R., Gioiello, A., Macchiarulo, A., Thomas, C., Rosatelli, E., Natalini, B., . . . Pastorini, E. (2009). Discovery of 6α-ethyl-23 (S)-methylcholic acid (S-EMCA, INT-777) as a potent and selective agonist for the TGR5 receptor, a novel target for diabesity. *Journal of medicinal chemistry, 52*(24), 7958-7961.

Pisani, P., Renna, M. D., Conversano, F., Casciaro, E., Di Paola, M., Quarta, E., . . . Casciaro, S. (2016). Major osteoporotic fragility fractures: risk factor updates and societal impact. *World journal of orthopedics, 7*(3), 171.

Posa, F., Di Benedetto, A., Colaianni, G., Cavalcanti-Adam, E. A., Brunetti, G., Porro, C., . . . Mori, G. (2016). Vitamin D effects on osteoblastic differentiation of mesenchymal stem cells from dental tissues. *Stem Cells International, 2016*.

Pun, K., Wong, F., Wang, C., Lau, P., Ho, P., Pun, W., . . . Young, R. (1990). Vitamin D status among patients with fractured neck of femur in Hong Kong. *Bone, 11*(5), 365-368.

Reginster, J.-Y., & Burlet, N. (2006). Osteoporosis: a still increasing prevalence. *Bone, 38*(2), 4-9.

Reid, I. R., Plank, L. D., & Evans, M. C. (1992). Fat mass is an important determinant of whole body bone density in premenopausal women but not in men. *The Journal of Clinical Endocrinology & Metabolism, 75*(3), 779-782.

Reisman, S. A., Aleksunes, L. M., & Klaassen, C. D. (2009). Oleanolic acid activates Nrf2 and protects from acetaminophen hepatotoxicity via Nrf2-dependent and Nrf2-independent processes. *Biochemical pharmacology, 77*(7), 1273-1282.

Rosenblum, J. L., Castro, V. M., Moore, C. E., & Kaplan, L. M. (2012). Calcium and vitamin D supplementation is associated with decreased abdominal visceral adipose tissue in overweight and obese adults. *The American journal of clinical nutrition, 95*(1), 101-108.

Samaras, K., Botelho, N. K., Chisholm, D. J., & Lord, R. V. (2010). Subcutaneous and visceral adipose tissue gene expression of serum adipokines that predict type 2 diabetes. *Obesity, 18*(5), 884-889.

Sato, H., Genet, C., Strehle, A., Thomas, C., Lobstein, A., Wagner, A., . . . Saladin, R. (2007). Anti-hyperglycemic activity of a TGR5 agonist isolated from Olea europaea. *Biochemical and biophysical research communications, 362*(4), 793-798.

Scheller, E. L., Doucette, C. R., Learman, B. S., Cawthorn, W. P., Khandaker, S., Schell, B., . . . Fazeli, P. K. (2015). Region-specific variation in the properties of skeletal adipocytes reveals regulated and constitutive marrow adipose tissues. *Nature communications, 6*(1), 1-15.

Scheller, E. L., Khoury, B., Moller, K. L., Wee, N. K., Khandaker, S., Kozloff, K. M., . . . Singer, K. (2016). Changes in skeletal integrity and marrow adiposity during high-fat diet and after weight loss. *Frontiers in endocrinology, 7*, 102.

Scheller, E. L., Troiano, N., VanHoutan, J. N., Bouxsein, M. A., Fretz, J. A., Xi, Y., . . . Church, C. D. (2014). Use of osmium tetroxide staining with microcomputerized tomography to visualize and quantify bone marrow adipose tissue in vivo. *Methods in enzymology, 537*, 123-139.

Schwartz, A. V., Sigurdsson, S., Hue, T. F., Lang, T. F., Harris, T. B., Rosen, C. J., . . . Oskarsdottir, D. (2013). Vertebral bone marrow fat associated with lower trabecular BMD and prevalent vertebral fracture in older adults. *The Journal of Clinical Endocrinology & Metabolism, 98*(6), 2294-2300.

Schwartz, G. G., Whitlatch, L. W., Chen, T. C., Lokeshwar, B. L., & Holick, M. F. (1998). Human prostate cells synthesize 1, 25-dihydroxyvitamin D3 from 25-hydroxyvitamin D3. *Cancer Epidemiology and Prevention Biomarkers, 7*(5), 391-395.

Shea, B., Wells, G., Cranney, A., Zytaruk, N., Robinson, V., Griffith, L., . . . Tugwell, P. (2002). Meta-analyses of therapies for postmenopausal osteoporosis. VII. Meta-analysis of calcium supplementation for the prevention of postmenopausal osteoporosis. *Endocrine Reviews, 23*(4), 552-559.

Shen, Q., & Christakos, S. (2005). The vitamin D receptor, Runx2, and the Notch signaling pathway cooperate in the transcriptional regulation of osteopontin. *Journal of Biological Chemistry, 280*(49), 40589-40598.

Sheng, L.-x., Huang, J.-y., Liu, C.-m., Zhang, J.-z., & Cheng, K.-g. (2019). Synthesis of oleanolic

acid/ursolic acid/glycyrrhetinic acid-hydrogen sulfide donor hybrids and their antitumor activity. *Medicinal Chemistry Research, 28*(8), 1212-1222.

Shu, B., Zhao, Y., Wang, Y., Wang, G., Shang, X., Britt, M., . . . Barton, S. (2017). Oleanolic acid enhances mesenchymal stromal cell osteogenic potential by inhibition of notch signaling. *Scientific reports, 7*(1), 1-8.

Shultz, T. D., Fox, J., Heath, H., & Kumar, R. (1983). Do tissues other than the kidney produce 1, 25-dihydroxyvitamin D3 in vivo? A reexamination. *Proceedings of the National Academy of Sciences, 80*(6), 1746-1750.

Somerman, M. J., Prince, C. W., Sauk, J. J., Foster, R. A., & Butler, W. T. (1987). Mechanism of fibroblast attachment to bone extracellular matrix: role of a 44 kilodalton bone phosphoprotein. *Journal of Bone and Mineral Research, 2*(3), 259-265.

Somjen, D., Weisman, Y., Kohen, F., Gayer, B., Limor, R., Sharon, O., . . . Stern, N. (2005). 25-Hydroxyvitamin D3-1α-hydroxylase is expressed in human vascular smooth muscle cells and is upregulated by parathyroid hormone and estrogenic compounds. *Circulation, 111*(13), 1666-1671.

Song, M., Hang, T.-j., Wang, Y., Jiang, L., Wu, X.-l., Zhang, Z., . . . Zhang, Y. (2006). Determination of oleanolic acid in human plasma and study of its pharmacokinetics in Chinese healthy male volunteers by HPLC tandem mass spectrometry. *Journal of pharmaceutical and biomedical analysis, 40*(1), 190-196.

Song, X., Liu, C.-C., Hong, Y.-R., & Zhu, X.-C. (2015). Anti-cancer activity of novel oleanolic acid methyl ester derivative in HeLa cervical cancer cells is mediated through apoptosis induction and reactive oxygen species production. ||| *Bangladesh Journal of Pharmacology, 10*(4), 896-902.

St‑Arnaud, R., Messerlian, S., Moir, J. M., Omdahl, J. L., & Glorieux, F. H. (1997). The 25‑hydroxyvitamin D 1‑alpha‑hydroxylase gene maps to the pseudovitamin D‑deficiency rickets (PDDR) disease locus. *Journal of bone and mineral research, 12*(10), 1552-1559.

Sung, H.-Y., Kang, S.-W., Kim, J.-L., Li, J., Lee, E.-S., Gong, J.-H., . . . Kang, Y.-H. (2010). Oleanolic acid reduces markers of differentiation in 3T3-L1 adipocytes. *Nutrition Research, 30*(12), 831-839.

Syed, F. A., Oursler, M. J., Hefferanm, T., Peterson, J. M., Riggs, B. L., & Khosla, S. (2008). Effects of estrogen therapy on bone marrow adipocytes in postmenopausal osteoporotic women. *Osteoporosis International, 19*(9), 1323-1330.

Szakiel, A., Grzelak, A., Dudek, P., & Janiszowska, W. (2003). Biosynthesis of oleanolic acid and its glycosides in Calendula officinalis suspension culture. *Plant Physiology and Biochemistry, 41*(3), 271-275.

Tajiri, M., Nakahashi, O., Kagawa, T., Masuda, M., Ohminami, H., Iwano, M., . . . Yamamoto, H. (2019). Association of increased renal Cyp24a1 gene expression with low plasma 1, 25-dihydroxyvitamin D levels in rats with streptozotocin-induced diabetes. *Journal of Clinical Biochemistry and Nutrition*, 19-79.

TAKEDA, E., YAMAMOTO, H., TAKETANI, Y., & MIYAMOTO, K. I. (1997). Vitamin D‑dependent rickets type I and type II. *Pediatrics International, 39*(4), 508-513.

Takeshita, S., Fumoto, T., Naoe, Y., & Ikeda, K. (2014). Age-related marrow adipogenesis is linked to increased expression of RANKL. *Journal of Biological Chemistry, 289*(24), 16699-16710.

Takeyama, K.-i., Kitanaka, S., Sato, T., Kobori, M., Yanagisawa, J., & Kato, S. (1997). 25-Hydroxyvitamin D3 1α-hydroxylase and vitamin D synthesis. *Science, 277*(5333), 1827-1830.

Tanaka, Y., Castillo, L., & DeLuca, H. (1976). Control of renal vitamin D hydroxylases in birds by sex hormones. *Proceedings of the National Academy of Sciences, 73*(8), 2701-2705.

Thomas, C., Gioiello, A., Noriega, L., Strehle, A., Oury, J., Rizzo, G., . . . Pruzanski, M. (2009). TGR5-mediated bile acid sensing controls glucose homeostasis. *Cell metabolism, 10*(3), 167-177.

Tian, A., Ma, J., Feng, K., Liu, Z., Chen, L., Jia, H., & Ma, X. (2019). Reference markers of bone turnover for prediction of fracture: a meta-analysis. *Journal of orthopaedic surgery and research, 14*(1), 1-10.

Tintut, Y., Morony, S., & Demer, L. L. (2004). Hyperlipidemia promotes osteoclastic potential of bone marrow cells ex vivo. *Arteriosclerosis, thrombosis, and vascular biology, 24*(2), e6-e10.

Tokuda, H., Ohigashi, H., Koshimizu, K., & Ito, Y. (1986). Inhibitory effects of ursolic and oleanolic ancid on skin tumor promotion by 12-O-tetradecanoylphorbol-13-acetate. *Cancer letters, 33*(3), 279-285.

Turner, A. G., Dwivedi, P. P., May, B. K., & Morris, H. A. (2007). Regulation of the CYP27B1 5′-flanking region by transforming growth factor-beta in ROS 17/2.8 osteoblast-like cells. *The Journal of Steroid Biochemistry and Molecular Biology, 103*(3-5), 322-325.

Van Der Meijden, K., Lips, P., van Driel, M., Heijboer, A. C., Schulten, E. A., den Heijer, M., & Bravenboer, N. (2014). Primary human osteoblasts in response to 25-hydroxyvitamin D 3, 1, 25-dihydroxyvitamin D 3 and 24R, 25-dihydroxyvitamin D 3. *PloS one, 9*(10), e110283.

Van der Meijden, K., Van Essen, H., Bloemers, F., Schulten, E., Lips, P., & Bravenboer, N. (2016). Regulation of CYP27B1 mRNA expression in primary human osteoblasts. *Calcified tissue international, 99*(2), 164-173.

van Driel, M., Koedam, M., Buurman, C., Hewison, M., Chiba, H., Uitterlinden, A., . . . Koedam, M. (2006). Evidence for auto/paracrine actions of vitamin D in bone: 1a‑hydroxylase expression

and activity in human bone cells. *The FASEB Journal, 20*(13), 2417-2419.

Van Schoor, N., Visser, M., Pluijm, S., Kuchuk, N., Smit, J., & Lips, P. (2008). Vitamin D deficiency as a risk factor for osteoporotic fractures. *Bone, 42*(2), 260-266.

Varela, N., Aranguiz, A., Lizama, C., Sepulveda, H., Antonelli, M., Thaler, R., . . . Van Wijnen, A. J. (2016). Mitotic inheritance of mRNA facilitates translational activation of the osteogenic-Lineage commitment factor runx2 in progeny of osteoblastic cells. *Journal of cellular physiology, 231*(5), 1001-1014.

Velazquez-Villegas, L. A., Perino, A., Lemos, V., Zietak, M., Nomura, M., Pols, T. W. H., & Schoonjans, K. (2018). TGR5 signalling promotes mitochondrial fission and beige remodelling of white adipose tissue. *Nature communications, 9*(1), 1-13.

Verma, S., Rajaratnam, J., Denton, J., Hoyland, J., & Byers, R. (2002). Adipocytic proportion of bone marrow is inversely related to bone formation in osteoporosis. *Journal of clinical pathology, 55*(9), 693-698.

Vieth, R., Pinto, T. R., Reen, B. S., & Wong, M. M. (2002). Vitamin D poisoning by table sugar. *The Lancet, 359*(9307), 672.

Wade, S., Strader, C., Fitzpatrick, L., Anthony, M., & O'Malley, C. (2014). Estimating prevalence of osteoporosis: examples from industrialized countries. *Archives of osteoporosis, 9*(1), 182.

Wagner, E. R., He, B.-C., Chen, L., Zuo, G.-W., Zhang, W., Shi, Q., . . . Luo, J. (2010). Therapeutic implications of PPAR in human osteosarcoma. *PPAR research, 2010*.

Wamberg, L., Christiansen, T., Paulsen, S., Fisker, S., Rask, P., Rejnmark, L., . . . Pedersen, S. (2013). Expression of vitamin D-metabolizing enzymes in human adipose tissue—the effect of obesity and diet-induced weight loss. *International journal of obesity, 37*(5), 651-657.

Wang, Q., Wang, G., Wang, B., & Yang, H. (2018). Activation of TGR5 promotes osteoblastic cell differentiation and mineralization. *Biomedicine & Pharmacotherapy, 108*, 1797-1803.

Wang, X., Chen, Y., Abdelkader, D., Hassan, W., Sun, H., & Liu, J. (2015). Combination therapy with oleanolic acid and metformin as a synergistic treatment for diabetes. *Journal of diabetes research, 2015*.

Wang, X., Ye, X.-l., Liu, R., Chen, H.-L., Bai, H., Liang, X., . . . Hai, C.-X. (2010). Antioxidant activities of oleanolic acid in vitro: possible role of Nrf2 and MAP kinases. *Chemico-biological interactions, 184*(3), 328-337.

Wat, W., Leung, J., Tam, S., & Kung, A. (2007). Prevalence and impact of vitamin D insufficiency in southern Chinese adults. *Annals of Nutrition and Metabolism, 51*(1), 59-64.

Watanabe, M., Houten, S. M., Mataki, C., Christoffolete, M. A., Kim, B. W., Sato, H., . . . Kodama, T. (2006). Bile acids induce energy expenditure by promoting intracellular thyroid hormone activation. *Nature, 439*(7075), 484-489.

Weaver, C., Gordon, C., Janz, K., Kalkwarf, H., Lappe, J. M., Lewis, R., . . . Zemel, B. (2016). The National Osteoporosis Foundation's position statement on peak bone mass development and lifestyle factors: a systematic review and implementation recommendations. *Osteoporosis international, 27*(4), 1281-1386.

Wei, J., Liu, M., Liu, H., Wang, H., Wang, F., Zhang, Y., . . . Lin, X. (2013). Oleanolic acid arrests cell cycle and induces apoptosis via ROS‐mediated mitochondrial depolarization and lysosomal membrane permeabilization in human pancreatic cancer cells. *Journal of Applied Toxicology, 33*(8), 756-765.

White, H., Ahmad, A., Durham, B., Patwala, A., Whittingham, P., Fraser, W., & Vora, J. (2005). Growth hormone replacement is important for the restoration of parathyroid hormone sensitivity and improvement in bone metabolism in older adult growth hormone-deficient patients. *The Journal of Clinical Endocrinology & Metabolism, 90*(6), 3371-3380.

Whitlatch, L. W., Young, M. V., Schwartz, G. G., Flanagan, J. N., Burnstein, K. L., Lokeshwar, B. L., . . . Chen, T. C. (2002). 25-Hydroxyvitamin D-1α-hydroxylase activity is diminished in human prostate cancer cells and is enhanced by gene transfer. *The Journal of steroid biochemistry and molecular biology, 81*(2), 135-140.

Williams, P., Brain, P., Peddie, M., & Taylor, T. (1988). Effects of estrone and estradiol-17β on 25-hydroxycholecalciferol hydroxylase activities in female Japanese quail. *General and comparative endocrinology, 71*(1), 97-104.

Wolf, S. L., Barnhart, H. X., Kutner, N. G., McNeely, E., Coogler, C., Xu, T., & Group, A. F. (1996). Reducing frailty and falls in older persons: an investigation of Tai Chi and computerized balance training. *Journal of the American Geriatrics Society, 44*(5), 489-497.

Xiong, J., Piemontese, M., Onal, M., Campbell, J., Goellner, J. J., Dusevich, V., . . . O'Brien, C. A. (2015). Osteocytes, not osteoblasts or lining cells, are the main source of the RANKL required for osteoclast formation in remodeling bone. *PloS one, 10*(9), e0138189.

Xu, Y., Chen, S., Yu, T., Qiao, J., & Sun, G. (2018). High-throughput metabolomics investigates anti-osteoporosis activity of oleanolic acid via regulating metabolic networks using ultra-performance liquid chromatography coupled with mass spectrometry. *Phytomedicine, 51*, 68-76.

Yan, S.-l., Huang, C.-y., Wu, S.-t., & Yin, M.-c. (2010). Oleanolic acid and ursolic acid induce apoptosis in four human liver cancer cell lines. *Toxicology in vitro, 24*(3), 842-848.

Yang, D., Atkins, G., Turner, A., Anderson, P., & Morris, H. (2012). Differential effects of 1, 25-dihydroxyvitamin D on in vitro mineral deposition: interaction between osteoblast stage of

maturation and culture medium calcium concentration. *J Bone Miner Res, 27*, SA0222.

Yong, L., Tang, G.-y., Tang, R.-b., Peng, Y.-f., & Wei, L. (2009). Assessment of bone marrow changes in postmenopausal women with varying bone densities: magnetic resonance spectroscopy and diffusion magnetic resonance imaging. *Chinese medical journal, 122*(12), 1524-1527.

Yoshida, N., Yoshida, T., Nakamura, A., Monkawa, T., Hayashi, M., & Saruta, T. (1999). Calcitonin induces 25-hydroxyvitamin D3 1α-hydroxylase mRNA expression via protein kinase C pathway in LLC-PK1 cells. *Journal of the American Society of Nephrology, 10*(12), 2474-2479.

Yoshimura, H., Sugawara, K., Saito, M., Saito, S., Murakami, S., Miyata, N., . . . Zhang, X. (2003). In vitro TGF-β1 antagonistic activity of ursolic and oleanolic acids isolated from Clerodendranthus spicatus. *Planta medica, 69*(07), 673-675.

Yu, Z., Sun, W., Peng, W., Yu, R., Li, G., & Jiang, T. (2016). Pharmacokinetics in vitro and in vivo of two novel prodrugs of oleanolic acid in rats and its hepatoprotective effects against liver injury induced by CCl4. *Molecular Pharmaceutics, 13*(5), 1699-1710.

Yunoki, K., Sasaki, G., Tokuji, Y., Kinoshita, M., Naito, A., Aida, K., & Ohnishi, M. (2008). Effect of dietary wine pomace extract and oleanolic acid on plasma lipids in rats fed high-fat diet and its DNA microarray analysis. *Journal of agricultural and food chemistry, 56*(24), 12052-12058.

Zehnder, D., Bland, R., Williams, M. C., McNinch, R. W., Howie, A. J., Stewart, P. M., & Hewison, M. (2001). Extrarenal expression of 25-hydroxyvitamin D3-1α-hydroxylase. *The Journal of Clinical Endocrinology & Metabolism, 86*(2), 888-894.

Zhao, D., Li, X., Zhao, Y., Qiao, P., Tang, D., Chen, Y., . . . Wang, J. (2018). Oleanolic acid exerts bone protective effects in ovariectomized mice by inhibiting osteoclastogenesis. *Journal of pharmacological sciences, 137*(1), 76-85.

Zhao, D., Shu, B., Wang, C., Zhao, Y., Cheng, W., Sha, N., . . . Wang, Y. (2020). Oleanolic acid exerts inhibitory effects on the late stage of osteoclastogenesis and prevents bone loss in osteoprotegerin knockout mice. *Journal of Cellular Biochemistry, 121*(1), 152-164.

Zhao, H., Zhou, M., Duan, L., Wang, W., Zhang, J., Wang, D., & Liang, X. (2013). Efficient synthesis and anti-fungal activity of oleanolic acid oxime esters. *Molecules, 18*(3), 3615-3629.

Zhao, J.-G., Zeng, X.-T., Wang, J., & Liu, L. (2017). Association between calcium or vitamin D supplementation and fracture incidence in community-dwelling older adults: a systematic review and meta-analysis. *Jama, 318*(24), 2466-2482.

Zhao, L.-J., Liu, Y.-J., Liu, P.-Y., Hamilton, J., Recker, R. R., & Deng, H.-W. (2007). Relationship of obesity with osteoporosis. *The Journal of Clinical Endocrinology & Metabolism, 92*(5), 1640-1646.

Zhao, X., Liu, M., & Li, D. (2015). Oleanolic acid suppresses the proliferation of lung carcinoma cells by miR-122/Cyclin G1/MEF2D axis. *Molecular and cellular biochemistry, 400*(1), 1-7.

Zhou, R., Zhang, Z., Zhao, L., Jia, C., Xu, S., Mai, Q., . . . Wang, X. (2011). Inhibition of mTOR signaling by oleanolic acid contributes to its anti‐tumor activity in osteosarcoma cells. *Journal of Orthopaedic Research, 29*(6), 846-852.

Zhou, S., Bueno, E. M., Kim, S. W., Amato, I., Shen, L., Hahne, J., . . . Glowacki, J. (2011). Effects of age on parathyroid hormone signaling in human marrow stromal cells. *Aging Cell, 10*(5), 780-788.

Zhou, S., Zilberman, Y., Wassermann, K., Bain, S. D., Sadovsky, Y., & Gazit, D. (2001). Estrogen modulates estrogen receptor α and β expression, osteogenic activity, and apoptosis in mesenchymal stem cells (MSCs) of osteoporotic mice. *Journal of cellular biochemistry, 81*(S36), 144-155.